132834

# TELEMETRY CODING STUDY FOR THE INTERNATIONAL MAGNETOSPHERE EXPLORERS— MOTHER/DAUGHTER AND HELIOCENTRIC MISSIONS

## VOL. II: FINAL REPORT

David E. Cartier
THE Magnavox COMPANY
Advanced Systems Analysis Office
8720 Georgia Avenue
Silver Spring, Maryland 20910

August 1973
Final Report



Prepared for
**GODDARD SPACE FLIGHT CENTER**
Greenbelt, Maryland 20771

| 1. Report No. | 2. Government Accession No. | 3. Recipient's Catalog No. |
|---|---|---|
| 4. Title and Subtitle<br>TELEMETRY CODING STUDY FOR THE INTERNATIONAL MAGNETOSPHERE EXPLORERS-MOTHER DAUGHTER AND HELIOCENTRIC MISSIONS VOL. II FINAL REPORT | | 5. Report Date<br><br>6. Performing Organization Code |
| 7. Author(s)<br>David E. Cartier | | 8. Performing Organization Report No.<br>ASAO-PR20046-4 |
| 9. Performing Organization Name and Address<br>The Magnavox Company<br>Advanced Systems Analysis Office<br>8720 Georgia Avenue, Suite 1000<br>Silver Spring, Maryland 20910 | | 10. Work Unit No.<br><br>11. Contract or Grant No.<br>NAS5-20386 |
| 12. Sponsoring Agency Name and Address<br>Dr. Ford Kalil<br>Goddard Space Flight Center<br>Greenbelt, Maryland 20771 | | 13. Type of Report and Period Covered<br>Final Report<br>14. Sponsoring Agency Code |

15. Supplementary Notes

This volume contains Vol. I (the only other volume) and as such is complete in itself.

16. Abstract

This is the final report for the convolutional coding study on the IME Mother-Daughter and Heliocentric spacecraft. It is a compilation of the three previously submitted task reports with supplemental material added to tie the three tasks together. It determines the amount of coding gain needed by the missions, studies and recommends an encoder/decoder system to provide the gain, and finally evaluates the impact of the system on the NASA space network in terms of cost and complexity.

| 17. Key Words (Selected by Author(s)) | 18. Distribution Statement |
|---|---|
| Telemetry Support Systems<br>Convolutional Coding<br>International Magnetosphere Explorers | |

| 19. Security Classif. (of this report) | 20. Security Classif. (of this page) | 21. No. of Pages | 22. Price* |
|---|---|---|---|
| UNCLASSIFIED | UNCLASSIFIED | | |

*For sale by the Clearinghouse for Federal Scientific and Technical Information, Springfield, Virginia 22151.

TABLE OF CONTENTS

TABLE OF CONTENTS (Cont.)

TABLE OF CONTENTS (Cont.)

TABLE OF CONTENTS (Cont.)



LIST OF APPENDICES

LIST OF ILLUSTRATIONS

LIST OF ILLUSTRATIONS (Cont.)

LIST OF ILLUSTRATIONS (Cont.)

LIST OF ILLUSTRATIONS (Cont.)



LIST OF TABLES

LIST OF TABLES (Cont.)

## 1.0 SUMMARY

The following document is the final report on a study of convolutional coding techniques for the International Magnetosphere Explorers (IME) Mother/Daughter and Heliocentric Missions (IMEMD/IMEH). Previous names for these missions were Interplanetary Monitoring Platform (IMP) KK' and L missions and also NASA/ESRO Mother/Daughter and NASA Heliocentric Missions (NEMD/NH). This report is a consolidation of the three task reports delivered to NASA Goddard Space Flight Center (GSFC) in December 1972, March 1973, and April 1973. All of the technical material found in those reports is duplicated here with explanatory material added.

The tasks imposed by GSFC in the contract statement of work will now be stated to provide a starting point for the rest of the report.

### 1.1 STATEMENT OF WORK

The Contractor will conduct a study to determine:

- the optimum cost-effective/efficient signal design for the Interplanetary Monitoring Platform, Mother/Daughter and Heliocentric Missions (IMP K-K') compatible with the Spaceflight Tracking and Data Network (STDN).
- the most cost-effective/efficient method(s) for ground handling of the one-half convolutionally coded, downlink telemetry received from these spacecraft. That is, should the data be transmitted from the remote sites to the Project Operations Control Center for decoding, or would noise interference significantly degrade the signal quality and so make it more desirable to decode the data at the remote sites. If the latter is more desirable, what are the most cost-effective augmentations, implementations and techniques for decoding at the remote sites?

#### 1.1.1 TASK REPORT NO. 1

The bit error rate enhancement capability of the planned convolutional coding technique significantly affects the optimum distribution of the

downlink signal power between the carrier range code and telemetry. Therefore, the Contractor will determine:

- The bit error rate enhancement that may be expected from the planned coding technique as well as other competitive techniques, for return link telemetry rates anticipated to be no greater than 16,384 information BPS for the IMP dual satellite mission and a maximum data rate of two information KBPS for the downlink telemetry for the IMP heliocentric mission. These rates will be programmable upon command to three lower bit rates which are multiples of $2^N$ of the maxima.
- Cost-effectiveness trade-offs, in especially those relating to the ground systems.
- Any interfacing problems associated with integrating decoding equipment techniques at the remote ground stations.

These results are to document the performance of the convolutional encoder-decoder in terms of bit error probability or coding gain for $10^{-5}$ bit error probability.

1.1.2 TASK REPORT NO. 2

Given the results of Task Report No. 1 plus system noise temperatures provided by NASA and using Effective Isotropic Radiated Power of .25 to 5.0 watts, the Contractor will determine the optimum power division among the carrier, ranging signal and telemetry signal for the return link. Parameters to be traded-off are range and range rate accuracy, time and signal power required for acquisition and "lack," and bit error probability.

1.1.3 TASK REPORT NO. 3

- The Contractor will determine the feasibility of decoding and decommutating in real and non-real time at the receiving ground station.
- He will determine whether or not hard-wired decoders are appropriate or whether the decoding can be accomplished at at the ground station with existing computer.

- He will determine the practicality of "tying up" the on-site computers for this purpose.

- He will examine the feasibility of transmitting the telemetry signal, which has been extracted from the return link but which has not been decoded or decommutated, over the NASCOM network via wideband or narrowband lines.

For instance, it may be possible to use wideband channels such as TELPAC A channels for real-time transmission to a central processor for decoding and decommutating, or it may be possible to use conventional voice bandwidth data lines for non-real time transmission to a central processor for decoding and decommutating. In these latter modes, the Contractor will assess the effect of the narrowband or wideband data transmission channels on the net bit error probability at the output of the decoder at the central processor.

- Cost figures will be developed to illustrate whether on-site decoding and decommutating or remote decoding and decommutating are advisable.

- The Contractor will provide definitive answers to the three following questions, which will be documented as a separate chapter of the final report.

  (a) What can be done with the present on-site equipment for the tasks outlined? This is primarily to establish a baseline for comparison purposes.

  (b) What would be the nature of a cost limited modification to accomplish some of the coding advantages?

  (c) What would be an optimum system with state of art approaches including costs and advantages?

## 1.2 STUDY PLAN

The method that was used to fulfill the work objectives was to perform Task 2 first, Task 1 second, and Task 3 third. The reason for this was that it was felt that a determination of the required coding enhancement

(gain) was in order before studying how such enhancement could be attained. After that was accomplished Task 3 could be performed to complete the study.

### 1.2.1 FIRST TASK SUMMARY

With the above reordering of priorities out of the way, the first task studied (Task 2 in the statement of work) performed a power budget analysis. The purpose was to determine the optimum modulation indices for the ranging and telemetry subcarrier and as a result derive the telemetry coding gain which would be necessary on the downlink.

The power budget is presented on several charts and is discussed on an item by item basis so that each factor of the system is brought into play with its associated impact. As the analysis progresses a series of tradeoffs are made and duly noted. Finally, as a result of all of these compromises, an optimal system is formed for the mission. Optimal here means that set of network elements which assures the greatest quality of data sent from the spacecrafts.

At the end of the analysis a section is presented which gathers, discusses, and explains, in terms of system impact, the conclusions reached in the items previously mentioned. After these conclusions are sufficiently expounded upon, recommendations are set forth which set the trend for the overall system design and its network support.

By way of highlighting the results of the first task, it was found that the coding gain required was 5 dB at $10^{-5}$ bit error probability; the solar noise factor on the downlink dictates that the minimum halo radius

on the Heliocentric mission be at least 60,000 km; the uplink signal-to-noise on the ranging is marginal in the case that the null of the omni receiving antenna is encountered on the Heliocentric mission; all other uplinks can be made to have good margins by efficient use of network facilities; finally, as expected, the Heliocentric mission is marginal on the downlink when near the earth-sun line.

### 1.2.2 SECOND TASK SUMMARY

A major result of the Task 1 report [1] was that the telemetry system for the IMEMD/H missions required an $E_b/N_o$ of 11.6 dB into the bit synchronizer to achieve an error probability of $10^{-5}$ without coding. Since only 7.2 dB was available in the IMEH mission when it was close to the sun (this was due to solar noise which degraded the system by about 10 dB) it was determined that at least a 5 dB coding gain should be designed into the system forward error control units.

The second task attacks the problem of achieving the 5 dB gain with a convolutional encoder used in conjunction with the appropriate decoder. It gives the theory of convolutional codes as found in the literature referenced in Section 5. After the theory is presented, the practical aspects of the encoding problem are discussed, and the important and complex subject of decoding is taken up. Three decoders are treated, namely, the Feedback Decoder, the Maximum Likelihood Decoder (also referred to as the Viterbi Decoder), and finally the Sequential Decoder. All of these are commonly used, however, only the last two provide the gain needed by the IMEMD/H missions. The Feedback Decoder is thus only touched upon to the extent necessary to eliminate it from consideration.

The algorithms upon which the two candidate decoders are based are fully developed, and then the practical aspects of implementing the algorithms into decoder hardware are detailed. The culmination of the above is the block diagram design of practical decoders with a discussion of each block.

Finally after the pros and cons of both the Viterbi and the Sequential Decoders have been weighed a recommendation is made to choose the Viterbi. This is based on a tradeoff among performance, complexity, and cost.

### 1.2.3 THIRD TASK SUMMARY

The third task completes the system study by looking at the the practical aspects of implementing the recommended encoding/decoding system. The limitations of actual hardware together with the costs involved are presented. Five possible configurations of the network (Figure 3.46) are analyzed on a block by block basis, i.e., each part of the system is scrutinized to ascertain whether or not it will prevent the realization of the system or to determine if it is too costly to be practical. After this is done the advantages and disadvantages are listed for each system.

In the conclusions and recommendations the material alluded to above is used to arrive at an optimum system to support the missions. This optimum system consists of the encoder arrived at in task 2 with each support station performing the decoding locally and transmitting the decoded data to Goddard Space Flight Center via the NASA Communications Network (NASCOM).

It will be shown in the text that follows that this system is relatively simple to implement, cost effective, flexible (can be used for future missions with a different bit rate and/or modulation scheme), and provides the experimenter with quality data.

## 2.0 INTRODUCTION

### 2.1 THE SOLAR WIND [2]

Both the IMEMD and IMEH missions will provide data on the solar wind, therefore, a few facts will be stated about it. The solar wind was virtually unknown until 1958 and it was only in 1962 that extensive measurements took place. It is an emission of subatomic particles from the sun's corona and consists mainly of protons and electrons. It is seen to be a significant part of the solar system and its effect on the components of the system is of great interest to scientists.

Its most prominent effect has been its influence on the comets as they come into proximity with the sun. An explanation for the acceleration of clouds of expelled gas from the heads of comets is that a force is exerted by an ionized gas or plasma streaming out from the sun at hundreds of miles per second.

Detecting devices were placed aboard early spacecraft to probe the solar wind. In 1962 the Venus mission, Mariner 2, and in 1959 the Russian mission, Lunik III both provided measurements which confirmed its existence and provided clues to its nature. It is a completely ionized gas consisting mainly of an average of 80 protons and electrons per cubic inch with the density varying from 1/10 to 10 times the average. The temperatures of the protons and electrons are 100,000 degrees and 400,000 degrees Fahrenheit, respectively. Heavier nucleis of helium, carbon, and oxygen also were found in it. The average speed near the earth is 300 miles per second with a variation of from 1/2 to 2 times the average.

Since the sun rotates the particles in the solar wind bend slightly in the direction of rotation; also due to the interaction with the sun's magnetic field a force on the sun is causing it to slow down. The solar wind causes the sun's magnetic field to expand so that the field extends farther than normally expected.

As far as the earth is concerned, the solar wind distorts the earth's magnetic field so that it forms a tail called the geomagnetic tail which is over three million miles in length. It is as if the magnetosphere of the earth were armor around a projectile (the earth) placed in a wind tunnel. The solar wind separates and passes around the armor coming together far behind it. The point of joining is called the magnetopause.

The region between the bow wave, or shock, and the magnetopause is called the magnetosheath, an area inhabited by the solar wind after passing through the shock and by irregular magnetic fields, tattered fragments of the sun's "elastic strings."

This complex interaction of solar wind and magnetic field may seem like a relatively stable affair. Yet highly sensitive compasses have shown that the Earth's magnetic field is subject to almost continuous aberrations. And changes in the density and velocity of the solar wind occur frequently. Occasionally solar flares erupt from the corona; vast dense streams of protons and electrons collide with the Earth's magnetic field, distorting it further and causing a wide range of geomagnetic storms and other activities, ranging from the magnificent sight of an aurora to a teletype machine typing out nonsense all by itself.

The solar wind was discovered so recently that it is barely mentioned in most undergraduate astronomy textbooks, and its role in the

solar system and beyond has only been glimpsed. (The answer is not known, among other questions, as to how far out from the sun the solar wind blows.) Not only will more be learned about this prominent presence in our corner of the universe but the solar wind itself will serve as an increasingly valuable tool for understanding other astronomical phemomena. For example, far beyond the Earth the solar wind collides with interstellar gas and observing its effects may shed light on the interstellar gas unobtainable by other methods. The solar wind, indeed, may become a large laboratory for investigating the nature of plasmas, the most common material of the universe.

## 2.2 THE IME MOTHER/DAUGHTER MISSION [3][4][5][6]

In this section the mission of the Mother/Daughter satellites will be described. To start the following material about the earth's magnetic field and perturbations in it is submitted.

The earth's magnetic field is closely approximated by a field emanating from a dipole source, similar to a bar magnet, which is tilted 11 degrees to the geographic equator. The postulated dipole source is also displaced from the earth's center several hundred miles westward and slightly to the north. As a result, the flux or field lines are anomalistic in distribution with reference to geographic coordinates. The most important feature of the field due to the source location is that a region of space above the South Atlantic Ocean has a much lower magnetic field strength for any given altitude than anywhere else around the earth. The result is that energetic charged particles, which are trapped on the field lines, come much closer to earth in this region, thereby producing a localized radiation hazard to space vehicles in low altitude orbits.

As described by Maxwell's equations, the earth's magnetic field acts to deflect approaching charged particles and therefore is a partial shield around the earth against cosmic particles. The magnetic field becomes severely distorted at high altitudes due to the steady outward movement of charged particles from the sun. The effects of this distortion are normally felt down to altitudes of five and six earth radii. However, in times of solar disturbances, surges of particles of higher than average energy cause the field to be temporarily unstable at these altitudes and below. This produces several effects, such as auroral and ionospheric disturbances, which are not well understood. When the disturbance is of solar flare intensity, the sun's particles penetrate the earth's magnetic field more effectively and can produce damaging radiation down to altitudes below 100,000 feet over the polar regions. Cosmic particles of galactic origin typically have sufficient energies to penetrate the magnetic field everywhere and to produce ionization in matter down to the earth's surface. However, the frequency of occurrence of these particles is so low that no particular hazard is involved.

There is a shock wave associated with the solar wind earth magnetic field interaction. This shock wave is analogous to the wave created by the bow of a ship cutting through the water, and it is thus termed a bow shock wave.

The Mother-Daughter mission has as its objectives the measurement of physical phenomena occurring in the bow shock of the earth. In order to do this, both mother and daughter will be placed into the same orbit by a single launch vehicle, and then their orbits will be

changed so that the two satellites go through their apogees at the same time, but separated by fixed distances of 100 km the first year, 1000 km the second year, and 5000 km the third year. The apogees themselves will range somewhere between 15 and 25 earth radii ($0.955 \times 10^4$ km and $1.59 \times 10^5$ km). The apogee separation allows measurement of the same phenomena at different points in the shock wave.

A sketch of the spacecraft is shown in Figure 2.1 while Figure 2.2 shows a typical orbit.

## 2.3 THE NASA HELIOCENTRIC MISSION[3][4][5][6]

In this section the mission of the heliocentric spacecraft will be described.

The earth-sun libration point is that point on a line connecting the centers of the sun and the earth where the gravitational forces of the two celestial bodies exactly cancel each other. Thus a spacecraft placed at this point would, theoretically, not move for all time. Of course, perturbations in the vehicle's position induced by outside forces, such as the solar wind, will cause it to leave the neutral point and eventually accelerate towards the body producing the stronger of the unbalanced gravitational forces.

The heliocentric S/C will be placed in an orbit about the earth-sun libration point which is perpendicular to the earth-sun center line. If it were placed on the libration point, reception of telemetry from the spacecraft would be made impossible due to solar noise entering

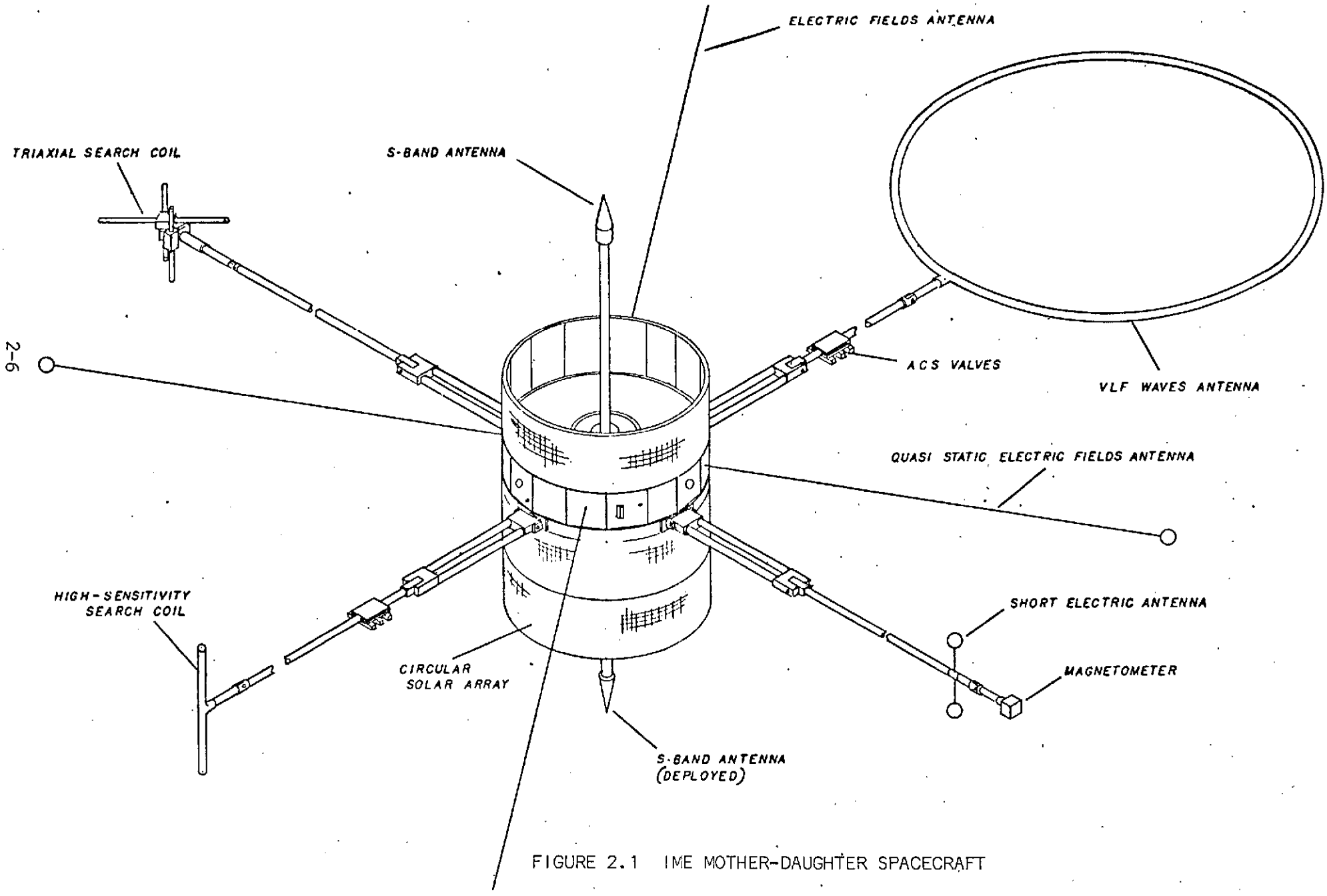


FIGURE 2.1 IME MOTHER-DAUGHTER SPACECRAFT

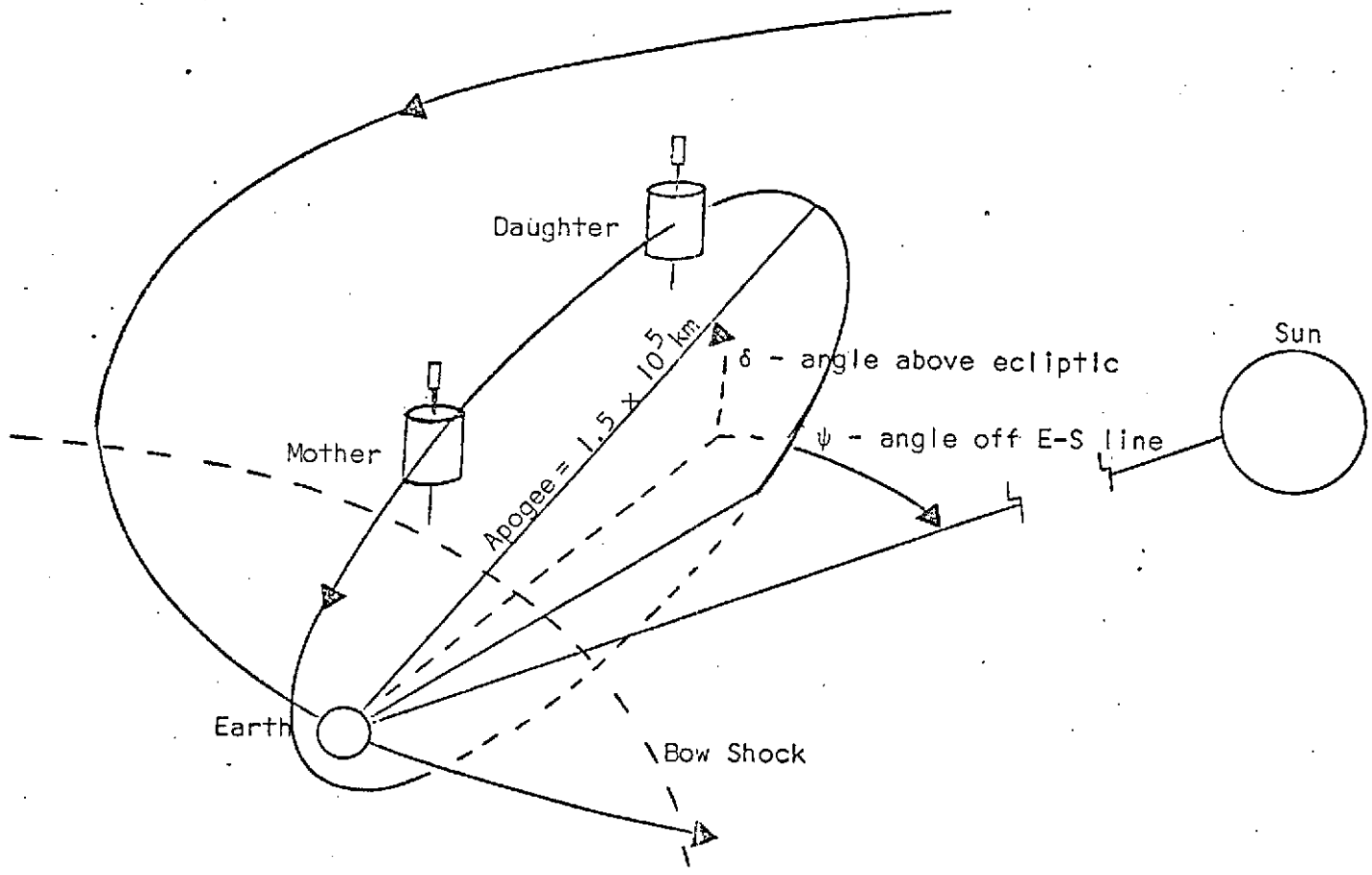


FIGURE 2.2 IMEMD TYPICAL ORBIT

the main beam of the earth receiving antenna. For this reason the "halo" orbit will be large enough so that any solar noise enters the ground system only by way of antenna side lobes which are controlled so as not to significantly contribute to the overall receiving system noise temperature.

Figure 2.3 shows a sketch of the IME Heliocentric spacecraft with Figure 2.4 showing the orbit concept together with the Earth-Sun libration points.

## 2.4 REPORT OBJECTIVES

### 2.4.1 TASK 1 OBJECTIVES

The primary purpose of the contract is to study the coding aspects of IME/Mother/Daughter and Heliocentric missions. It is thus imperative that a power budget analysis be performed, an optimum adjustment be made in available parameters, and the best use of system components be made. This results in the amount of coding gain needed and subsequently in the impact of the various coding systems on the network.

In this task the budget and tradeoffs alluded to above have been performed. The analysis proceeded as follows. A worst case and best case link calculation was determined for each spacecraft. The best case used all the system components and parameters in such a way as to enhance the margins available at various points throughout the link. As an example of the thought processes involved here, the most antenna gain was used rather than the least, i.e., 85 foot over 30 foot dishes, medium gain directional on the spacecraft over the omni, etc.; the least circuit losses were used; etc. It should be mentioned that care was taken not to be optimistic to the point of unrealistic in choices of parameters. The best

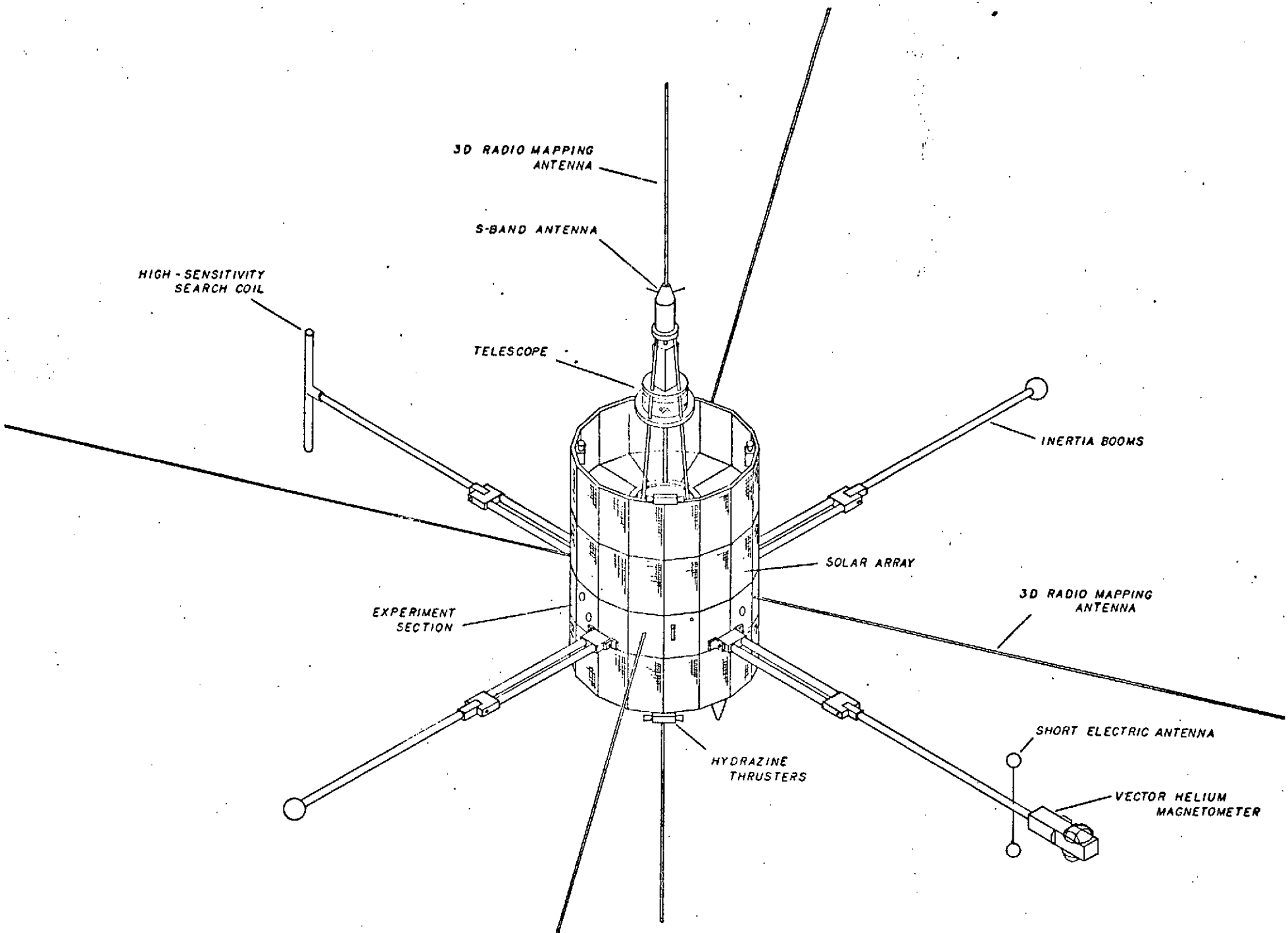


FIGURE 2:3 IME HELIOCENTRIC SPACECRAFT

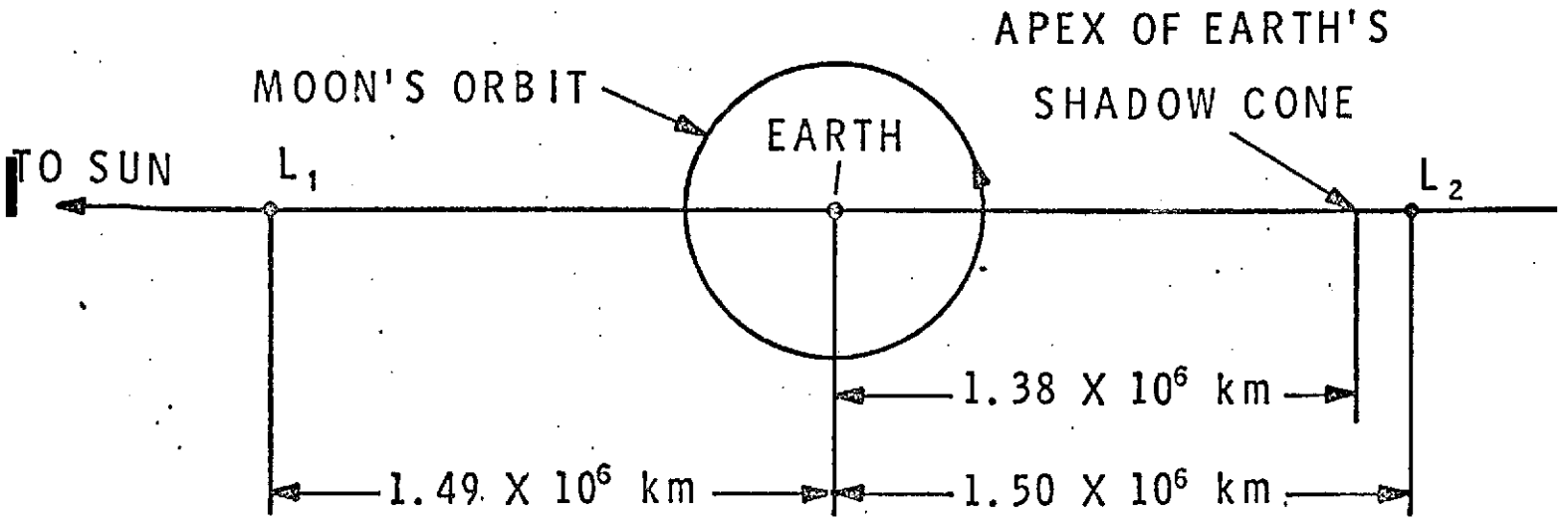


FIGURE 2.4a EARTH-SUN LIBRATION POINTS

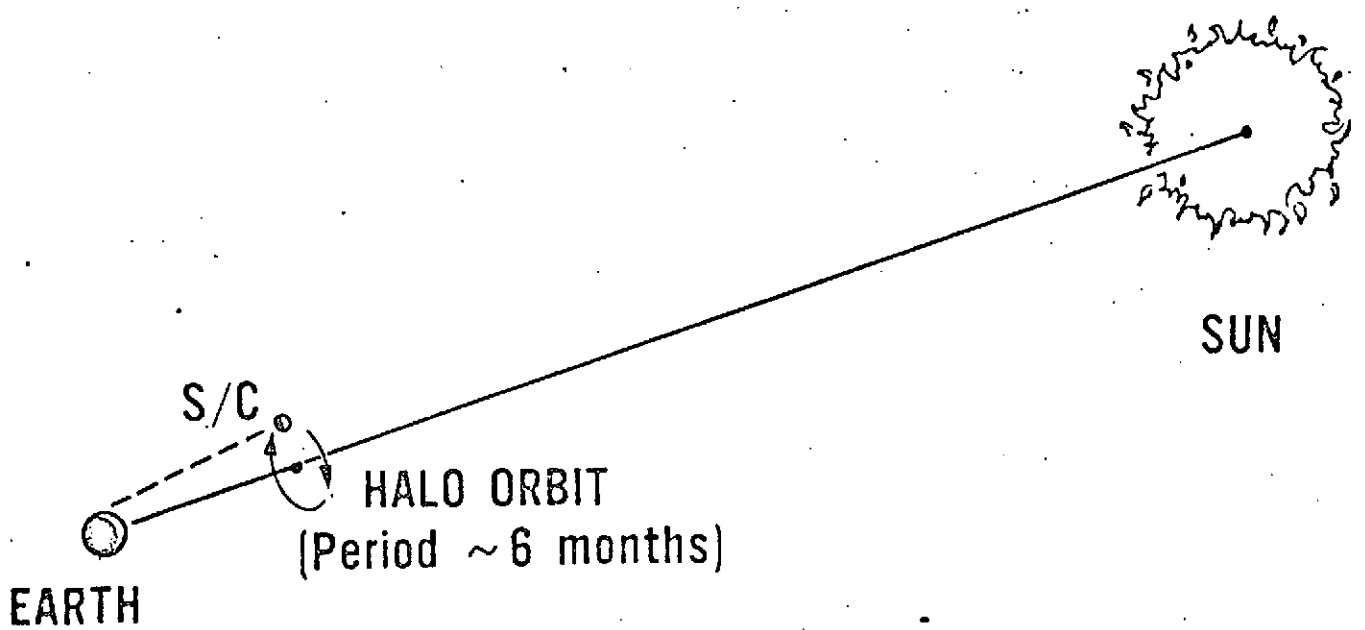


FIGURE 2.4b IMEH HALO ORBIT

case is considered plausible in that system parameters and components can be chosen to give this case under normal operating conditions. It should also be noted in addition, that there may be times when certain components, such as the 85 foot dish, may not be available and so a "less than best" case must be used. In summary, the best case merely uses the best combination of subsystems, etc. to enhance the link performance while it is in a configuration favorable to the mission.

The worst case, on the other hand, started off as the worst use of all systems in the link (assuming all could be employed). As the analysis progressed certain limitations were reached. At these points tradeoffs were made so that the limitation was removed. For example, the 30 foot dish was replaced by the 85 foot dish, or a lower bit rate was used. By continuing in this manner, the minimum operational worst case system was obtained together with conclusions and recommendations derived as a result of the tradeoffs. The above rationale will become clear as the report develops.

The main vehicle for budgeting the power in this report will be a series of link calculation charts. As each limitation, referred to above, is reached a compromise is made and the old chart is superseded by a new chart with the compromise reflected within it.* Finally a chart is presented which supersedes all previous charts and shows the optimum choice of parameters and subsystems which have resulted from the aggregate of all the individual compromises made through the report.

---

* The appropriate value is changed and marked by a "†" for clarity on the updated chart.

It is the belief of the author that this hands-on approach will let the reader follow the thoughts of the designer as he progressed through the task.

It should also be noted that due to the large number of parameters in the system, the highest bit rate was assumed, i.e., all other parameters were traded-off before the bit rate was compromised. Lowering the bit rate would lessen the strain on the link and allow "sub-optimum" network components to be used. This will be discussed later.

### 2.4.2 TASK 2 OBJECTIVES

A major result of the Task 1 study[1] was that a coding gain of at least 5 dB was desirable in order to support the IMEMD/H missions. The full gain was needed for the Heliocentric spacecraft when its "halo" radius was at a minimum thereby allowing close to 10 dB degradation* in the signal to noise ratio (SNR) due to solar noise entering the antenna beam. Less coding gain was needed in other configurations, however, if the full 5 dB was used then this allowed greater flexibility in the choice of ground station equipment, e.g., smaller diameter antenna or an uncooled rather than cooled parametric amplifier in the front end system.

The primary objective of this task is to provide the background material necessary to confidently recommend a complete forward error control system which will result in a 5 dB coding gain. The way that this is done is to study convolutional coding theory in general (other forward error control schemes such as Reed-Solomon[7][8][9] or Hamming codes[7][8][9] were not considered since convolutional codes are far superior when applied to a space channel) and then to study the practical implementation factors of a coding system design.

* The solar noise data was supplied by GSFC.

The important outputs of this task are the design of a maximum likelihood decoder and the design of a sequential decoder with complexity taken into account. Having done this a tradeoff was made to arrive at a recommended decoder for the missions. The tradeoff was based upon many factors; included among these were:

- complexity of decoder
- cost of decoder
- burst error recovery factors (for decoding at GSFC)
- network interface complexity
- error rate versus SNR characteristics
- synchronization factors.

Used in the final tradeoff was a method found in reference 10 which looks at the complexity of the decoders in terms of "complexity bits." These indicate storage and/or computation requirements of the decoder in question.

### 2.4.3 TASK 3 OBJECTIVES

In the previous two tasks [1][11] the problem of providing good quality telemetry data from the IMEMD/H spacecraft was considered. As a result of these studies it was found that, due to low signal to noise ratios available at the ground stations, at least a 5 dB coding gain was needed in the downlink. It was also recommended that a constraint length seven (7), rate 1/2 convolutional encoder be placed aboard the spacecraft and that the received coded information be decoded using a decoder implementing the maximum likelihood (Viterbi) algorithm in order to achieve the needed gain. Several reasons were given for this choice, among which were the low cost (~$5000) per decoder, the provision for handling higher data

rates in future missions without any modification to the station, the better synchronization properties of the Viterbi algorithm, and the graceful degradation in error rate versus input signal to noise.

Having arrived at the decoding algorithm to be used via the preceeding tasks, the third task will answer the following questions:

- Is real or non real time decoding feasible at the ground station?
- Should software or hardware be used to implement the algorithm?
- What is the impact on the station computer for a software implementation?
- Should the decoding be done at the ground stations themselves or should it be done at some central location, such as Goddard Space Flight Center, after the received baseband has been transmitted via NASCOM?
- What are the cost factors involved with the above schemes?
- What is the station impact?
- What is the optimum system?

In order to answer these questions five systems were set up which "in theory" could implement the telemetry/codec scheme previously settled upon. By "in theory" it is meant that if all practical problems were ignored, such as bit slippage in a bit synchronizer at low signal to noise ratios, or quantized block resynchronization after parallel to serial and serial to parallel conversion, or limited tape recorder response, then the system was capable of presenting the experimenter with quality data.

In the course of this task the practical factors of the systems will be "cranked in," thereby eliminating some altogether and hopefully

arranging the rest in a list of decreasing optimality. Optimality here means the system which will do the best job theoretically while being cost effective and also practical to implement.

Throughout the task the 1975-1977 STDN will be assumed with the bulk of the information drawn from reference 34. In this time frame the network should have settled into a reasonably stable configuration and Stadac I and Stadac II should be in operation. It should be noted that the network in 1975 will be more sophisticated than at present with such things as "third generation" soft bit synchronizers in the field and more wideband lines available.

Each of the five systems mentioned above will be analyzed on a block by block basis thereby pinpointing the weak links of the system and, if such is the case, isolate the reason for rejecting the overall system. As the material is developed it is hoped that a clear understanding of the "real world" factors in designing a codec system will be obtained. This is, in the author's opinion, one of the most important goals of task 3, for theory is fine as far as it goes, but unless the hardware and/or software can be built, and unless network personnel and project experimenters can be convinced that the theory does indeed produce the promised results, there is little hope for allocations in the network budgets.

In closing this section, then, the present task really comes down to the last question stated above, namely, what is the optimum system

for receiving coded telemetry data at the ground stations and delivering experimental data to the network users, where optimality weighs:

- Quality of the output data
- Availability of equipment
- System cost
- Network loading
- System complexity
- System reliability.

## 3.0 DISCUSSION AND RESULTS

This section of the report present the results of the three tasks set forth by the statement of work in the contract together with any discussion, analysis, and technical material needed to support them. The present section is broken down into three major subsections, each of which are the discussion and results of the individual tasks.

### 3.1 TASK 1 DISCUSSION AND RESULTS

In this section of the report a power budget for the IME Mother Daughter and the IME Heliocentric mission will be presented. The discussion will follow the exact line of reasoning which was used to arrive at the results shown in the following pages. Charts, equations, and figures will be interlaced with the text to clarify and demonstrate conclusions and recommendations.

The coding aspects of this report require a prediction of the total power available in the downlink together with the allocation of power among the PN ranging signal, the carrier, and the telemetry.

Referring to Figure 3.1, the modes of operation for both missions are as follows.

Case A: Ranging only directly through the medium gain antenna

Case B: Telemetry only directly through the medium gain antenna

Case C: Ranging and Telemetry diplexed through the medium gain antenna

Case D: Ranging and Telemetry subcarrier directly through the medium gain antenna

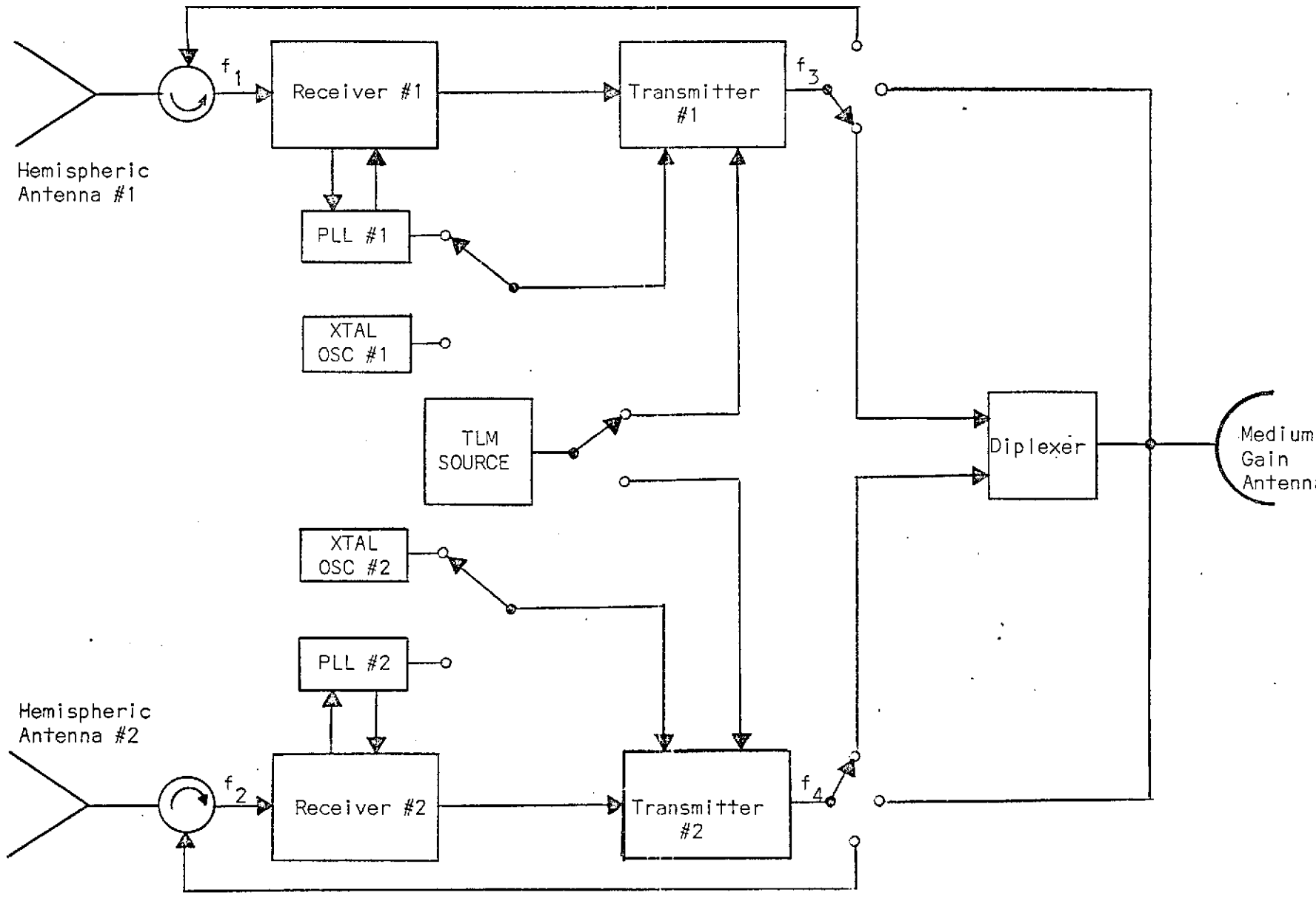


FIGURE 3.1 IME COMMUNICATIONS BLOCK DIAGRAM

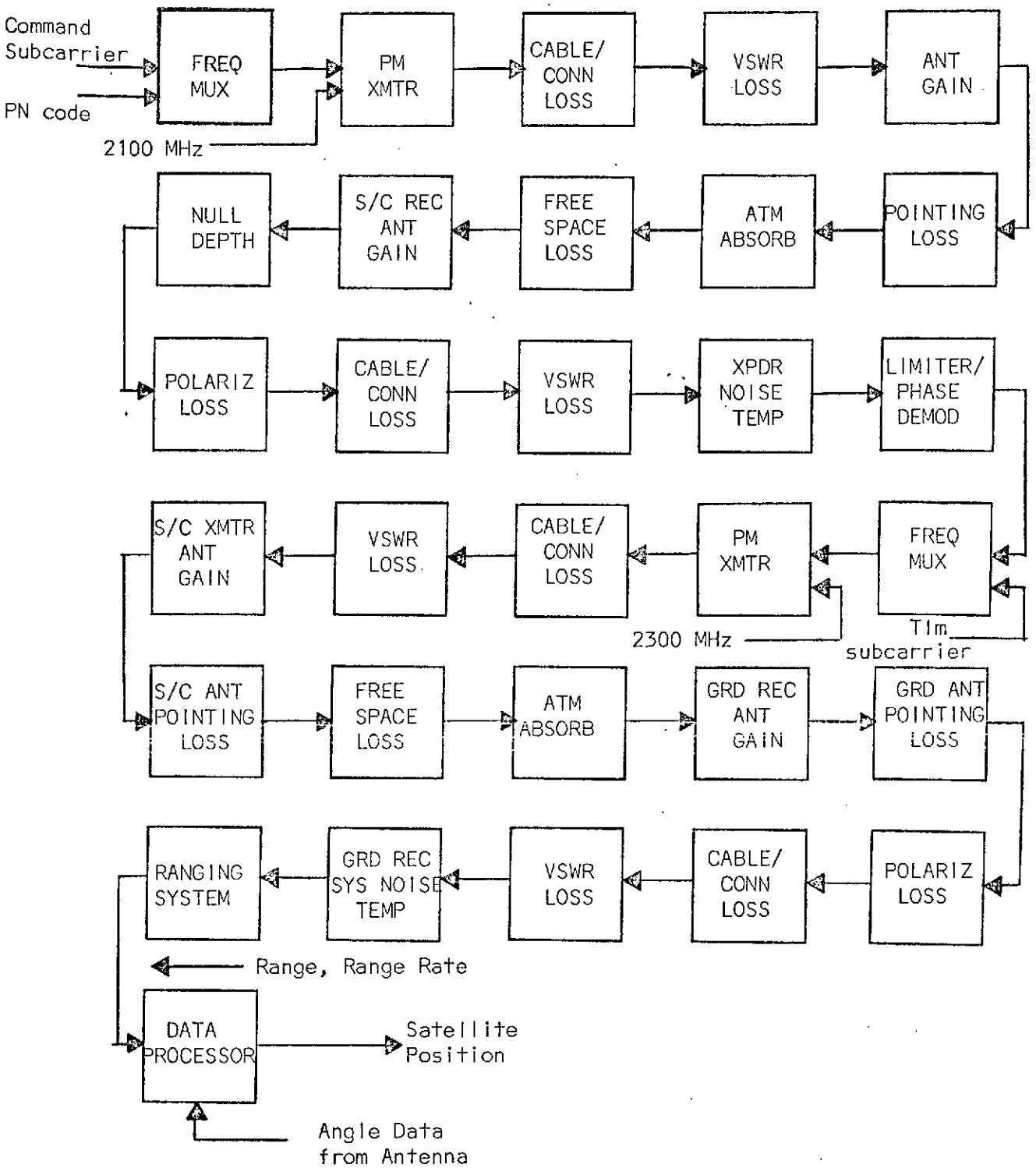


FIGURE 3.2 RANGING SYSTEM BLOCK DIAGRAM

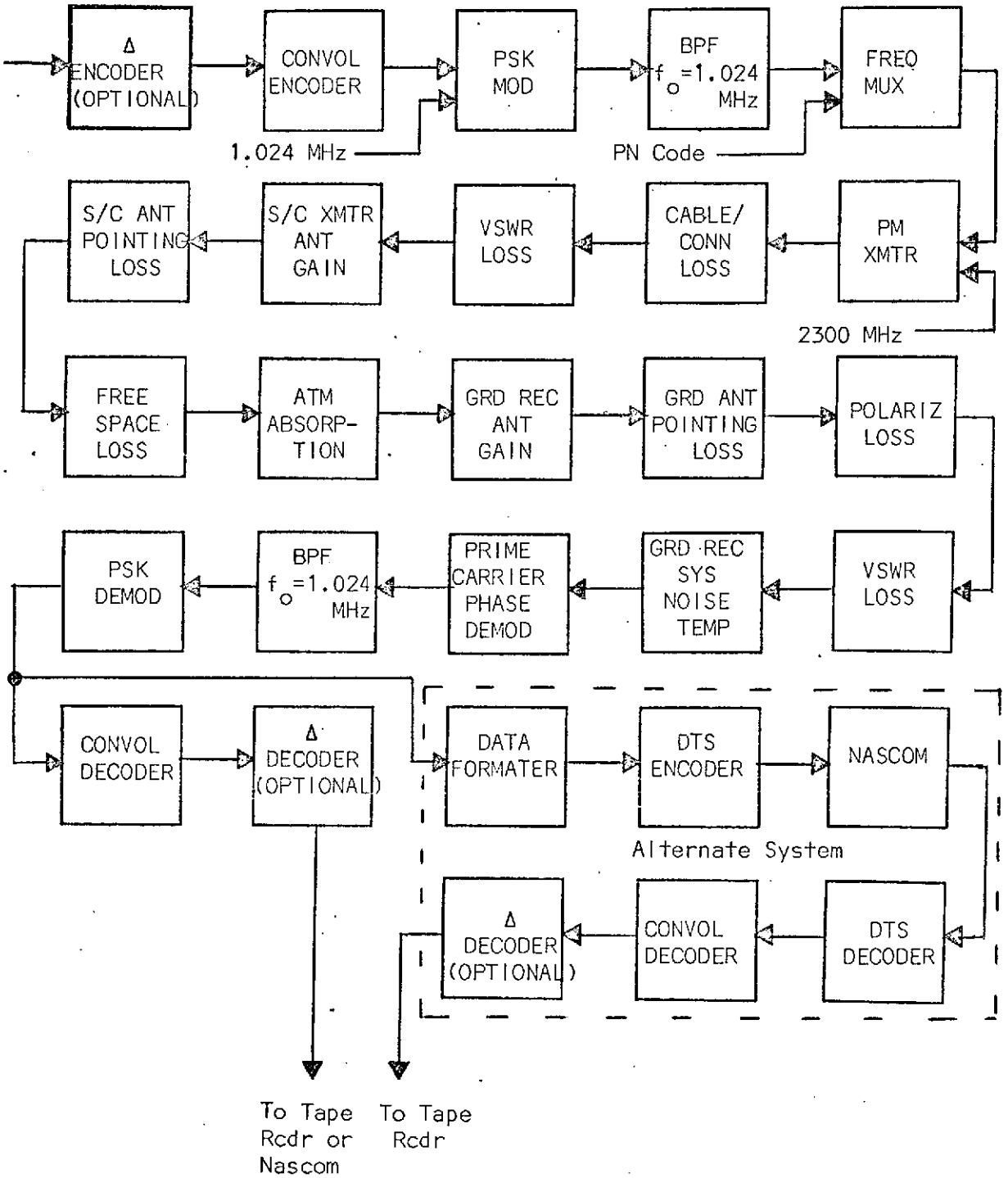


FIGURE 3.3 TELEMETRY SYSTEM BLOCK DIAGRAM (SUBCARRIER OPTION)

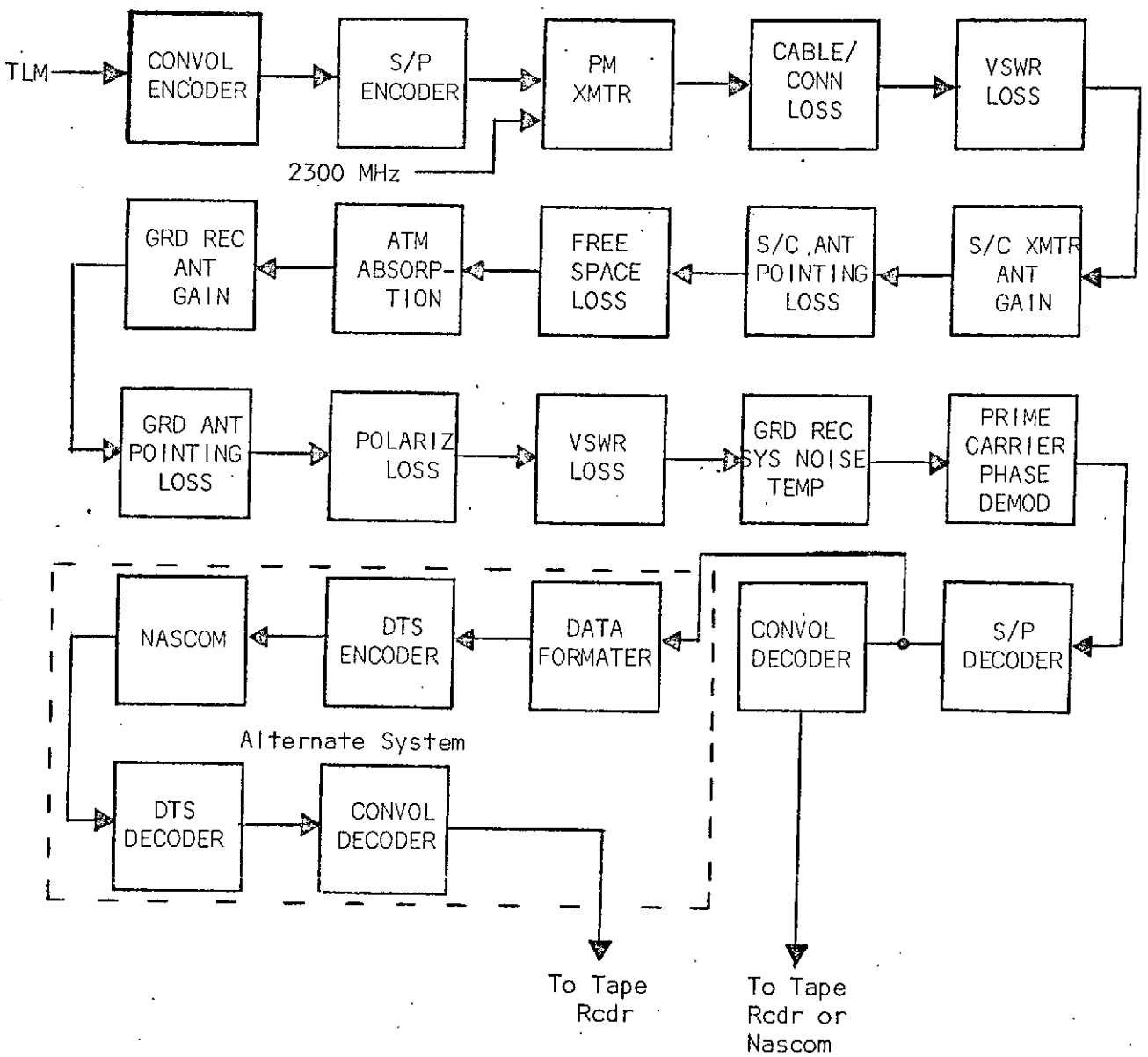


FIGURE 3.4 TELEMETRY SYSTEM BLOCK DIAGRAM (PRIME CARRIER OPTION)

Case E: Ranging only directly through the hemispherical antenna

Case F: Telemetry only directly through the hemispherical antenna

The above modes can be generalized with respect to link calculations as reflected in Figures 3.2, 3.3, and 3.4.

Using these figures as a guide link calculation charts were derived. Having determined the parameters needed, a computer program was written which when fed with the parameters of the system for each case given above outputted the data necessary to make the appropriate tradeoffs. The program is general enough to handle more than the above modes and can be readily modified to be used with other missions (see Appendix D).

### 3.1.1 UPLINK POWER BUDGET ANALYSIS

At this point the first chart will be introduced. It will be noted that each line has an item number. These numbers will be referred to continually throughout the discussion. Also changes in the charts will reflect the conclusions within the report. This two way referencing will allow the reader to either follow the text and refer to the chart or vice versa, thus adding flexibility to the discussion. This it is hoped will increase the usefulness of the report.

Consider Table 3.1. Item 1 is the ground transmitter power which is available for the uplink command/ranging signal. The Unified S-band stations have 20 KW maximum. In dBm, then, the power is 73 dBm. Note that any less available power than that stated would be considered a degraded operational status for the supporting stations. It should be mentioned that due to the frequency diversity which can be employed for

| ITEM | ITEM DESCRIPTION | | IME-H. BEST CASE | IME-H. WORST CASE | IME-M.-D. BEST CASE | IME-M.-D. WORST CASE |
|---|---|---|---|---|---|---|
| 1. | Grd Xmtr Power (USB 20KW) | (dbm) | 73.0 | 73.0 | 73.0 | 73.0 |
| 2. | Xmtr to Antenna Xmssn Losses | (db) | -0.1 | -0.5 | -0.1 | -0.5 |
| 3. | Grd Xmtr Antenna Gain (85'-52.5db, 30'-43db) | (db) | 52.5 | 43.0 | 52.5 | 43.0 |
| 4. | Path Loss (H.-1.5x10*6KM, M.-D.-1.5x10*5Km, 2.1GHz) | (db) | -222.1 | -222.1 | -202.1 | -202.1 |
| 5. | Power at S/C Rcvr Antenna | (dbm) | -96.7 | -106.6 | -76.7 | -86.6 |
| 6. | S/C Rcvr Antenna Gain (Omni) | (db) | 2.0 | -3.0 | 2.0 | -3.0 |
| 7. | Antenna to Rcvr Xmssn Losses | (db) | -1.0 | -2.0 | -1.0 | -2.0 |
| 8. | Power at S/C Rcvr Input (S(u)) | (dbm) | -95.7 | -111.6 | -75.7 | -91.6 |
| 9. | Uplink Solar Noise Factor | (db) | 0.0 | 0.0 | 0.0 | 0.0 |
| 10. | S/C Rcvr Noise Density (N(ou)) | (dbm/Hz) | -160.6 | -166.1 | -151.7 | -157.8 |
| 11. | Uplink Total (S(u)/N(ou)) | (db-Hz) | 64.9 | 54.5 | 76.0 | 66.2 |

TABLE 3.1A IME LINK CALCULATION (RISING DENSITY)



| ITEM | ITEM DESCRIPTION | | IME-H. BEST CASE | IME-H. WORST CASE | IME-M.-D. BEST CASE | IME-M.-D. WORST CASE |
|---|---|---|---|---|---|---|
| 1. | Grd Xmtr Power (USB 20KW) | (dbm) | 73.0 | 73.0 | 73.0 | 73.0 |
| 2. | Xmtr to Antenna Xmssn Losses | (db) | -0.1 | -0.5 | -0.1 | -0.5 |
| 3. | Grd Xmtr Antenna Gain (85'-52.5db, 30'-43db) | (db) | 52.5 | 43.0 | 52.5 | 43.0 |
| 4. | Path Loss (H.-1.5x10*6KM, M.-D.-1.5x10*5Km, 2.1GHz) | (db) | -222.1 | -222.1 | -202.1 | -202.1 |
| 5. | Power at S/C Rcvr Antenna | (dbm) | -96.7 | -106.6 | -76.7 | -86.6 |
| 6. | S/C Rcvr Antenna Gain (Omni) | (db) | 2.0 | -3.0 | 2.0 | -3.0 |
| 7. | Antenna to Rcvr Xmssn Losses | (db) | -1.0 | -2.0 | -1.0 | -2.0 |
| 8. | Power at S/C Rcvr Input (S(u)) | (dbm) | -95.7 | -111.6 | -75.7 | -91.6 |
| 9. | Uplink Solar Noise Factor | (db) | 0.0 | 0.0 | 0.0 | 0.0 |
| 10. | S/C Rcvr Noise Density (N(ou)) | (dbm/Hz) | -166.8 | -166.8 | -166.8 | -166.8 |
| 11. | Uplink Total (S(u)/N(ou)) | (db-Hz) | 71.1 | 55.2 | 91.1 | 75.2 |

TABLE 3.1B IME LINK CALCULATION (NON RISING DENSITY)

the ranging channel the power could be 70 dBm per channel, however, once the strong channel is chosen the full power of 73 dBm is available for the uplink.

Item 2 is an estimate of the transmission losses incurred between the transmitter and the antenna; these include diplexer loss, cable loss, etc.

Item 3 is the gain of the command transmitting antennas. The 85 foot parabolic dish has a gain of 52.5 dB at 2.1 GHz, and the 30 foot parabolic dish has a gain of 43 dB at 2.1 GHz. If both were available then the 85 foot would be best case and the 30 foot would be worst.

Item 4 is the free space path loss. For IME-Mother-Daughter the apogee is $1.5 \times 10^5$ km. Using the equation[12]

$$L_{FS} = (4\pi)^2 \, d^2/\lambda^2, \tag{3.1}$$

where $L_{FS}$ is the loss in free space between isotropic antennas, d is the distance in meters between the antennas, and $\lambda$ is the wavelength in meters of the electromagnetic wave propagating through the medium, the loss is

$$[(4\pi)^2(1.5 \times 10^8)^2]/[(2.99793 \times 10^8/2.1 \times 10^9)^2]$$
$$= 10^{+20.21} \ (+202.1 \text{ dB}). \tag{3.2}$$

For IME-Heliocentric the same reasoning with a distance of $1.5 \times 10^6$ km instead of $1.5 \times 10^5$ km gives a loss of +222.1 dB.

Item 5 is simply the sum of Items 1 through 4 and gives the power level appearing at the spacecraft receiving antenna.

Item 6 is the spacecraft receiving antenna gain. One half of the pattern for this antenna is shown in Figure 3.5 (actually two of these patterns will make up the overall receiving antenna).[13] The maximum gain is 2 dB, whereas the minimum gain appearing at the junction of the two halves is -3 dB. These are the best and worst case respectively.

Item 7 estimates the spacecraft transmission line losses at -1 dB and -2 dB, best and worst case, respectively.

Item 8 is the sum of Items 5, 6, and 7 and is the power level appearing at the input to the spacecraft receiver, i.e., the ranging transponder in this instance.

Item 9 is the uplink solar noise factor. Due to the large solid angle seen by the spacecraft hemispheric antennas, i.e., wide field of view the uplink solar noise is negligible and is therefore assumed to be 0 dB.

Item 10 is the transponder noise density. Some discussion is in order here. Per reference 14, the noise density of an Apollo type of transponder which could be used in the IME missions has a rising characteristic as shown in Figure 3.6. This increase in noise density is due to the AGC circuits internal to the transponder. As can be seen in the figure at an input signal level of -90 dBm the slope becomes almost 1:1 and constant thereafter. This is very degrading in terms of signal margin and negates the high command power transmitted from the ground.

With the above discussion in mind, the curve in Figure 3.6 can be used to find the noise density required in Item 10 by translating the

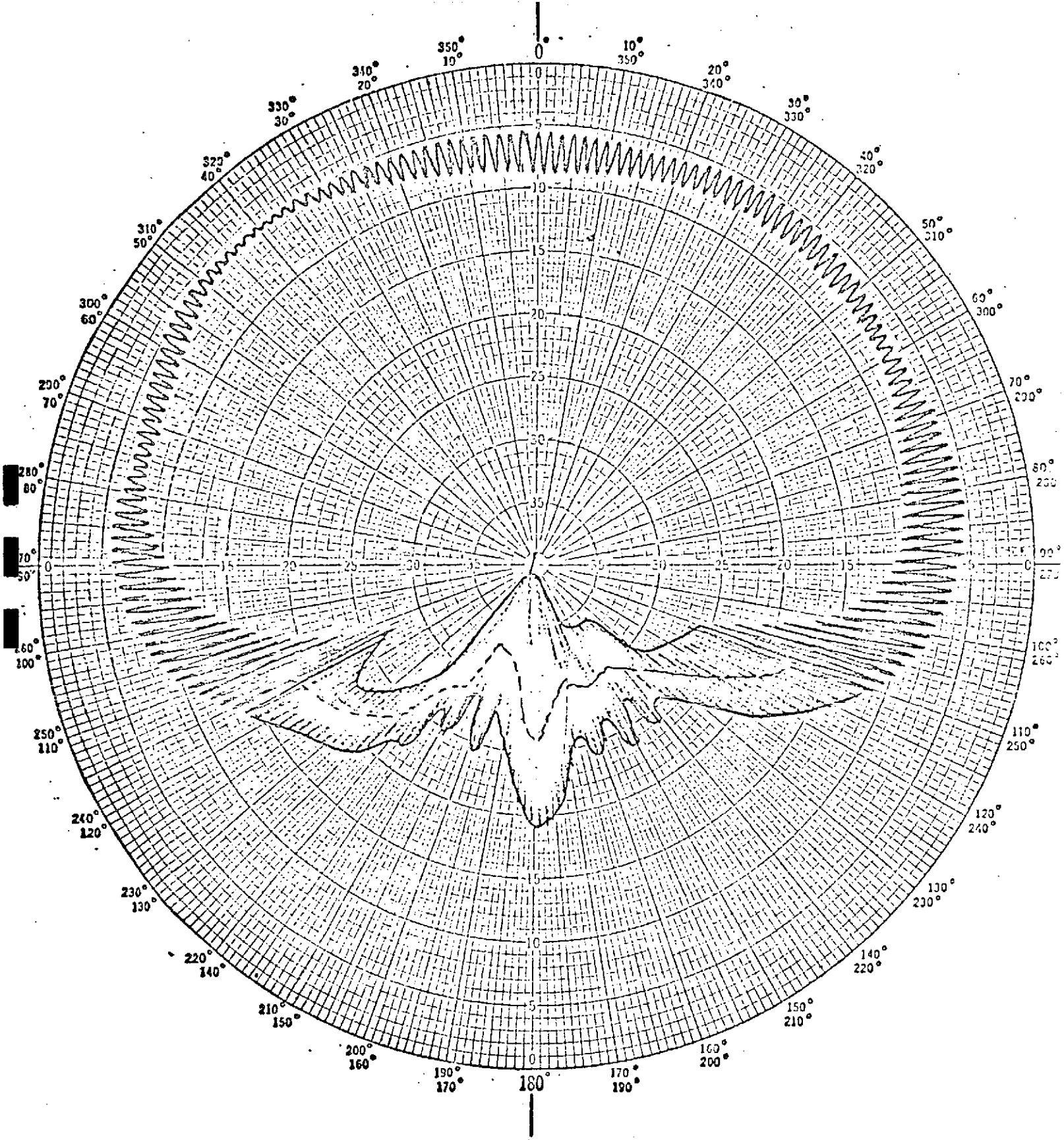


Note: 0 = +7 dB, 5 = +2 dB, etc. (data taken at 2.3 GHz)

FIGURE 3.5 ONE HALF OF IME OMNI PATTERN

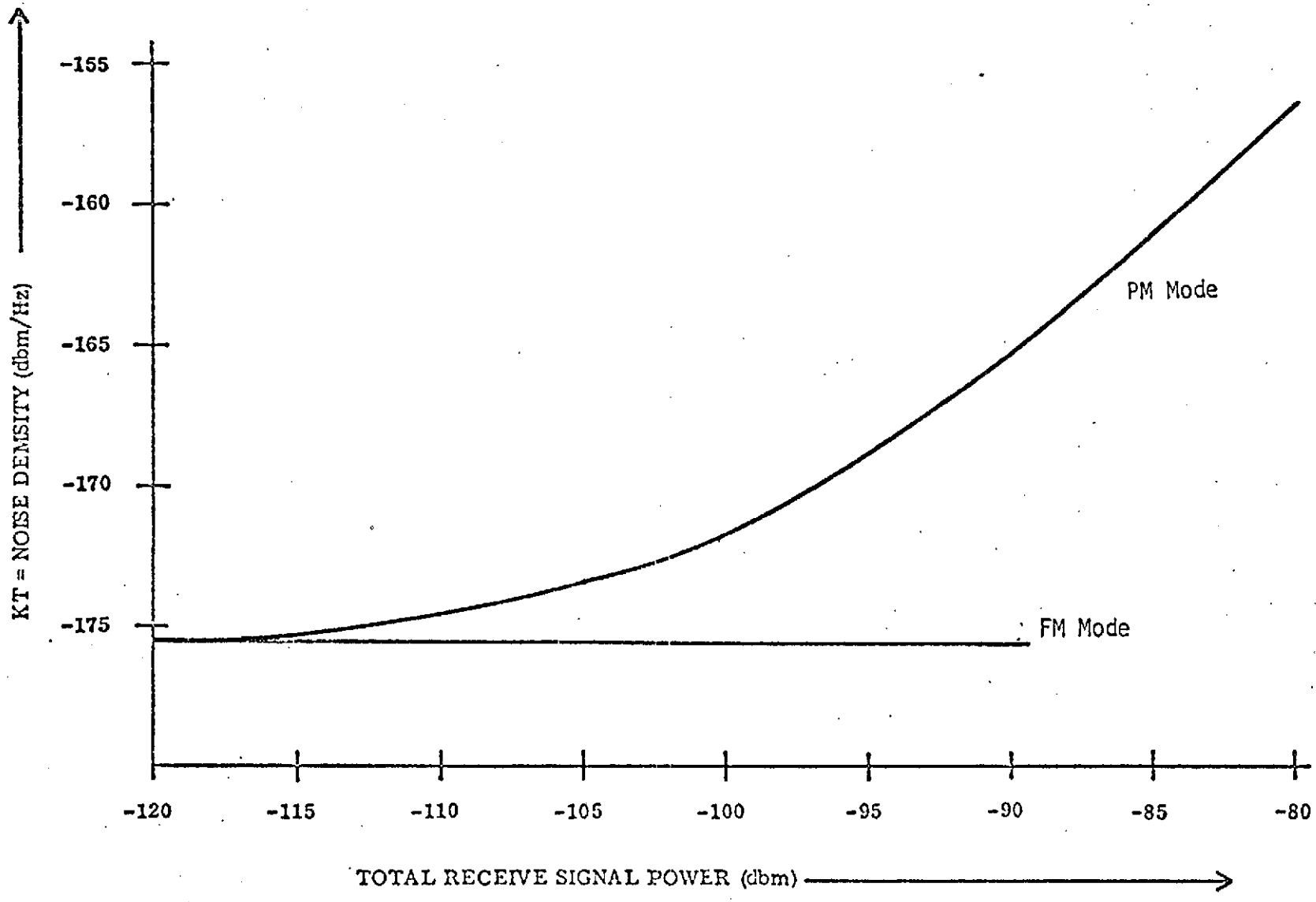


FIGURE 3.6 NOISE DENSITY VERSUS TOTAL RECEIVE SIGNAL POWER, USB RECEIVER PM MODE AND FM MODE

threshold value from -175.7 dBm/Hz as shown to -166.8 dBm/Hz (1500°K), which is applicable to the spacecraft transponder, and then using the received input level to read off the noise density. For example, the power level best case for IME-Heliocentric is -95.7 dBm (item 8). The curve gives -169.5 dBm/Hz. Since the difference in thresholds is 8.9 dB (+175.7 - 166.8), the appropriate noise density is -169.5 dBm/Hz + 8.9 dB = -160.6 dBm/Hz. This value is shown as the best case on IME-Heliocentric Item 10 for the rising density type of transponder. In the computer program a curve fit was done and the above rationale was used.

If the rising noise density were not present the density would be that given at threshold, i.e., -166.8 dBm/Hz, that is, 6.2 dB better! Table 3.1 gives the results for rising density and no rise type receivers. Since the present plans are to use a non rising density type of transponder on the IME missions the rest of the charts will assume this. The inclusion of the rising density type of transponder in the first chart was to show how degrading its use would be in the IME missions.

Item 11 is the sum of Item 8 and Item 9 minus Item 10 and is the uplink total signal-to-noise ratio with the noise normalized to a one hertz bandwidth, i.e., signal-to-noise density. Out of this total must come a certain amount for the ranging code and an amount for the command signal. This is implemented by subtracting off a modulation factor. The resultant is the power ratio after modulation has taken place.

At this point the first observation/tradeoff will be made. Consider Item 11 of the IME-Heliocentric mission for the no rise case. Its value is 55.2 dB-Hz. As stated above this is the amount of signal-

to-noise density available prior to modulation considerations. If all the power were put into the ranging sidebands 55.2 dB-Hz would apply. This, of course, cannot happen due to the need for carrier power to lock onto and command power to command the spacecraft, however, 55.2 dB-Hz would be the absolute upper limit of ranging ratio that could be used. The point is that if 55.2 dB-Hz is not enough to do the job, then there is no hope of doing it with any less power ratio.

Now for transponding purposes it is desirable to have as much $S/N_o$ as possible so that the uplink noise is negligible in the overall turnaround. This is usually the case due to high ground antenna gain and transmitter power. In the case of the item in question, however, this is not true.

The ranging spectrum (Figure 3.7) is such that at least twice the chip rate of the code must be passed, i.e., 2 x 1 MHz, thus in dB the passband is 63 dB-Hz. The predetection signal-to-noise ratio is then 55.2 dB-Hz - 63 dB-Hz, i.e., -7.8 dB. This large negative margin is due to the "worst case" use of the 30 foot dish together with the null in the spacecraft receive antenna (the rest of the factors are secondary).

Suppose an 85 foot dish were used. The improvement would be (52.5 dB - 43 dB), i.e., 9.5 dB. Table 3.2 shows what the result of the added gain would be. Realizing that some improvement is enjoyed in coherent detection, it appears that there is now a chance of obtaining a positive SNR prior to modulating the downlink carrier.

The conclusion is that for the IME-Heliocentric mission uplink the USB stations must be used with its 85 foot dish.

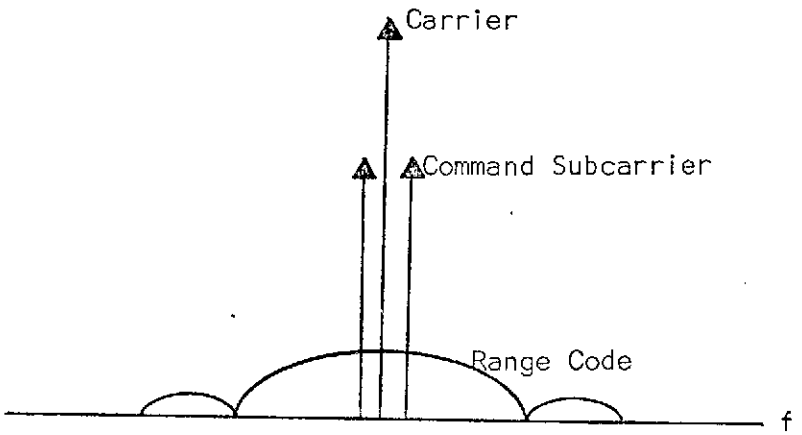


FIGURE 3.7 UPLINK POWER SPECTRUM

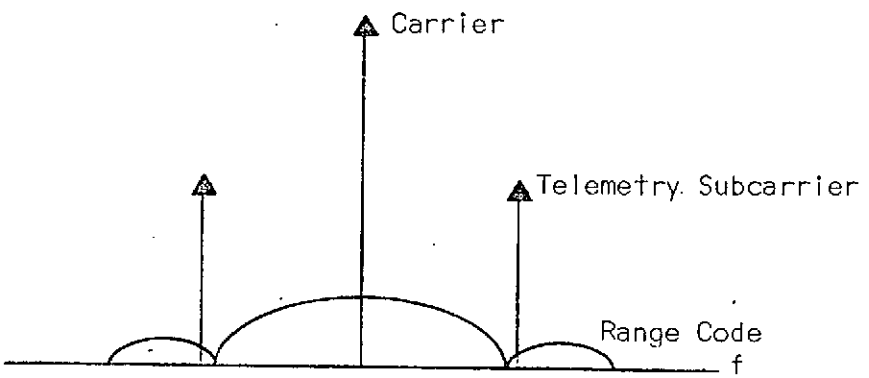


FIGURE 3.8A DOWNLINK POWER SPECTRUM (SUBCARRIER OPTION)

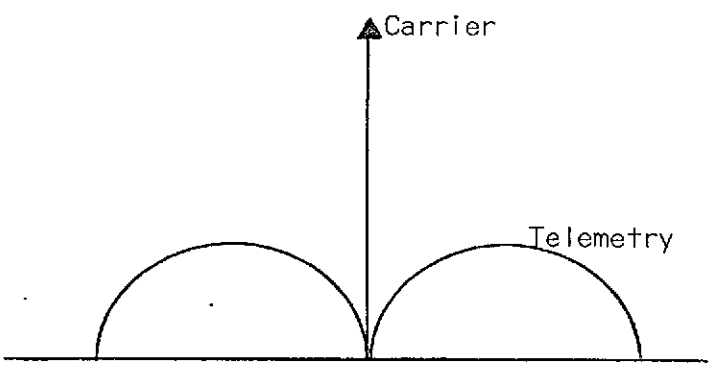


FIGURE 3.8B DOWNLINK POWER SPECTRUM (PRIME CARRIER OPTION)

At this point in the discussion Table 3.1 is superseded by Table 3.2, i.e., Table 3.1 is discarded in favor of Table 3.2. Items between now and the next tradeoff are those of Table 3.2.

The uplink signal is bandpass limited before demodulation, therefore, as is well known, either it is enhanced, unchanged, or degraded depending upon the prelimiter signal-to-noise ratio. Considering the limiter bandwidth to have a nominal value of 2 MHz (63 dB-Hz) the signal-to-noise densities of Item 11 give the limiter factors of Item 12. For example, the IME-Mother-Daughter best case $S/N_o$ corresponds to an SNR of 28 dB (91.1 dB-Hz - 63 dB-Hz) and thus gives a 3.0 dB enhancement. Table 3.3 lists the output SNR versus input SNR for the ideal bandpass limiter.[15]

As can be seen from Table 3.2, the spacecraft using an omni-direction antenna can be supported with the USB stations, and the downlink ranging becomes essentially noisefree in all cases except the IME-Heliocentric worst case where it is marginal at 1.6 dB.

Getting back now to the other cases, Item 13 reflects the modulation loss incurred on the uplink by using indices of 0.8 and 0.9 for ranging and command, respectively, per reference 16.

Item 14 is a result of coherent demodulation, which only looks at the in-phase noise and eliminates the quadrature noise, and the filtering involved.

Item 15 is the sum of items 11 through 14 minus the RF bandwidth of 63 dB-Hz.

| ITEM | ITEM DESCRIPTION | | IME-H. BEST CASE | IME-H. WORST CASE | IME-M.-D. BEST CASE | IME-M.-D. WORST CASE |
|---|---|---|---|---|---|---|
| 1. | Grd Xmtr Power (USB 20KW) | (dbm) | 73.0 | 73.0 | 73.0 | 73.0 |
| 2. | Xmtr to Antenna Xmssn Losses | (db) | -0.1 | -0.5 | -0.1 | -0.5 |
| 3. | Grd Xmtr Antenna Gain (85'-52.5db, 30'-43db) | (db) | 52.5 | 52.5† | 52.5 | 43.0 |
| 4. | Path Loss (H.-1.5x10*6KM, M.-D.-1.5x10*5Km, 2.1GHz) | (db) | -222.1 | -222.1 | -202.1 | -202.1 |
| 5. | Power at S/C Rcvr Antenna | (dbm) | -96.7 | -97.1† | -76.7 | -86.6 |
| 6. | S/C Rcvr Antenna Gain (Omni) | (dbJ | 2.0 | -3.0 | 2.0 | -3.0 |
| 7. | Antenna to Rcvr Xmssn Losses | (db) | -1.0 | -2.0 | -1.0 | -2.0 |
| 8. | Power at S/C Rcvr Input (S(u)) | (dbm) | -95.7 | -102.1† | -75.7 | -91.6 |
| 9. | Uplink Solar Noise Factor | (db) | 0.0 | 0.0 | 0.0 | 0.0 |
| 10. | S/C Rcvr Noise Density (N(ou)) | (dbm/Hz) | -166.8 | -166.8 | -166.8 | -166.8 |
| 11. | Uplink Total (S(u)/N(ou)) | (db-Hz) | 71.1 | 64.7† | 91.1 | 75.2 |
| 12. | Bandpass Limiter Gain/Loss Factor | (db) | 2.6 | 1.6 | 3.0 | 2.8 |
| 13. | Uplink Ranging Factor | (db) | -4.7 | -4.7 | -4.7 | -4.7 |
| 14. | Coherent Demodulation Factor (W(rf)/W(v)) | (db) | 3.0 | 3.0 | 3.0 | 3.0 |
| 15. | Premodulation Signal to Noise Ratio | (db) | 9.0 | 1.6 | 29.4 | 13.3 |
| 16. | Uplink Ranging Threshold | (db) | 0.0 | 0.0 | 0.0 | 0.0 |
| 17. | Uplink Ranging Margin | (db) | 9.0 | 1.6 | 29.4 | 13.3 |
| 18. | Ranging Low Pass Bandwidth | (db-Hz) | 60.0 | 60.0 | 60.0 | 60.0 |
| 19. | S/C Xmtr Power (into Xmssn Line) | (dbm) | | | | |
| 20. | Xmtr to Antenna Xmssn Losses | (db) | | | | |
| 21. | S/C Antenna Gain (Medium Gain Directional, Omni) | (db) | | | | |
| 22. | S/C Antenna Pointing Loss | (db) | | | | |
| 23. | Path Loss (See Item 4, 2.3GHz) | (db) | | | | |
| 24. | Power at Grd Rcvr Antenna | (dbm) | | | | |
| 25. | Grd Rcvr Antenna Gain (See Item 3) | (db) | | | | |
| 26. | Antenna to Rcvr Xmssn Losses | (db) | | | | |
| 27. | Power at Grd Rcvr Input (S(d)) | (dbm) | | | | |
| 28. | Downlink Solar Noise Factor | (db) | | | | |
| 29. | Grd Rcvr Noise Density (N(od)),(Maser, Cool P., Hot P.) | (dbm/Hz) | | | | |
| 30. | Downlink Total (S(d)/N(od)) | (db-Hz) | | | | |
| 31. | Downlink Ranging Factor | (db) | | | | |
| 32. | Downlink Carrier Factor | (db) | | | | |
| 33. | Downlink Telemetry Factor | (db) | | | | |
| 34. | Downlink Ranging (S(rd)/N(od)) | (db-Hz) | | | | |
| 35. | Downlink Carrier (S(cd)/Nod)) | (db-Hz) | | | | |
| 36. | Downlink Telemetry (S(td)/N(od)) | (db-Hz) | | | | |
| 37. | Downlink Effective Ranging (S(erd)/N(od)) | (db-Hz) | | | | |
| 38. | Grd Rcvr Ranging Threshold (Mark 1A) | (db-Hz) | | | | |
| 39. | Grd Rcvr Carrier Threshold | (db-Hz) | | | | |
| 40. | Grd Rcvr Telemetry Threshold (10*-5 BEP) | (db-Hz) | | | | |
| 41. | Ranging Margin | (db) | | | | |
| 42. | Carrier Margin | (db) | | | | |
| 43. | Telemetry Margin | (db) | | | | |
| 44. | Coding Gain | (db) | | | | |
| 45. | Telemetry Margin with Coding | (db) | | | | |

TABLE 3.2 IME LINK CALCULATION

| INPUT SNR (dB) | OUTPUT SNR (dB) |
|---|---|
| -20.0 | -21.00 |
| -19.0 | -19.98 |
| -18.0 | -18.97 |
| -17.0 | -17.95 |
| -16.0 | -16.92 |
| -15.0 | -15.89 |
| -14.0 | -14.85 |
| -13.0 | -13.80 |
| -12.0 | -12.74 |
| -11.0 | -11.67 |
| -10.0 | -10.59 |
| -9.0 | -9.48 |
| -8.0 | -8.36 |
| -7.0 | -7.22 |
| -6.0 | -6.06 |
| -5.0 | -4.88 |
| -4.0 | -3.69 |
| -3.0 | -2.48 |
| -2.0 | -1.25 |
| -1.0 | -0.02 |
| 0.0 | 1.20 |
| 1.0 | 2.43 |
| 2.0 | 3.64 |
| 3.0 | 4.84 |
| 4.0 | 6.02 |
| 5.0 | 7.18 |
| 6.0 | 8.32 |
| 7.0 | 9.44 |
| 8.0 | 10.54 |
| 9.0 | 11.63 |
| 10.0 | 12.70 |
| 11.0 | 13.76 |
| 12.0 | 14.81 |
| 13.0 | 15.85 |
| 14.0 | 16.88 |
| 15.0 | 17.91 |
| 16.0 | 18.93 |
| 17.0 | 19.94 |
| 18.0 | 20.96 |
| 19.0 | 21.97 |
| 20.0 | 22.98 |

TABLE 3.3 BANDPASS LIMITER ENHANCEMENT/DEGRADATION

Item 16 was chosen as a minimum SNR for the downlink ranging signal. A 10 dB SNR is desirable but 0 dB is considered minimum.

Item 17 is the margin available just prior to modulating the downlink carrier. Anything over 10 dB will result in an almost perfect, although time delayed, replica of the originally transmitted ranging code. As can be seen from this item all downlink ranging signals are essentially noisefree with the lone exception of the IME-Heliocentric worst case. In this case the modulating waveform is ranging plus noise. This will impact on the final ranging SNR and will be discussed later in Item 37.

A general comment would be that the worst case is not likely to occur in the Heliocentric mission since it is stabilized and as such will, on one of its channels, have the peak of the antenna pattern pointed toward the earth. In case of a malfunction, however, a tumbling spacecraft could encounter this condition.

### 3.1.2 DOWNLINK POWER BUDGET ANALYSIS

In this section the more relevant, in terms of the coding study, part of the IMP power budget will be detailed. The only reason for performing the uplink analysis was to obtain the "effective" ranging SNR. This will be discussed fully later in connection with Item 37.

Refer now to Tables 3.4, 3.5, and 3.6 which are merely Table 3.2 with the downlink factors added. In Table 3.4 the two transponders are diplexed into the medium gain antenna; as such the total power available is 3 dB lower than the maximum per channel. This is reflected in Item 19 on Table 3.4. In the other two tables there is no diplexer and full power is utilized.

Note that Cases A and B do not appear. This was done for design purposes, i.e., Cases A and B can be derived from Case C by adding 3 dB to the transmitter power. It was felt that the added 3 dB should be used for margin when the link was weak. With this in mind Case C was used for the optimization of the link parameters.

Item 20 is an estimate of the best (-1.5 dB) and the worst (-3 dB) transmission losses that can be expected from the transmitter to the antenna on the spacecraft.

Item 21 is the transmitting antenna gain. Cases C and D use the medium gain antenna (9 dB) while Cases E and F use the hemispheric antenna for a peak of 2 dB and a null of -3 dB.

Item 22 reflects the possible pointing loss for the antennas. When the hemispheric antenna is used there is no pointing loss (actually it is incorporated into the gain) while the medium gain can suffer 2 dB loss (chosen arbitrarily).

Item 23 is the path loss at the transmitting frequency of 2.3 GHz and is about 1 dB higher than the uplink.

Item 24 is the sum of items 19 through 23 and is the received signal power available at the ground antenna.

Item 25 is the ground antenna gain for the 85 foot dish (52.5 dB) or the 30 foot dish (43 dB).

Item 26 is an estimate of the transmission losses.

Item 27 is the received signal power, i.e., the sum of Items 24, 25, and 26.

Item 28 is the downlink solar noise factor. This factor is a result of the ground receiving antenna looking towards the sun. Per information received by the author from Goddard personnel the minimum halo orbit radius of the Heliocentric mission will range from 40,000 km to 60,000 km. This converts to angle offsets from the earth-sun line of 1.5° to 2.3°. Preliminary data taken by Goddard shows that the increase in system noise density will be -11.2 dB for the 40,000 km radius and -9.8 dB for the 60,000 km radius as compared with the quiet sky readings.

Since a smaller radius conserves fuel it was assumed as a first iteration and is reflected in Item 28 of Tables 3.4, 3.5, and 3.6. The solar noise factors away from the sun are assumed to be negligible.

Item 29 is the system noise density of the following choices of ground receiver front ends:[17] maser (70°K), cooled parametric amplifier (96°K), or uncooled parametric amplifier (170°K). The maser is only available with the 85' receiving antennas, whereas the cooled and uncooled paramp are available with the 30' dishes. The noise densities of Item 29 are for a quiet sky.

By the IME mission time frame all sites will have multifunctional receivers, but even if USB types were used the received signal power is so low that the rising noise density is not applicable, i.e., the receiver is at threshold. The noise densities are then "KT", where "K" is Boltzman's constant (-198.6°dBm/ K-Hz). It should be mentioned here that the above noise temperatures for the maser, etc., include antenna temperature.

| ITEM | ITEM DESCRIPTION | | IME-H. BEST CASE | | | IME-H. WORST CASE | | | IME-M.-D. BEST CASE | | | IME-M.-D. WORST CASE | | |
|---|---|---|---|---|---|---|---|---|---|---|---|---|---|---|
| 1. | Grd Xmtr Power (USB 20KW) | (dbm) | 73.0 | | | 73.0 | | | 73.0 | | | 73.0 | | |
| 2. | Xmtr to Antenna Xmssn Losses | (db) | -0.1 | | | -0.5 | | | -0.1 | | | -0.5 | | |
| 3. | Grd Xmtr Antenna Gain (85'-52.5db, 30'-43db) | (db) | 52.5 | | | 52.5 | | | 52.5 | | | 43.0 | | |
| 4. | Path Loss (H.-1.5x10*6KM, M.-D.-1.5x10*5Km, 2.1GHz) | (db) | -222.1 | | | -222.1 | | | -202.1 | | | -202.1 | | |
| 5. | Power at S/C Rcvr Antenna | (dbm) | -96.7 | | | -97.1 | | | -76.7 | | | -86.6 | | |
| 6. | S/C Rcvr Antenna Gain (Omni) | (db) | 2.0 | | | -3.0 | | | 2.0 | | | -3.0 | | |
| 7. | Antenna to Rcvr Xmssn Losses | (db) | -1.0 | | | -2.0 | | | -1.0 | | | -2.0 | | |
| 8. | Power at S/C Rcvr Input (S(u)) | (dbm) | -95.7 | | | -102.1 | | | -75.7 | | | -91.6 | | |
| 9. | Uplink Solar Noise Factor | (db) | 0.0 | | | 0.0 | | | 0.0 | | | 0.0 | | |
| 10. | S/C Rcvr Noise Density (N(ou)) | (dbm/Hz) | -166.8 | | | -166.8 | | | -166.8 | | | -166.8 | | |
| 11. | Uplink Total (S(u)/N(ou)) | (db-Hz) | 71.1 | | | 64.7 | | | 91.1 | | | 75.2 | | |
| 12. | Bandpass Limiter Gain/Loss Factor | (db) | 2.6 | | | 1.6 | | | 3.0 | | | 2.8 | | |
| 13. | Uplink Ranging Factor | (db) | -4.7 | | | -4.7 | | | -4.7 | | | -4.7 | | |
| 14. | Coherent Demodulation Factor (W(rf)/W(v)) | (db) | 3.0 | | | 3.0 | | | 3.0 | | | 3.0 | | |
| 15. | Premodulation Signal to Noise Ratio | (db) | 9.0 | | | 1.6 | | | 29.4 | | | 13.3 | | |
| 16. | Uplink Ranging Threshold | (db) | 0.0 | | | 0.0 | | | 0.0 | | | 0.0 | | |
| 17. | Uplink Ranging Margin | (db) | 9.0 | | | 1.6 | | | 29.4 | | | 13.3 | | |
| 18. | Ranging Low Pass Bandwidth | (db-Hz) | 60.0 | | | 60.0 | | | 60.0 | | | 60.0 | | |
| 19. | S/C Xmtr Power (into Xmssn Line) | (dbm) | 31.0 | | | 31.0 | | | 27.0 | | | 27.0 | | |
| 20. | Xmtr to Antenna Xmssn Losses | (db) | -1.5 | | | -3.0 | | | -1.5 | | | -3.0 | | |
| 21. | S/C Antenna Gain (Medium Gain Directional, Omni) | (db) | 9.0 | | | 9.0 | | | 9.0 | | | 9.0 | | |
| 22. | S/C Antenna Pointing Loss | (db) | 0.0 | | | -2.0 | | | 0.0 | | | -2.0 | | |
| 23. | Path Loss (See Item 4, 2.3GHz) | (db) | -223.1 | | | -223.1 | | | -204.9 | | | -204.9 | | |
| 24. | Power at Grd Rcvr Antenna | (dbm) | -184.6 | | | -188.1 | | | -170.4 | | | -173.9 | | |
| 25. | Grd Rcvr Antenna Gain (See Item 3) | (db) | 52.5 | | | 43.0 | | | 52.5 | | | 43.0 | | |
| 26. | Antenna to Rcvr Xmssn Losses | (db) | -0.2 | | | -0.5 | | | -0.2 | | | -0.5 | | |
| 27. | Power at Grd Rcvr Input (S(d)) | (dbm) | -132.5 | | | -145.6 | | | -118.1 | | | -131.4 | | |
| 28. | Downlink Solar Noise Factor | (db) | 0.0 | | | -11.2 | | | 0.0 | | | 0.0 | | |
| 29. | Grd Rcvr Noise Density (N(od)),(Maser, Cool P., Hot P.) | (dbm/Hz) | -180.1 | -178.8 | -176.3 | -180.1 | -178.8 | -176.3 | -180.1 | -178.8 | -176.3 | -180.1 | -178.8 | -176.3 |
| 30. | Downlink Total (S(d)/N(od)) | (db-Hz) | 47.8 | 46.5 | 44.0 | 23.3 | 22.0 | 19.5 | 62.0 | 60.7 | 58.2 | 48.7 | 47.4 | 44.9 |
| 31. | Downlink Ranging Factor | (db) | | | | | | | | | | | | |
| 32. | Downlink Carrier Factor | (db) | | | | | | | | | | | | |
| 33. | Downlink Telemetry Factor | (db) | | | | | | | | | | | | |
| 34. | Downlink Ranging (S(rd)/N(od)) | (db-Hz) | | | | | | | | | | | | |
| 35. | Downlink Carrier (S(cd)/Nod)) | (db-Hz) | | | | | | | | | | | | |
| 36. | Downlink Telemetry (S(td)/N(od)) | (db-Hz) | | | | | | | | | | | | |
| 37. | Downlink Effective Ranging (S(erd)/N(od)) | (db-Hz) | | | | | | | | | | | | |
| 38. | Grd Rcvr Ranging Threshold (Mark 1A) | (db-Hz) | 23.0 | 23.0 | 23.0 | 23.0 | 23.0 | 23.0 | 23.0 | 23.0 | 23.0 | 23.0 | 23.0 | 23.0 |
| 39. | Grd Rcvr Carrier Threshold | (db-Hz) | 30.0 | 30.0 | 30.0 | 30.0 | 30.0 | 30.0 | 30.0 | 30.0 | 30.0 | 30.0 | 30.0 | 30.0 |
| 40. | Grd Rcvr Telemetry Threshold (10*-5 BEP) | (db-Hz) | 44.7 | 44.7 | 44.7 | 44.7 | 44.7 | 44.7 | 53.8 | 53.8 | 53.8 | 53.8 | 53.8 | 53.8 |
| 41. | Ranging Margin | (db) | | | | | | | | | | | | |
| 42. | Carrier Margin | (db) | | | | | | | | | | | | |
| 43. | Telemetry Margin | (db) | | | | | | | | | | | | |
| 44. | Coding Gain | (db) | | | | | | | | | | | | |
| 45. | Telemetry Margin with Coding | (db) | | | | | | | | | | | | |

TABLE 3.4 IME LINK CALCULATION (CASE C)

| ITEM | ITEM DESCRIPTION | | IME-H. BEST CASE | | | IME-H. WORST CASE | | | IME-M.-D. BEST CASE | | | IME-M.-D. WORST CASE | | |
|---|---|---|---|---|---|---|---|---|---|---|---|---|---|---|
| 1. | Grd Xmtr Power (USB 20KW) | (dbm) | 73.0 | | | 73.0 | | | 73.0 | | | 73.0 | | |
| 2. | Xmtr to Antenna Xmssn Losses | (db) | -0.1 | | | -0.5 | | | -0.1 | | | -0.5 | | |
| 3. | Grd Xmtr Antenna Gain (85'-52.5db, 30'-43db) | (db) | 52.5 | | | 52.5 | | | 52.5 | | | 43.0 | | |
| 4. | Path Loss (H.-1.5x10*6KM, M.-D.-1.5x10*5Km, 2.1GHz) | (db) | -222.1 | | | -222.1 | | | -202.1 | | | -202.1 | | |
| 5. | Power at S/C Rcvr Antenna | (dbm) | -96.7 | | | -97.1 | | | -76.7 | | | -86.6 | | |
| 6. | S/C Rcvr Antenna Gain (Omni) | (db) | 2.0 | | | -3.0 | | | 2.0 | | | -3.0 | | |
| 7. | Antenna to Rcvr Xmssn Losses | (db) | -1.0 | | | -2.0 | | | -1.0 | | | -2.0 | | |
| 8. | Power at S/C Rcvr Input (S(u)) | (dbm) | -95.7 | | | -102.1 | | | -75.7 | | | -91.6 | | |
| 9. | Uplink Solar Noise Factor | (db) | 0.0 | | | 0.0 | | | 0.0 | | | 0.0 | | |
| 10. | S/C Rcvr Noise Density (N(ou)) | (dbm/Hz) | -166.8 | | | -166.8 | | | -166.8 | | | -166.8 | | |
| 11. | Uplink Total (S(u)/N(ou)) | (db-Hz) | 71.1 | | | 64.7 | | | 91.1 | | | 75.2 | | |
| 12. | Bandpass Limiter Gain/Loss Factor | (db) | 2.6 | | | 1.6 | | | 3.0 | | | 2.8 | | |
| 13. | Uplink Ranging Factor | (db) | -4.7 | | | -4.7 | | | -4.7 | | | -4.7 | | |
| 14. | Coherent Demodulation Factor (W(rf)/W(v)) | (db) | 3.0 | | | 3.0 | | | 3.0 | | | 3.0 | | |
| 15. | Premodulation Signal to Noise Ratio | (db) | 9.0 | | | 1.6 | | | 29.4 | | | 13.3 | | |
| 16. | Uplink Ranging Threshold | (db) | 0.0 | | | 0.0 | | | 0.0 | | | 0.0 | | |
| 17. | Uplink Ranging Margin | (db) | 9.0 | | | 1.6 | | | 29.4 | | | 13.3 | | |
| 18. | Ranging Low Pass Bandwidth | (db-Hz) | 60.0 | | | 60.0 | | | 60.0 | | | 60.0 | | |
| 19. | S/C Xmtr Power (into Xmssn Line) | (dbm) | 34.0 | | | 34.0 | | | 30.0 | | | 30.0 | | |
| 20. | Xmtr to Antenna Xmssn Losses | (db) | -1.5 | | | -3.0 | | | -1.5 | | | -3.0 | | |
| 21. | S/C Antenna Gain (Medium Gain Directional, Omni) | (db) | 9.0 | | | 9.0 | | | 9.0 | | | 9.0 | | |
| 22. | S/C Antenna Pointing Loss | (db) | 0.0 | | | -2.0 | | | 0.0 | | | -2.0 | | |
| 23. | Path Loss (See Item 4, 2.3GHz) | (db) | -223.1 | | | -223.1 | | | -204.9 | | | -204.9 | | |
| 24. | Power at Grd Rcvr Antenna | (dbm) | -181.6 | | | -185.1 | | | -167.4 | | | -170.9 | | |
| 25. | Grd Rcvr Antenna Gain (See Item 3) | (db) | 52.5 | | | 43.0 | | | 52.5 | | | 43.0 | | |
| 26. | Antenna to Rcvr Xmssn Losses | (db) | -0.2 | | | -0.5 | | | -0.2 | | | -0.5 | | |
| 27. | Power at Grd Rcvr Input (S(d)) | (dbm) | -129.3 | | | -142.6 | | | -115.1 | | | -128.4 | | |
| 28. | Downlink Solar Noise Factor | (db) | 0.0 | | | -11.2 | | | 0.0 | | | 0.0 | | |
| 29. | Grd Rcvr Noise Density (N(od)),(Masar, Cool P., Hot P.) | (dbm/Hz) | -180.1 | -178.8 | -176.3 | -180.1 | -178.8 | -176.3 | -180.1 | -178.8 | -176.3 | -180.1 | -178.8 | -176.3 |
| 30. | Downlink Total (S(d)/N(od)) | (db-Hz) | 50.8 | 49.5 | 47.0 | 26.3 | 25.0 | 22.5 | 65.0 | 63.7 | 61.2 | 51.7 | 50.4 | 47.9 |
| 31. | Downlink Ranging Factor | (db) | | | | | | | | | | | | |
| 32. | Downlink Carrier Factor | (db) | | | | | | | | | | | | |
| 33. | Downlink Telemetry Factor | (db) | | | | | | | | | | | | |
| 34. | Downlink Ranging (S(rd)/N(od)) | (db-Hz) | | | | | | | | | | | | |
| 35. | Downlink Carrier (S(cd)/Nod)) | (db-Hz) | | | | | | | | | | | | |
| 36. | Downlink Telemetry (S(td)/N(od)) | (db-Hz) | | | | | | | | | | | | |
| 37. | Downlink Effective Ranging (S(erd)/N(od)) | (db-Hz) | | | | | | | | | | | | |
| 38. | Grd Rcvr Ranging Threshold (Mark 1A) | (db-Hz) | 23.0 | 23.0 | 23.0 | 23.0 | 23.0 | 23.0 | 23.0 | 23.0 | 23.0 | 23.0 | 23.0 | 23.0 |
| 39. | Grd Rcvr Carrier Threshold | (db-Hz) | 30.0 | 30.0 | 30.0 | 30.0 | 30.0 | 30.0 | 30.0 | 30.0 | 30.0 | 30.0 | 30.0 | 30.0 |
| 40. | Grd Rcvr Telemetry Threshold (10*-5 BEP) | (db-Hz) | 44.7 | 44.7 | 44.7 | 44.7 | 44.7 | 44.7 | 53.8 | 53.8 | 53.8 | 53.8 | 53.8 | 53.8 |
| 41. | Ranging Margin | (db) | | | | | | | | | | | | |
| 42. | Carrier Margin | (db) | | | | | | | | | | | | |
| 43. | Telemetry Margin | (db) | | | | | | | | | | | | |
| 44. | Coding Gain | (db) | | | | | | | | | | | | |
| 45. | Telemetry Margin with Coding | (db) | | | | | | | | | | | | |

TABLE 3.5 IME LINK CALCULATION (CASE D)

| ITEM | ITEM DESCRIPTION | | IME-H. BEST CASE | | | IME-H. WORST CASE | | | IME-M.-D. BEST CASE | | | IME-M.-D. WORST CASE | | |
|---|---|---|---|---|---|---|---|---|---|---|---|---|---|---|
| 1. | Grd Xmtr Power (USB 20KW) | (dbm) | 73.0 | | | 73.0 | | | 73.0 | | | 73.0 | | |
| 2. | Xmtr to Antenna Xmssn Losses | (db) | -0.1 | | | -0.5 | | | -0.1 | | | -0.5 | | |
| 3. | Grd Xmtr Antenna Gain (85'-52.5db, 30'-43db) | (db) | 52.5 | | | 52.5 | | | 52.5 | | | 43.0 | | |
| 4. | Path Loss (H.-1.5x10*6KM, M.-D.-1.5x10*5Km, 2.1GHz) | (db) | -222.1 | | | -222.1 | | | -202.1 | | | -202.1 | | |
| 5. | Power at S/C Rcvr Antenna | (dbm) | -96.7 | | | -97.1 | | | -76.7 | | | -86.6 | | |
| 6. | S/C Rcvr Antenna Gain (Omni) | (db) | 2.0 | | | -3.0 | | | 2.0 | | | -3.0 | | |
| 7. | Antenna to Rcvr Xmssn Losses | (db) | -1.0 | | | -2.0 | | | -1.0 | | | -2.0 | | |
| 8. | Power at S/C Rcvr Input (S(u)) | (dbm) | -95.7 | | | -102.1 | | | -75.7 | | | -91.6 | | |
| 9. | Uplink Solar Noise Factor | (db) | 0.0 | | | 0.0 | | | 0.0 | | | 0.0 | | |
| 10. | S/C Rcvr Noise Density (N(ou)) | (dbm/Hz) | -166.8 | | | -166.8 | | | -166.8 | | | -166.8 | | |
| 11. | Uplink Total (S(u)/N(ou)) | (db-Hz) | 71.1 | | | 64.7 | | | 91.1 | | | 75.2 | | |
| 12. | Bandpass Limiter Gain/Loss Factor | (db) | 2.6 | | | 1.6 | | | 3.0 | | | 2.8 | | |
| 13. | Uplink Ranging Factor | (db) | -4.7 | | | -4.7 | | | -4.7 | | | -4.7 | | |
| 14. | Coherent Demodulation Factor (W(rf)/W(v)) | (db) | 3.0 | | | 3.0 | | | 3.0 | | | 3.0 | | |
| 15. | Premodulation Signal to Noise Ratio | (db) | 9.0 | | | 1.6 | | | 29.4 | | | 13.3 | | |
| 16. | Uplink Ranging Threshold | (db) | 0.0 | | | 0.0 | | | 0.0 | | | 0.0 | | |
| 17. | Uplink Ranging Margin | (db) | 9.0 | | | 1.6 | | | 29.4 | | | 13.3 | | |
| 18. | Ranging Low Pass Bandwidth | (db-Hz) | 60.0 | | | 60.0 | | | 60.0 | | | 60.0 | | |
| 19. | S/C Xmtr Power (into Xmssn Line) | (dbm) | 34.0 | | | 34.0 | | | 30.0 | | | 30.0 | | |
| 20. | Xmtr to Antenna Xmssn Losses | (db) | -1.5 | | | -3.0 | | | -1.5 | | | -3.0 | | |
| 21. | S/C Antenna Gain (Medium Gain Directional, Omni) | (db) | 2.0 | | | -3.0 | | | 2.0 | | | -3.0 | | |
| 22. | S/C Antenna Pointing Loss | (db) | 0.0 | | | 0.0 | | | 0.0 | | | 0.0 | | |
| 23. | Path Loss (See Item 4, 2.3GHz) | (db) | -223.1 | | | -223.1 | | | -204.9 | | | -204.9 | | |
| 24. | Power at Grd Rcvr Antenna | (dbm) | -188.6 | | | -195.1 | | | -174.4 | | | -180.9 | | |
| 25. | Grd Rcvr Antenna Gain (See Item 3) | (db) | 52.5 | | | 43.0 | | | 52.5 | | | 43.0 | | |
| 26. | Antenna to Rcvr Xmssn Losses | (db) | -0.2 | | | -0.5 | | | -0.2 | | | -0.5 | | |
| 27. | Power at Grd Rcvr Input (S(d)) | (dbm) | -136.3 | | | -152.6 | | | -122.1 | | | -138.4 | | |
| 28. | Downlink Solar Noise Factor | (db) | 0.0 | | | -11.2 | | | 0.0 | | | 0.0 | | |
| 29. | Grd Rcvr Noise Density (N(od)),(Maser, Cool P., Hot P.) | (dbm/Hz) | -180.1 | -178.8 | -176.3 | -180.1 | -178.8 | -176.3 | -180.1 | -178.8 | -176.3 | -180.1 | -178.8 | -176.3 |
| 30. | Downlink Total (S(d)/N(od)) | (db-Hz) | 43.8 | 42.5 | 40.0 | 16.3 | 15.0 | 12.5 | 58.0 | 56.7 | 54.2 | 41.7 | 40.4 | 37.9 |
| 31. | Downlink Ranging Factor | (db) | | | | | | | | | | | | |
| 32. | Downlink Carrier Factor | (db) | | | | | | | | | | | | |
| 33. | Downlink Telemetry Factor | (db) | | | | | | | | | | | | |
| 34. | Downlink Ranging (S(rd)/N(od)) | (db-Hz) | | | | | | | | | | | | |
| 35. | Downlink Carrier (S(cd)/Nod)) | (db-Hz) | | | | | | | | | | | | |
| 36. | Downlink Telemetry (S(td)/N(od)) | (db-Hz) | | | | | | | | | | | | |
| 37. | Downlink Effective Ranging (S(erd)/N(od)) | (db-Hz) | | | | | | | | | | | | |
| 38. | Grd Rcvr Ranging Threshold (Mark 1A) | (db-Hz) | 23.0 | 23.0 | 23.0 | 23.0 | 23.0 | 23.0 | 23.0 | 23.0 | 23.0 | 23.0 | 23.0 | 23.0 |
| 39. | Grd Rcvr Carrier Threshold | (db-Hz) | 30.0 | 30.0 | 30.0 | 30.0 | 30.0 | 30.0 | 30.0 | 30.0 | 30.0 | 30.0 | 30.0 | 30.0 |
| 40. | Grd Rcvr Telemetry Threshold (10*-5 BEP) | (db-Hz) | 44.7 | 44.7 | 44.7 | 44.7 | 44.7 | 44.7 | 53.8 | 53.8 | 53.8 | 53.8 | 53.8 | 53.8 |
| 41. | Ranging Margin | (db) | | | | | | | | | | | | |
| 42. | Carrier Margin | (db) | | | | | | | | | | | | |
| 43. | Telemetry Margin | (db) | | | | | | | | | | | | |
| 44. | Coding Gain | (db) | | | | | | | | | | | | |
| 45. | Telemetry Margin with Coding | (db) | | | | | | | | | | | | |

TABLE 3.6 IME LINK CALCULATION (CASE E OR F)

Item 30 is the total (modulation sidebands and all) signal power minus the noise densities of Item 29. The values shown are very important due to the following discussion.

The purpose of this study is to find the telemetry coding impact on the IME missions. In doing so the required coding gain must be determined, and so the "optimum" choice of power distribution must be obtained. By optimum it is meant: that choice of modulation indices which simultaneously yields the most margin in the cases of ranging, carrier lock, and telemetry. In this regard a computer program was written which solved for the power drop from the total signal power versus the ranging modulation index with the telemetry index as a parameter. The output from the program is listed in Appendix C.

Since the decoder will be used for both missions, the worst case of both was used to choose the indices.

Prior to choosing the indices the ranging, telemetry, and carrier thresholds must be found. These are shown in Items 38 through 40. The ranging threshold (23 dB) was determined by assuming a Mark IA ranging system.[18] Referring to Figure 3.9, the value of 23 dB was chosen because it was the threshold for the 12 Hz bandwidth clock loop. It should be noted that for the manned missions a value of 43 dB-Hz is used, but this was felt to be far too stringent for the present case.

The carrier loop threshold was chosen to be 30.0 dB-Hz to provide 12 dB in a noise bandwidth of 60 Hz.

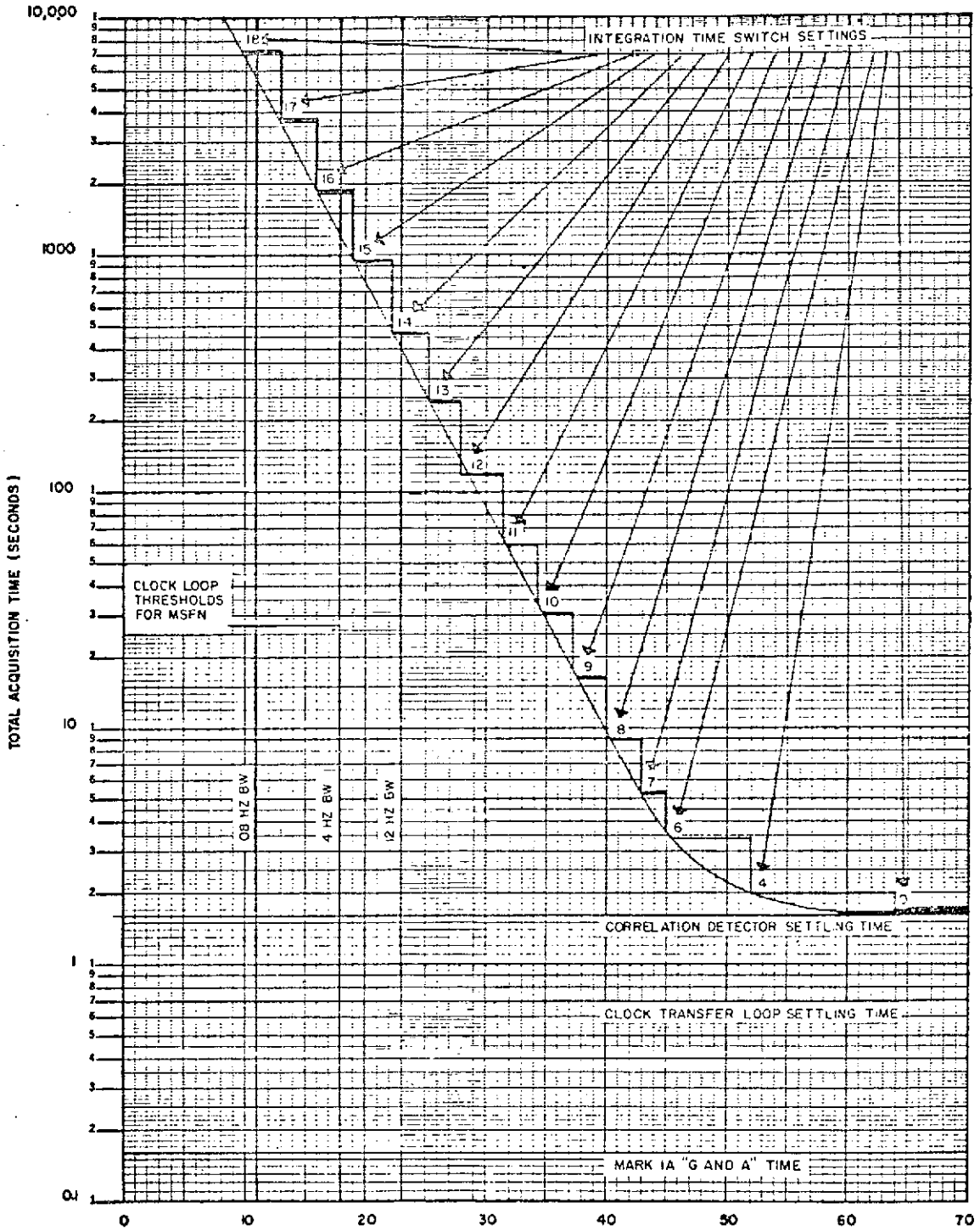


FIGURE 3.9 MARK 1A RANGING SUBSYSTEM ACQUISITION TIME

The maximum telemetry thresholds were chosen to be 35.7 dB-Hz for the 256 bps case, 44.7 dB-Hz for the 2048 bps case, and 53.8 dB-Hz for the 16 kbps case. These were derived by taking the ideal PSK ($E_b/N_o$) threshold of 9.6 dB for $10^{-5}$ bit error probability, adding 2 dB for practical systems and then using the appropriate bit rates given above, e.g., 9.6 dB + 2 dB + 10 log 2048.

Now, having found the needed thresholds and knowing the total signal-to-noise density available, together with a nominal range for the coding gain achievable (3-5 dB), the tables in Appendix C were used to pick the modulation indices.

Looking at the downlink total signal-to-noise densities for Case C (Item 30 of Table 3.4), the lowest is 19.5 dB-Hz. There is no way that this can work due to the carrier requirement of 30 dB-Hz, therefore go to an 85' dish. Going to the 85' dish forces the use of the maser front end hence the 19.5 is replaced by 23.3 plus the added antenna gain of 9.5 for a total of 32.8 dB-Hz.

There is now a chance of supporting the mission, however, no modulation loss has been accounted for. The only other factor to be traded off is to increase the halo radius on the Heliocentric mission which gives a solar noise factor of -9.8 dB instead of -11.2 dB, a pickup of 1.4 dB. The total $S/N_o$ is now 32.8 + 1.4 = 34.2 dB-Hz.

The above allowed the locking of the carrier, but looking at the telemetry threshold, too much coding gain is needed. The conclusion is to go to the lowest bit rate for this mission (44.7 dB-Hz goes to 35.7 dB-Hz).

| ITEM | ITEM DESCRIPTION | | IME-H. BEST CASE | | | IME-H. WORST CASE | | | IME-M.-D. BEST CASE | | | IME-M.-D. WORST CASE | | |
|---|---|---|---|---|---|---|---|---|---|---|---|---|---|---|
| 1. | Grd Xmtr Power (USB 20KW) | (dbm) | 73.0 | | | 73.0 | | | 73.0 | | | 73.0 | | |
| 2. | Xmtr to Antenna Xmssn Losses | (db) | -0.1 | | | -0.5 | | | -0.1 | | | -0.5 | | |
| 3. | Grd Xmtr Antenna Gain (85'-52.5db, 30'-43db) | (db) | 52.5 | | | 52.5 | | | 52.5 | | | 43.0 | | |
| 4. | Path Loss (H.-1.3x10*6Km, M.-D.-1.5x10*5Km, 2.1GHz) | (db) | -222.1 | | | -222.1 | | | -202.1 | | | -202.1 | | |
| 5. | Power at S/C Rcvr Antenna | (dbm) | -96.7 | | | -97.1 | | | -76.7 | | | -86.6 | | |
| 6. | S/C Rcvr Antenna Gain (Omni) | (db) | 2.0 | | | -3.0 | | | 2.0 | | | -3.0 | | |
| 7. | Antenna to Rcvr Xmssn Losses | (db) | -1.0 | | | -2.0 | | | -1.0 | | | -2.0 | | |
| 8. | Power at S/C Rcvr Input (S(u)) | (dbm) | -95.7 | | | -102.1 | | | -75.7 | | | -91.6 | | |
| 9. | Uplink Solar Noise Factor | (db) | 0.0 | | | 0.0 | | | 0.0 | | | 0.0 | | |
| 10. | S/C Rcvr Noise Density (N(ou)) | (dbm/Hz) | -166.8 | | | -166.8 | | | -166.8 | | | -166.8 | | |
| 11. | Uplink Total (S(u)/N(ou)) | (db-Hz) | 71.1 | | | 64.7 | | | 91.1 | | | 75.2 | | |
| 12. | Bandpass Limiter Gain/Loss Factor | (db) | 2.6 | | | 1.6 | | | 3.0 | | | 2.8 | | |
| 13. | Uplink Ranging Factor | (db) | -4.7 | | | -4.7 | | | -4.7 | | | -4.7 | | |
| 14. | Coherent Demodulation Factor (W(rf)/W(v)) | (db) | 3.0 | | | 3.0 | | | 3.0 | | | 3.0 | | |
| 15. | Premodulation Signal to Noise Ratio | (db) | 9.0 | | | 1.6 | | | 29.4 | | | 13.3 | | |
| 16. | Uplink Ranging Threshold | (db) | 0.0 | | | 0.0 | | | 0.0 | | | 0.0 | | |
| 17. | Uplink Ranging Margin | (db) | 9.0 | | | 1.6 | | | 29.4 | | | 13.3 | | |
| 18. | Ranging Low Pass Bandwidth | (db-Hz) | 60.0 | | | 60.0 | | | 60.0 | | | 60.0 | | |
| 19. | S/C Xmtr Power (into Xmssn Line) | (dbm) | 31.0 | | | 31.0 | | | 27.0 | | | 27.0 | | |
| 20. | Xmtr to Antenna Xmssn Losses | (db) | -1.5 | | | -3.0 | | | -1.5 | | | -3.0 | | |
| 21. | S/C Antenna Gain (Medium Gain Directional, Omni) | (db) | 9.0 | | | 9.0 | | | 9.0 | | | 9.0 | | |
| 22. | S/C Antenna Pointing Loss | (db) | 0.0 | | | -2.0 | | | 0.0 | | | -2.0 | | |
| 23. | Path Loss (See Item 4, 2.3GHz) | (db) | -223.1 | | | -223.1 | | | -204.9 | | | -204.9 | | |
| 24. | Power at Grd Rcvr Antenna | (dbm) | -184.6 | | | -188.1 | | | -170.4 | | | -173.9 | | |
| 25. | Grd Rcvr Antenna Gain (See Item 3) | (db) | 52.5 | | | 52.5† | | | 52.5 | | | 52.5† | | |
| 26. | Antenna to Rcvr Xmssn Losses | (db) | -0.2 | | | -0.5 | | | -0.2 | | | -0.5 | | |
| 27. | Power at Grd Rcvr Input (S(d)) | (dbm) | -132.3 | | | -136.1† | | | -118.1 | | | -121.9† | | |
| 28. | Downlink Solar Noise Factor | (db) | 0.0 | | | -9.8† | | | 0.0 | | | 0.0 | | |
| 29. | Grd Rcvr Noise Density (N(od)),(Maser, Cool P., Hot P.) | (dbm/Hz) | -180.1 | -178.8 | -176.3 | -180.1 | -178.8 | -176.3 | -180.1 | -178.8 | -176.3 | -180.1 | -178.8 | -176.3 |
| 30. | Downlink Total (S(d)/N(od)) | (db-Hz) | 47.8 | 46.5 | 44.0 | 34.2† | 32.9† | 30.4† | 62.0 | 60.7 | 58.2 | 58.2† | 56.9† | 54.4† |
| 31. | Downlink Ranging Factor | (db) | -6.4 | -6.4 | -6.4 | -6.4 | -6.4 | -6.4 | -8.2 | -8.2 | -8.2 | -8.2 | -8.2 | -8.2 |
| 32. | Downlink Carrier Factor | (db) | -1.1 | -1.1 | -1.1 | -1.1 | -1.1 | -1.1 | -0.7 | -0.7 | -0.7 | -0.7 | -0.7 | -0.7 |
| 33. | Downlink Telemetry Factor | (db) | | | | | | | | | | | | |
| 34. | Downlink Ranging (S(rd)/N(od)) | (db-Hz) | 41.4 | 40.1 | 37.6 | 27.8 | 26.5 | 24.0 | 53.8 | 52.5 | 50.0 | 50.0 | 48.7 | 46.2 |
| 35. | Downlink Carrier (S(cd)/Nod)) | (db-Hz) | 46.7 | 45.4 | 42.9 | 33.1 | 31.8 | 29.3 | 61.3 | 60.0 | 57.5 | 57.5 | 56.2 | 53.7 |
| 36. | Downlink Telemetry (S(td)/N(od)) | (db-Hz) | | | | | | | | | | | | |
| 37. | Downlink Effective Ranging (S(erd)/N(od)) | (db-Hz) | 40.9 | 39.6 | 37.1 | 25.5 | 24.2 | 21.7 | 53.8 | 52.5 | 50.0 | 49.8 | 48.5 | 46.0 |
| 38. | Grd Rcvr Ranging Threshold (Mark 1A) | (db-Hz) | 23.0 | 23.0 | 23.0 | 23.0 | 23.0 | 23.0 | 23.0 | 23.0 | 23.0 | 23.0 | 23.0 | 23.0 |
| 39. | Grd Rcvr Carrier Threshold | (db-Hz) | 30.0 | 30.0 | 30.0 | 30.0 | 30.0 | 30.0 | 30.0 | 30.0 | 30.0 | 30.0 | 30.0 | 30.0 |
| 40. | Grd Rcvr Telemetry Threshold (10*-5 BEP) | (db-Hz) | | | | | | | | | | | | |
| 41. | Ranging Margin | (db) | 17.9 | 16.6 | 14.1 | 2.5 | 1.2 | -1.3 | 30.8 | 29.5 | 27.0 | 26.8 | 25.5 | 23.0 |
| 42. | Carrier Margin | (db) | 16.7 | 15.4 | 12.9 | 3.1 | 1.8 | -0.7 | 31.3 | 30.0 | 27.5 | 27.5 | 26.2 | 23.7 |
| 43. | Telemetry Margin | (db) | | | | | | | | | | | | |
| 44. | Coding Gain | (db) | | | | | | | | | | | | |
| 45. | Telemetry Margin with Coding | (db) | | | | | | | | | | | | |

TABLE 3.7 IME LINK CALCULATION (CASE C, RANGE PRINTOUT)

| ITEM | ITEM DESCRIPTION | | IME-H, BEST CASE | | | IME-H, WORST CASE | | | IME-M,-D, BEST CASE | | | IME-M,-D, WORST CASE | | |
|---|---|---|---|---|---|---|---|---|---|---|---|---|---|---|
| 1. | Grd Xmtr Power (USB 20KW) | (dbm) | | 73.0 | | | 73.0 | | | 73.0 | | | 73.0 | |
| 2. | Xmtr to Antenna Xmssn Losses | (db) | | -0.1 | | | -0.5 | | | -0.1 | | | -0.5 | |
| 3. | Grd Xmtr Antenna Gain (85'-52.5db, 30'-43db) | (db) | | 52.5 | | | 52.5 | | | 52.5 | | | 43.0 | |
| 4. | Path Loss (H.-1.5x10*6KM, M.-D.-1.5x10*5Km, 2.1GHz) | (db) | | -222.1 | | | -222.1 | | | -202.1 | | | -202.1 | |
| 5. | Power at S/C Rcvr Antenna | (dbm) | | -96.7 | | | -97.1 | | | -76.7 | | | -86.6 | |
| 6. | S/C Rcvr Antenna Gain (Omni) | (db) | | 2.0 | | | -3.0 | | | 2.0 | | | -3.0 | |
| 7. | Antenna to Rcvr Xmssn Losses | (db) | | -1.0 | | | -2.0 | | | -1.0 | | | -2.0 | |
| 8. | Power at S/C Rcvr Input (S(u)) | (dbm) | | -95.7 | | | -102.1 | | | -75.7 | | | -91.6 | |
| 9. | Uplink Solar Noise Factor | (db) | | 0.0 | | | 0.0 | | | 0.0 | | | 0.0 | |
| 10. | S/C Rcvr Noise Density (N(ou)) | (dbm/Hz) | | -166.8 | | | -166.8 | | | -166.8 | | | -166.8 | |
| 11. | Uplink Total (S(u)/N(ou)) | (db-Hz) | | 71.1 | | | 64.7 | | | 91.1 | | | 75.2 | |
| 12. | Bandpass Limiter Gain/Loss Factor | (db) | | 2.6 | | | 1.6 | | | 3.0 | | | 2.8 | |
| 13. | Uplink Ranging Factor | (db) | | -4.7 | | | -4.7 | | | -4.7 | | | -4.7 | |
| 14. | Coherent Demodulation Factor (W(rf)/W(v)) | (db) | | 3.0 | | | 3.0 | | | 3.0 | | | 3.0 | |
| 15. | Premodulation Signal to Noise Ratio | (db) | | 9.0 | | | 1.6 | | | 29.4 | | | 13.3 | |
| 16. | Uplink Ranging Threshold | (db) | | 0.0 | | | 0.0 | | | 0.0 | | | 0.0 | |
| 17. | Uplink Ranging Margin | (db) | | 9.0 | | | 1.6 | | | 29.4 | | | 13.3 | |
| 18. | Ranging Low Pass Bandwidth | (db-Hz) | | 60.0 | | | 60.0 | | | 60.0 | | | 60.0 | |
| 19. | S/C Xmtr Power (into Xmssn Line) | (dbm) | | 31.0 | | | 31.0 | | | 27.0 | | | 27.0 | |
| 20. | Xmtr to Antenna Xmssn Losses | (db) | | -1.5 | | | -3.0 | | | -1.5 | | | -3.0 | |
| 21. | S/C Antenna Gain (Medium Gain Directional, Omni) | (db) | | 9.0 | | | 9.0 | | | 9.0 | | | 9.0 | |
| 22. | S/C Antenna Pointing Loss | (db) | | 0.0 | | | -2.0 | | | 0.0 | | | -2.0 | |
| 23. | Path Loss (See Item 4, 2.3GHz) | (db) | | -223.1 | | | -223.1 | | | -204.9 | | | -204.9 | |
| 24. | Power at Grd Rcvr Antenna | (dbm) | | -184.6 | | | -188.1 | | | -170.4 | | | -173.9 | |
| 25. | Grd Rcvr Antenna Gain (See Item 3) | (db) | | 52.5 | | | 52.5† | | | 52.5 | | | 52.5† | |
| 26. | Antenna to Rcvr Xmssn Losses | (db) | | -0.2 | | | -0.5 | | | -0.2 | | | -0.5 | |
| 27. | Power at Grd Rcvr Input (S(d)) | (dbm) | | -132.3 | | | -136.1† | | | -118.1 | | | -121.9† | |
| 28. | Downlink Solar Noise Factor | (db) | | 0.0 | | | -9.8† | | | 0.0 | | | 0.0 | |
| 29. | Grd Rcvr Noise Density (N(od)), (Maser, Cool P., Hot P.) | (dbm/Hz) | -180.1 | -178.8 | -176.3 | -180.1 | -178.8 | -176.3 | -180.1 | -178.8 | -176.3 | -180.1 | -178.8 | -176.3 |
| 30. | Downlink Total (S(d)/N(od)) | (db-Hz) | 47.8 | 46.5 | 44.0 | 34.2† | 32.9† | 30.4† | 62.0 | 60.7 | 58.2 | 58.2† | 56.9† | 54.4† |
| 31. | Downlink Ranging Factor | (db) | | | | | | | | | | | | |
| 32. | Downlink Carrier Factor | (db) | -3.1 | -3.1 | -3.1 | -3.1 | -3.1 | -3.1 | -15.4 | -15.4 | -15.4 | -15.4 | -15.4 | -15.4 |
| 33. | Downlink Telemetry Factor | (db) | -2.9 | -2.9 | -2.9 | -2.9 | -2.9 | -2.9 | -0.1 | -0.1 | -0.1 | -0.1 | -0.1 | -0.1 |
| 34. | Downlink Ranging (S(rd)/N(od)) | (db-Hz) | | | | | | | | | | | | |
| 35. | Downlink Carrier (S(cd)/Nod)) | (db-Hz) | 44.7 | 43.4 | 40.9 | 31.1 | 29.8 | 27.3 | 46.6 | 45.3 | 42.8 | 42.8 | 41.5 | 39.0 |
| 36. | Downlink Telemetry (S(td)/N(od)) | (db-Hz) | 44.9 | 43.6 | 41.1 | 31.3 | 30.0 | 27.5 | 61.9 | 60.6 | 58.1 | 58.1 | 56.8 | 54.3 |
| 37. | Downlink Effective Ranging (S(erd)/N(od)) | (db-Hz) | | | | | | | | | | | | |
| 38. | Grd Rcvr Ranging Threshold (Mark 1A) | (db-Hz) | | | | | | | | | | | | |
| 39. | Grd Rcvr Carrier Threshold | (db-Hz) | 30.0 | 30.0 | 30.0 | 30.0 | 30.0 | 30.0 | 30.0 | 30.0 | 30.0 | 30.0 | 30.0 | 30.0 |
| 40. | Grd Rcvr Telemetry Threshold (10*-5 BEP) | (db-Hz) | 44.7 | 44.7 | 44.7 | 35.7† | 35.7† | 35.7† | 53.8 | 53.8 | 53.8 | 53.8 | 53.8 | 53.8 |
| 41. | Ranging Margin | (db) | | | | | | | | | | | | |
| 42. | Carrier Margin | (db) | 14.7 | 13.4 | 10.9 | 1.1 | -0.2 | -2.7 | 16.6 | 15.3 | 12.8 | 12.8 | 11.5 | 9.0 |
| 43. | Telemetry Margin | (db) | 0.2 | -1.1 | -3.6 | -4.4 | -5.7 | -8.2 | 8.1 | 6.8 | 4.3 | 4.3 | 3.0 | 0.5 |
| 44. | Coding Gain | (db) | 5.0 | 5.0 | 5.0 | 5.0 | 5.0 | 5.0 | 5.0 | 5.0 | 5.0 | 5.0 | 5.0 | 5.0 |
| 45. | Telemetry Margin with Coding | (db) | 5.2 | 3.9 | 1.4 | 0.6 | -0.7 | -3.2 | 13.1 | 11.8 | 9.3 | 9.3 | 8.0 | 5.5 |

TABLE 3.8 IME LINK CALCULATION (CASE C, TELEMETRY PRINTOUT)

Summarizing so far there is 34.2 dB-Hz to play with prior to modulation losses and it must be apportioned among thresholds of 30 dB-Hz, 23 dB-Hz, and 35.7 dB-Hz, for the carrier, ranging, and telemetry respectively.

Consider the ranging channel, (34.2 - 30 = 4.2) and (34.2 - 23 = 11.2) together with the loss factors of Appendix C give 0.5 for the ranging index.[19] This index optimizes the margins for the ranging and the carrier (see Table 3.7) by making both as large as possible.

For the telemetry channel, (34.2 - 35.7 = -1.5) indicates that a large coding gain is needed. It is at this point that a coding gain of 5 dB is chosen. The -1.5 becomes (-1.5 + 5 = 3.5) and there is 4.2 dB and 3.5 dB to be accounted for between the modulation losses and the margins.

The range of indices applicable are

| | | |
|---|---|---|
| 0.8 | (-3.14 | -2.89)* |
| 0.$\dot{9}$ | (-4.13 | -2.12.) |

Since there is slightly more carrier difference than telemetry (4.2 over 3.5) a telemetry index of 0.8 will do the job (the -4.13 loss is too much). The results of this choice are shown in Table 3.8.

Now going to the Mother-Daughter Mission, the worst case is 44.9 dB-Hz. The ranging and carrier are alright, but the telemetry will not work. In keeping with the philosophy stated previously, the bit rate is the last thing to be traded, hence, an 85' dish and maser replace the 30' dish and cooled or uncooled paramps. This gives 58.2 dB-Hz to play with.

---

* see Appendix C

Using the same rationale as before the ranging and telemetry indices are 0.4 and 1.4 respectively.

The rest of the modulation indices for the Cases D, E, and F follow the same procedure with the results shown in Tables 3.9, 3.10, and 3.11. In the case of Table 3.9 another iteration was needed due to the effect of the low uplink signal-to-noise ratio, that is, the effective signal-to-noise density is not a linear function of the downlink signal-to-noise density.

After the appropriate modulation factors (Items 31, 32, 33) are taken into account the available $S/N_o$ for ranging, carrier, and telemetry can be found (Items 34, 35, 36).

The last item to be calculated prior to ascertaining the relevant signal margins is the effective ranging signal-to-noise density. An explanation is in order.

In turning around the ranging signal the uplink noise is modulated onto the downlink carrier together with the uplink ranging waveform. The resultant is a noisy ranging signal even if no downlink noise was present. If K is the downlink power gain, S is the uplink noisefree premodulation ranging in the spacecraft, $N_1$ is the uplink noise power, and $N_2$ is the downlink noise power, then the total received ranging signal for ground system processing is

$$KS + KN_1 + N_2 \tag{3.3}$$

Defining

$$A \triangleq (KS + KN_1)/N_2 \tag{3.4}$$

$$B \triangleq S/N_1 \tag{3.5}$$

| ITEM | ITEM DESCRIPTION | | IME-H. BEST CASE | | | IME-H. WORST CASE | | | IME-M.-D. BEST CASE | | | IME-M.-D. WORST CASE | | |
|---|---|---|---|---|---|---|---|---|---|---|---|---|---|---|
| 1. | Grd Xmtr Power (USB 20KW) | (dbm) | | 73.0 | | | 73.0 | | | 73.0 | | | 73.0 | |
| 2. | Xmtr to Antenna Xmssn Losses | (db) | | -0.1 | | | -0.5 | | | -0.1 | | | -0.5 | |
| 3. | Grd Xmtr Antenna Gain (85'-52.5db, 30'-43db) | (db) | | 52.5 | | | 52.5 | | | 52.5 | | | 43.0 | |
| 4. | Path Loss (H.-1.5x10*6KM, M.-D.-1.5x10*5Km, 2.1GHz) | (db) | | -222.1 | | | -222.1 | | | -202.1 | | | -202.1 | |
| 5. | Power at S/C Rcvr Antenna | (dbm) | | -96.7 | | | -97.1 | | | -76.7 | | | -86.6 | |
| 6. | S/C Rcvr Antenna Gain (Omni) | (db) | | 2.0 | | | -3.0 | | | 2.0 | | | -3.0 | |
| 7. | Antenna to Rcvr Xmssn Losses | (db) | | -1.0 | | | -2.0 | | | -1.0 | | | -2.0 | |
| 8. | Power at S/C Rcvr Input (S(u)) | (dbm) | | -95.7 | | | -102.1 | | | -75.7 | | | -91.6 | |
| 9. | Uplink Solar Noise Factor | (db) | | 0.0 | | | 0.0 | | | 0.0 | | | 0.0 | |
| 10. | S/C Rcvr Noise Density (N(ou)) | (dbm/Hz) | | -166.8 | | | -166.8 | | | -166.8 | | | -166.8 | |
| 11. | Uplink Total (S(u)/N(ou)) | (db-Hz) | | 71.1 | | | 64.7 | | | 91.1 | | | 75.2 | |
| 12. | Bandpass Limiter Gain/Loss Factor | (db) | | 2.6 | | | 1.6 | | | 3.0 | | | 2.8 | |
| 13. | Uplink Ranging Factor | (db) | | -4.7 | | | -4.7 | | | -4.7 | | | -4.7 | |
| 14. | Coherent Demodulation Factor (W(rf)/W(v)) | (db) | | 3.0 | | | 3.0 | | | 3.0 | | | 3.0 | |
| 15. | Premodulation Signal to Noise Ratio | (db) | | 9.0 | | | 1.6 | | | 29.4 | | | 13.3 | |
| 16. | Uplink Ranging Threshold | (db) | | 0.0 | | | 0.0 | | | 0.0 | | | 0.0 | |
| 17. | Uplink Ranging Margin | (db) | | 9.0 | | | 1.6 | | | 29.4 | | | 13.3 | |
| 18. | Ranging Low Pass Bandwidth | (db-Hz) | | 60.0 | | | 60.0 | | | 60.0 | | | 60.0 | |
| 19. | S/C Xmtr Power (into Xmssn Line) | (dbm) | | 34.0 | | | 34.0 | | | 30.0 | | | 30.0 | |
| 20. | Xmtr to Antenna Xmssn Losses | (db) | | -1.5 | | | -3.0 | | | -1.5 | | | -3.0 | |
| 21. | S/C Antenna Gain (Medium Gain Directional, Omni) | (db) | | 9.0 | | | 9.0 | | | 9.0 | | | 9.0 | |
| 22. | S/C Antenna Pointing Loss | (db) | | 0.0 | | | -2.0 | | | 0.0 | | | -2.0 | |
| 23. | Path Loss (See Item 4, 2.3GHz) | (db) | | -223.1 | | | -223.1 | | | -204.9 | | | -204.9 | |
| 24. | Power at Grd Rcvr Antenna | (dbm) | | -181.6 | | | -185.1 | | | -167.4 | | | -170.9 | |
| 25. | Grd Rcvr Antenna Gain (See Item 3) | (db) | | 52.5 | | | 52.5† | | | 52.5 | | | 52.5† | |
| 26. | Antenna to Rcvr Xmssn Losses | (db) | | -0.2 | | | -0.5 | | | -0.2 | | | -0.5 | |
| 27. | Power at Grd Rcvr Input (S(d)) | (dbm) | | -129.3 | | | -133.1† | | | -115.1 | | | -118.9† | |
| 28. | Downlink Solar Noise Factor | (db) | | 0.0 | | | -9.8† | | | 0.0 | | | 0.0 | |
| 29. | Grd Rcvr Noise Density (N(od)),(Maser, Cool P., Hot P.) | (dbm/Hz) | -180.1 | -178.8 | -176.3 | -180.1 | -178.8 | -176.3 | -180.1 | -178.8 | -176.3 | -180.1 | -178.8 | -176.3 |
| 30. | Downlink Total (S(d)/N(od)) | (db-Hz) | 50.8 | 49.5 | 47.0 | 37.2† | 35.9† | 33.4† | 65.0 | 63.7 | 61.2 | 61.2† | 59.9† | 57.4† |
| 31. | Downlink Ranging Factor | (db) | -11.0 | -11.0 | -11.0 | -11.0 | -11.0 | -11.0 | -27.3 | -27.3 | -27.3 | -27.3 | -27.3 | -27.3 |
| 32. | Downlink Carrier Factor | (db) | -3.6 | -3.6 | -3.6 | -3.6 | -3.6 | -3.6 | -19.9 | -19.9 | -19.9 | -19.9 | -19.9 | -19.9 |
| 33. | Downlink Telemetry Factor | (db) | -4.3 | -4.3 | -4.3 | -4.3 | -4.3 | -4.3 | -2.8 | -2.8 | -2.8 | -2.8 | -2.8 | -2.8 |
| 34. | Downlink Ranging (S(rd)/N(od)) | (db-Hz) | 39.8 | 38.5 | 36.0 | 26.2 | 24.9 | 22.4 | 37.7 | 36.4 | 33.9 | 33.9 | 32.6 | 30.1 |
| 35. | Downlink Carrier (S(cd)/Nod)) | (db-Hz) | 47.2 | 45.9 | 43.4 | 33.6 | 32.3 | 29.8 | 45.1 | 43.8 | 41.3 | 41.3 | 40.0 | 37.5 |
| 36. | Downlink Telemetry (S(td)/N(od)) | (db-Hz) | 46.5 | 45.2 | 42.7 | 32.9 | 31.6 | 29.1 | 62.2 | 60.9 | 58.4 | 58.4 | 57.1 | 54.6 |
| 37. | Downlink Effective Ranging (S(erd)/N(od)) | (db-Hz) | 39.3 | 38.0 | 35.5 | 23.9 | 22.6 | 20.1 | 37.7 | 36.4 | 33.9 | 33.7 | 32.4 | 29.9 |
| 38. | Grd Rcvr Ranging Threshold (Mark 1A) | (db-Hz) | 23.0 | 23.0 | 23.0 | 23.0 | 23.0 | 23.0 | 23.0 | 23.0 | 23.0 | 23.0 | 23.0 | 23.0 |
| 39. | Grd Rcvr Carrier Threshold | (db-Hz) | 30.0 | 30.0 | 30.0 | 30.0 | 30.0 | 30.0 | 30.0 | 30.0 | 30.0 | 30.0 | 30.0 | 30.0 |
| 40. | Grd Rcvr Telemetry Threshold (10*-5 BEP) | (db-Hz) | 44.7 | 44.7 | 44.7 | 35.7† | 35.7† | 35.7† | 53.8 | 53.8 | 53.8 | 53.8 | 53.8 | 53.8 |
| 41. | Ranging Margin | (db) | 16.3 | 15.0 | 12.5 | 0.9 | -0.4 | -2.9 | 14.7 | 13.4 | 10.9 | 10.7 | 9.4 | 6.9 |
| 42. | Carrier Margin | (db) | 17.2 | 15.9 | 13.4 | 3.6 | 2.3 | -0.2 | 15.1 | 13.8 | 11.3 | 11.3 | 10.0 | 7.5 |
| 43. | Telemetry Margin | (db) | 1.8 | 0.5 | -2.0 | -2.8 | -4.1 | -6.6 | 8.4 | 7.1 | 4.6 | 4.6 | 3.3 | 0.8 |
| 44. | Coding Gain | (db) | 5.0 | 5.0 | 5.0 | 5.0 | 5.0 | 5.0 | 5.0 | 5.0 | 5.0 | 5.0 | 5.0 | 5.0 |
| 45. | Telemetry Margin with Coding | (db) | 6.8 | 5.5 | 3.0 | 2.2 | 0.9 | -1.6 | 13.4 | 12.1 | 9.6 | 9.6 | 8.3 | 5.8 |

TABLE 3.9 IME LINK CALCULATION (CASE D, ITERATION 1)

| ITEM | ITEM DESCRIPTION | | IME-H. BEST CASE | | | IME-H. WORST CASE | | | IME-M.-D. BEST CASE | | | IME-M.-D. WORST CASE | | |
|---|---|---|---|---|---|---|---|---|---|---|---|---|---|---|
| 1. | Grd Xmtr Power (USB 20KW) | (dbm) | | 73.0 | | | 73.0 | | | 73.0 | | | 73.0 | |
| 2. | Xmtr to Antenna Xmssn Losses | (db) | | -0.1 | | | -0.5 | | | -0.1 | | | -0.5 | |
| 3. | Grd Xmtr Antenna Gain (85'-52.5db, 30'-43db) | (db) | | 52.5 | | | 52.5 | | | 52.5 | | | 43.0 | |
| 4. | Path Loss (H.-1.5x10*6KM, M.-D.-1.5x10*5Km, 2.1GHz) | (db) | | -222.1 | | | -222.1 | | | -202.1 | | | -202.1 | |
| 5. | Power at S/C Rcvr Antenna | (dbm) | | -96.7 | | | -97.1 | | | -76.7 | | | -86.6 | |
| 6. | S/C Rcvr Antenna Gain (Omni) | (db) | | 2.0 | | | -3.0 | | | 2.0 | | | -3.0 | |
| 7. | Antenna to Rcvr Xmssn Losses | (db) | | -1.0 | | | -2.0 | | | -1.0 | | | -2.0 | |
| 8. | Power at S/C Rcvr Input (S(u)) | (dbm) | | -95.7 | | | -102.1 | | | -75.7 | | | -91.6 | |
| 9. | Uplink Solar Noise Factor | (db) | | 0.0 | | | 0.0 | | | 0.0 | | | 0.0 | |
| 10. | S/C Rcvr Noise Density (N(ou)) | (dbm/Hz) | | -166.8 | | | -166.8 | | | -166.8 | | | -166.8 | |
| 11. | Uplink Total (S(u)/N(ou)) | (db-Hz) | | 71.1 | | | 64.7 | | | 91.1 | | | 75.2 | |
| 12. | Bandpass Limiter Gain/Loss Factor | (db) | | 2.6 | | | 1.6 | | | 3.0 | | | 2.8 | |
| 13. | Uplink Ranging Factor | (db) | | -4.7 | | | -4.7 | | | -4.7 | | | -4.7 | |
| 14. | Coherent Demodulation Factor (W(rf)/W(v)) | (db) | | 3.0 | | | 3.0 | | | 3.0 | | | 3.0 | |
| 15. | Premodulation Signal to Noise Ratio | (db) | | 9.0 | | | 1.6 | | | 29.4 | | | 13.3 | |
| 16. | Uplink Ranging Threshold | (db) | | 0.0 | | | 0.0 | | | 0.0 | | | 0.0 | |
| 17. | Uplink Ranging Margin | (db) | | 9.0 | | | 1.6 | | | 29.4 | | | 13.3 | |
| 18. | Ranging Low Pass Bandwidth | (db-Hz) | | 60.0 | | | 60.0 | | | 60.0 | | | 60.0 | |
| 19. | S/C Xmtr Power (into Xmssn Line) | (dbm) | | 34.0 | | | 34.0 | | | 30.0 | | | 30.0 | |
| 20. | Xmtr to Antenna Xmssn Losses | (db) | | -1.5 | | | -3.0 | | | -1.5 | | | -3.0 | |
| 21. | S/C Antenna Gain (Medium Gain Directional, Omni) | (db) | | 2.0 | | | -3.0 | | | 2.0 | | | -3.0 | |
| 22. | S/C Antenna Pointing Loss | (db) | | 0.0 | | | 0.0 | | | 0.0 | | | 0.0 | |
| 23. | Path Loss (See Item 4, 2.3GHz) | (db) | | -223.1 | | | -223.1 | | | -204.9 | | | -204.9 | |
| 24. | Power at Grd Rcvr Antenna | (dbm) | | -188.6 | | | -195.1 | | | -174.4 | | | -180.9 | |
| 25. | Grd Rcvr Antenna Gain (See Item 3) | (db) | | 52.5 | | | 52.5† | | | 52.5 | | | 52.5† | |
| 26. | Antenna to Rcvr Xmssn Losses | (db) | | -0.2 | | | -0.5 | | | -0.2 | | | -0.5 | |
| 27. | Power at Grd Rcvr Input (S(d)) | (dbm) | | -136.3 | | | -143.1† | | | -122.1 | | | -128.9† | |
| 28. | Downlink Solar Noise Factor | (db) | | 0.0 | | | -9.8† | | | 0.0 | | | 0.0 | |
| 29. | Grd Rcvr Noise Density (N(od)),(Maser, Cool P., Hot P.) | (dbm/Hz) | -180.1 | -178.8 | -176.3 | -180.1 | -178.8 | -176.3 | -180.1 | -178.8 | -176.3 | -180.1 | -178.8 | -176.3 |
| 30. | Downlink Total (S(d)/N(od)) | (db-Hz) | 43.8 | 42.5 | 40.0 | 27.2† | 25.9† | 23.4† | 58.0 | 56.7 | 54.2 | 51.2† | 49.9† | 47.4† |
| 31. | Downlink Ranging Factor | (db) | -8.2 | -8.2 | -8.2 | -8.2 | -8.2 | -8.2 | -8.2 | -8.2 | -8.2 | -8.2 | -8.2 | -8.2 |
| 32. | Downlink Carrier Factor | (db) | -0.7 | -0.7 | -0.7 | -0.7 | -0.7 | -0.7 | -0.7 | -0.7 | -0.7 | -0.7 | -0.7 | -0.7 |
| 33. | Downlink Telemetry Factor | (db) | | | | | | | | | | | | |
| 34. | Downlink Ranging (S(rd)/N(od)) | (db-Hz) | 35.6 | 34.3 | 31.8 | 19.0 | 17.7 | 15.2 | 49.8 | 48.5 | 46.0 | 43.0 | 41.7 | 39.2 |
| 35. | Downlink Carrier (S(cd)/Nod)) | (db-Hz) | 43.1 | 41.8 | 39.3 | 26.5 | 25.2 | 22.7 | 57.3 | 56.0 | 53.5 | 50.5 | 49.2 | 46.7 |
| 36. | Downlink Telemetry (S(td)/N(od)) | (db-Hz) | | | | | | | | | | | | |
| 37. | Downlink Effective Ranging (S(erd)/N(od)) | (db-Hz) | 35.1 | 33.8 | 31.3 | 16.7 | 15.4 | 12.9 | 49.8 | 48.5 | 46.0 | 43.8 | 41.5 | 39.0 |
| 38. | Grd Rcvr Ranging Threshold (Mark 1A) | (db-Hz) | 23.0 | 23.0 | 23.0 | 23.0 | 23.0 | 23.0 | 23.0 | 23.0 | 23.0 | 23.0 | 23.0 | 23.0 |
| 39. | Grd Rcvr Carrier Threshold | (db-Hz) | 30.0 | 30.0 | 30.0 | 30.0 | 30.0 | 30.0 | 30.0 | 30.0 | 30.0 | 30.0 | 30.0 | 30.0 |
| 40. | Grd Rcvr Telemetry Threshold (10*-5 BEP) | (db-Hz) | | | | | | | | | | | | |
| 41. | Ranging Margin | (db) | 12.1 | 10.8 | 8.3 | -6.3 | -7.6 | -10.1 | 26.8 | 25.5 | 23.0 | 19.8 | 18.5 | 16.0 |
| 42. | Carrier Margin | (db) | 13.1 | 11.8 | 9.3 | -3.5 | -4.8 | -7.3 | 27.3 | 26.0 | 23.5 | 20.5 | 19.2 | 16.7 |
| 43. | Telemetry Margin | (db) | | | | | | | | | | | | |
| 44. | Coding Gain | (db) | | | | | | | | | | | | |
| 45. | Telemetry Margin with Coding | (db) | | | | | | | | | | | | |

TABLE 3.10 IME LINK CALCULATION (CASE E)

| ITEM | ITEM DESCRIPTION | | IME-H. BEST CASE | | | IME-H. WORST CASE | | | IME-M.-D. BEST CASE | | | IME-M.-D. WORST CASE | | |
|---|---|---|---|---|---|---|---|---|---|---|---|---|---|---|
| 1. | Grd Xmtr Power (USB 20KW) | (dbm) | 73.0 | | | 73.0 | | | 73.0 | | | 73.0 | | |
| 2. | Xmtr to Antenna Xmssn Losses | (db) | -0.1 | | | -0.5 | | | -0.1 | | | -0.5 | | |
| 3. | Grd Xmtr Antenna Gain (85'-52.5db, 30'-43db) | (db) | 52.5 | | | 52.5 | | | 52.5 | | | 43.0 | | |
| 4. | Path Loss (H.-1.5x10*6KM, M.-D.-1.5x10*5Km, 2.1GHz) | (db) | -222.1 | | | -222.1 | | | -202.1 | | | -202.1 | | |
| 5. | Power at S/C Rcvr Antenna | (dbm) | -96.7 | | | -97.1 | | | -76.7 | | | -86.6 | | |
| 6. | S/C Rcvr Antenna Gain (Omni) | (db) | 2.0 | | | -3.0 | | | 2.0 | | | -3.0 | | |
| 7. | Antenna to Rcvr Xmssn Losses | (db) | -1.0 | | | -2.0 | | | -1.0 | | | -2.0 | | |
| 8. | Power at S/C Rcvr Input (S(u)) | (dbm) | -95.7 | | | -102.1 | | | -75.7 | | | -91.6 | | |
| 9. | Uplink Solar Noise Factor | (db) | 0.0 | | | 0.0 | | | 0.0 | | | 0.0 | | |
| 10. | S/C Rcvr Noise Density (N(ou)) | (dbm/Hz) | -166.8 | | | -166.8 | | | -166.8 | | | -166.8 | | |
| 11. | Uplink Total (S(u)/N(ou)) | (db-Hz) | 71.1 | | | 64.7 | | | 91.1 | | | 75.2 | | |
| 12. | Bandpass Limiter Gain/Loss Factor | (db) | 2.6 | | | 1.6 | | | 3.0 | | | 2.8 | | |
| 13. | Uplink Ranging Factor | (db) | -4.7 | | | -4.7 | | | -4.7 | | | -4.7 | | |
| 14. | Coherent Demodulation Factor (W(rf)/W(v)) | (db) | 3.0 | | | 3.0 | | | 3.0 | | | 3.0 | | |
| 15. | Premodulation Signal to Noise Ratio | (db) | 9.0 | | | 1.6 | | | 29.4 | | | 13.3 | | |
| 16. | Uplink Ranging Threshold | (db) | 0.0 | | | 0.0 | | | 0.0 | | | 0.0 | | |
| 17. | Uplink Ranging Margin | (db) | 9.0 | | | 1.6 | | | 29.4 | | | 13.3 | | |
| 18. | Ranging Low Pass Bandwidth | (db-Hz) | 60.0 | | | 60.0 | | | 60.0 | | | 60.0 | | |
| 19. | S/C Xmtr Power (into Xmssn Line) | (dbm) | 34.0 | | | 34.0 | | | 30.0 | | | 30.0 | | |
| 20. | Xmtr to Antenna Xmssn Losses | (db) | -1.5 | | | -3.0 | | | -1.5 | | | -3.0 | | |
| 21. | S/C Antenna Gain (Medium Gain Directional, Omni) | (db) | 2.0 | | | -3.0 | | | 2.0 | | | -3.0 | | |
| 22. | S/C Antenna Pointing Loss | (db) | 0.0 | | | 0.0 | | | 0.0 | | | 0.0 | | |
| 23. | Path Loss (See Item 4, 2.3GHz) | (db) | -223.1 | | | -223.1 | | | -204.9 | | | -204.9 | | |
| 24. | Power at Grd Rcvr Antenna | (dbm) | -188.6 | | | -195.1 | | | -174.4 | | | -180.9 | | |
| 25. | Grd Rcvr Antenna Gain (See Item 3) | (db) | 52.5 | | | 52.5† | | | 52.5 | | | 52.5† | | |
| 26. | Antenna to Rcvr Xmssn Losses | (db) | -0.2 | | | -0.5 | | | -0.2 | | | -0.5 | | |
| 27. | Power at Grd Rcvr Input (S(d)) | (dbm) | -136.3 | | | -143.1† | | | -122.1 | | | -128.9† | | |
| 28. | Downlink Solar Noise Factor | (db) | 0.0 | | | -9.8† | | | 0.0 | | | 0.0 | | |
| 29. | Grd Rcvr Noise Density (N(od)),(Maser, Cool P., Hot P.) | (dbm/Hz) | -180.1 | -178.8 | -176.3 | -180.1 | -178.8 | -176.3 | -180.1 | -178.8 | -176.3 | -180.1 | -178.8 | -176.3 |
| 30. | Downlink Total (S(d)/N(od)) | (db-Hz) | 43.8 | 42.5 | 40.0 | 27.2† | 25.9† | 23.4† | 58.0 | 56.7 | 54.2 | 51.2† | 49.9† | 47.4† |
| 31. | Downlink Ranging Factor | (db) | | | | | | | | | | | | |
| 32. | Downlink Carrier Factor | (db) | -8.8 | -8.8 | -8.8 | -8.8 | -8.8 | -8.8 | -15.4 | -15.4 | -15.4 | -15.4 | -15.4 | -15.4 |
| 33. | Downlink Telemetry Factor | (db) | -0.6 | -0.6 | -0.6 | -0.6 | -0.6 | -0.6 | -0.1 | -0.1 | -0.1 | -0.1 | -0.1 | -0.1 |
| 34. | Downlink Ranging (S(rd)/N(od)) | (db-Hz) | | | | | | | | | | | | |
| 35. | Downlink Carrier (S(cd)/Nod)) | (db-Hz) | 35.0 | 33.7 | 31.2 | 18.4 | 17.1 | 14.6 | 42.6 | 41.3 | 38.8 | 35.8 | 34.5 | 32.0 |
| 36. | Downlink Telemetry (S(td)/N(od)) | (db-Hz) | 43.2 | 41.9 | 39.4 | 26.6 | 25.3 | 22.8 | 57.9 | 56.6 | 54.1 | 51.1 | 49.8 | 47.3 |
| 37. | Downlink Effective Ranging (S(erd)/N(od)) | (db-Hz) | | | | | | | | | | | | |
| 38. | Grd Rcvr Ranging Threshold (Mark 1A) | (db-Hz) | | | | | | | | | | | | |
| 39. | Grd Rcvr Carrier Threshold | (db-Hz) | 30.0 | 30.0 | 30.0 | 30.0 | 30.0 | 30.0 | 30.0 | 30.0 | 30.0 | 30.0 | 30.0 | 30.0 |
| 40. | Grd Rcvr Telemetry Threshold (10*-5 BEP) | (db-Hz) | 44.7 | 44.7 | 44.7 | 35.7† | 35.7† | 35.7† | 53.8 | 53.8 | 53.8 | 53.8 | 53.8 | 53.8 |
| 41. | Ranging Margin | (db) | | | | | | | | | | | | |
| 42. | Carrier Margin | (db) | 5.0 | 3.7 | 1.2 | -11.6 | -12.9 | -15.4 | 12.6 | 11.3 | 8.8 | 5.8 | 4.5 | 2.0 |
| 43. | Telemetry Margin | (db) | -1.5 | -2.8 | -5.3 | -9.1 | -10.4 | -12.9 | 4.1 | 2.8 | 0.3 | -2.7 | -4.0 | -6.5 |
| 44. | Coding Gain | (db) | 5.0 | 5.0 | 5.0 | 5.0 | 5.0 | 5.0 | 5.0 | 5.0 | 5.0 | 5.0 | 5.0 | 5.0 |
| 45. | Telemetry Margin with Coding | (db) | 3.5 | 2.2 | -0.3 | -4.1 | -5.4 | -7.9 | 9.1 | 7.8 | 5.3 | 2.3 | 1.0 | -1.5 |

TABLE 3.11 IME LINK CALCULATION (CASE F)

then A is the composite signal-to-noise, i.e., considering $S + N_1$ as the downlink premodulation signal, and B is the uplink signal-to-noise. The effective SNR is the one which actually is effective in producing the ranging data and is given by

$$C \triangleq (KS)/(KN_1 + N_2) = AB/(1 + A + B). \tag{3.6}$$

Note that if A<<B then

$$C \doteq A, \tag{3.7}$$

and if B<<A, then

$$C \doteq B. \tag{3.8}$$

An example may help to solidify ideas. Consider Items 15 and 34. Item 34, adjusted for the ranging bandwidth gives the composite SNR. Looking at Table 3.12 for example, A = 40.9 - 63 and B = 9.0 (Heliocentric maser best case); hence B>>A. Essentially, then, the uplink factor, B, can be ignored and the effective $S/N_o$, Item 37 is almost the same as Item 34.

At this point all the pertinent factors have been taken into account and the margins may be calculated (Items 41, 42, 43, 45). Task 1 is therefore completed.

| ITEM | ITEM DESCRIPTION | | IME-H. BEST CASE | | | IME-H. WORST CASE | | | IME-M.-D. BEST CASE | | | IME-M.-D. WORST CASE | | |
|---|---|---|---|---|---|---|---|---|---|---|---|---|---|---|
| 1. | Grd Xmtr Power (USB 20KW) | (dbm) | | 73.0 | | | 73.0 | | | 73.0 | | | 73.0 | |
| 2. | Xmtr to Antenna Xmssn Losses | (db) | | -0.1 | | | -0.5 | | | -0.1 | | | -0.5 | |
| 3. | Grd Xmtr Antenna Gain (85°-52.5db, 30°-43db) | (db) | | 52.5 | | | 52.5 | | | 52.5 | | | 43.0 | |
| 4. | Path Loss (H.-1.5x10*6Km, M.-D.-1.5x10*5Km, 2.1GHz) | (db) | | -222.1 | | | -222.1 | | | -202.1 | | | -202.1 | |
| 5. | Power at S/C Rcvr Antenna | (dbm) | | -96.7 | | | -97.1 | | | -76.7 | | | -86.6 | |
| 6. | S/C Rcvr Antenna Gain (Omni) | (db) | | 2.0 | | | -3.0 | | | 2.0 | | | -3.0 | |
| 7. | Antenna to Rcvr Xmssn Losses | (db) | | -1.0 | | | -2.0 | | | -1.0 | | | -2.0 | |
| 8. | Power at S/C Rcvr Input (S(u)) | (dbm) | | -95.7 | | | -102.1 | | | -75.7 | | | -91.6 | |
| 9. | Uplink Solar Noise Factor | (db) | | 0.0 | | | 0.0 | | | 0.0 | | | 0.0 | |
| 10. | S/C Rcvr Noise Density (N(ou)) | (dbm/Hz) | | -166.8 | | | -166.8 | | | -166.8 | | | -166.8 | |
| 11. | Uplink Total (S(u)/N(ou)) | (db-Hz) | | 71.1 | | | 64.7 | | | 91.1 | | | 75.2 | |
| 12. | Bandpass Limiter Gain/Loss Factor | (db) | | 2.6 | | | 1.6 | | | 3.0 | | | 2.8 | |
| 13. | Uplink Ranging Factor | (db) | | -4.7 | | | -4.7 | | | -4.7 | | | -4.7 | |
| 14. | Coherent Demodulation Factor (W(rf)/W(v)) | (db) | | 3.0 | | | 3.0 | | | 3.0 | | | 3.0 | |
| 15. | Premodulation Signal to Noise Ratio | (db) | | 9.0 | | | 1.6 | | | 29.4 | | | 13.3 | |
| 16. | Uplink Ranging Threshold | (db) | | 0.0 | | | 0.0 | | | 0.0 | | | 0.0 | |
| 17. | Uplink Ranging Margin | (db) | | 9.0 | | | 1.6 | | | 29.4 | | | 13.3 | |
| 18. | Ranging Low Pass Bandwidth | (db-Hz) | | 60.0 | | | 60.0 | | | 60.0 | | | 60.0 | |
| 19. | S/C Xmtr Power (into Xmssn Line) | (dbm) | | 34.0 | | | 34.0 | | | 30.0 | | | 30.0 | |
| 20. | Xmtr to Antenna Xmssn Losses | (db) | | -1.5 | | | -3.0 | | | -1.5 | | | -3.0 | |
| 21. | S/C Antenna Gain (Medium Gain Directional, Omni) | (db) | | 9.0 | | | 9.0 | | | 9.0 | | | 9.0 | |
| 22. | S/C Antenna Pointing Loss | (db) | | 0.0 | | | -2.0 | | | 0.0 | | | -2.0 | |
| 23. | Path Loss (See Item 4, 2.3GHz) | (db) | | -223.1 | | | -223.1 | | | -204.9 | | | -204.9 | |
| 24. | Power at Grd Rcvr Antenna | (dbm) | | -181.6 | | | -185.1 | | | -167.4 | | | -170.9 | |
| 25. | Grd Rcvr Antenna Gain (See Item 3) | (db) | | 52.5 | | | 52.5 | | | 52.5 | | | 52.5 | |
| 26. | Antenna to Rcvr Xmssn Losses | (db) | | -0.2 | | | -0.5 | | | -0.2 | | | -0.5 | |
| 27. | Power at Grd Rcvr Input (S(d)) | (dbm) | | -129.3 | | | -133.1 | | | -115.1 | | | -118.9 | |
| 28. | Downlink Solar Noise Factor | (db) | | 0.0 | | | -9.8 | | | 0.0 | | | 0.0 | |
| 29. | Grd Rcvr Noise Density (N(od)),(Maser, Cool P., Hot P.) | (dbm/Hz) | -180.1 | -178.8 | -176.3 | -180.1 | -178.8 | -176.3 | -180.1 | -178.8 | -176.3 | -180.1 | -178.8 | -176.3 |
| 30. | Downlink Total (S(d)/N(od)) | (db-Hz) | 50.8 | 49.5 | 47.0 | 37.2 | 35.9 | 33.4 | 65.0 | 63.7 | 61.2 | 61.2 | 59.9 | 57.4 |
| 31. | Downlink Ranging Factor | (db) | -9.9 | -9.9 | -9.9 | -9.9 | -9.9 | -9.9 | -27.3 | -27.3 | -27.3 | -27.3 | -27.3 | -27.3 |
| 32. | Downlink Carrier Factor | (db) | -4.6 | -4.6 | -4.6 | -4.6 | -4.6 | -4.6 | -19.9 | -19.9 | -19.9 | -19.9 | -19.9 | -19.9 |
| 33. | Downlink Telemetry Factor | (db) | -4.2 | -4.2 | -4.2 | -4.2 | -4.2 | -4.2 | -2.8 | -2.8 | -2.8 | -2.8 | -2.8 | -2.8 |
| 34. | Downlink Ranging (S(rd)/N(od)) | (db-Hz) | 40.9 | 39.6 | 37.1 | 27.3 | 26.0 | 23.5 | 37.7 | 36.4 | 33.9 | 33.9 | 32.6 | 30.1 |
| 35. | Downlink Carrier (S(cd)/Nod)) | (db-Hz) | 46.2 | 44.9 | 42.4 | 32.6 | 31.3 | 28.8 | 45.1 | 43.8 | 41.3 | 41.3 | 40.0 | 37.5 |
| 36. | Downlink Telemetry (S(td)/N(od)) | (db-Hz) | 46.6 | 45.3 | 42.8 | 33.0 | 31.7 | 29.2 | 62.2 | 60.9 | 58.4 | 58.4 | 57.1 | 54.6 |
| 37. | Downlink Effective Ranging (S(erd)/N(od)) | (db-Hz) | 40.4 | 39.1 | 36.6 | 25.0 | 23.7 | 21.2 | 37.7 | 36.4 | 33.9 | 33.7 | 32.4 | 29.9 |
| 38. | Grd Rcvr Ranging Threshold (Mark 1A) | (db-Hz) | 23.0 | 23.0 | 23.0 | 23.0 | 23.0 | 23.0 | 23.0 | 23.0 | 23.0 | 23.0 | 23.0 | 23.0 |
| 39. | Grd Rcvr Carrier Threshold | (db-Hz) | 30.0 | 30.0 | 30.0 | 30.0 | 30.0 | 30.0 | 30.0 | 30.0 | 30.0 | 30.0 | 30.0 | 30.0 |
| 40. | Grd Rcvr Telemetry Threshold (10*-5 BEP) | (db-Hz) | 44.7 | 44.7 | 44.7 | 35.7 | 35.7 | 35.7 | 53.8 | 53.8 | 53.8 | 53.8 | 53.8 | 53.8 |
| 41. | Ranging Margin | (db) | 17.4 | 16.1 | 13.6 | 2.0 | 0.7 | -1.8 | 14.7 | 13.4 | 10.9 | 10.7 | 9.4 | 6.9 |
| 42. | Carrier Margin | (db) | 16.2 | 14.9 | 12.4 | 2.6 | 1.3 | -1.2 | 15.1 | 13.8 | 11.3 | 11.3 | 10.0 | 7.5 |
| 43. | Telemetry Margin | (db) | 1.0 | 0.6 | -1.9 | -2.7 | -4.0 | -6.5 | 8.4 | 7.1 | 4.6 | 4.6 | 3.3 | 0.8 |
| 44. | Coding Gain | (db) | 5.0 | 5.0 | 5.0 | 5.0 | 5.0 | 5.0 | 5.0 | 5.0 | 5.0 | 5.0 | 5.0 | 5.0 |
| 45. | Telemetry Margin with Coding | (db) | 6.9 | 5.6 | 3.1 | 2.3 | 1.0 | -1.5 | 13.4 | 12.1 | 9.6 | 9.6 | 8.3 | 5.8 |

TABLE 3.12 IME LINK CALCULATION (CASE D, ITERATION 2)

## 3.2 TASK 2 DISCUSSION AND RESULTS

In this section of the report both the theoretical and practical aspects of convolutional encoding and decoding will be presented. The discussion will start with the general theory as found in the literature, look at the encoding problem, and finally pursue the important subject of decoding convolutional codes.

Decoders will be designed and cost factors shown for the maximum likelihood and sequential decoding algorithms. While feedback decoding will be discussed due to its importance as a major decoding technique, no costing or design will be done for it since it is well known that the complexity required for the high coding gains needed by IMEMD/H (>5 dB) is impractical to implement. More will be said on this subject in the section on feedback decoding.

### 3.2.1 CONVOLUTIONAL CODING THEORY

This part of the section will review the theory of convolutional coding as it relates to the general topic of communication. A minimum of mathematics will be used, however, since coding is a mathematical animal, so to speak, the results of the literature, i.e., equations, inequalities, etc., will be presented. These results together with heuristic explanations, tables, and figures will, it is hoped, transfer the maximum amount of information with the minimum amount of confusion; they should also serve to provide a basis upon which the encoding/decoding technique can be built.

The majority of this subsection is drawn from reference 20, however, the author's own experience, and that of others will be interlaced to embellish the basic treatise.

The best and most common way of introducing convolutional codes is by way of an example. This will be followed here. Consider Figure 3.10

the data (information) sequence enters the three bit ($B_0$, $B_1$, $B_2$) shift register in a serial manner (prior to the data the $B_i$'s were set to zero). After each bit is shifted into the encoder the multiplex switch (S) samples the two outputs of the exclusive-ors ($M_1$, $M_2$) which have added their inputs via register taps from the various stages. The addition here is that of the binary Galois field, i.e., modulo-2 (mod-2) (See Table 3.13)

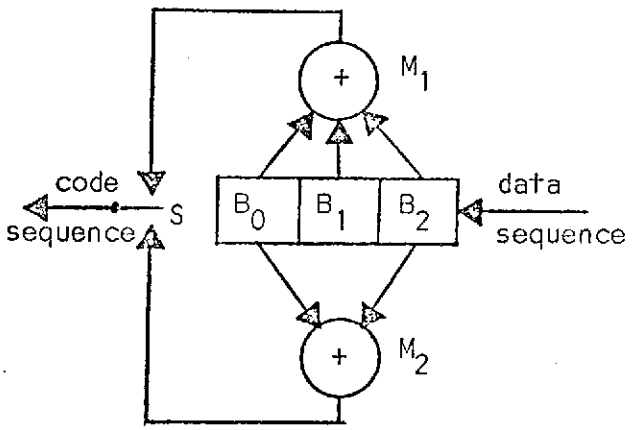


FIGURE 3.10 CONVOLUTIONAL ENCODER

| | |
|---|---|
| 0 + 0 = 0 | |
| 1 + 1 = 0 | |
| 0 + 1 = 1 | |
| 1 + 0 = 1 | |

TABLE 3.13 MODULO-2 ADDITION

The two bits (n=2) outputted from the multiplexer per data bit are the so called code bits, and the sequence of these bits are the encoded bit stream. Thus a sequence of data bits, say, $\underline{X} = (X_0, X_1, \ldots X_N)$ has, via the encoder, resulted in another bit stream, the encoded bits, say, $\underline{Y} = (Y_0, Y_1, \ldots Y_M)$.

At this point it is of interest to point out why this type of code is called a convolutional code. The key is in how $\underline{Y}$ is related to $\underline{X}$. Consider the output of $M_1$ for a moment; call it $\underline{Z}$. If a vector $\underline{g} = (g_0, g_1, g_2)$ is defined to be the connection vector to the mod-2 adder $M_1$, that is, $g_i = 1$ if the register stage $B_i$ is connected to $M_1$ and $g_i = 0$ if not, then it is clear that the time waveform Z(t) corresponding to $\underline{Z}$ is a linear function of the waveform X(t) corresponding to $\underline{X}$ since Z(t) is the result of adding

various portions of the input waveform; therefore Z(t) is related to X(t) by convolution, i.e.,

$$Z(t) = X(t) * h(t), \tag{3.9}$$

where h(t) is some equivalent encoder filter impulse response. In fact h(t) can be found as follows. Let

$$X_1(t) = u(t) - u(t-T) \tag{3.10}$$

i.e., a pulse at time t = 0 and ending at t = T (u(t) is the unit step function). The output $Z_1(t)$ is

$$\begin{aligned} Z_1(t) &= g_0 X_1(t) \quad : 0 \leq t < T \\ &= g_1 X_1(t-T) \quad : T \leq t < 2T \\ &\vdots \quad\quad \vdots \\ &= g_n X_1(t-nT) \quad : nT \leq t < (n+1)T \end{aligned} \tag{3.11}$$

Due to the choice of $X_1(t)$ (non-overlapping pulse)

$$Z_1(t) = \sum_{n=0}^{k} g_n X_1(t-nT) \tag{3.12}$$

The Laplace Transform of h(t) is therefore

$$H(s) = \left[ \sum_{n=0}^{k} g_n \left( \frac{e^{-nTs} - e^{-(n+1)Ts}}{s} \right) \right] \div \left( \frac{1-e^{-Ts}}{s} \right) \tag{3.13}$$

$$H(s) = \sum_{n=0}^{k} g_n e^{-nTs} \tag{3.14}$$

which implies that

$$h(t) = \sum_{n=0}^{k} g_n \, \delta(t-nT) \tag{3.15}$$

where $\delta(t)$ is the dirac delta function. The encoder, then, is a linear filter with its response given by its tap arrangement, and the output is the convolution of the input with the impulse response. The code stream is merely the time multiplexing of several filter outputs.

The specific encoder in Figure 3.10 can be described as a rate 1/2, constraint length 3, nonsystematic encoder. The rate of a code is the number of data bits encoded per code bit outputted, e.g., if two data bits were shifted into the encoder per multiplex cycle the rate would be 2/2 = 1. In the following text "b" will be the number of data bits encoded per cycle and "n" will be the number of coded bits per cycle; thus a general encoder rate is R = b/n.

Logically it would seem to be best to have R small so that many code bits contain information about a given data bit. The drawback is that more code bits per cycle mean high code symbol rates and thus more bandwidth is used. Obviously, a tradeoff is involved.

The code is nonsystematic because the data bits are not part of the coded bits. A systematic encoder would send data bits along with coded (sometimes called parity) bits. Figure 3.11 shows a systematic encoder. Note that the data bits are alternated with the parity bits due to the direct connection to one stage of the register.

Again logic dictates that less information is sent, in terms of coding, if a systematic code is used. It has been shown that a nonsystematic code of constraint length K is equivalent to systematic code of constraint length 2K if a rate 1/2 code is assumed.[21] Similar results hold for other rates.

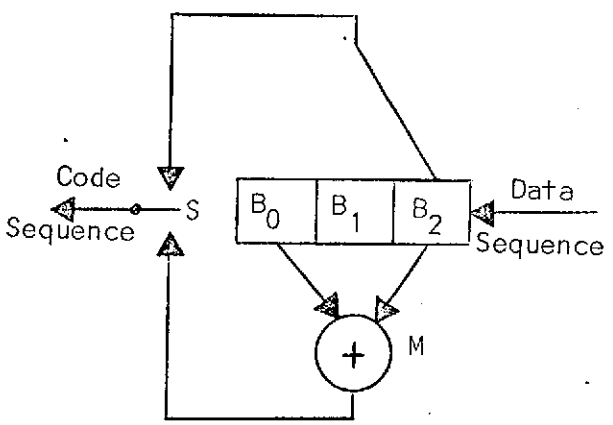


FIGURE 3.11 SYSTEMATIC CONVOLUTIONAL ENCODER FOR K=3, b/n=1/2

The last qualifier used above was the constraint length, K. This quantity is defined in a number of different ways in different papers; here, however, it will mean the number of stages in the encoder. Note that the set of all tap coefficients (for all adders) must include $g_1$ and $g_K$, otherwise one end register stage is not used and can be dropped.

The constraint length governs the number of code bits which contain information about, i.e., which are a function of, a given data bit. Obviously the more information supplied about a data bit the less the chance of making an error in a decision on that bit.

Getting back to the example now, consider Figures 3.12, 3.13, and 3.14. All of these figures are equivalent representations of the encoder shown in Figure 3.10; the information is merely contained in different forms.

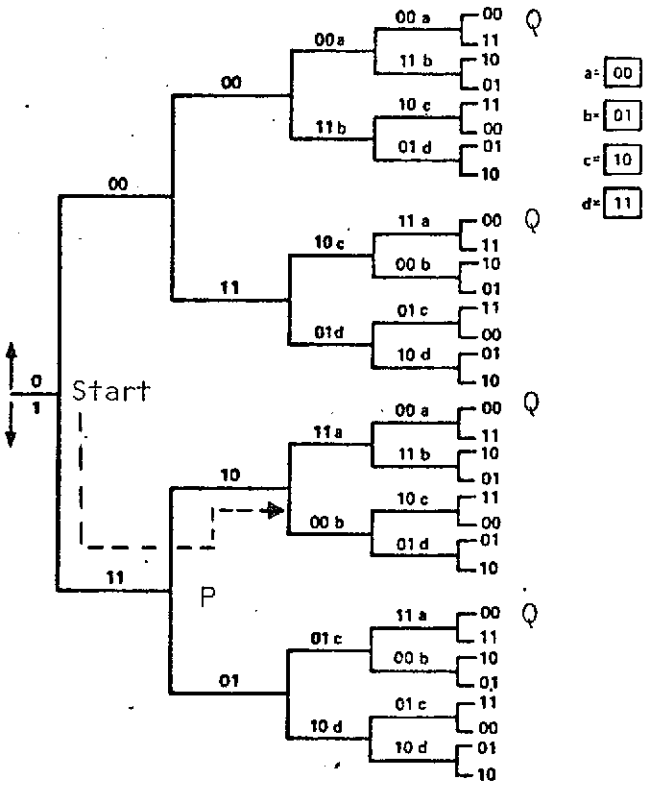


FIGURE 3.12 TREE DIAGRAM FOR ENCODER OF FIGURE 3.10

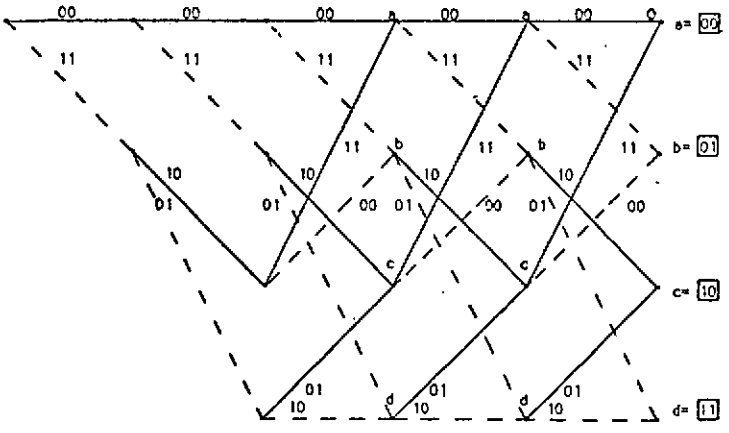


FIGURE 3.13 TRELLIS DIAGRAM FOR ENCODER OF FIGURE 3.10

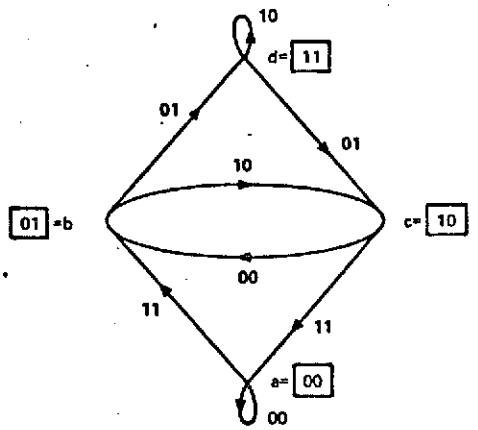


FIGURE 3.14 STATE DIAGRAM FOR ENCODER OF FIGURE 3.10

Figure 3.12 is the tree representation of the encoder. It works as follows. Beginning at the "Start" point, if a data bit entering the encoder is a 0 the upper branch of the tree is chosen. If a 1 enters the lower branch is chosen. For example, if the first data bit was a 1 then the dotted branch of Figure 3.12 is picked and the bits on this path, viz., "11" indicate that a "11" was the output of the encoder due to the 1 input. Looking at Figure 3.10, the output of $M_1$ is $B_0 + B_1 + B_2 = 0 + 0 + 1 = 1$, and the output of $M_2$ is $B_0 + B_2 = 0 + 1 = 1$; hence the output of S is indeed 11.

We are now at point (node) P in the tree. Suppose the second data bit is a 0 then the upper branch from P is chosen and an output of 10 is indicated. Continuing in this manner any input data sequence can be found to result in a code sequence given by the path through the tree.

The tree is simplest to understand, but it is complex to draw after only a few data shifts. This is where Figure 3.13 comes into play. This is the trellis representation of the encoder. Where the tree grew in two dimensions, the trellis grows only in one dimension. The trellis is a result of the observation that once a data bit "drops" out of the encoder stage $B_0$, its influence must disappear. Because of this the tree must repeat, i.e., $B_0 = d_0$, $B_1 = d_1$, $B_2 = d_2$ must give the same output regardless of where the consecutive data bits $d_0$, $d_1$, $d_2$ occur within the data stream. As a concrete example consider the data sequences 00000, 10000, 11000, and 01000. All of these sequences lead to the point Q in the tree (see also Q in the trellis). Since any sixth data bit will load the register in the <u>same</u> way for all of the four 5 data bit sequences above the four points Q in the tree may be tied together. This is exactly the trellis.

The trellis is better to draw than the tree and yet contains all the information that the tree contains, however, it still grows in one dimension as more data bits are added to the input. Figure 3.14 is the state diagram of the encoder; it eliminates this last drawback, and loses no information about the encoder. The state diagram is a result of the observation that the encoder output for each shift is completely determined by what is in the register prior to the shift and immediately following the shift, i.e., if $B_0 = 0$, $B_1 = 1$, $B_2 = 0$, then a data bit entry must result in $B_0 = 1$, $B_1 = 0$, $B_2$ = new data bit. In other words the only bit in doubt is $B_2$ when given the state $B_0\ B_1$.

Looking now at Figure 3.14 suppose we have all zeros in the register, and an input of 1 is shifted into it. Well the $B_0 = 0$, $B_1 = 0$ implies a present state of "a" in the figure, whereas, the $B_1 = 0$, $B_2 = 1$ implies that the next state will be "b". Thus the state diagram travels from state "a" to "b" and the path label gives the output bits as a "11." Continuing in this manner any given data sequence will result in the corresponding coded sequence.

Each of these representations of the code has its usefulness and should be understood to fully realize the workings of a convolutional code. Also the mathematical properties of the code are developed by these diagrams. As a side note sequential and feedback decoding are best understood by using the tree, whereas, maximum likelihood decoding uses the trellis or state diagrams.

At this point in the section several important results of the theory of convolutional codes will be stated without all of the developmental material. The reader interested in the details leading up to the results can refer to the papers referenced at the end of this report.

The space channel involved in the IMEMD/H study can be accurately modeled by the additive white Gaussian noise (AWGN) channel with no memory, that is, the channel noise is added to the transmitted symbols independent of which symbols are sent, the noise is gaussianly distributed, and has a constant power density ($N_0/2$) over a frequency range which is large compared with the signal bandwidth. Also the filtering, etc. of the channel is such that each symbol is transmitted independent of any other one, i.e., memoryless.

It will be assumed that ideal PSK is used, i.e., a $+\pi/2$ shift of the carrier represents a 1 while $-\pi/2$ shift represents a 0.

If each symbol is assumed to be equally likely to occur, then it is well known that a receiver which calculates the probability of the received sequence given that a particular coded sequence was sent, does this for each coded sequence, and then picks that coded sequence which gives the highest probability is optimum in the a posteriori sense. In the following this type of receiver is assumed.

Speaking heuristically the more dissimilar a set of sequences are the more errors correctable, e.g., if a 0 is sent and an error causes it to change to a 1 there is no way to tell if a 1 wasn't sent, i.e., no errors correctable. If a 000 is sent and one error occurs, say, 010 it can be guessed that a 000 was sent rather than a 111 because a 000 is closer in digits to 010 than 111 is. Continuing further a 00000 and 11111 are even more dissimilar and thus will correct more errors. This is an example of simple redundancy coding. It gains little because the energy per symbol decreases linearly with the number of symbols. General coding allows an

increase in dissimilarity, i.e., an increase in distance between two symbols, without an equal decrease in energy per symbol; the energy does decrease, but not as fast as the increase in dissimilarity.

The above discussion was to introduce the concept of distance between code words. Mathematically distance becomes a metric in the Hilbert Space of code symbols. This metric is used to determine the error correcting capability of the code. Let "d" be the minimum distance (metricwise) between code words.

One other concept must be introduced before the bit error probability can be bounded, and that is the code transfer function, T(D,N). Let D and N be dummy variables, i.e., of no particular interest in themselves. Let the power of D be a number equal to the number of ones outputted by the encoder when switching states, e.g., in Figure 3.14 a 11 is outputted when going from state c to a or a to b therefore replace the 11 by a $D^2$ (see Figure 3.15).

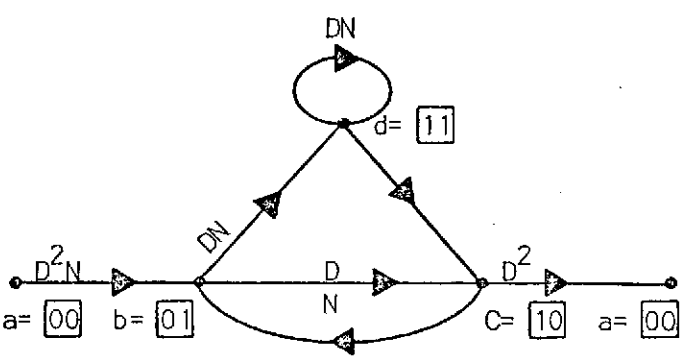


FIGURE 3.15 STATE DIAGRAM LABELED ACCORDING TO DISTANCE AND NUMBER OF ONES

### 3.2.2 CONVOLUTIONAL ENCODING

Two examples of convolutional encoders were shown in Figures 3.10 and 3.11. In general the encoder is a finite-state linear machine having K shift register stages and n linear algebraic function generators. Although the input data need not be binary, the binary case is by far the most common, and so it will be assumed hereafter.

The constraint length of an encoder was defined in Section 3.2.1 to be the number of stages in the register. This is deceiving except in the case that one bit is shifted per multiplexer cycle, i.e., b = 1. If b = 2, for example, a constraint length K = 2 encoder can be as shown in Figure 3.16 with its state diagram shown in Figure 3.17.

A less ambiguous definition of constraint length is "the number of multiplexer cycles over which a given data bit has influence on the output." The longer the constraint length, the longer is the influence of a given bit, and the more information that is sent about that bit. In Figure 3.16 it is seen that due to the two bit shift per cycle a given data bit only stays in the encoder for two cycles; thus the constraint length is two.

The major question to be answered in this section is what is the best way to connect the mod-2 adders to the register stages, i.e., given a certain length shift register and a particular number of adders what is the connection set which will make "d" the largest. Simply stated the only way to find out is to try all of the combinations and measure the results.

One other factor is important in choosing a code. It is possible to pick a code which will generate an infinite number of errors if certain

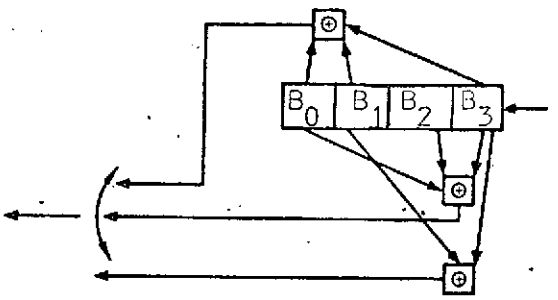


FIGURE 3.16 CODER FOR K=2, b=2, n=3, AND R=2/3

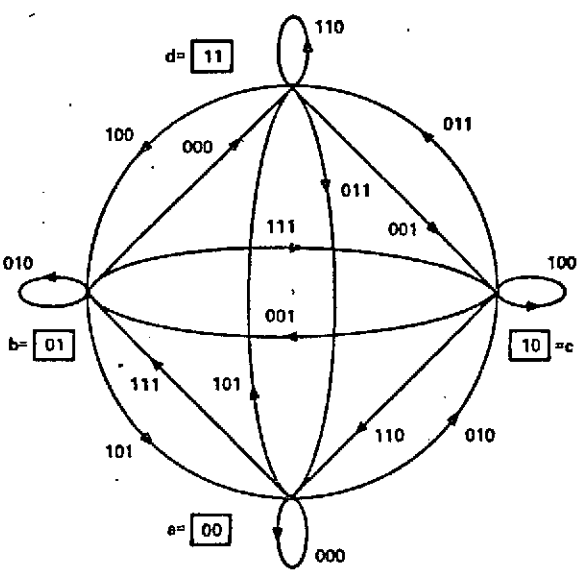


FIGURE 3.17 STATE DIAGRAM FOR CODE OF FIGURE 3.16

conditions occur. This is called a catastrophic error code. An example is shown in Figure 3.18. Suppose all zeros were sent, i.e., we should stay at state "a" forever, and suppose an error caused us to go to state "d," then we can never get back to the "a" state because the self loop of state "d" outputs coded 0's for input 1's just like it would for input 0's. The decoder would assume that 1's came in instead of 0's, thus one error in the channel causes a decoder to output an infinite number of 1's, i.e., errors (all 0's sent).

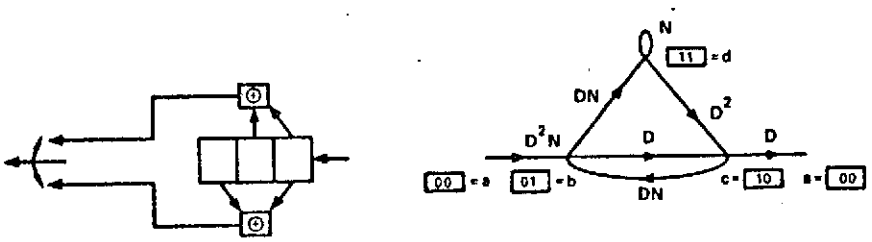


FIGURE 3.18 CODER DISPLAYING CATASTROPHIC ERROR PROPAGATION

The object of the game, therefore, is to pick a code with the largest minimum distance which is not catastrophic. This has been done for a number of constraint lengths, rates, etc.

Further discussion of choosing codes will be found in the sections on decoding since some codes are better suited to, say, sequential decoding than, say, feedback decoding and vice versa.

As a final comment on encoding it can be seen that the complexity of the encoder is negligible, thus the impact on a power/space/weight limited vehicle is very small. This is not true of the decoders in general but they are usually on the ground where this is not a severe problem. This is a big advantage of convolutional coding.

### 3.2.3 CONVOLUTIONAL DECODING

While the encoding procedure and hardware is well defined, the method to be used for decoding a convolutional code is not. There are probably as many decoding schemes as there are people to think them up. In the following three sections of the report, the three most common methods used for decoding convolutional codes will be presented. The decoding algorithms will be developed, and typical implementations shown. For sequential decoding and maximum likelihood decoders much more detailed designs which are geared towards the IMEMD/H missions will be found. This is because the required coding gain of the missions (>5 dB) eliminates feedback decoding from consideration, i.e., long constraint lengths are required in feedback decoders to achieve this gain and this makes them too complex and costly. This will be seen more clearly after the next section is introduced.

#### 3.2.3.1 FEEDBACK DECODING[23]

Feedback decoding of convolutional codes is the most straightforward of the three major decoding techniques discussed in this section, and it is also the easiest to implement when short constraint length codes are involved. Feedback decoders grew quite naturally out of well known decoding schemes for block codes. An example will help to introduce the algorithm. Consider Figure 3.19; this is the same as Figure 3.12 with less branches shown.

The operation of a feedback decoder is as follows. Suppose a data stream of 101 was sent. This implies that the coded symbols are 111000. The decoder looks at the first two branches (box A) of received data, viz., 1010; it compares it with all possiblities in the tree. The closest branches are 1110, therefore, it assumes an error was made and that the data 10 was sent to give the branches 1110.

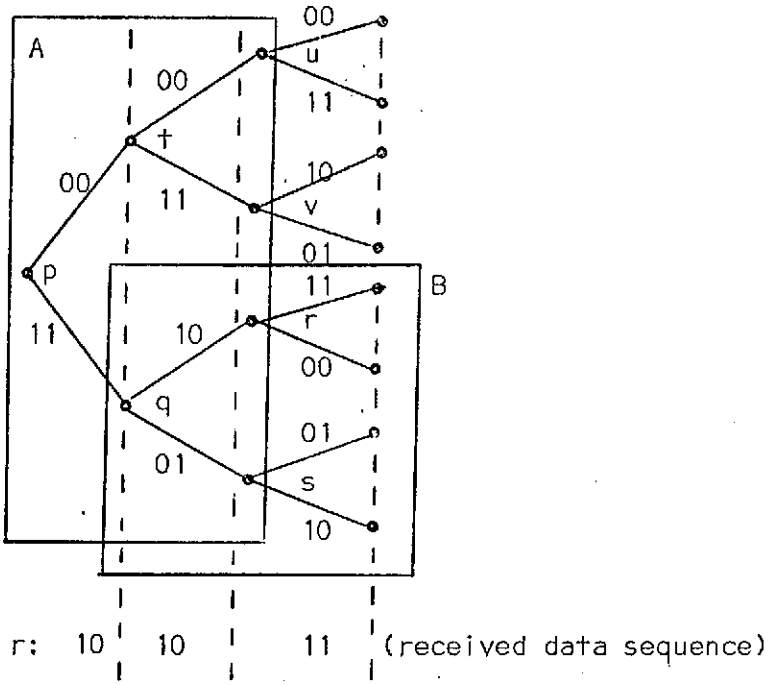


FIGURE 3.19 TREE CODE AND RECEIVED DATA

At this point the first information bit is decoded as a 1, and sent out of the decoder. The decoder now assumes that the upper paths of the tree leading to points u and v are eliminated and creates a new tree with point q as the starting point instead of point p. The whole procedure starts over again, i.e., the next two received bits are brought in and the 1011 is compared with 1011, 1000, 0101, and 0110. The closest is 1011 and so the next data bit is outputted as a 0.

Two things are important to note; they are that the number of comparisons does <u>not</u> grow (remains constant) thus the number of comparisons is dependent upon the depth into the tree chosen by the designer, and that once a decision is made there is no court of appeals, i.e., the data bit is lost forever. Overcoming this will be seen to be an advantage of sequential decoders.

Next let the power of N be a 0 if a data input 0 caused the state transition and a 1 if a data input 1 did. Figure 3.15 shows the result of relabling the state diagram as defined above.

The method introduced above is general for any system where path parameters are to be accumulated, i.e., transfer functions multiply and their exponents accumulate. The exponents are the key here. By Mason's rule [22] the overall transfer function through any path can be calculated. Define it to be T(D, N).

An important side point is that Figure 3.15 has broken the "a to a" loop in Figure 3.14 with one "a" as the input and the other as the output of the diagram. This can be done with any state, but the all zeros path is convenient, and the results of the analysis of bit probability will not change with the loop choice. This is so because of a property of the code called the group property, namely, the error correcting capability of a group code is independent of the data input, i.e., if three errors are corrected when all zeros are sent, then three errors will be corrected if any other data sequence of the same length was sent.

With the above assumptions the probability of error, $P(\varepsilon)$ for a given encoder is less than a certain function, viz.,

$$P(\varepsilon) < \operatorname{erfc}\sqrt{\frac{E_s 2d}{N_0}} \quad \exp\left(\frac{E_s d}{N_0}\right) \left.\frac{\partial T(D,N)}{\partial N}\right|_{N=1,\ D=\exp(-E_s/N_0)} \qquad (3.16)^*$$

where $E_s$ is the energy per coded symbol (recall d was the minimum distance between code words).

---

* $\operatorname{erfc}(x) \triangleq \frac{2}{\sqrt{\pi}} \int_x^\infty e^{-\alpha^2}\, d\alpha$

Expression (3.16) looks complicated, but what it says is the following. If no coding is used, then,

$$P_{NC}(\varepsilon) = \frac{1}{2}\,\mathrm{erfc}\sqrt{\frac{E_s}{N_0}}\ , \tag{3.17}$$

whereas if coding is used the probability of error is less than this. The reasons are because $d \geq 1$ implies the argument of the erfc in (3.16) is larger by the factor $2d > 1$ and because the factor

$$\exp\left(\frac{E_s d}{N_0}\right) \times \left.\frac{\partial T(D,N)}{\partial N}\right]_{N=1,\ D=\exp(-E_s/N_0)}$$

can be made less than 1.

As a concrete example, for the encoder of Figure 3.10

$$P(\varepsilon) < \frac{1}{2}\ \mathrm{erfc}\sqrt{\frac{5E_s}{N_0}}\ \left(\frac{2}{1-2^{-E_s/N_0}}\right). \tag{3.18}$$

Comparing performance with the uncoded system at $E_s/N_0 = 3$ dB we get

$$P_{NC}(\varepsilon) = 2.3 \times 10^{-2} \quad \text{uncoded} \tag{3.19}$$

$$P(\varepsilon) < 1.6 \times 10^{-5} \quad \text{coded} \tag{3.20}$$

Suppose $P(\varepsilon) = 1.6 \times 10^{-5}$ then the $E_s/N_0$ needed in an uncoded system is 9.4 dB, which means that coding has produced at least a 6.4 dB gain over an uncoded one, i.e., less than 1/4 the power need be transmitted with a coded system. In a power limited project this is significant.

By way of summarizing this section on coding theory, it can be said that in an ideal system using coding much less power has to be transmitted due to the increased dissimilarity in the output symbols. The next few subsections of the report deal with the degradations due to a practical system's departure from the ideal case assumed in the preceeding discussion.

Now what determines how powerful the decoder is, i.e., why would one decoder make less errors than another? It will be recalled that the information about a particular data is related intimately to the constraint length, K, therefore it would be best to choose the depth into the tree in any set of comparisons to be at least as great as the constraint length. This however increases the complexity by $2^K$ since the number of branches grows by this factor. It can be seen then that if K needs to be large then the complexity gets out of hand rapidly.

It can be shown that the bit error probability decreases exponentially with K under the appropriate conditions, i.e.,

$$P(\varepsilon) < \frac{2^{-K\,R_o/R}}{1-2^{-[(R_o/R)-1]}} \quad . \qquad (3.21)$$

*

This was derived under the assumption of a maximum likelihood decoder. Feedback decoding cannot be expected to be as powerful and indeed it is not. The conclusion then is that the K needed with feedback decoding is much larger than maximum likelihood decoding, and so feedback decoding is only practical for moderate coding gains, say, 1 to 2 dB.

One might ask why feedback decoding is ever considered for system designs. The answer is that sequential, maximum likelihood, and feedback decoders are very sensitive to bursts of errors, such as might be due to lightning or switching transients, and feedback decoding is the only one of the three where this problem can be circumvented in the least complex manner. This is done by delaying adjacent code bits long enough so that bursts of errors do not corrupt a string of data related bits, and the process is called interleaving. In a feedback decoder the interleaving can be done as

---

* $R_o$ is the practical channel capacity.

an integral part of the encoder and decoder, whereas in the other two schemes for decoding the interleaving must be done externally.

Since feedback decoding will not be considered any further for this study due to the reasons given above a detailed design will not be attempted, however, two examples of these decoders will be presented below in the interest of completing the topic.

Consider[8] the operation of the single error correcting decoder shown in Figure 3.20. A 1/2 rate systematic code is assumed so that every other bit is an information bit. The commutator alternates so that information bits are supplied to the data register and parity bits are supplied to the lower adder. The upper adder recomputes the parity bits using the received data bits. If there are no errors the lower adder output injects all zeros into the 2-bit error register.

Now suppose that a single error occurs in the form of a received parity bit error. The lower adder injects a "1" into the $E_1$ position. Since only a single error is assumed to occur no "correct pulse" is sent ("and" gate is disabled). Subsequent parity bits are correct and so zeros are shifted into $E_1$, eventually discarding the 1 out of $E_2$, thus a single parity error has no effect.

Suppose that a single error occurs in the form of a received data bit error. The upper adder outputs a "1" to the lower adder which, in turn, injects a "1" into position $E_1$ of the error register. Now since the error is propagated to the $B_2$ position the same process occurs and results in a "1" being injected into position $E_2$ from $E_1$ and a "1" injected into position $E_1$. This enables the "and" gate which sends an invert (correct bit) pulse to the $B_2$ position.

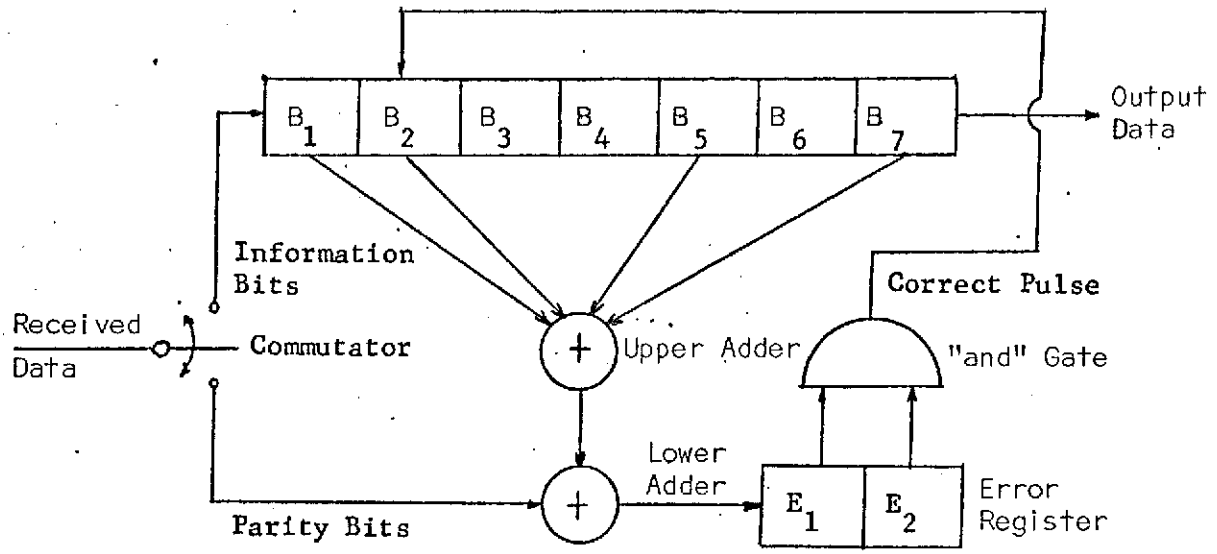


FIGURE 3.20 CONVOLUTIONAL DECODER (SINGLE ERROR CORRECTING)

In terms of the tree of the code this decoder looks at seven branches per decoding cycle. The upper register of the decoder is simply a replica of the encoder used to generate the code. Everything works fine as long as two consecutive errors do not occur. If this happens the decoder fails.

The next example of a decoder shows how bursts of errors can be corrected. In between burst errors there are good pulses for a fairly long period of time so the codes developed previously are wasteful and inadequate when the noise bursts do occur (mechanization complexity must always remain a factor). A code which works well in burst noise (sometimes called impulse noise) is one which makes use of the sequence of good bits in the stream to

correct the bad bits and in doing so reduces complexity. Consider the following block diagram (Figure 3.21). The encoder shown operates by

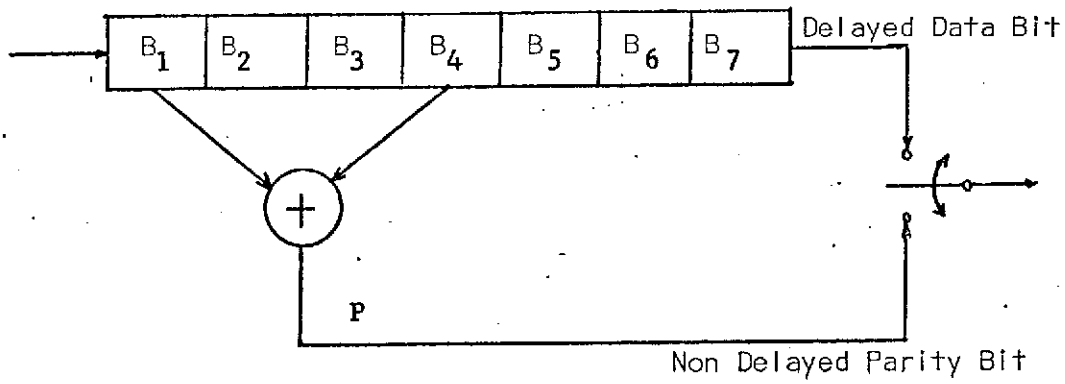


FIGURE 3.21 BURST ERROR ENCODER

performing a parity check on positions $B_1$ and $B_4$. It sends the parity bit on alternate shifts of the register. An output code word might look like

$P_1 O P_2 O P_3 O P_4 O P_5 O P_6 O P_7 I_1 P_8 I_2 P_9 I_3 P_{10} \ldots$*

if the encoder operation started after $I_1$ was shifted into position $S_1$.

The burst correcting properties appear in the decoder as shown in Figure 3.22. Assume that $B_1$ thru $B_7$ and $T_1$ thru $T_{10}$ contain correct values, i.e., that a stream of good bits has been received. Now suppose that a bad data or parity bit enters the decoder. The bad parity bit doesn't alter anything since the "tap" in the parity register is in the $T_7$ position. However, a wrong data bit entering $B_1$ generates an error in

* Note that the parity check $P_1$ is sent long before $I_1$ is sent. This fact will have more significance when the decoder is studied.

the R circuit causing an output of "1" to the "and" gate. Since the data bit error is not present in the $B_4$ and $B_7$ positions, the Q circuit sends a "0" to the "and" gate. This situation disables the gate and causes it to disable the "$B_4/B_5$ inverting circuit" so that the information bit in $B_4$ shifts to the $B_5$ position without inverting (correcting).

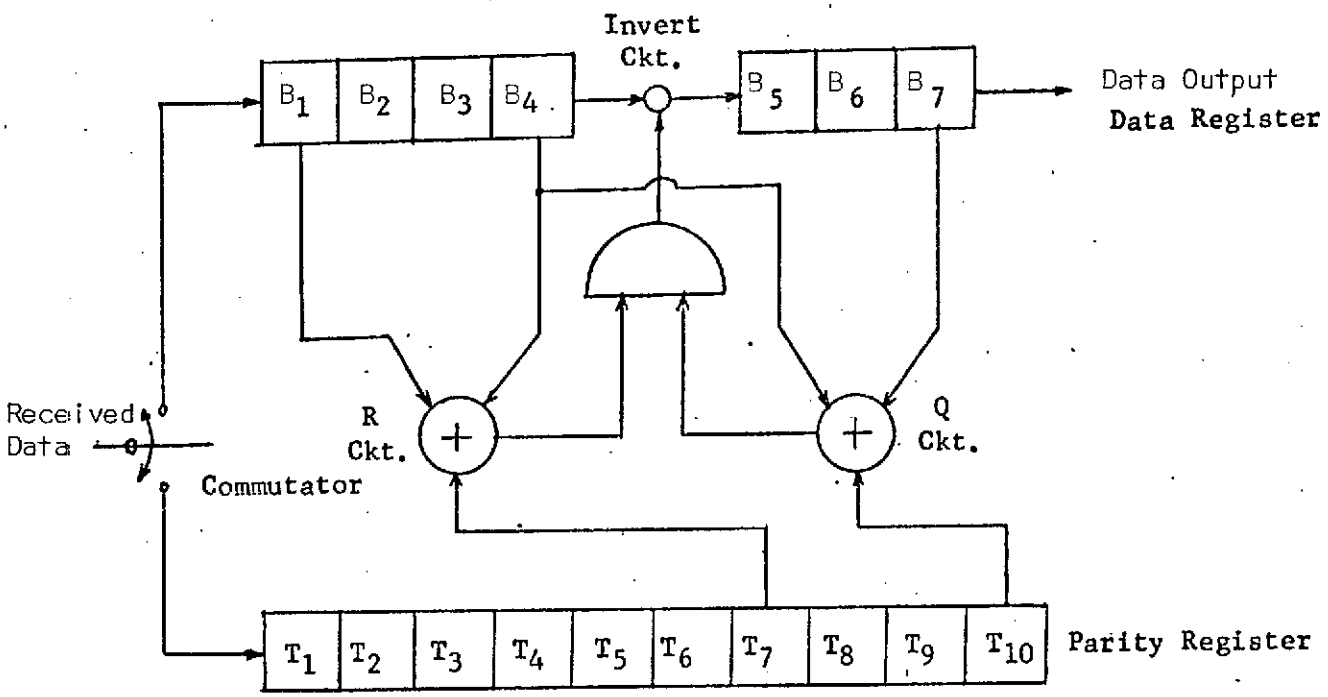


FIGURE 3.22 BURST ERROR DECODER

When the data error propagates so that it is in the $B_4$ position it causes an error in the Q circuit thus outputting a "1" to the gate. Now assuming that $B_1$ is correct the $B_4$ error also causes the R circuit to output a "1" to the gate. This enables the gate and it inverts the bit in $B_4$ as it shifts to the $B_5$ position (note that when the data bit error is in the $B_4$ position any parity bit error still hasn't reached the tap on the parity register).

The encoder/decoder discussed on the previous page corrects a burst of length six, i.e., there can be at most three data bit errors and three parity bit errors. Under this assumption there will be a "cleansing" of the decoder before any new bursts of length six enter it. It should be noted that since the parity taps are three bits apart any parity errors cannot cause the R and Q circuits to simultaneously output 1's to the gate. This encoder/decoder pair is much simpler than the circuits studied before and yet corrects up to six errors, but it must be kept in mind that it fails miserably if the bursts are not far enough apart.

For communications channels which are noiseless for long periods of time, but for which many word errors are probable for short periods of time, burst error coding works. The code depends on the long noiseless periods to provide enough good bits to cleanse the decoder so that it can correct the next burst of errors.

In summary, then, many different types of feedback decoders are available depending on the application. These decoders are especially applicable to burst error channels, and are not powerful enough to be of much use on random error channels.

### 3.2.3.2 MAXIMUM LIKELIHOOD DECODING

#### 3.2.3.2.1 Maximum Likelihood Decoding Theory [20]

In this section, the Maximum Likelihood Decoder (MLD) and its algorithm will be described. Since the MLD is one of two convolutional decoders which can provide the coding gain needed for the IMEMD/H missions (>5 dB) it will be analyzed to an extent sufficient to provide a firm basis for a decision between it and sequential decoding (SD) in the final tradeoff.

Cost, hardware complexity, network interface, and other factors will be presented together with a block diagram of a practical decoder.

Maximum Likelihood Decoding of convolutional codes was first introduced by Viterbi[24] and his description of it will for the most part be followed here. More detail will be given, though, so that the algorithm can be better understood. It will be recalled from the convolutional coding theory that a trellis representation of the code contained all of the information about a particular encoder, i.e., given an encoder and the trellis, the code output for any data input could be generated.

The encoder of Figure 3.10 and its trellis of Figure 3.13 are reshown in Figure 3.23 below. Consider in detail how the trellis comes about. The encoder stages $B_0$ and $B_1$ are <u>defined</u> to be the state of the encoder. Now given any two consecutive states the value of the encoder stages and the coded output can be found, e.g., let the two consecutive states be, say, a = 00, b = 01 then the register had $B_0 = 0$, $B_1 = 0$ prior to the shift and $B_0 = 0$, $B_1 = 1$ after the shift, but since $B_1 = 1$ after a shift implies $B_2 = 1$ before the shift, the register loading before the shift must have been $B_0 = 0$, $B_1 = 0$, $B_2 = 1$. Looking at the encoder adder inputs, the code output must be

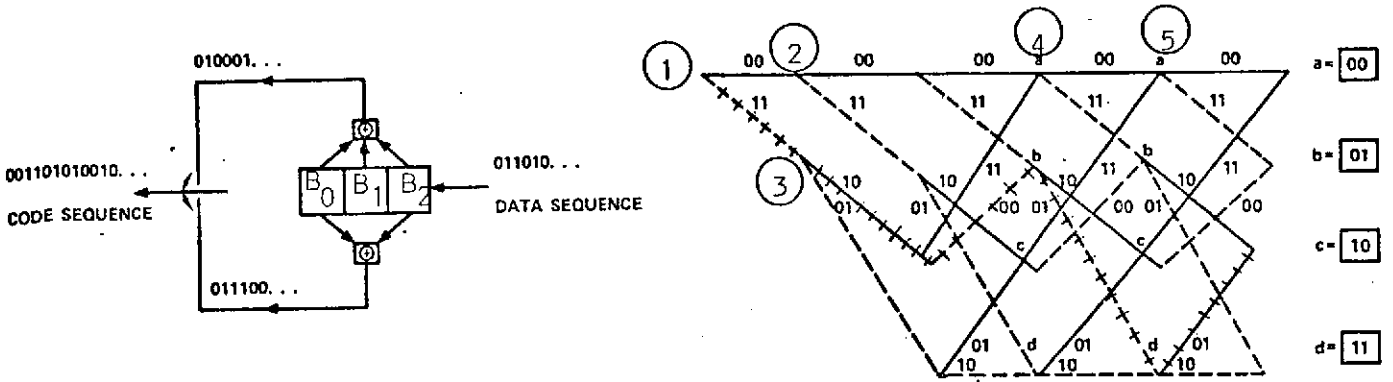


FIGURE 3.23 CONVOLUTIONAL ENCODER WITH TRELLIS DIAGRAM

$(B_0 + B_1 + B_2)$, $(B_0 + B_2)$, i.e., (1), (1). In the trellis then we use a dashed line if $B_2 = 1$ prior to a shift and a solid line if $B_2 = 0$. In the example above looking at <u>any</u> point labeled "a", we follow a dashed line to a "b".

Note that the word "any" was underlined in the above paragraph. This is because the encoder doesn't care where the $B_0B_1$ stages got the zeros or where in the data stream this occurred. It only knows that it has $B_0 = 0$ and $B_1 = 0$ right now! This concept is vital and is the basis for drawing a trellis.

Now to draw a trellis from a particular encoder (assume binary data, i.e., 0, 1 and one bit per shift) start with $B_0 = 0$, and $B_1 = 0$ and define this as state "a"; this is point ① in the trellis (see Figure 3.23). Now $B_2$ will be assumed to have in it the first data bit. Suppose $B_2 = 0$, then the next shift will cause the state to switch to $B_0 = 0$, $B_1 = 0$, i.e., state "a" this happen via a 0 data bit, therefore use a solid line from "a to a" (point ② in the trellis). Suppose by contrast that the first data bit was a 1 instead, i.e., $B_2 = 1$, then after the first shift the state would be $B_0 = 0$, $B_1 = 1$ (point ③ in the trellis). Define $B_0 = 0$, $B_1 = 1$ as state "b". Since a data bit of 1 was used to get from state "a to b" use a dashed line in the trellis.

As can be seen in the trellis the output of the adders can be put as labels on the branches from state to state to allow a user of the trellis to find the coded stream. Note that given state "a" one can only end up at state "a" or state "b" after a shift due to only two data bit possibilities, viz., 0 or 1.

Now given that we are either at state "a" (point ②) or state b, (point ③) the previous process can be repeated indefinitely until the trellis is drawn. To give a concrete example suppose the input data stream was 10110. Assuming an initial state of "a" the state sequence goes as follows; 00, 01, 10, 01, 11, 10, i.e., a to b to c to b to d to c where the states are defined as in Table 3.14.

state a: $B_0 = 0, B_1 = 0$

state b: $B_0 = 0, B_1 = 1$

state c: $B_0 = 1, B_1 = 0$

state d: $B_0 = 1, B_1 = 1$

TABLE 3.14 STATE DEFINITIONS

This path is shown as a cross hatched path in Figure 3.23. Note that if the states are overlapped that the data bit stream is recovered. In the example above one has

$$\left\{\begin{matrix} a\ c\ d \\ b\ b\ c \end{matrix} \Rightarrow \begin{matrix} 001011 \\ 010110 \end{matrix}\right\} \Rightarrow 10110.$$

In terms of a decoding algorithm consideration of the trellis shows a technique to follow. Assume for the moment that the Hamming distance, i.e., the number of bits different between two binary sequences, is applicable, e.g., d(000,101) = 2 and d(000,111) = 3. Suppose the first six received (noise corrupted) bits were 010001. Looking at the trellis this sequence is closer to 000000 than 111011, i.e., the two paths to the first state "a" (point ④ in Figure 3.23). The distances are 2 and 3, respectively.

Consider now the first eight received bits, say, 01000111. The distances to state "a" after eight code bits (point ⑤ in the trellis) assuming it has passed through state "a" after six code bits (point ④ in the trellis) is 4 or 5. There are two ways of arriving at these figures. The first is to brute force compare 00000000 with 01000111 and 11101100 with 01000111. The other way, which is the basis of the algorithm, is to simply take the distances up to state "a" after six code bits and add on the differential (transition) distance to the next state "a", i.e., $\Delta d(00,11) = 2$.

The important point of the above is that once the best path up to state "a" has been determined there is no need to keep any inferior paths because the total distance will only change with new code bits.

The algorithm is then as follows:

1. Initially, calculate the distances between all paths leading to all of the states and the received sequence up to and including a depth into the trellis or tree of K branches.
2. Pick the least distance path to each state (call these the survivor paths) and throw away the others, i.e., drop them from memory.
3. Again for all the states, calculate the differential distances between all paths leading to the states and the next received code sequence branch.
4. Add these differential distances to the appropriate survivor distances so that a continuous path results to a state.
5. Comparing all distances to a particular state, choose the path (survivor + differential path) with the least distance (this is the new survivor to the state). Do this for all states.
6. After a suitable* number of branches have been received look at the first bit of all hypothesized data sequences (a result of iterations of the above). Choose the bit which is in the majority.

---

* Elaborated on later

7. Continue in this manner until all data has been decoded realizing that the last state will be forced to state "a" by injection of zeros into the encoder at the end.

If the decoder follows the above algorithm, it can be shown that the decoder is a maximum likelihood decoder, thus all the theory developed previously applies to data decoded in the above manner.

In a practical decoder there are several details and implications of the MLD which must be considered. These are:

- Choice and calculation of the distance function (metric)
- Comparison of paths
- Storage requirements
- Branch synchronization, i.e., where does a branch start?
- Quantization of the distance function (metric) for digital processing
- Overflow of metric storage
- Underflow of metric storage
- Number of branches stored before making a data bit decision (path delay)
- Provision for coin flipping in case of a tie in decisions
- Parallel versus serial implemenation (depends of data rates)
- Code restart after burst errors
- Logic speed versus code rate
- Transparent versus non transparent codes
- decoding delay
- noisy reference and timing
- memory and buffer size

Some of the above are an obvious consequences of a practical rather than theoretical decoder implementation and will not be discussed;

the rest will be touched upon as the design of the decoder given below evolves.

3.2.3.2.2 Maximum Likelihood Decoder Design

The error correction unit described in this section will consist of a rate 1/2 convolutional encoder* with a Viterbi (Maximum Likelihood) decoder. The encoder/decoder design will accommodate bit rates up to 20 kb/s, thus the maximum desired operating rate of 16 kb/s will be covered with leeway for some adjustment in the rate. The units can use large scale integrated (LSI) circuitry to optimize speed, space, and power if required.

The performance of Viterbi decoding when used with optimal (maximum distance) codes is shown in Table 3.15 along with a non-optimal transparent code chosen for comparison purposes. The values in the table were obtained by computer simulation.

The error correction unit which was chosen was a K=7, nonsystematic, transparent, and noncatastrophic convolutional code with the corresponding Viterbi decoder. This decision was based on the following factors:

1) The required value of $E_b/N_0$ can be obtained by the encoder/decoder design.

2) Low power considerations can be met with the design.

3) The transparency of the code offers no degradation in $E_b/N_0$ if differential encoding were not used.

4) The K=7 specification requires the least amount of complexity in hardware for the coding gain required.

The following sections, however, offer trade-off performance curves for the constraint lengths of five, six, and seven for completeness.

* The encoder design is discussed here since it is matched to the decoder.

| Output Error Rate | Uncoded CPSK $E_b/N_0$ | Uncoded DCPSK $E_b/N_0$ | K =7 | | K = 6 | | K = 5 Optimal Code | | |
|---|---|---|---|---|---|---|---|---|---|
| | | | $E_b/N_0$ | Coding Gain over CPSK | $E_b/N_0$ | Coding Gain over CPSK | $E_b/N_0$ | Coding Gain over CPSK | Coding Gain over DCPSK |
| $1\times10^{-5}$ | 9.6 | 9.9 | 4.4 | 5.2 | 4.9 | 4.7 | 5.2 | 4.4 | 4.7 |
| $1\times10^{-4}$ | 8.4 | 8.8 | 3.7 | 4.7 | 4.1 | 4.3 | 4.4 | 4.0 | 4.4 |
| $1\times10^{-3}$ | 6.8 | 7.3 | 3.0 | 3.8 | 3.3 | 3.5 | 3.5 | 3.3 | 3.8 |
| $1\times10^{-2}$ | 4.3 | 5.2 | 2.1 | 2.2 | 2.3 | 2.0 | 2.4 | 1.9 | 2.8 |

| K = 5 Transparent Code (Δ-Decoded) | | | |
|---|---|---|---|
| Output Error Rate | $E_b/N_0$ | Coding Gain over CPSK | Coding Gain over DCPSK |
| $1\times10^{-5}$ | 5.6 | 4.0 | 4.3 |
| $1\times10^{-4}$ | 4.8 | 3.6 | 4.0 |
| $1\times10^{-3}$ | 3.9 | 2.9 | 3.4 |
| $1\times10^{-2}$ | 2.8 | 1.5 | 2.4 |

TABLE 3.15

VITERBI DECODING OUTPUT ERROR RATE PERFORMANCE

Soft Decision Q = 8
(No Δ-decoding except the K=5 transparent code)

Interface considerations are offered in the following sections together with the hardware approach and some design factors for the coder/decoder unit.

3.2.3.2.2.1 Performance of the Maximum Likelihood Decoder

In this section, the performance of the maximum likelihood decoder for K=5, 6 and 7; rate 0.5; convolutional codes will be presented. The codes studied are listed in Table 3.16. The constraint length 5 and 6 optimal codes are nontransparent to phase reversals while the constraint length 5 nonoptimal and constraint length 7 optimal codes are transparent.

| CONSTRAINT LENGTH | CODE POLYNOMIAL |
|---|---|
| 5 (nonoptimal) | {10011}<br>{11001} |
| 5 (optimal) | {10011}<br>{11101} |
| 6 (optimal) | {111101}<br>{101011} |
| 7 (optimal) | {1111001}<br>{1011011} |

TABLE 3.16
CONVOLUTIONAL CODES STUDIED

A code is transparent if the coded output sequences of two complementary information input sequences are themselves complements of one another. Transparency of the code can be useful in a system which may have a phase polarity ambiguity but it is in no way a requirement, e.g., a phase reversal detector can be incorporated into the decoder itself in lieu of the transparency.

The codes shown in Table 3.16 are the optimal codes for their constraint length except as noted. Optimality is defined here as possessing the largest minimum free distance among all codes of identical constraint length.

From a hardware standpoint, it is desirable to use a code of short constraint length (K) since as the constraint length of the code is increased, the hardware growth is exponential (due to the increase number of states). Another hardware problem is to choose the length of the path memory truncation or decoding delay. The problem here is to determine the minimum number of bits to be retained in the path memory without a significant loss in performance. Since there are $2^{K-1}$ path memories, storage must be allocated for $(N \cdot 2^{K-1})$ bits where N is the number of bits retained in each path. It will be seen later that five constraint lengths will be sufficient (N=5K).

The channel will be modeled as an Additive White Gaussian Noise Channel for all simulations in this section. This is an accurate model for satellite links. As a reference, the probability of a bit error as a function of the signal-to-noise ratio ($E_b/N_0$) for ideal CPSK and differentially encoded PSK (DCPSK) is shown in Figure 3.24. A typical error rate of interest is $10^{-5}$ which for CPSK is achieved at $E_b/N_0$ = 9.6 dB; and for DCPSK, at 9.9 dB.

3.2.3.2.2.2 Decoder Delay and Constraint Length

The performance as a function of code constraint length and decoding delay is considered in this section. For the results presented in the following, the decision statistic for the most delayed bit* in the path memory is the most likely path metric. Also, the allocated metric storage is four bits with provisions for clamping and resetting.

* Due to the most recently received branch

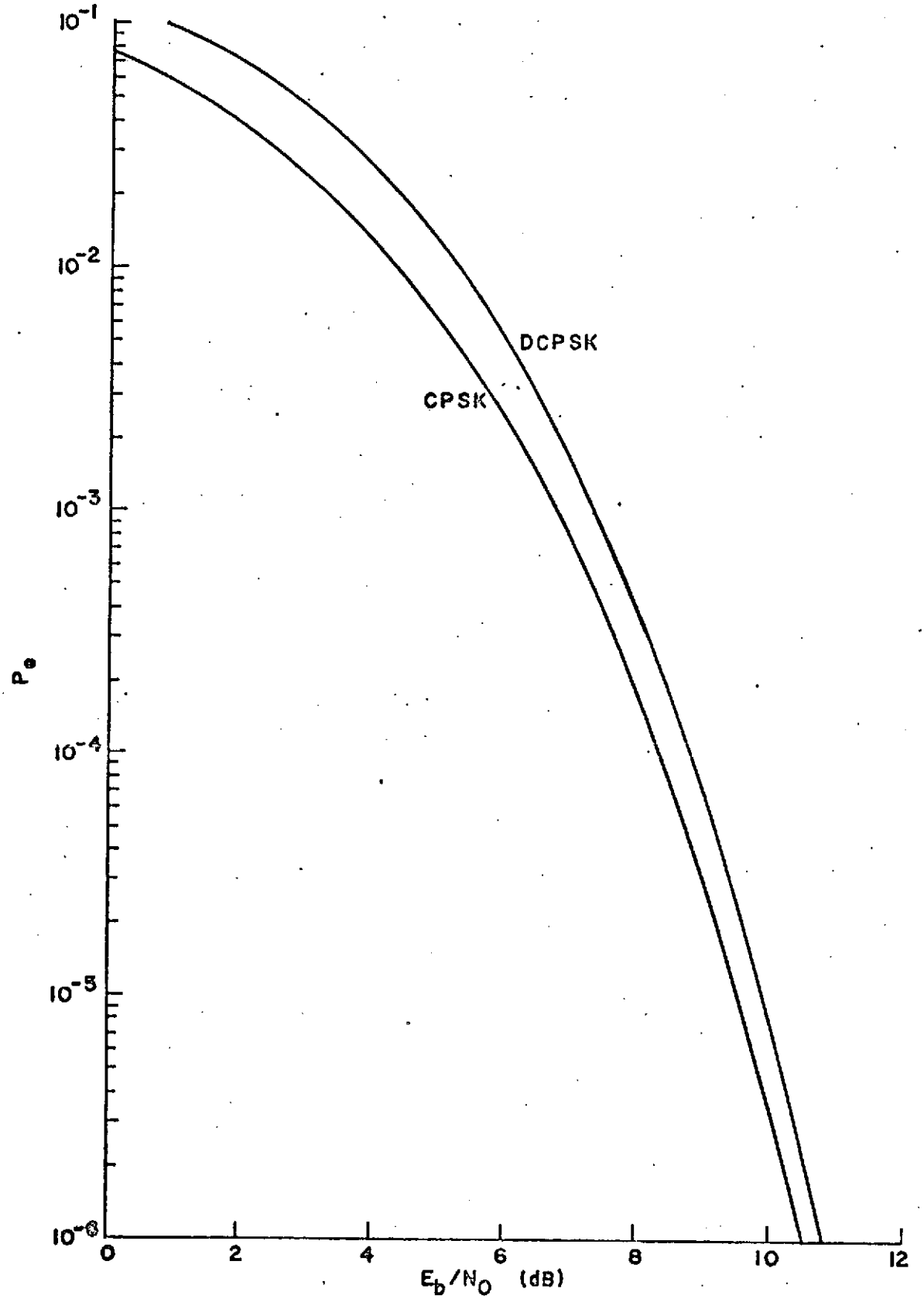


FIGURE 3.24 PROBABILITY OF A RAW BIT ERROR VS. $E_b/N_0$ FOR IDEAL CPSK AND DCPSK ON THE ADDITIVE GAUSSIAN NOISE CHANNEL

The performance curves for the soft-decision maximum likelihood decoders for constraint length 5, 6, and 7 codes are shown in Figures 3.25, 3.26, and 3.27. The soft-decision inputs are uniformly quantized to three bits.

Figure 3.25 shows the performance of the constraint length 5 soft-decision maximum likelihood decoder for various decoding delays. The performance of the soft-decision decoder improves with increasing decoding delay. However, for a decoding delay greater than 5 constraint lengths, the return is insignificant. An average error rate of $10^{-5}$ for the constraint length five optimal code with a decoding delay of five constraint lengths is achieved at $E_b/N_0$ = 5.25 dB. This represents a coding gain of 4.4 dB over ideal two-phase PSK.

In the case of the transparent code there is a 0.2 dB loss over the optimal code shown in Figure 3.25 because the distance is 6 as opposed to the optimal of 7. At $10^{-5}$ bit error rate, then, the coding gain is only 4.2 dB over coherent PSK.

Figure 3.26 shows the results of the simulation of the soft-decision maximum likelihood decoder for the constraint length six code with variable decoding delay. The chosen decoding delay is five constraint lengths. For a decoding delay of five constraint lengths, the constraint length six soft-decision maximum likelihood decoder achieves an average error rate of $10^{-5}$ at $E_b/N_0$ = 4.9 dB for a coding gain of 4.75 dB over ideal two-phase PSK.

Figure 3.27 shows the result of the simulation of the constraint length seven soft-decision maximum likelihood decoder with variable decoding

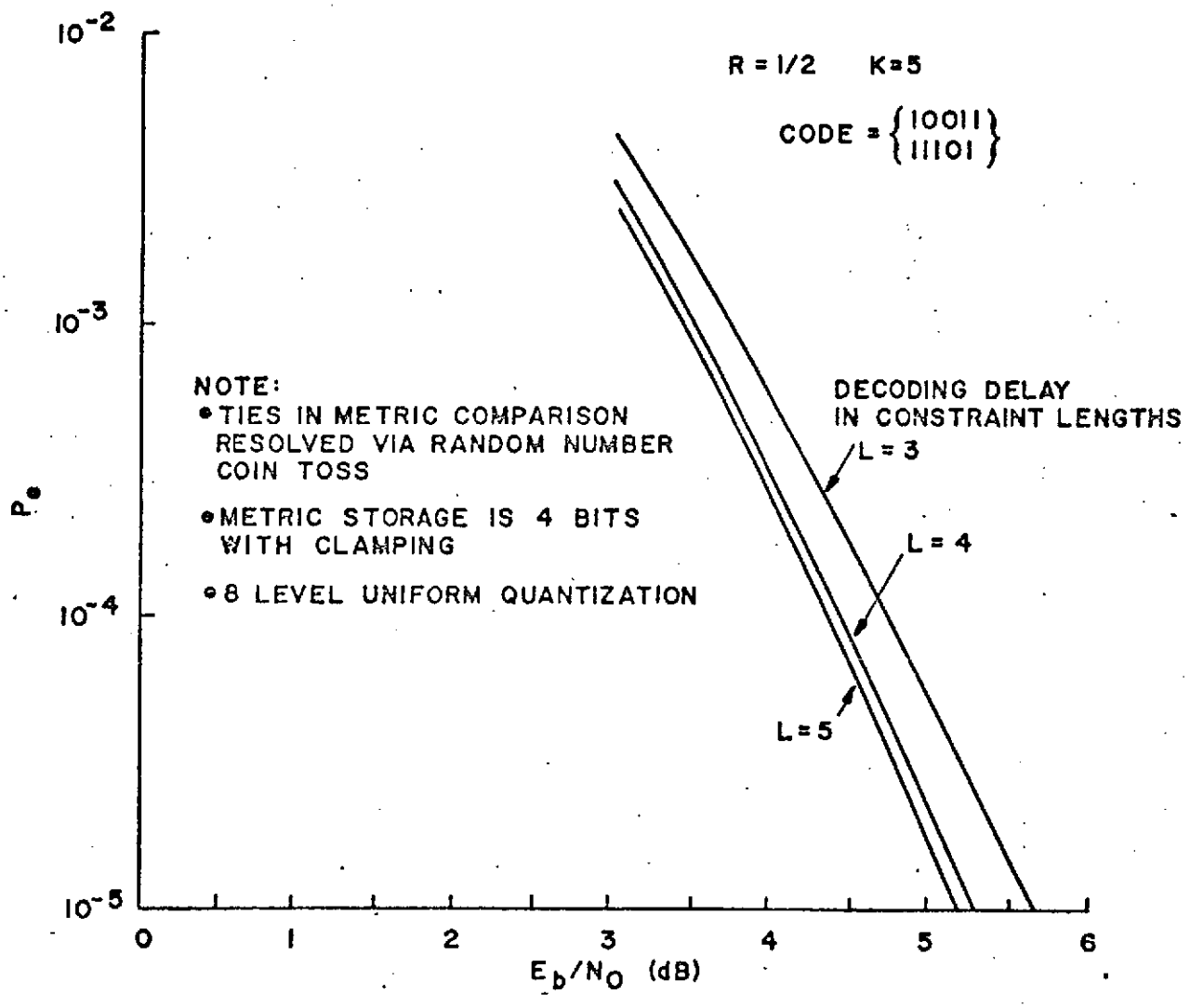


FIGURE 3.25. SOFT DECISION MAXIMUM LIKELIHOOD (K=5) DECODER PERFORMANCE USING MOST LIKELY PATH DECISION RULE ON THE ADDITIVE GAUSSIAN CHANNEL

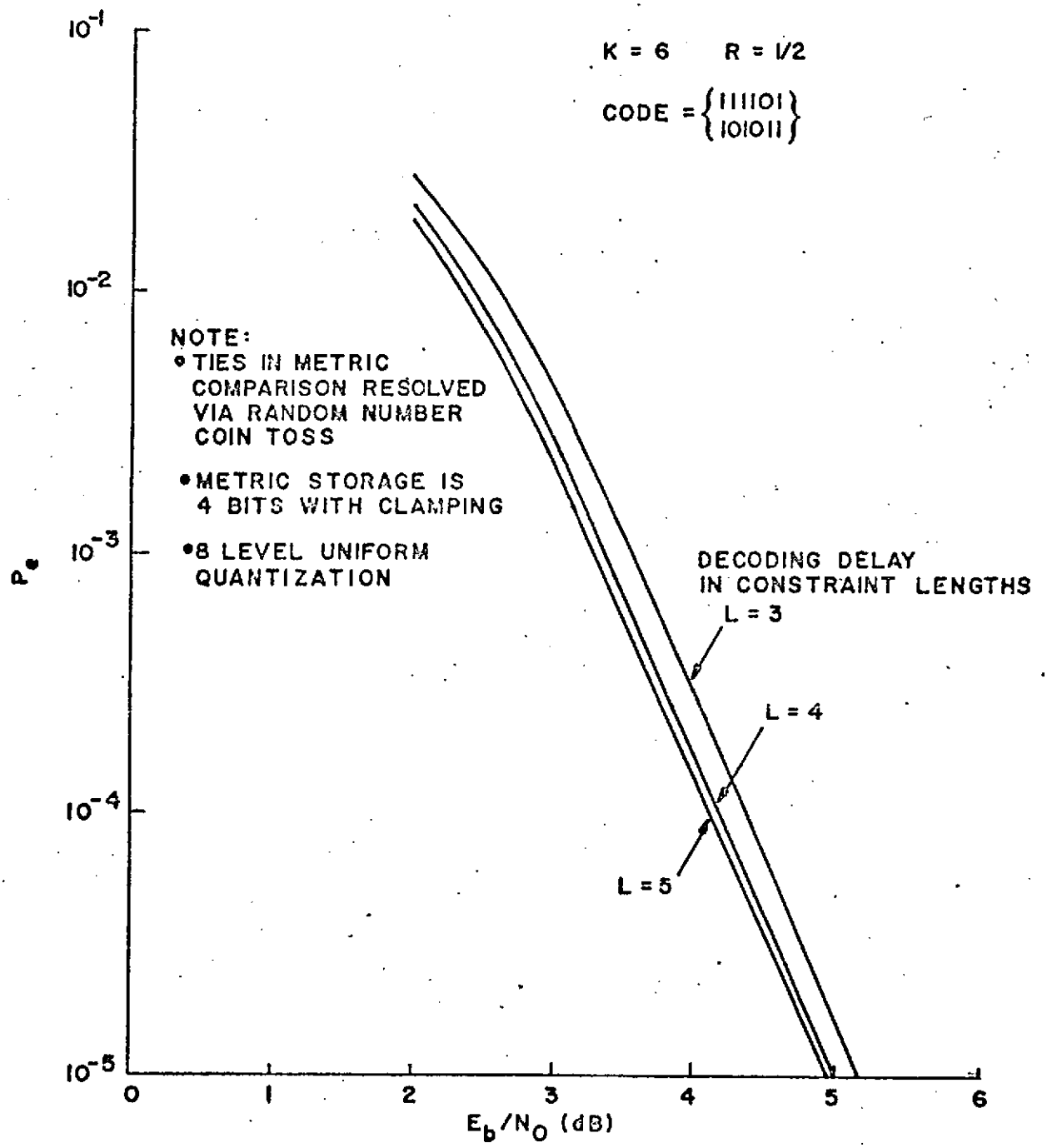


FIGURE 3.26 SOFT DECISION MAXIMUM LIKELIHOOD (K=6) DECODER PERFORMANCE USING MOST LIKELY PATH DECISION RULE ON THE ADDITIVE GAUSSIAN NOISE CHANNEL

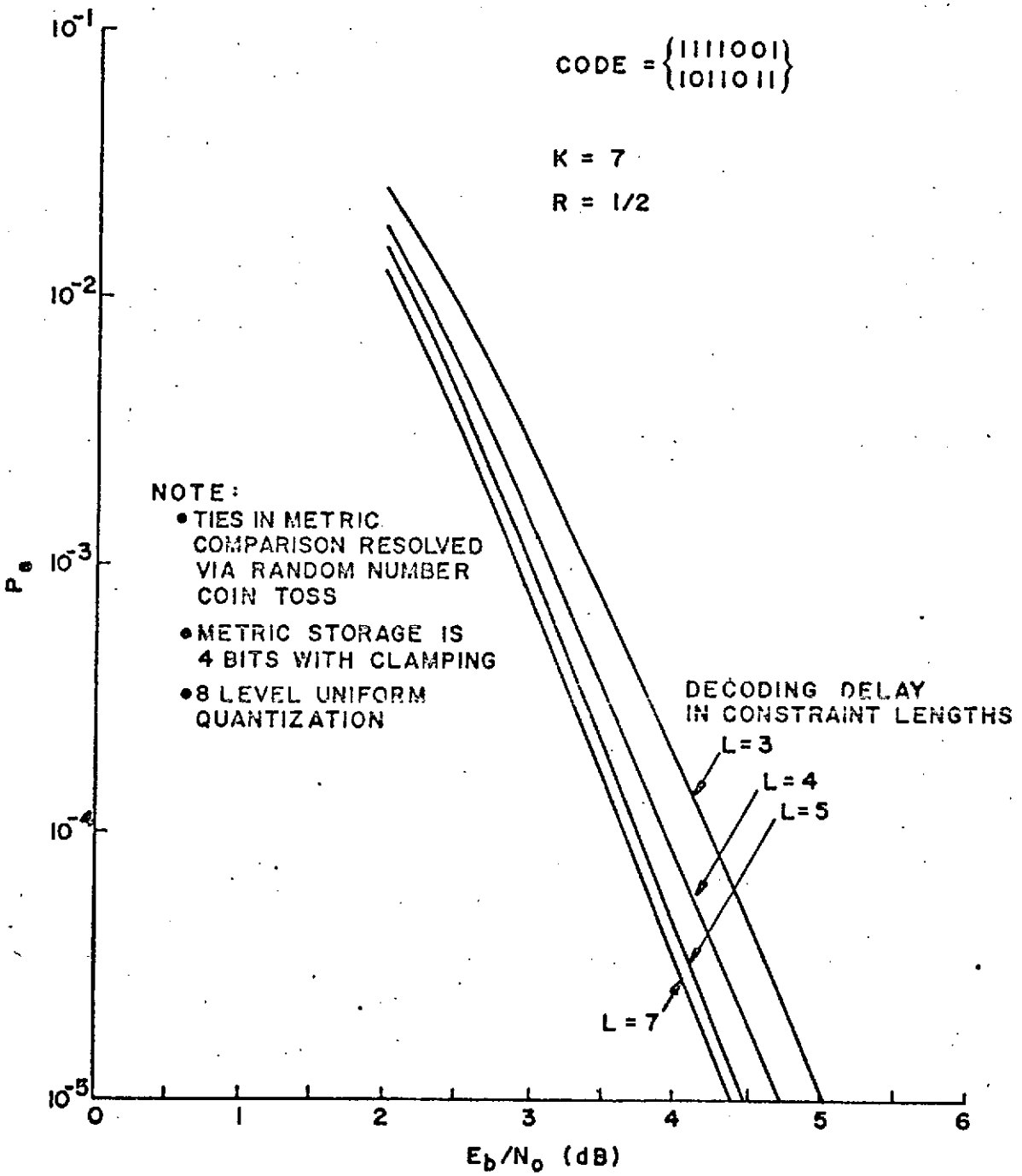


FIGURE 3.27 SOFT DECISION MAXIMUM LIKELIHOOD (K=7) DECODER PERFORMANCE USING MOST LIKELY PATH DECISION STATISTIC ON THE ADDITIVE GAUSSIAN NOISE CHANNEL

delay. To attain a coding gain of 5.0 dB or greater over ideal two-phase PSK, the decoding delay necessary is five constraint lengths. For a decoding delay of five constraint lengths, the system performs at $E_b/N_0$ = 4.4 dB for a coding gain of 5.25 dB. This was a prime reason for choosing K = 7 for the decoder design.

3.2.3.2.2.3 System Interface Considerations

The influence of the system interface on the coder/decoder is summarized in the synchronization, inversions due to phase slips in the PSK demodulator, and the quantization of the inputs to the decoder.

One of the most critical parts of the system is the quantization of the soft decisions. The equally spaced quantizer is shown in Figure 3.28 for eight levels. The input analog voltage is limited to a maximum signal excursion of $\pm K\sqrt{E_s}$ where $\sqrt{E_s}$ is the mean value of the magnitude of the received waveform. The spacing between the levels is given by

$$Q = \frac{2K\sqrt{E_s}}{N} \tag{3.22}$$

The output of the quantizer is a three-bit number. The sign bit represents the hard decision on the received channel symbol and the remaining two bits represent the magnitude of the associated confidence level.

The error performance of the decoder is sensitive to the spacing Q selected. Since the level of quantization is fixed to be three bits and to be uniformly spaced, the problem is the selection of the optimum signal excursion as input to the quantizer.

Figure 3.29 shows the results of the optimization procedure simulated on a computer for the constraint length 7 optimal code with a soft-

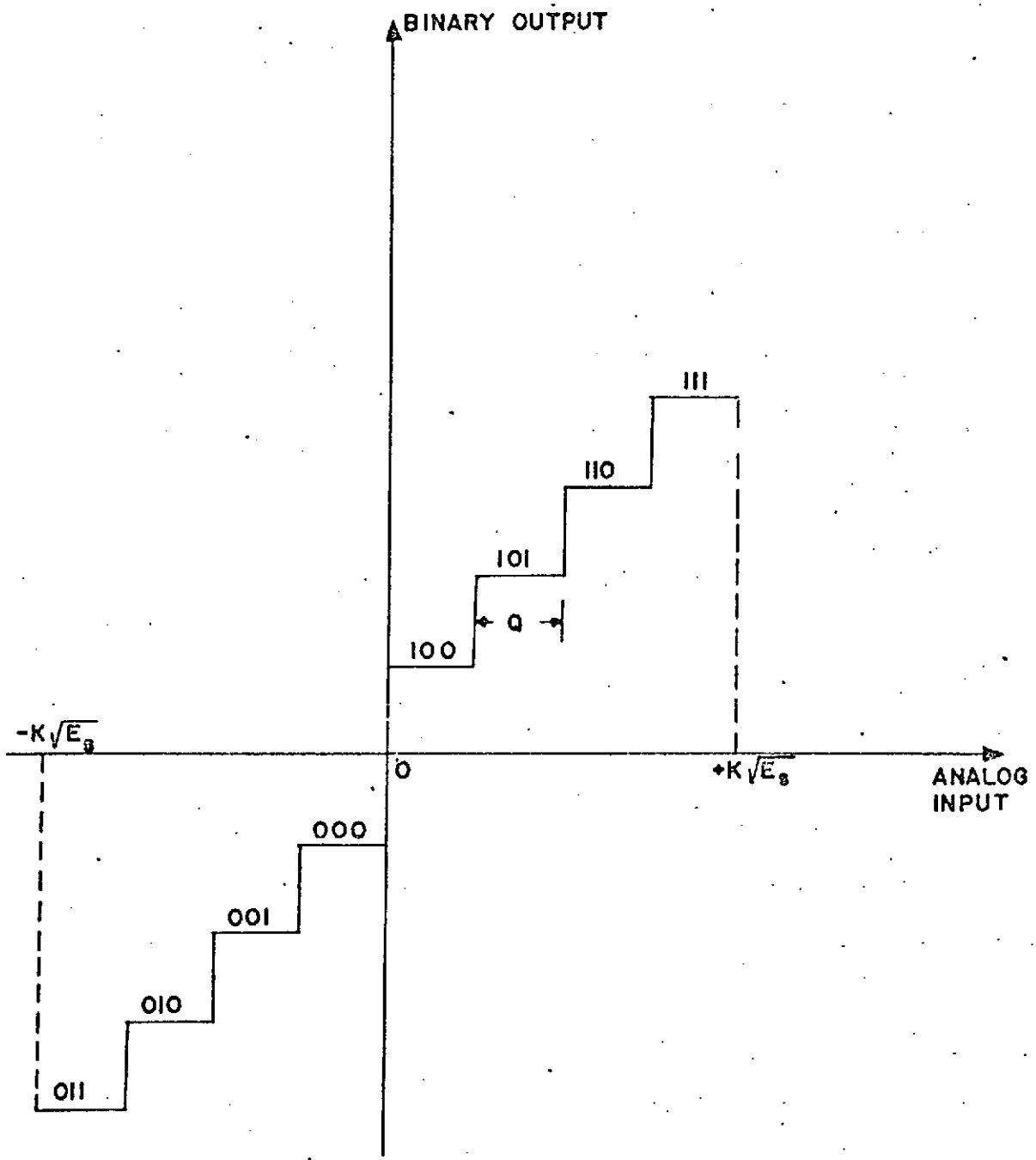


FIGURE 3.28 UNIFORM QUANTIZER (N=8 LEVELS)

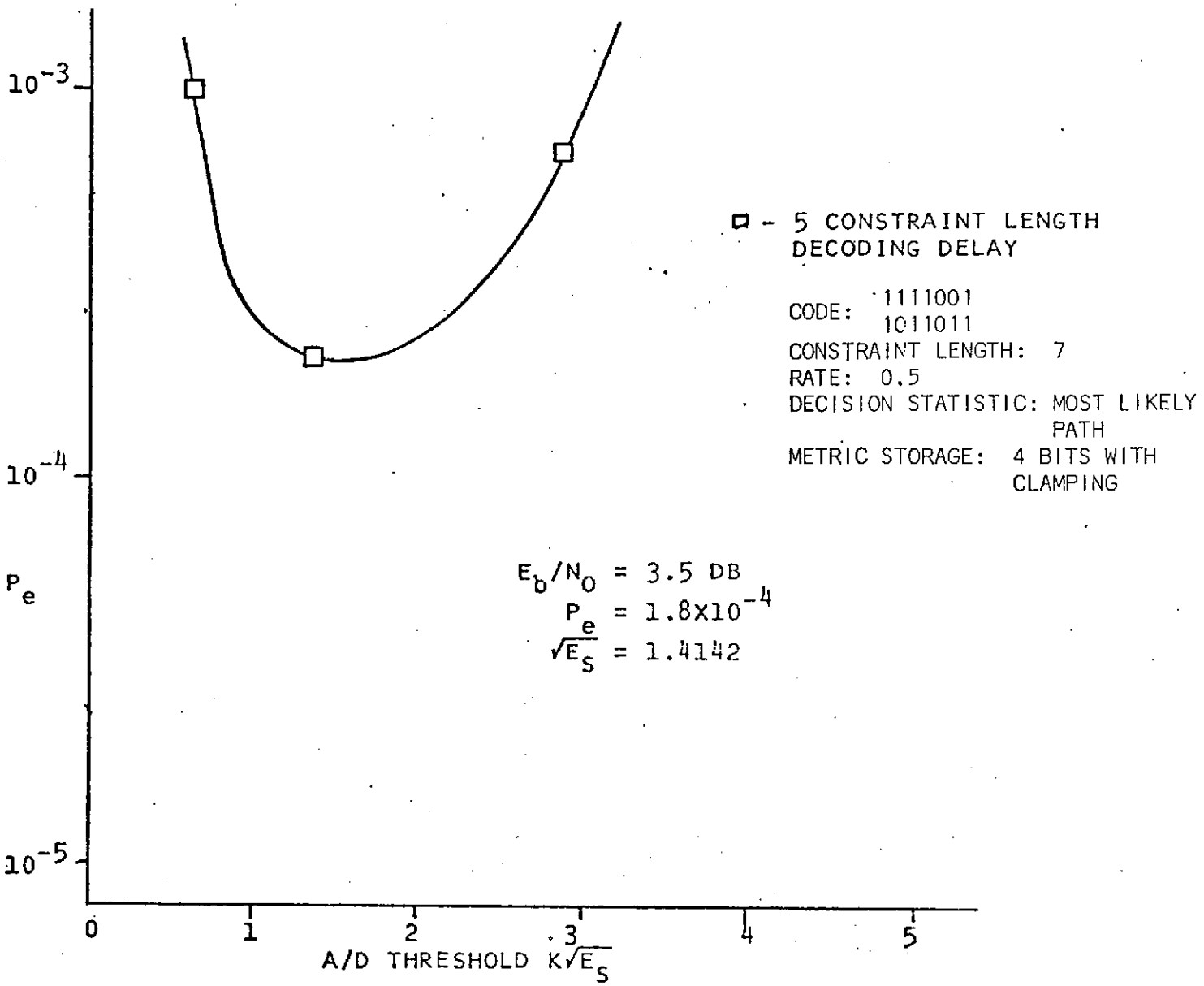


FIGURE 3.29 MAXIMUM LIKELIHOOD DECODER PERFORMANCE

decision input of 3 bits. An optimum spacing can be chosen using results such as these.

At the receiver (decoder) two timing problems arise during the transmission of data by a two-phase PSK system. They are the initial node synchronization on the code symbol pair of the rate 1/2 convolutional code and the monitoring of this synchronization. To monitor sync, the receiver is required to detect when a sync error (bit slip) has occurred and initiate action to recover from sync error.

Code symbol (node) synchronization within a branch is necessary. Clearly, if the wrong decision of code symbol pairs is made, the decoder will constantly make errors thereafter. This situation can be detected because the mismatch of code symbols will cause all path metrics to be large, i.e., there will be no correct paths.

A method of detecting this condition is to count the number of metric resets that occur over a specific time interval. If the resets occur too frequently, the decoder can assume that it is out of sync and initiate the appropriate action for correction. Figure 3.30 shows the number of metric resets per bit as a function of $E_b/N_0$ for the contraint length 5 maximum likelihood decoder operating in the out-of-sync and in-sync modes. Note that the number of metric resets is essentially constant for the out-of-sync mode, whereas for the in-sync mode, the number of resets decreases as $E_b/N_0$ increases. Similar results hold for the K = 7 length code.

Another method of detecting sync errors is to accumulate the most likely path metric and compare it to a threshold after a specific time interval. This can be considered as a finer grating of the reset counting method.

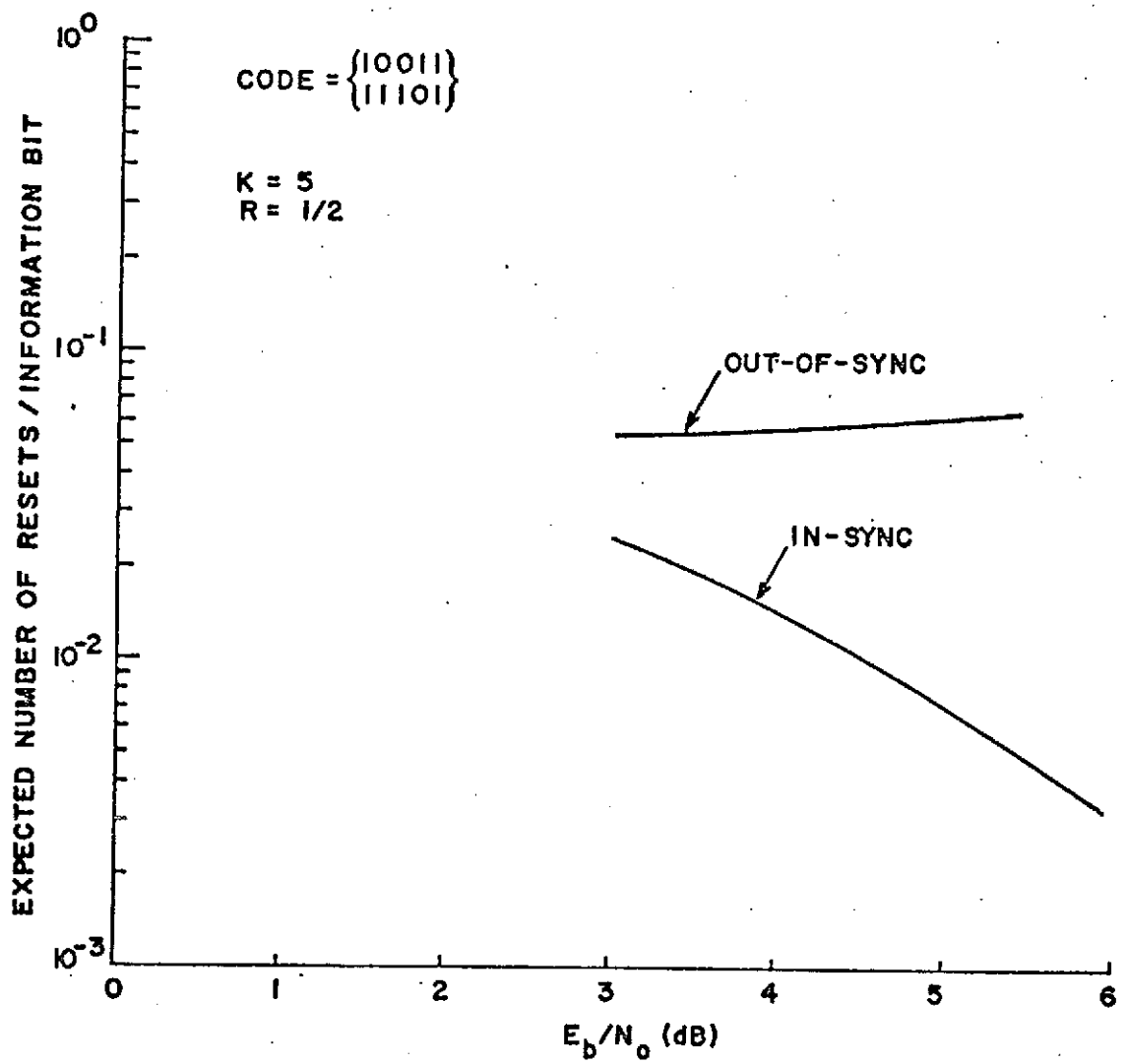


FIGURE 3.30 EXPECTED NUMBER OF RESETS PER INFORMATION BIT VS. $E_b/N_o$ FOR MOST LIKELY PATH DETECTION RULE USING 4 BITS OF METRIC STORAGE WITH CLAMPING AND 3-BIT UNIFORM QUANTIZATION

The first of these methods was chosen for the initial synchronization and monitoring problems since it is simplest to implement.

The carrier tracking loop introduces another problem. The tracking loop is subject to phase flips which will cause the coded bits to be inverted. That is, a zero will be received as a one and a one as a zero.

If the convolutional code is transparent, however, the bit inversions can be compensated by DCPSK encoding. The maximum likelihood decoder will operate without loss of performance after the phase flip has occurred and the decoding memory associated with the actual time of the phase flip is shifted out.

If a nontransparent code was used, the maximum likelihood decoder will act as if it were out of sync. Errors will propagate and the metric will grow rapidly. When a nontransparent code is used, the decoder can be in the following out-of-sync modes:

1) bit inversion and in-sync
2) bit inversion and out-of-sync
3) out-of-sync without a bit inversion

Figure 3.31 applies for conditions 1) and 2) above. Therefore, it may take longer for the decoder to obtain synchronization.

It should be noted also that when a nontransparent code is used bit inversions due to phase flips must be accounted for within the decoder. On the other hand, when a transparent code is used bit inversions are accounted for by external sources, i.e., with DCPSK coding and decoding.

In order to obtain an indication of the decoded error rate (error rate after decoding), one can just integrate the average number of resets

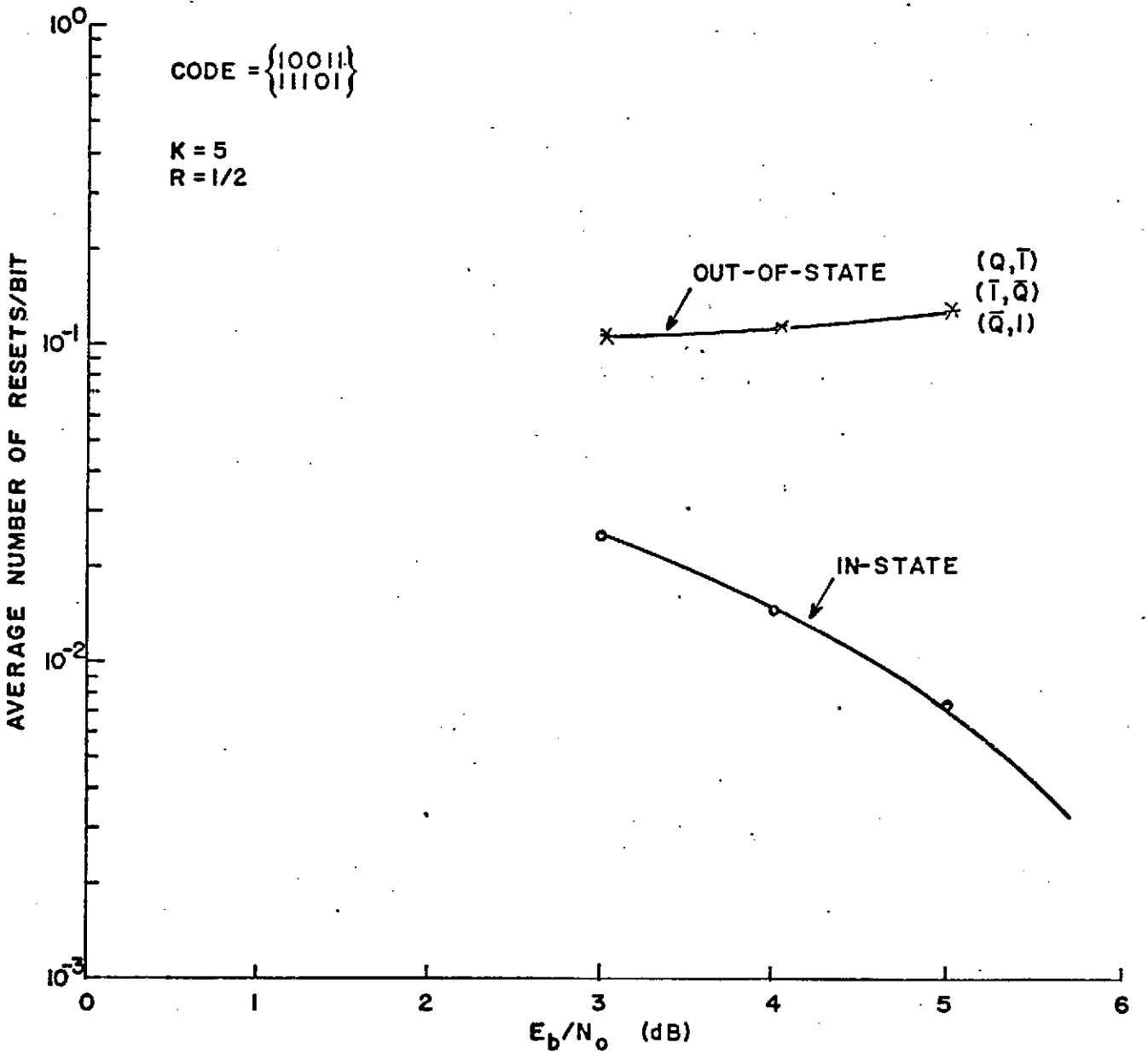


FIGURE 3.31 EXPECTED NUMBER OF METRIC RESETS PER INFORMATION DIGIT VS. $E_b/N_0$ FOR A MOST LIKELY PATH DETECTION RULE USING 4 BITS OF METRIC STORAGE WITH CLAMPING AND 3-BIT UNIFORM QUANTIZATION

which is monotonically related to the probability of an error. Figure 3.32 illustrates this point by plotting the probability of an error as a function of the average of resets.

3.2.3.2.2.4 Design of a Coder/Decoder with Constraint Length 7

The following section describes the design of a convolutional encoder and decoder for transmission of data at rates up to 20 Kb/s, and therefore will more than accommodate the data rates for the telemetry links in the IMEMD/H missions.

The parameters chosen are given in Table 3.17.

| |
|---|
| Code Rate: 1/2 (nonsystematic) |
| Constraint Length: K=7 bits |
| Decoder Input Quantization: 3 bits (8 uniformly spaced levels) |
| Path Delay: 5 constraint lengths |
| Path Selection: Most likely according to metrics |

TABLE 3.17
PARAMETERS FOR CODER/DECODER DESIGN

Figure 3.33 is a block diagram showing the inputs and outputs of the convolutional encoder. The encoder operates with the channel modulator. Clock signals at rates R and 2R are derived from a local reference. Data at clock rate R are fed into the convolutional encoder from a synchronous source. The output of the convolutional encoder is the serial coded data sequence at a clock rate 2R. Output data from the convolutional encoder switches in response to positive-going edges of the clock.

Figure 3.34 shows the configuration for the maximum likelihood convolutional decoder. Three-bit soft-decision statistics are brought from

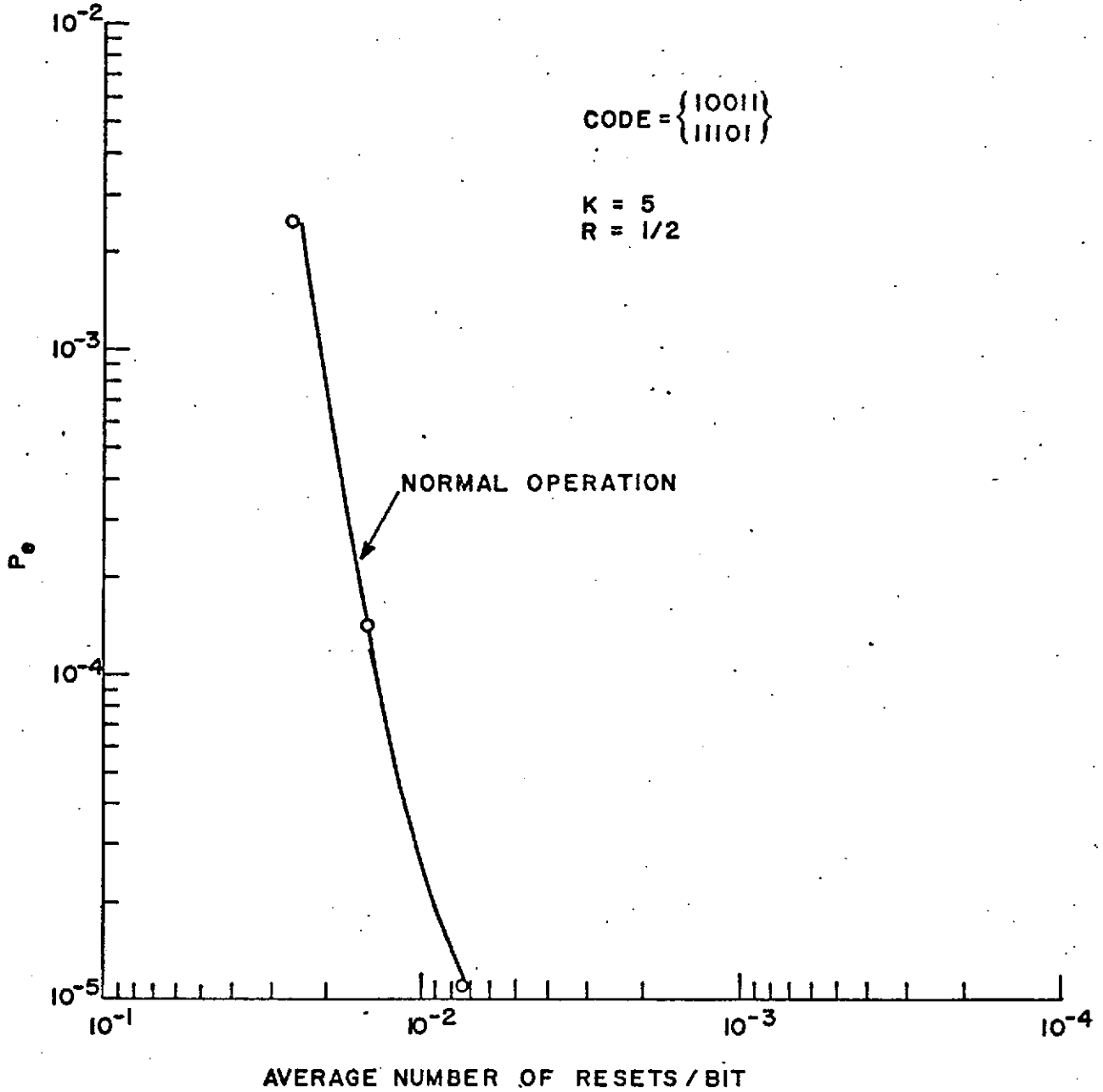


FIGURE 3.32 PROBABILITY OF ERROR VS. AVERAGE NUMBER OF RESETS/INFORMATION BIT USING MOST LIKELY PATH DETECTION RULE WITH 4 BITS OF METRIC STORAGE WITH CLAMPING AND 3-BIT UNIFORM QUANTIZATION

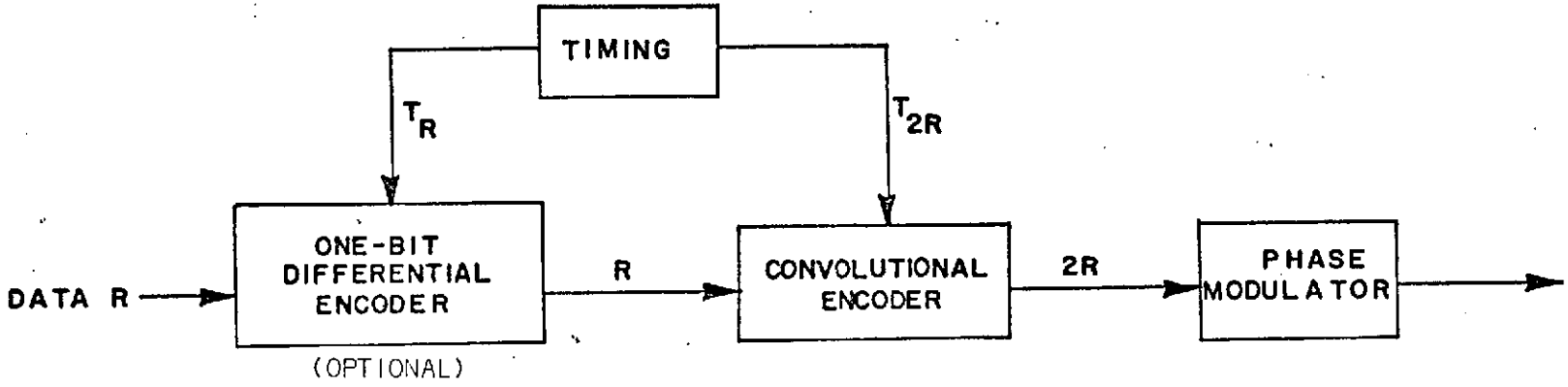


FIGURE 3.33 ENCODER CONFIGURATION



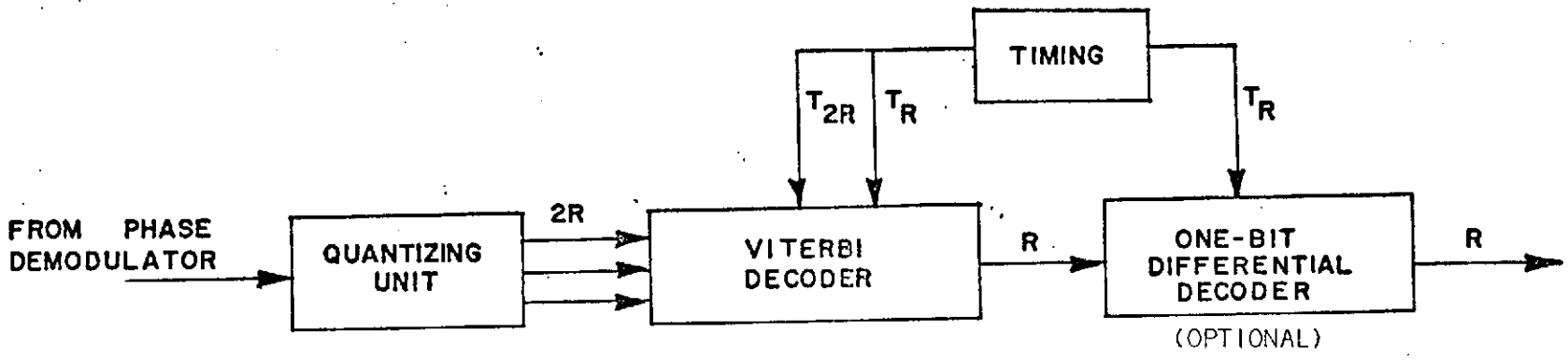


FIGURE 3.34 DECODER CONFIGURATION

the quantizing unit on three parallel lines, one line for each bit of the soft decisions. The output of the convolutional decoder is the reconstructed data sequence that appeared at the input to the convolutional encoder. The convolutional decoder requires clocks of R and 2R. All output data moves in response to the positive edge of clock R.

Figure 3.35 shows the rate = 1/2, K=7 convolutional encoder. Data bits are entered serially into a seven-bit shift register. For each new input data bit two coded bits are generated by the encoder. Each coded bit is generated by a modulo-2 adder that derives its input from several of the seven stages of the shift register. In this manner each coded bit is a function of the new data bit in the register and the six data bits preceding the new data bit in time. The six previous data bits which occupy the last six stages of the shift register are by definition the encoder state.

The coded bit pair is time-multiplexed into a single line for transmission at twice the data clock rate. Interface circuits are provided at the input and output of the encoder to translate the logic levels of interfacing equipment to that of the logic used in this system.

The function of the decoder is to reconstruct the data stream fed into the encoder from the soft-decision coded bit pair that the decoder receives from the channel modem. The reconstruction is achieved by determining the most probable sequence of states progressed through by the encoder.

Figure 3.36 is the block diagram for the decoder. The three-bit soft decisions from the quantizing unit are received serially by the Metric Transition Generator at twice the data rate (i.e., at the coded data

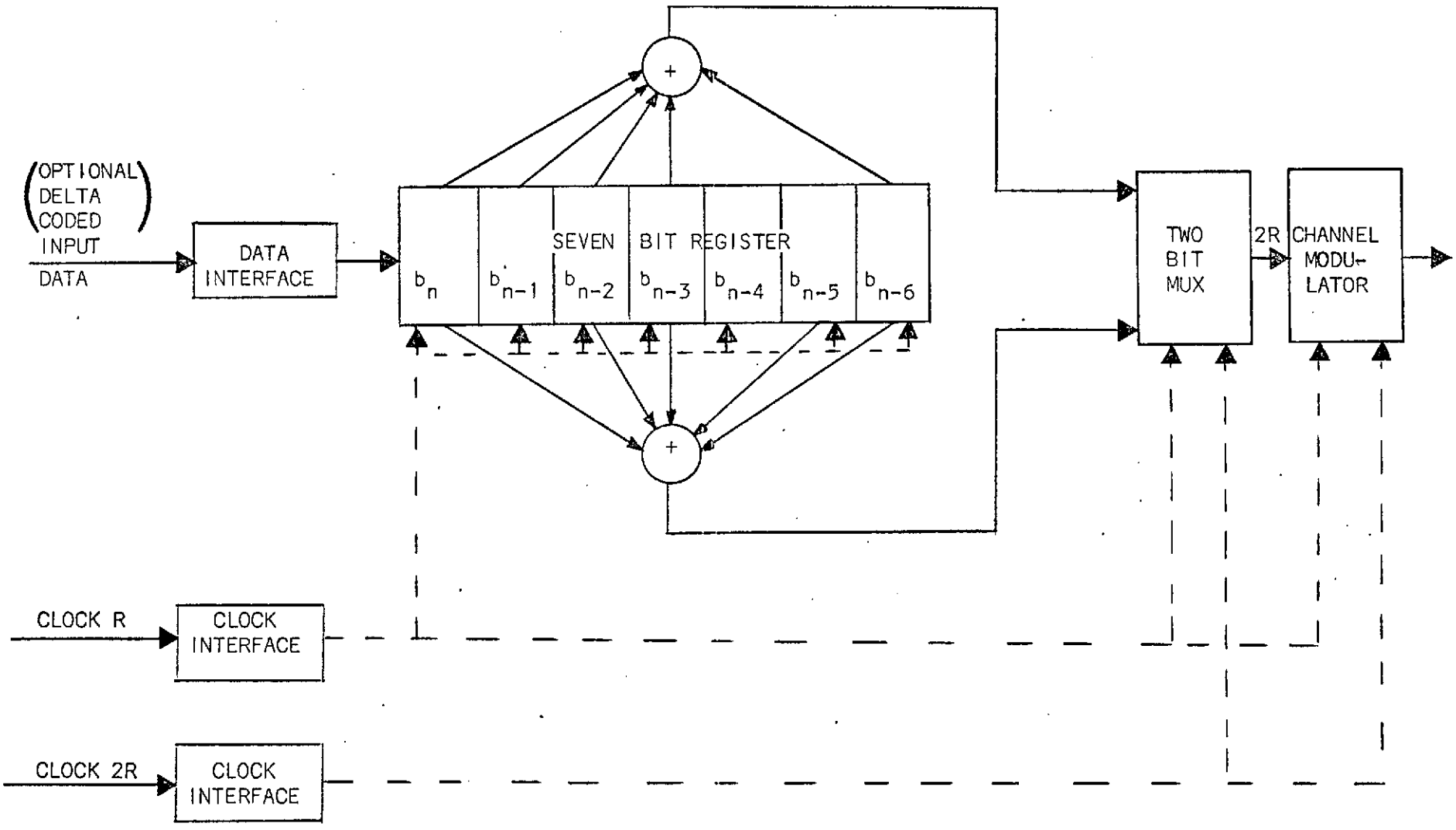


FIGURE 3.35 CONVOLUTIONAL ENCODER R=1/2, K=7

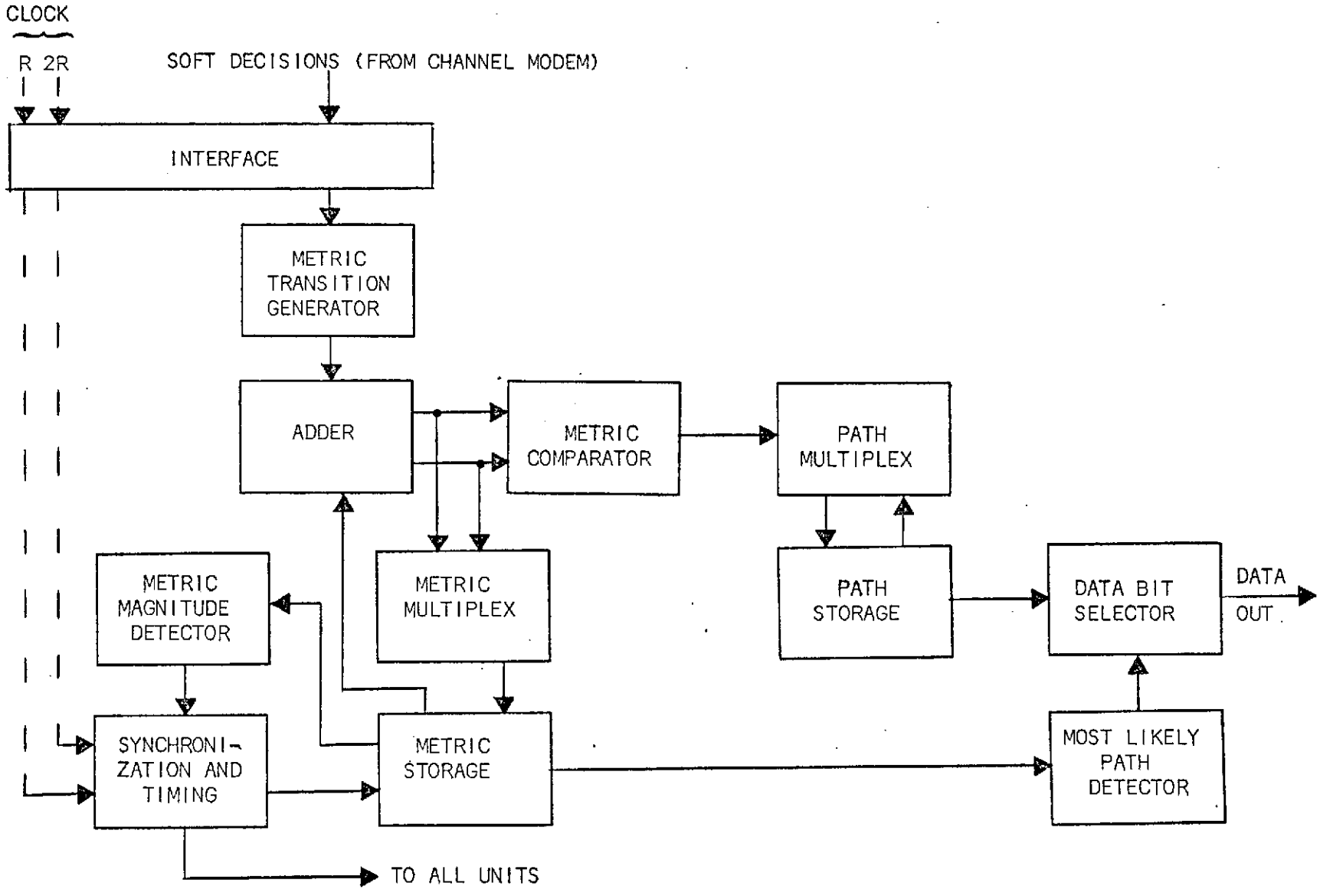


FIGURE 3.36 MAXIMUM LIKELIHOOD CONVOLUTIONAL DECODER

rate 2R). From each pair of soft-decisions received the Metric Transition Generator calculates a probability measure on each of the four possible magnitude values (i.e., 00, 01, 10, 11) of the associated bit pair. The metric transitions are combined with the metrics from the past in order to generate a new set of metrics. Since the data rate is low, the above can be done serially thereby reducing the complexity.

Each metric indicates the reliability of the most probable data path ending in a specific encoder state. Since for a K=7 code there are 64 encoder states, it is necessary to generate 64 metrics in a sequential manner. From an examination of the possible sequence of encoder states, it is known that for each new data bit an encoder state can go to only one of two encoder states and conversely any encoder state can be accessed from only two encoder states. From each metric two new metrics are generated, corresponding to the two new states the old state could have progressed to with a new data bit. The two new metrics are calculated from the old metric in the following manner. The first new metric is the old metric added to the metric transition resulting from a zero (0) as the new data bit in the encoder register. The second new metric is the old metric added to the metric transition if a one (1) had been the new data bit.

In this manner a set of 128 new metrics is eventually generated by the adder. The metric comparator performs a pairwise comparison for each pair of metrics leading to the same states. Each comparison selects the most probable of the two metrics. The most probable metric is indicated by the metric of minimum numerical value. The surviving metrics are then placed via the metric multiplex in the position assigned to their states in the metric storage. The surviving metrics now become the old metrics for the next coded bit pair received.

In addition to determining the surviving metric, each comparison makes a decision on the most delayed bit in the encoder register. This is due to the fact that the states from which each set of parallel paths is derived can only differ in the most delayed bit position. Therefore, each path bit decision from the metric comparisons is, in effect, delayed six bit intervals from the time it was estimated to enter the encoder register. The bits resulting from each comparison are stored in the path storage.

The path storage corresponds to the sequence of bits or path leading to the state of its corresponding metric. When a comparison and a new bit decision are made, that bit must be added to the path associated with the metric from which the new metric was derived. The new path must then be placed in the storage position associated with the new metric. The result is that the path storage will contain 64 paths, each of which is associated with a metric in the metric storage. The paths are allowed to accumulate for a number of bits equivalent to five constraint lengths of delay from the new data bit positions of the encoder. For any one path five constraint lengths of delay is equivalent to thirty-five bits, therefore, each path consists of 35 bits.

At each data bit interval the most probable metric in the metric storage is detected. The most delayed bit (i.e., the 35-th bit) in the path associated with that metric is chosen as the decoded data bit by the data bit selector.

The metric transition generator calculates a probability measure on the received coded bit pair for each of the four possible received sequences. The four metric transitions ($L_{C_1C_2}$) are defined as follows.

Let $r_1$, $r_2$ be the quantized soft decisions on received bits #1 and #2, respectively, of the coded bit pair (see Figure 3.28). Let

$$C_1 = \begin{cases} 0 \text{ if } r_1<0 \\ 1 \text{ if } r_1>0 \end{cases} \tag{3.23}$$

$$C_2 = \begin{cases} 0 \text{ if } r_2<0 \\ 1 \text{ if } r_2>0 \end{cases} \tag{3.24}$$

and

$$\alpha_1 = |r_1| \tag{3.25}$$

$$\alpha_2 = |r_2| \tag{3.26}$$

Then the metric transitions are given by (see Appendix E)

$$L_{00} = \alpha_1 \cdot C_1 + \alpha_2 \cdot C_2 \tag{3.27}$$

$$L_{11} = \alpha_1 \cdot \bar{C}_1 + \alpha_2 \cdot \bar{C}_2 \tag{3.28}$$

$$L_{10} = \alpha_1 \cdot \bar{C}_1 + \alpha_2 \cdot C_2 \tag{3.29}$$

$$L_{01} = \alpha_1 \cdot C_1 + \alpha_2 \cdot \bar{C}_2 \tag{3.30}$$

where a bar over a number indicates its complement and $\alpha_i$ is the absolute value of the soft decision. These metric transitions are chosen such that a positive soft decision represents a received 1 and a negative soft decision represents a 0.

Figure 3.37 is the block diagram for the metric transition generator. The three-bit soft decisions are entered into the $r_2$ and $r_1$ registers at the coded data rate. The least significant two bits of $r_1$ and $r_2$ (i.e., $\alpha_1$, $\alpha_2$) are fed to the inputs of a two-bit adder via NAND gates. The NAND gates will allow or block the adder inputs* as dictated by the most

* $\alpha_i C_i = 0$ if $C_i = 0$ (blocked $\alpha_i$); $\alpha_i C_i = \alpha_i$ if $C_i = 1$ (allowed $\alpha_i$)

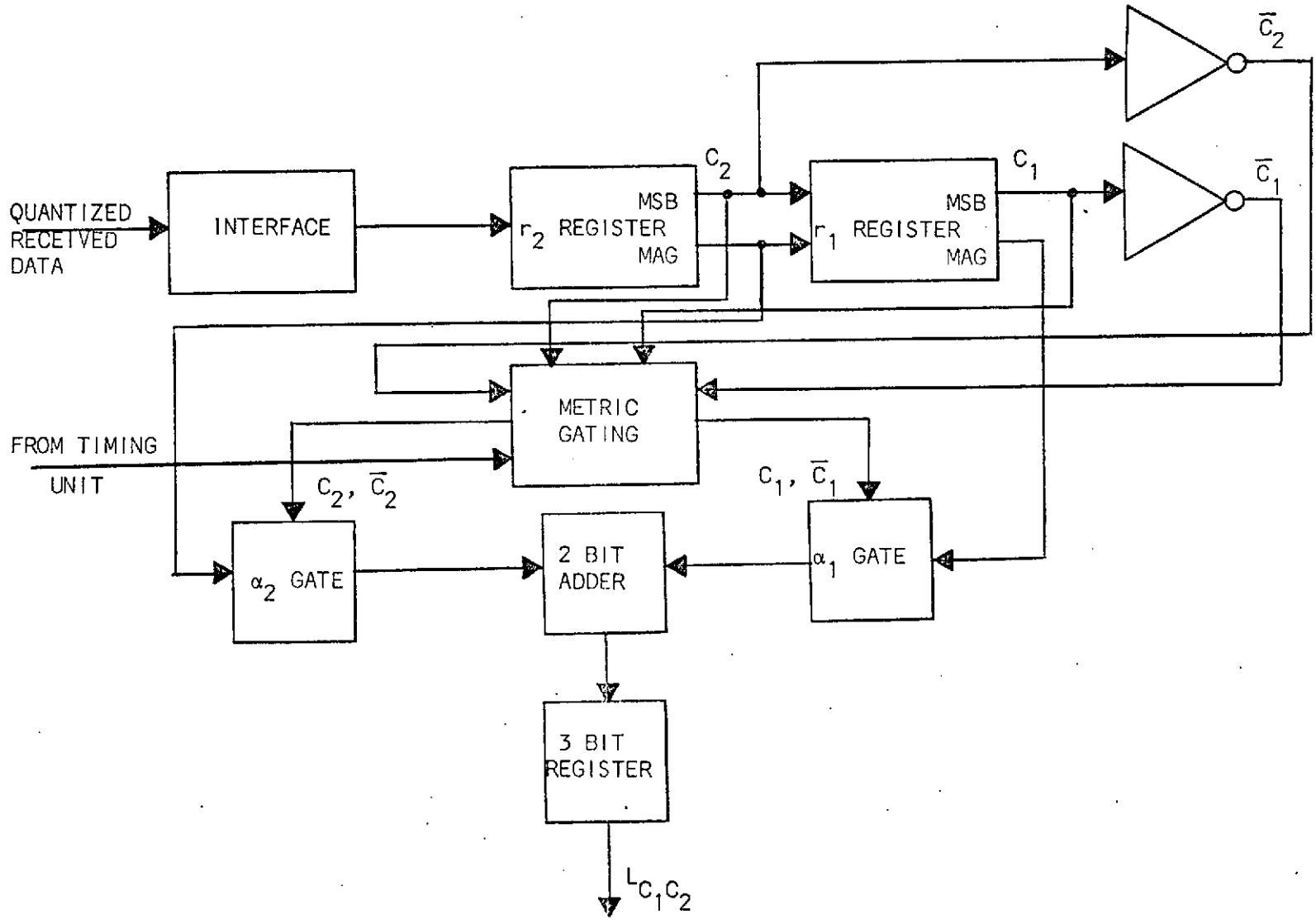


FIGURE 3.37 METRIC TRANSITION GENERATOR

the metrics. This is accomplished by detecting when the most significant bits of all metrics are set and then causing them all to reset at the same time. By employing these overflow protections it is possible to limit the metric storage for each metric to four bits and still obtain a performance which is essentially the same as that possible for infinite metric storage.

For each encoder state, there is a path memory which contains a record of the surviving path leading to that encoder state. Hence there are 64 path memories for the constraint length 7 code. Each comparison between parallel paths leading to the new encoder state, in addition to determining the surviving metric, also determines the surviving path and the newest member of that path. The newest member is a zero or a one depending on the old state from which the transition occurred. If the old state has a zero (one) in the most delayed state position, a zero (one) is appended to the surviving path. The choice of the most probable of the two metric states dictates the selection of this bit.

Selection of the most likely path is made on the basis of comparison of magnitudes of the metrics; the path register output corresponding to the lowest metric is selected. The most likely path is obtained by selecting one of 32 paths, using five levels of comparison and selection logic; then extending this comparison to one more level, selection of one of 64 paths is accomplished. The path register final stage outputs are connected to the first level inputs. A typical "cell" contains a four-bit parallel comparator, a two-input four-bit multiplexer and an AND-OR-INVERT circuit which serves as a two-input one-bit multiplexer. The comparator produces a logic ONE at the output opposite the input of smaller magnitude, or at both outputs if the inputs are equal. The smaller metric input to each cell

thus appears at an input to the following cell. At the same time, the path register output corresponding to the smaller metric is routed through the AND-OR-INVERT circuit. Note that if the metric inputs to a cell are equal, both path register outputs are OR-gated; a logic ONE at either produces a ONE at the output, an acceptable situation since either choice of path is equally good in such a case.

The input to the decoder consists of a succession of soft decision A/D outputs following the integrate-and-dump circuit of the quantization unit. The soft decisions are processed in pairs, each pair corresponding to the pair of coded bits generated by the encoder each time a new data bit is generated.

Computer simulation shows that the metric corresponding to the most likely path increases in magnitude considerably faster when out of synchronization than when properly synchronized. Therefore, resetting of the most significant bit of all metrics (which occurs at times determined by the smallest metric, which is by definition that corresponding to the most likely path) occurs more frequently in the out-of-synchronization condition.

As seen previously a phase reversal can cause node synchronization difficulty; the decoder must monitor the metrics to recognize a two-correct-out-of-four condition. Table 3.18 summarizes this. The metric resets provide the clue to any difficulty.

| SYNC | PHASE SLIP | CORRECT/INCORRECT |
|---|---|---|
| in | 0 radians | correct |
| out | 0 radians | incorrect |
| in | $\pi$ radians | correct |
| out | $\pi$ radians | incorrect |

TABLE 3.18
SYNCHRONIZATION AND PHASE REFERENCE MODES

3.2.3.2.3 Maximum Likelihood Decoder Cost

The decoder presented previously is similar in theory to any state of the art decoder; as such it was felt that an available hardware design would be the most helpful in representing typical costs of a Viterbi decoder of the kind presented in this report. Per reference 25 the following data is listed.

- Manufacturer: Linkabit Corporation
- Model: LV7015
- Coding Gain: 5.1 dB at $10^{-5}$ bit error probability
- IC Complement: 82 units, TTL
- Data Rates: up to 100 kbps
- Code Rate: 1/2, nonsytematic
- Constraint Length: K=7
- Decision Scheme: soft, Q=8
- Cost: $5,000 each in lots of one
  $4,500 each in lots of five

3.2.3.3 SEQUENTIAL DECODING

In this section the theory and implementation of sequential decoding will be discussed. As with the Maximum Likelihood Decoder (MLD) enough detail will be given in the decoder design so that a recommendation between it and the MLD can be made.

3.2.3.3.1 Sequential Decoding Theory (Fano Algorithm)

Consider the code tree representation of the example convolutional code given in Figure 3.10 repeated here as Figure 3.38.

To oversimplify things for the moment, a sequential decoder assumes a path through the tree is correct; it calculates the metric between

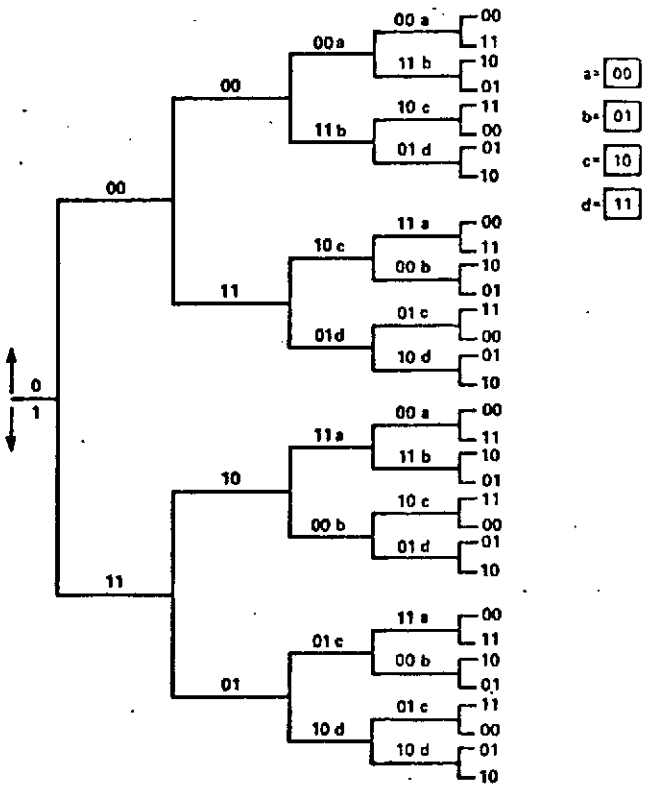


FIGURE 3.38 TREE-CODE REPRESENTATION FOR CODER OF FIGURE 3.10

this "best path" and the received sequence up to that time. If this metric value does not violate a running threshold, which changes constantly, then the decoder assumes the path is correct. If, however, the threshold is violated then other paths are tried until the threshold is not violated. If, as often happens, the threshold is violated for all paths then it is increased, and all paths are tried again, etc., etc..

As can be readily deduced from the above if a wrong path is chosen at any point in the algorithm, then the decoder must back up; this consumes time. If the errors are few and far between the chances are that the correct path will be chosen and the decoding will keep moving deeper into the tree at a rapid rate. On the other hand if, say, a burst of errors

came in or a great number of random errors occurred then the decoder would have to back up frequently; but data keeps coming, therefore, the decoder buffers finally reach a point where they cannot store anymore data, and they overflow resulting in a complete breakdown of the decoder error correction ability.

The probability of overflow is one of the most important design criteria in a sequential decoder design since the results of an overflow are so disastrous. Unfortunately it depends on the number of computations done per node in the tree, call it N, which is a random variable dependent in a very complex way on the code and the channel noise. It is generally agreed that N follows a Pareto distribution[26][27] in the cases of interest, i.e.,

$$P(N \geq N_a) \approx kN^{-\beta} \quad .^{*} \tag{3.31}$$

Once a particular code has been chosen a simulation can be done. From the results of the simulation the above distribution can be determined by a curve fit; for that matter, the simulation will also give the bit error rate charcteristics of the code with sequential decoding. As can be seen from the above, most of the work in designing a good convolutional encoder/sequential decoder (CE/SD) system is in preparing and evaluating the output from computer simulations.

To be a bit more precise now, the following sections will introduce and analyze a basic form of sequential decoding, viz., the Fano algorithm; although there are many variations on it the essentials remain the same. The algorithm is shown as a flowchart in Figure 3.39.[28] The parameters in the figure will be defined as the discussion progresses.

---

* $\beta$ is the Pareto exponent.

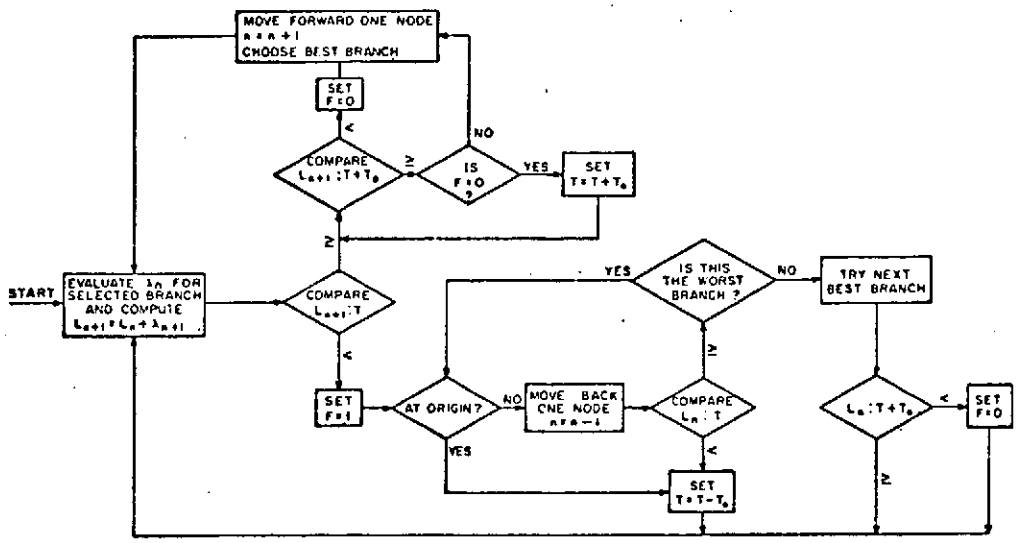


$\lambda_n$ = transition metric, $L_n$ = path metric, T = threshold, $T_0$ = constant

FIGURE 3.39 FLOWCHART FOR THE FANO ALGORITHM

The algorithm is started at the origin of the tree. The metrics for all paths leading from the origin to the next nodes are calculated; there are usually only two, but there could be more if more than one bit per shift were implemented in the encoder. The path metrics are compared and the largest metric ($L_1$) path chosen, i.e., "the best." Next $L_1$ is compared with the running threshold, T. If no errors occurred and T wasn't too large, then $L_1 \geq T$ and the upper path out of the decision block is taken. After this $L_1$ is compared with $T+T_o$, where $T_o$ is a predetermined constant; this is to allow T to be set to its maximum value without $L_1$ violating it. If it is violated, i.e., $L_1 < T+T_o$ then the algorithm moves to the node #1 and recycles from the beginning. If $L_1 \geq T+T_o$ the threshold is increased or if F=0 left alone and recycled.

The above was if $L_1 \geq T$. If $L_1 < T$ then F is set to 1, and the lower path is taken. If the node under consideration is not the origin, the algorithm backs up one node. If the previous node also violates T then the next best branch is chosen (next highest metric) unless of course there isn't any, in which case the algorithm backs up again. If the previous node didn't violate T then it is assumed that the threshold was too large; it is lessened and the algorithm recycled.

From the brief description above, it is seen that the parameter $T_o$ affects the amount of computational effort during a search. As $T_o$ is reduced the decoder becomes more responsive to incorrect decisions but at the same time makes it more prone to label a correct path as incorrect due to noise. This, on the average, results in numerous short searches. Conversely, a large value of $T_o$ means a correct path is less likely to be confused with an incorrect one due to noise but the decoder will take longer to respond to a wrong decision. This results in fewer but longer searches on the average. The best choice for $T_o$ depends on channel conditions and thus should be determined experimentally or by simulation. Investigation of the behavior of $T_o$ is discussed in a later section.

At this point in the discussion, it may be of interest to compare the maximum likelihood and sequential algorithms. If the same metric is used for both, then the essential difference between the two is that the maximum likelihood looks at all paths leading to a point in the tree and picks the best one, whereas the sequential doesn't look at all paths, but rather only looks at those paths which do not violate a threshold. The best path in the maximum likelihood algorithm, then, as it becomes longer is allowed to exceed the threshold of the sequential algorithm as long as

it eventually (whenever a decision is made) ends up as the one with the best overall metric. This best path, if a sequential decoder were used could be thrown out at an interim point in the algorithm, but hopefully would be chosen again as the threshold was adjusted.

The conclusion is that since the maximum likelihood algorithm looks at all paths, it is better; in fact Viterbi[24] has shown that it is optimum. The sequential algorithm is therefore suboptimum. Since all paths in a MLD must be looked at for a given constraint length K, the operations required increase by $2^K$. The sequential decoder thus has an advantage here.

Proceeding now with the sequential algorithm discussion, it will be recalled that the code rate was defined to be the number of information bits encoded per code bit output, e.g., a rate 1/2 code implies that two code bits come out of the encoder for every data bit going into it. Ideally, the larger the code rate the better since this requires less bandwidth, however, just as in FM, there is a point where the "improvement" of the coding system disappears, sort of its threshold. The applicable parameter in sequential coding is called $R_{comp}$, i.e., the computational cutoff rate. For example, if $R_{comp}=0.5$ then the practical maximum rate that can be used on this channel with sequential decoding is $R=R_{comp}=0.5$. It is generally true, however, that if R is much more than 0.9 $R_{comp}$ then the sequential decoder requires too many computations to do the error correcting job and is thus very ineffective; at $R=R_{comp}$ the computations become enormous.

The $R_{comp}$ of a channel is dependent on the $E_b/N_o$ available since if $E_b/N_o$ were, say, infinite, then no coding would be needed,

i.e., $R_{comp}=R=1$. On the other hand, as $E_b/N_o$ decreases $R_{comp}$ also decreases which forces more code bits per data bit to be used. All that is really being said here is that a trade can be made between the quality of data decoded and channel bandwidth. This is true in nonlinear modulation such as FM and is a general property of communications systems. The key is to make the "best trade."

Getting back to the main topic, the value of $R_{comp}$ for the infinitely quantized AWGN channel with a phase coherent modem is given by[27]

$$R_{comp} = 1 - \log_2(1 + \exp(-R\, E_b/N_0)) \tag{3.32}$$

Defining $E = R\, E_b/N_0$ Figure 3.40 [28] plots $R_{comp}$ versus $E/N_0$ per waveform received.

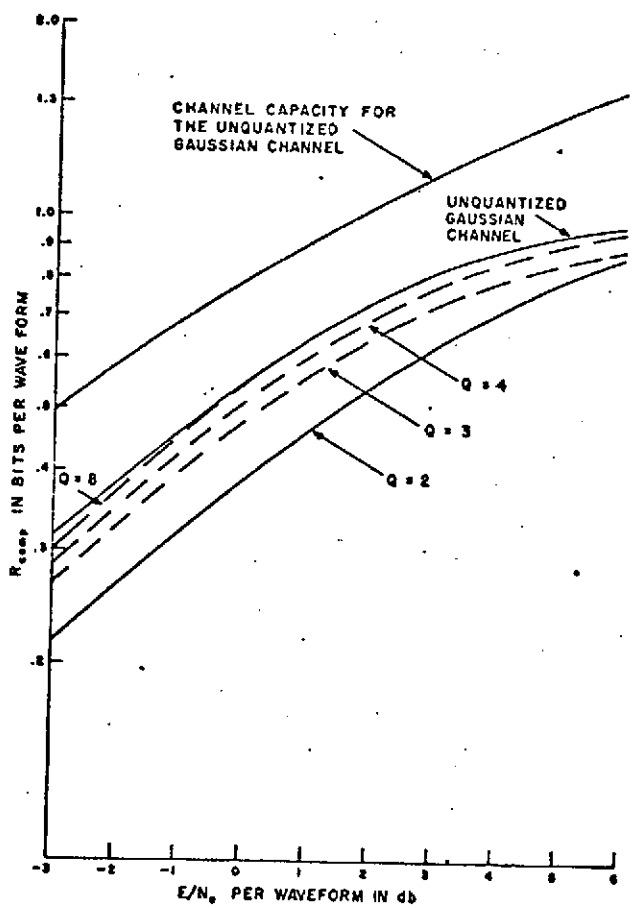


FIGURE 3.40 $R_{COMP}$ FOR A COHERENT GAUSSIAN CHANNEL

Also shown is the effect of quantizing the output of the channel into Q levels; this was discussed in the Viterbi decoder section.

Another curve in Figure 3.40 is the channel capacity of the AWGN channel. As can be seen in the figure, $R_{comp}$ is well below the capacity of the channel; in fact even if $R=R_{comp}$ the minimum $E_b/N_0$ that can be used with the channel is found by letting $E/N_0 = E_b R_{comp}/N_o$ go to zero. Using L' Hopital's rule with respect to $E/N_0$

$$\lim_{E/N_0 \to 0} E_b/N_0 = \frac{E/N_0}{R_{comp}} = \frac{2}{\log_2 e} = 1.386 \text{ (1.42 dB)}. \tag{3.33}$$

Shannon's limit is -1.6 dB, therefore CE/SD is even theoretically suboptimum. Since 1.42 dB is such a low number, though, sequential decoding with convolutional encoding is a very powerful error correction technique.

From curves like Figure 3.40 $R_{comp}$ can be determined, i.e., a link calculation is performed; the minimum $E_b/N_0$ is found; then the curves give the value of $R_{comp}$ for a given quantization scheme.

The next task is find the metric to be used in evaluating paths through the tree. The "log a posteriori" metric is optimum and is given in one form (binary) by

$$L_n = \sum_{i=1}^{n-1} \left[ \log_2 \frac{p(y_i | x_i^*)}{p(y_i)} - U \right] = \sum_{i=1}^{n-1} \lambda_i \tag{3.34}$$

where $L_n$ is the metric, n is the number of nodes in the path, $y_i$ is the received branch, $x_i^*$ is the uncorrupted i'th received branch, p( ) is the

probability density function, and U is a constant chosen to make $L_n$ increase on the average if correct paths are chosen and decrease if incorrect ones are chosen.

It is found that U=R gives good results; also theoretically $p(y_i|x_i^*)$ and $p(y_i)$ requires a knowledge of the variance of $y_i$ and $y_i|x_i^*$ which is precisely a knowledge of $N_0$, i.e., the noise density. This can't be known a priori, but if the minimum $E_b/N_0$ is found as described in finding $R_{comp}$ then the $N_0$ corresponding to this can be used. Any less noise gives smaller $N_0$, but then $E_b/N_0$ is greater and the nonoptimality of $N_0$ is compensated for by the greater signal to noise ratio available.

Finally the threshold increment $T_0$ must be chosen. Since it affects the average number of computations required per node, it is chosen to minimize this. A value of 5 bits (between binary representation of analog thresholds) seems to be acceptable (actually the minimum is quite broad).

Knowing all of the above together with the logic speed being employed in the decoder several simulations are performed. From these the probability of overflow is found, and the decoded error rate is determined. The reader interested in more design detail is referred to (27), (28).

A general comment on the sequential decoding technique is that it is highly dependent on the incoming symbol rate and the logic speed, thus if the rates are low (<50 kbps) then the sequential decoder complexity is small. This is true even though the constraint length may increase. This is the prime advantage of sequential decoding over maximum likelihood decoding, and is the reason why it has remained a powerful decoding tool even though it is a suboptimum algorithm.

3.2.3.3.2 Sequential Decoder Design

The error correction unit described in this section will consist of a rate 1/2 encoder with a sequential decoder. The design will accommodate bit rates up to 20 kbps, (information rate). Since the speed factor is so important in a sequential decoder, it is not prudent to overdesign for bit rates much higher than needed.

3.2.3.3.2.1 Performance of the Sequential Decoder

The following set of curves shows the performance of the sequential decoding algorithm for several constraint lengths (Figure 3.41). Since the Fano algorithm was used in all of the curves, it can be seen that for the coding gain required by the IMEMD/H missions a constraint length of at least K=24 must be used for Q=8 and K=47 for Q=2. Because of this and because the encoder selected by NASA[5] has a constraint length sufficient to do the job, i.e., K=24 nonsystematic (equivalent to K=48 systematic), the analysis in the next sections will be for it. This encoder is shown in Figure 3.42. It is readily seen to be a non transparent code.

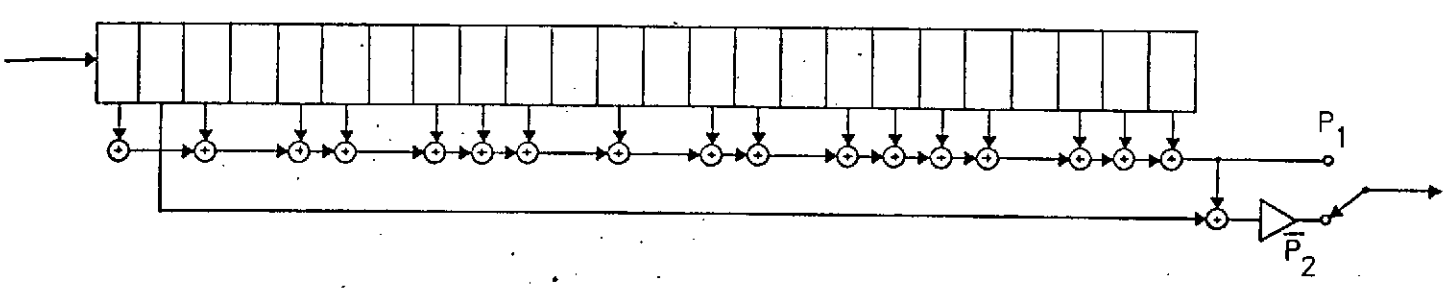


FIGURE 3.42 K=24 NONSYSTEMATIC CONVOLUTIONAL ENCODER

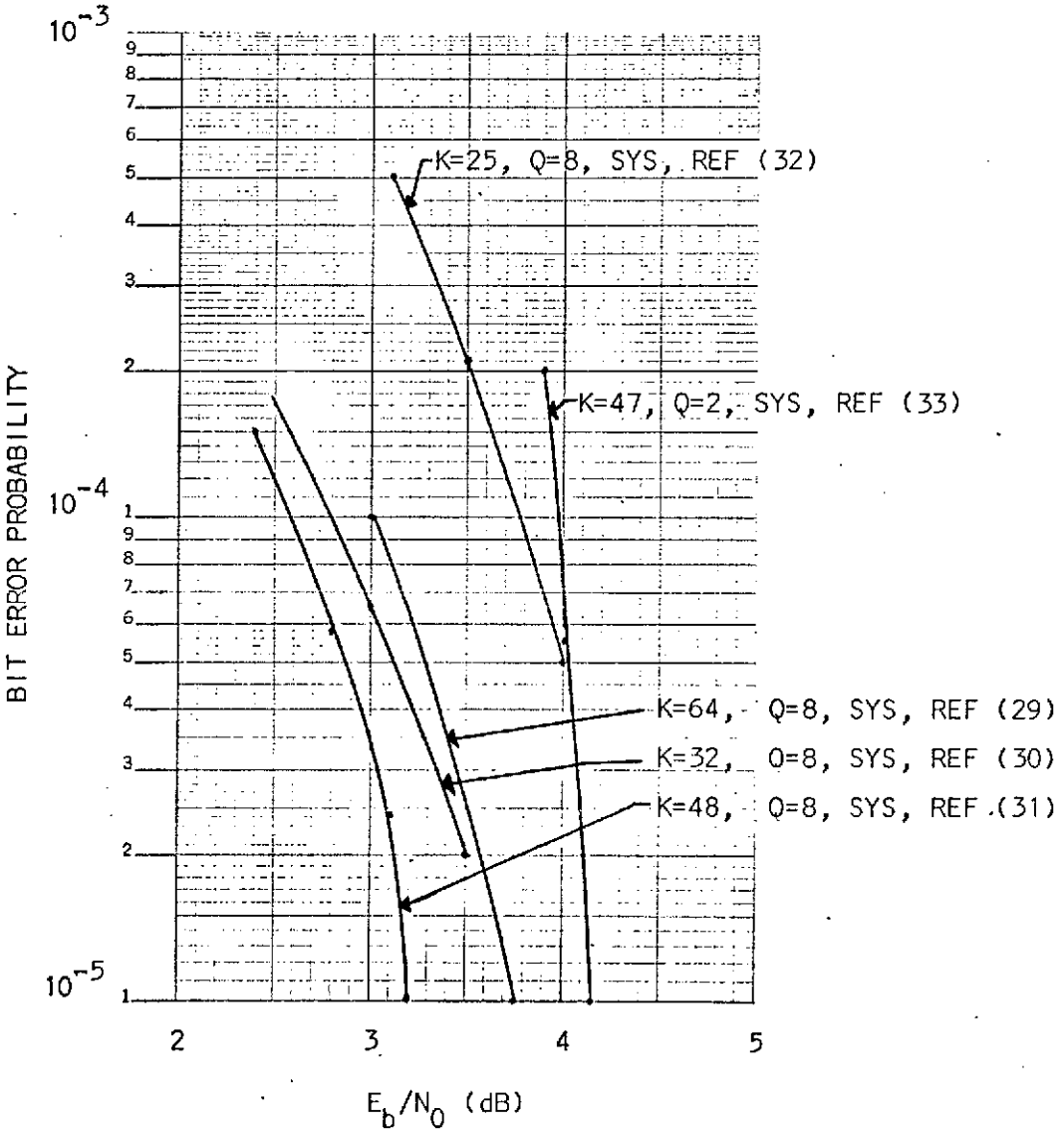


FIGURE 3.41 PERFORMANCE OF 1/2 RATE SEQUENTIAL DECODERS ON AWGN CHANNEL

This encoder has the nice property that even though it is nonsystematic, the information bits can be recovered very easily by simply inverting $\overline{P}_2$ and summing it modulo-2 with $P_1$ since 0 + 0 = 1 + 1 = 0 modulo-2. This property can be used for a "quick look" at the data or to bypass the decoding in case of a failure or in the event that high signal levels are encountered (hot transmitter, etc.).

3.2.3.3.2.2 Soft Decision Metric

As discussed in Section 3.2.3.2.2.2 in connection with the MLD it is wise to use soft decisions. As a side note the only practical reasons for going to hard decisions, Q=2, is to decrease the complexity and increase the speed of the decoder, however, at rates considered here (16 kbps) this is not a factor. The use of soft decisions makes much fuller use of the available information transmitted through the channel and thus lowers the $E_b/N_0$ required for a given error rate; compare, for example, the constraint length 47 hard decision and 48 soft decision curves in Figure 3.41.

3.2.3.3.2.3 System Interface Considerations

As discussed in Section 3.2.3.2.2.3 the decoder must be synchronized. In the case of the MLD only branch synch was required since the decoder does not care where it is in the tree, but rather only in the relative positional location within any given branch. This is not true with a sequential decoder and is a major implementation problem.

The sequential decoder must know where it is in the tree at all times. Suppose for example that a loss of lock occurred in the tracking loop causing the decoder to overflow. Since the decoder was backing up at the time and more data came in than it could handle, it has lost track of

where it was in the tree. Some way must be found to start things going again. A simple method is to reset the whole system (encoder and all) and start over. This, however, would require a command to the spacecraft and timing problems; also it is slow with a lot of data held up or lost.

A more practical way is to periodically send a known bit or a sequence of bits which can be used as a guide by the decoder in synchronizing, restarting, and as an overall check of the system sync. Sandwiching these bits into the data stream decreases the energy per data bit, however, with some loss in coding gain. A tradeoff is involved to optimize sync capability and coding gain.

Other schemes for restarting and synching have been proposed. All of them somehow produce data at the decoder input which has a high probability of being correct and has a known position within the code tree.

Another interface consideration is the transparency versus non-transparency of the code. If the code is not transparent then differential coding could be inserted after the convolutional encoder and prior to the decoder to correct the situation. In doing this, however, an error in one received bit out of the differential decoder causes the adjacent bit to be in error. The implication is that the error rate into the decoder is doubled and also that the errors are correlated. This degrades the system significantly.

Another way is to use a transparent code so that the decoder is oblivious to phase flips; differential encoding/decoding can be done prior to/after the CE/SD system.

Still another method is to use the restart bits discussed above to accomplish the phase ambiguity. All three of these schemes are shown in Figure 3.43. Since the code chosen for the missions by NASA is not transparent the "decoder resolves phase ambiguity" scheme will have to be used.

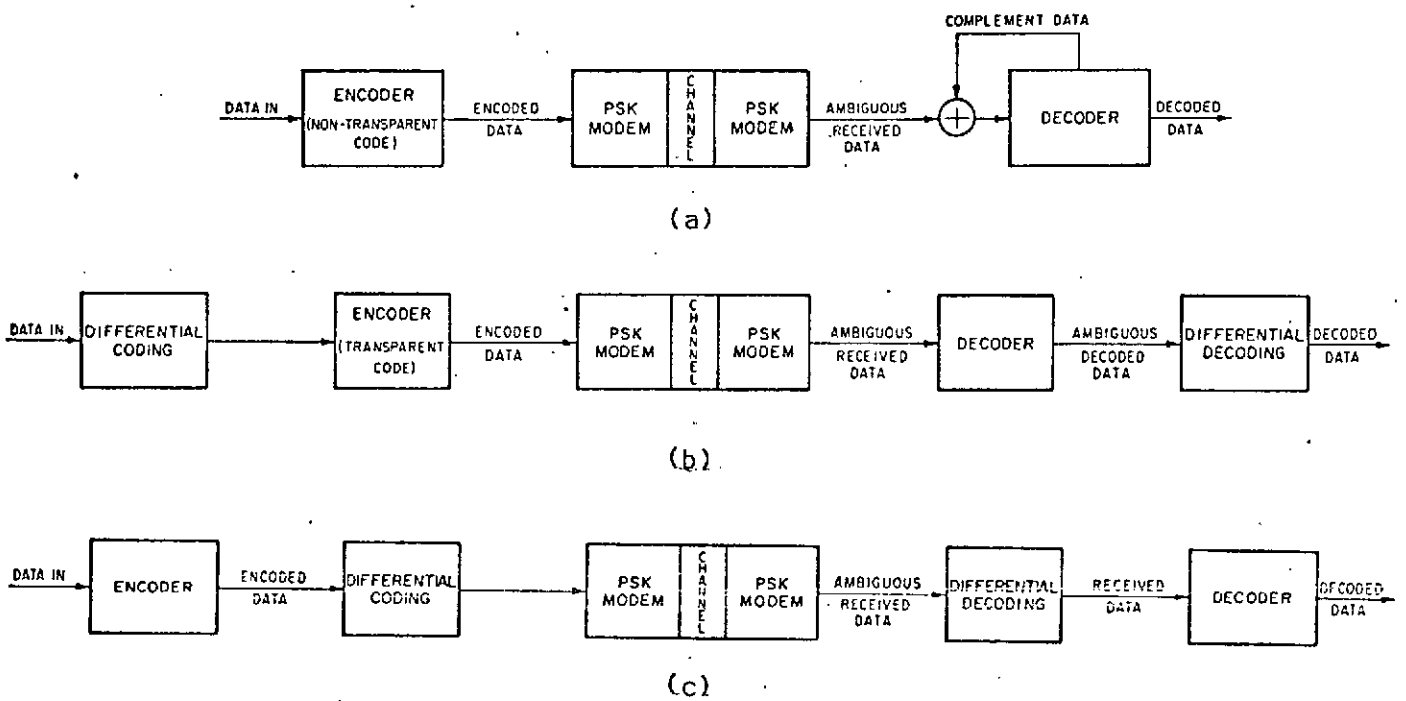


FIGURE 3.43 PHASE AMBIGUITY RESOLVING METHODS

(a) Decoder resolves phase ambiguity. (b) Differential coding external to transparent error-control coding. (c) Differential coding internal to error-control coding (undesirable).

3.2.3.3.2.4 Design of a Sequential Decoder for a Constraint Length 24 Code

The following section describes the design of a sequential decoder to be used with the encoder of Figure 3.42. The parameters for the decoder are given in Table 3.19.

A block diagram of the sequential decoder is shown in Figure 3.44. Note the similarity to the MLD; this is to be expected since the differences are threshold rather than path comparisons and back up (input buffering) versus no back up capability.

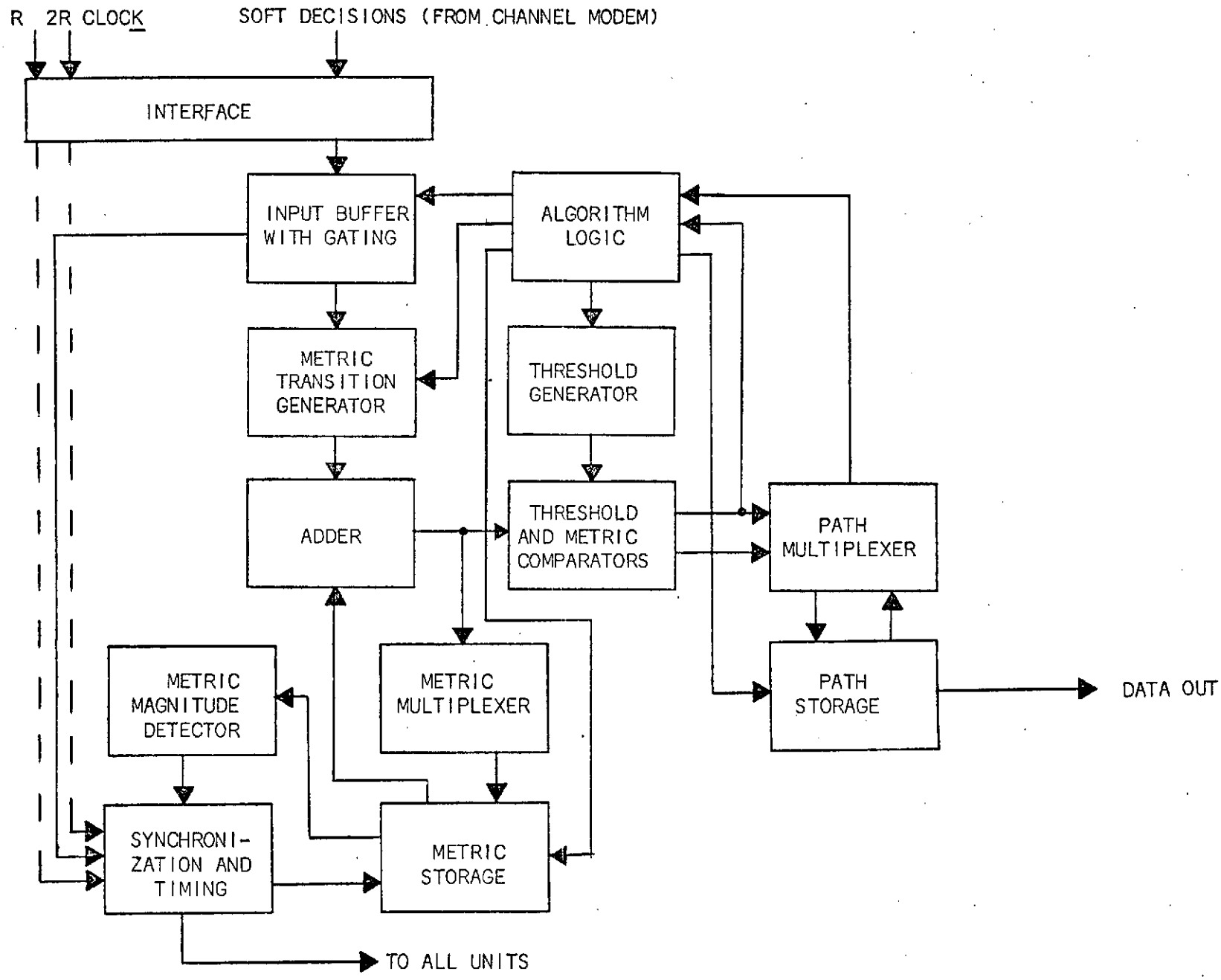


FIGURE 3.44 A SEQUENTIAL CONVOLUTIONAL DECODER

Code Rate: 1/2 (Nonsystematic)
Constraint Length: K=24 bits
Decoder Input Quantization: 3 bits (8 uniformly spaced levels)
Path Delay: 8 constaint lengths
Path Selection: Best Path not violating threshold

TABLE 3.19 PARAMETERS FOR DECODER DESIGN

The operation of the decoder is as follows. The received data is quantized into eight levels as in the MLD and stored in an input buffer (this is the one which can overflow) for back up search. The proper received data is sent to the transition generator along with information necessary to calculate the transition metrics; this depends on the node under consideration. The past node metric (accumulated) is added to the transition metrics giving two new accumulated metrics which are then compared for the best path of the two (highest metric). This best metric is tested for threshold violation; if okay the comparator notifies the algorithm logic which initiates a tightening procedure or other path as dictated by the flow diagram. It also outputs a tentative data bit selection to the path multiplexer which multiplexes it with the accumulated data path up to that point. The result is stored. If the threshold is violated the logic is also notified and the lower level of the flow diagram is implemented including, if necessary, a back up. In the case of a back up, the algorithm erases the corresponding node from path storage and metric storage; it then selects the appropriate input bits for calculation of the next best path to a node or if none exists it backs up again. If that fails it finally reduces the threshold by resetting the threshold generator and proceeds forward.

Since the same transition metric is used in sequential decoding as was in the MLD, except for a bias term, its calculation is the same as in

the MLD with the bias term subtracted from it, i.e.,

$$L_{00} = \alpha_1 C_1 + \alpha_2 C_2 - B_{00} \tag{3.35}$$

$$L_{11} = \alpha_1 \overline{C}_1 + \alpha_2 \overline{C}_2 - B_{11} \tag{3.36}$$

$$L_{10} = \alpha_1 \overline{C}_1 + \alpha_2 C_2 - B_{10} \tag{3.37}$$

$$L_{01} = \alpha_1 C_1 + \alpha_2 \overline{C}_2 - B_{01} \tag{3.38}$$

The modification to Figure 3.37 is the addition of the bias term, $B_{uj}$, to the adder (in binary, of course).

The metric multiplex, metric storage, metric magnitude detector, synchronization and timing, path multiplex, path storage, and metric comparator remain essentially the same as in the MLD design with the notable exceptions of erase capability in the storage units in the case of a back up and restart capability in synchronization.

The threshold generator is a dual function full adder (threshold loosening) and subtracter (threshold tightening) with the algorithm logic controlling the add/subtract functions.

The input buffer is a 2048 bit serial in/parallel out shift register with its input receiving the three bit quantized bits from the channel modem and its outputs connected to the input buffer gates. These gates, which are controlled by the algorithm logic allow the selection of any set of received data as required for metric calculation.

Finally, the algorithm logic is essentially a minicomputer, which reacts per the Fano flow diagram to "threshold satisfy/violate" inputs and information so as to generate the algorithm.

Note that no data bit selector or most likely path detector blocks exists in the sequential decoder. This is because the data bit selection is a natural result of a particular path having survived the threshold criterion as opposed to any direct comparison of path metrics in the MLD.

Phase reversal detection and other timing/sync functions are provided by the synchronization and timing unit. Basically the metric is monitored as in the MLD, however, added circuitry is needed to obtain restart in the case of buffer overflow and to routinely check on the periodic reference bits sent by the encoder, e.g., frame sync words.

3.2.3.3.3 Sequential Decoder Cost

The cost of a sequential decoder operating at the low bit rates of interest here should be higher than the Viterbi decoder because the previously decribed Viterbi decoder used serial operations which essentially makes it a sequential machine, however, the sequential decoding algorithm is by its very nature more complex, hence more logic is needed. The machine described below is one presently available and was chosen because of this. If one had to be developed the development costs would have to be added onto it. Also the decoder is overdesigned for the application here since it operates at much higher rates than necessary and uses hard decisions, however it shows what can be done.

- Manufacturer: Linkabit Corporation
- Model: LS4157
- Coding Gain: approximately 6 dB* at $10^{-5}$ bit error probability
- IC Complement: approximately 600 units, MECL III
- Data Rate: up to 40 MBPS

* at data rates well below 40 MBPS

- Code Rate: 1/2, systematic
- Constraint Length: K=41
- Decision Scheme: hard, Q=2
- Cost: approximately $35000 each

### 3.2.4 SEQUENTIAL VERSUS VITERBI DECODER TRADEOFF FACTORS

The primary vehicle used in this section for performing the tradeoff between the sequential and maximum likelihood decoders is a paper by Huth[10]. In the paper Huth has used the storage and computation requirements of the two algorithms together with their performance on the AWGN channel to analyze them. He plots complexity bits, which are defined as a bit of storage or latch, a bit in an addition or comparison, or a switch, versus $E_b/N_0$ with constraint length, quantization levels, and bit rate as parameters.

Along with the above criterion other factors will be brought into play which are pertinent to the IMEMD/H missions. Consider Figure 3.45[10]. In order to apply the curve to an output probability of error of $10^{-5}$ rather than the $10^{-4}$ shown the coding gain variation could be taken into account, but since K=7 has already been determined for the Viterbi decoder, this is unnecessary (it is the constraint length that fixes the complexity). In the case of sequential decoding the curve is vertical and independent of constraint length hence for a given bit rate the complexity at $10^{-5}$ will be the same as that for $10^{-4}$.

With the above in mind it is seen that a K=7, Q=8 Viterbi decoder requires 6000 complexity bits and the K=24, Q=8 sequential decoder requires 3500 complexity bits. Per a private conversation with Dr. Jerrold Heller of Linkabit Corporation[25], it is felt that Huth's results are pessimistic

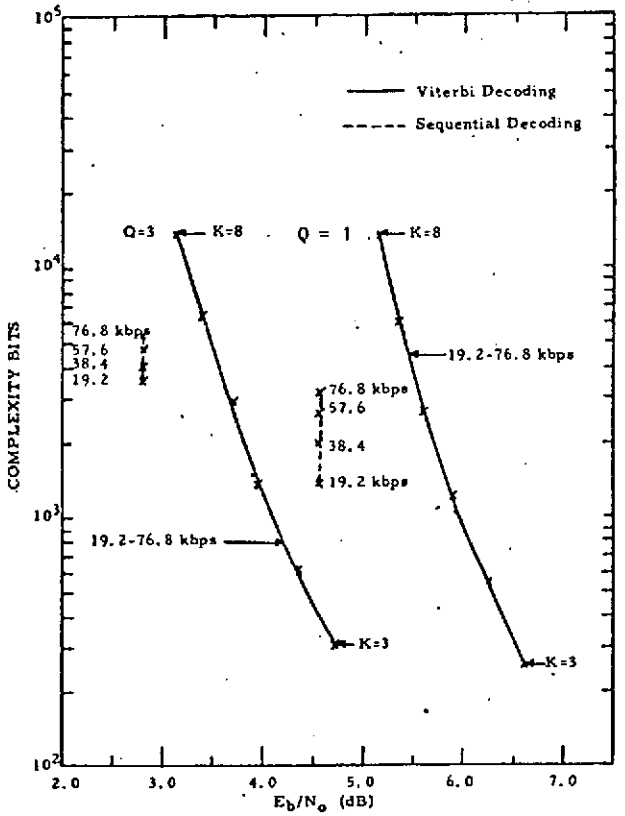


FIGURE 3.45 Comparison of Complexity Versus Performance of Viterbi Decoding and Sequential Decoding with Code Rate 1/2 and Output Probability of Error Per Bit of $10^{-4}$

in that he uses the brute force approach. In fact Linkabit and General Atronics Corporation have proposed Viterbi units with considerably less complexity. In the conversation with Linkabit it was learned that they have available a K=7 decoder, Model LV7015 which provides the gain necessary and yet uses only 82 IC units. The unit costs $5000 in lots of one and $4500 in lots of five.*

The reason for the discrepancy is that at the low rates considered here (<100 kbps) a serial rather than parallel operation is possible (much like the sequential decoder). This decreases the complexity to at or below the sequential machine. Another factor is that a more sophisticated algorithm is used in the present decoder. It is thus felt that the complexity of the

* see Section 3.2.3.2.3

MLD and the sequential decoder is about the same, thus neither has the edge here.

With the complexity issue resolved, other factors will be analyzed which are essential to any decision between the two decoders. The first is very important and that is the burst error performance. While the space channel is a random error medium, the signals could be subjected to burst errors in several ways, e.g., due to tape speed fluctuation if recorded prior to decoding, switching transients or transients, caused by lightening, entering a transmission line while the code is being sent to, say, Goddard for central decoding, or temporary loss of sync at the ground station due to power transients, signal fade, etc. The Viterbi decoder, since it does not require restart after loss of sync will recover rapidly whereas the sequential decoder needs a complete restart as discussed in its section. The Viterbi decoder therefore has the edge here.

Another factor to be considered is the steepness of the coding curves. Figure 3.45a contrasts typical Viterbi and sequential error curves. The steepness of the sequential curve is an asset if very low error rates are desired ($\leq 10^{-6}$) since less $E_b/N_0$ is needed to achieve them, however it is a detriment if the system $E_b/N_0$ fluctuates very much about the knee of the curve. For example consider Table 3.20 with values taken from Figure 3.45a.

| Error Rate | $E_b/N_0$ (Viterbi) | $E_b/N_0$ (Sequential) |
|---|---|---|
| $10^{-5}$ | 4.1 dB | 4.2 dB |
| $10^{-2}$ | 1.8 dB | 3.5 dB |

TABLE 3.20 ERROR RATE DEGRADATION

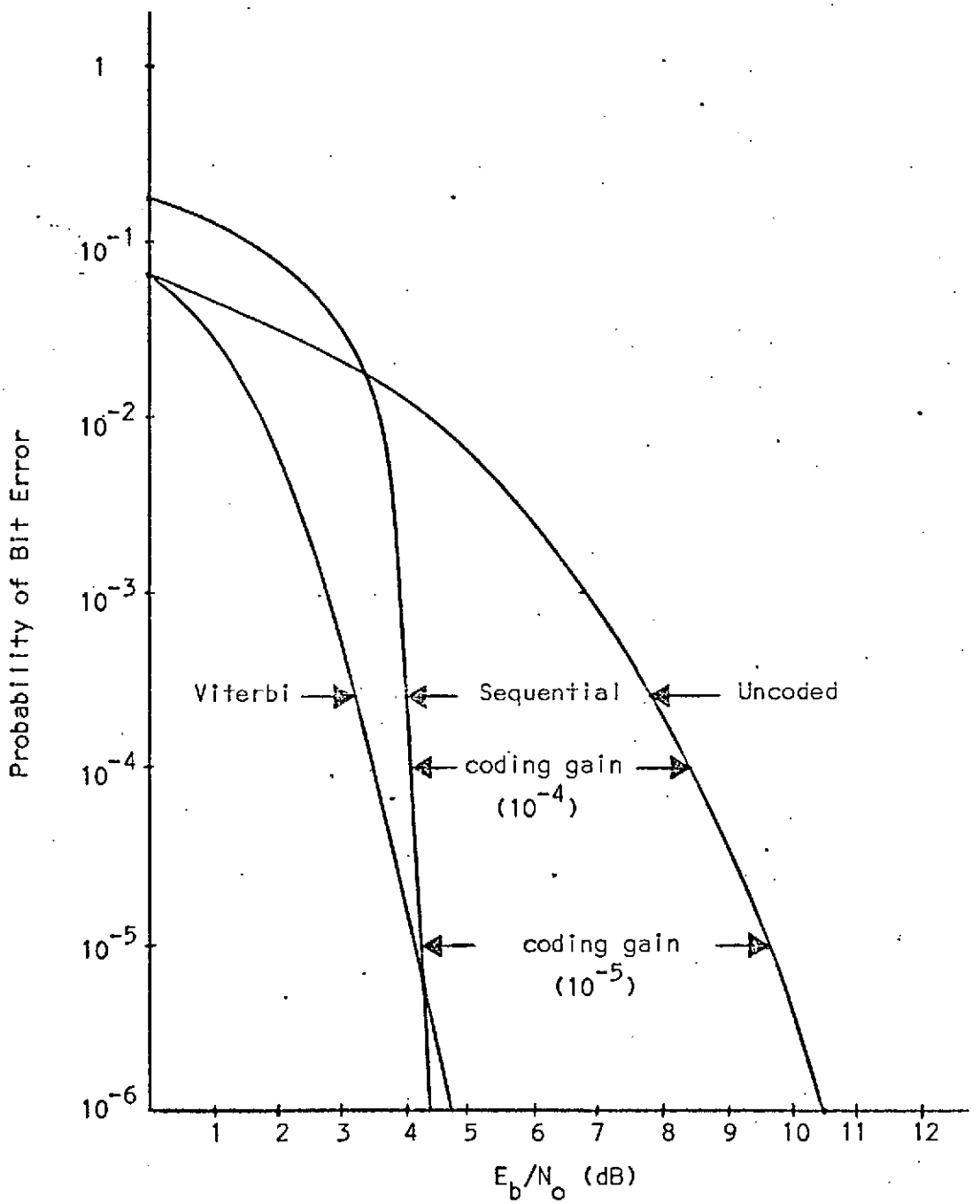


FIGURE 3.45a CONVOLUTION CODING GAIN EXAMPLE

As seen in the table, it only takes a 0.7 dB drop in $E_b/N_0$ to degrade the error rate from $10^{-5}$ to $10^{-2}$ with a sequential decoder where as it takes 2.3 dB with the Viterbi. Thus if a fade occurs in the signal due to transmitter power drop or an antenna off axis problem, the Viterbi decoder is more graceful.

A third factor is the elimination of any off line decoding due to sequential buffer overflow if a Viterbi decoder is used.

A fourth minor factor is that the constraint length of 7 encoder is cheaper and easier to build than one of 24.

A fifth factor is that the Viterbi decoder is insensitive to the AGC levels presented to it, especially in a soft decision decoder, e.g., a $\pm$ 3 dB level change only affects the gain by about 0.1 dB. In the sequential decoder the number of computations increases drastically as the levels deviate from designed values.

The above items are considered to be the most important in the tradeoff between the two decoders. In the next section these items will be employed to recommend the decoder to be used on the IMEMD/H missions.

## 3.3 TASK 3 DISCUSSION AND RESULTS

This section of the report studies five network configurations (Figure 3.46) for delivering experimental data to a user via a convolutionally encoded/Viterbi decoded telemetry system. Each configuration will be analyzed individually on a block by block basis. In so doing the system as a whole can be evaluated in terms of efficiency, cost, etc. and as such can be compared against the others. The result of these comparisons will be the optimum system for the IMEMD/H missions.

### 3.3.1 SOFTWARE VERSUS HARDWARE

As can be seen from Figure 3.46 the systems can be grouped into two broad headings; either the decoding is done at the ground station or it is done remotely. The bulk of this section will be devoted to the problem of which is best and which system in the group is best. A major concern before proceeding to this phase of the report, however, is what is the implementation of the decoder to be, i.e., should it be hard wired such as the one analyzed in task 2, or should the algorithm be performed by a general purpose or possibly a special purpose digital computer? To answer this question, consider the following material on software decoding.

The first point to be determined in making a decision between hardware versus software is the number and type of operations to be performed in the algorithm. With this in mind the Viterbi algorithm was analyzed in detail. Consider the flow diagram of Figure 3.47. Each block will be explained in terms of its function in the algorithm, and the major operations required to perform it will be investigated.

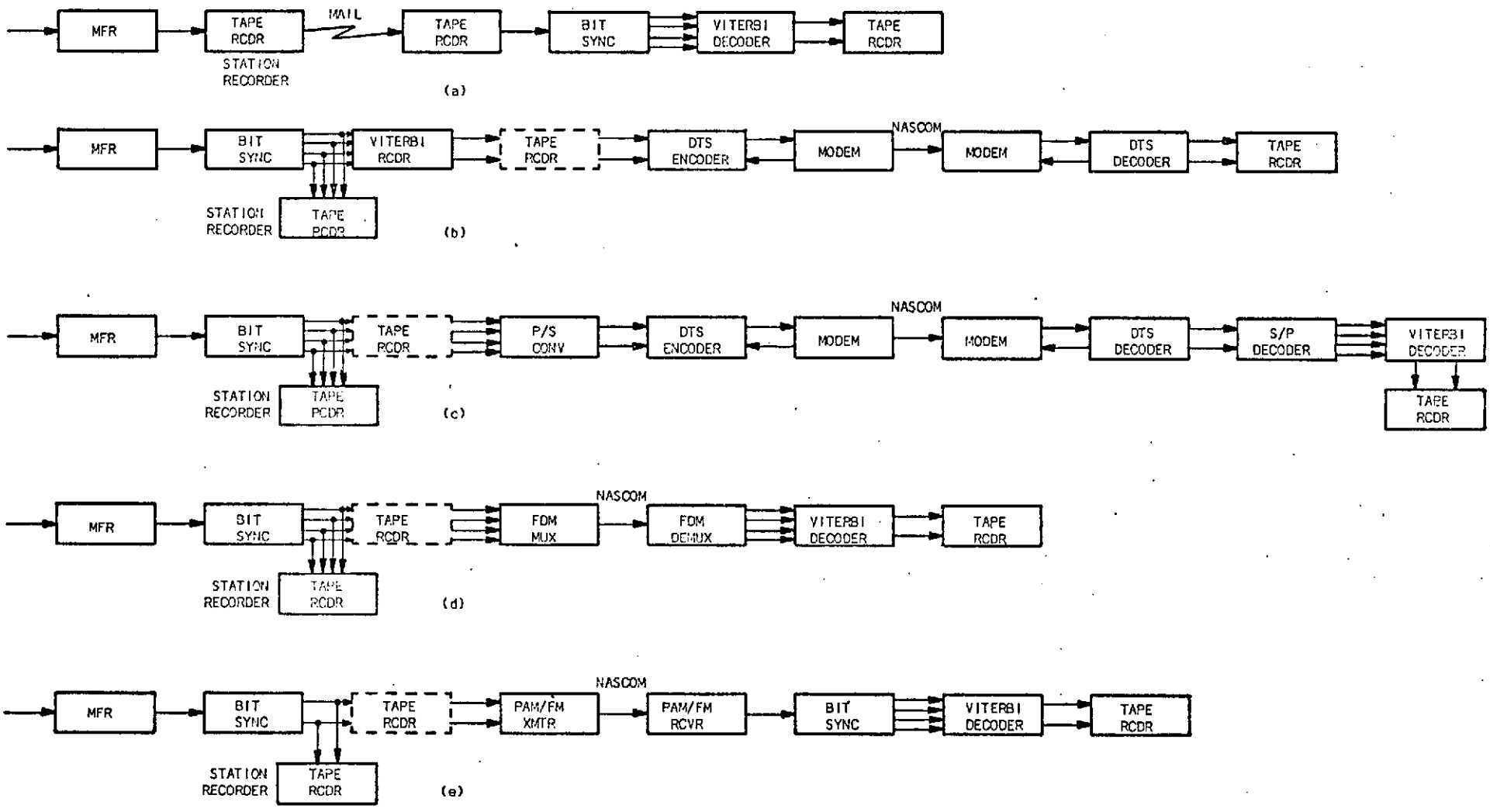


FIGURE 3.46 TELEMETRY/CODEC CONFIGURATIONS

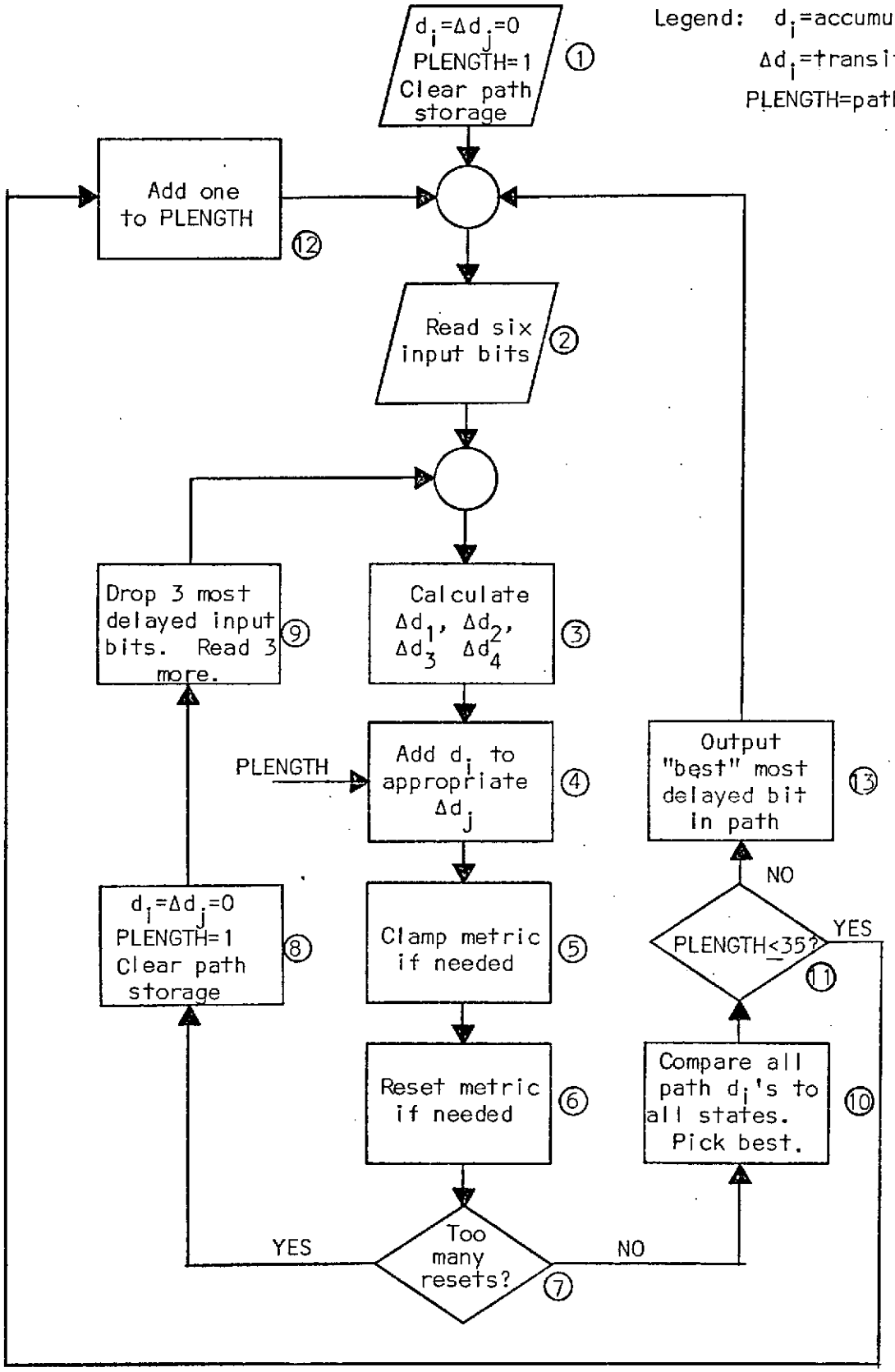


FIGURE 3.47 VITERBI ALGORITHM FLOW DIAGRAM

Block 1 sets the metric storage (accumulated and transition) to zero to start the algorithm at the tree origin. It also clears the path registers and sets the path length counter to one. This is needed since the number of allowable states increases up to $64=2^6$ and stays there; also the information bits start to be outputted from the decoder after 5 constraint lengths, i.e., 35 path bits.

Block 2 reads in the first six (6) received bits from the A/D converter output of the bit synchronizer.

Block 3 calculates the transition metrics $\Delta d_j$ : j=1,2,3,4. There are four of them because a 1/2 rate code allows the possibilities 00, 01, 10, 11 as transmitted (noisefree) code bits out of the spacecraft encoder.

Block 4 calculates the accumulated metric for all paths leading to a given state. There are $128=2^7$ of these metrics. Note that the path length counter content is an input to the block. This is needed because at the start the number of accumulated metrics is less than 128. After K-1 branches have been received, where K is the constraint length, the number of metrics is 128 and stays at this value for the rest of the algorithm.

Block 5 clamps the accumulated metric at some value if it tries to grow too much. Since we are only interested in the lowest metric the clamping will have negligible effect.

Block 6 resets all metrics by a fixed amount so that the relative distances remain the same. This keeps the lowest metric from getting too large which is not advantageous for storage purposes.

Block 7 examines the number of resets that have occurred. Too many resets means that the error rate is large which usually means that branch sync has not been achieved.

Blocks 8 and 9 restart the algorithm and slip the received branches by one half. Since there are only two bits (noisefree) per branch out of the encoder, the decoder is either in sync or out. Slipping one half a branch when out of sync puts the decoder in sync again.

Block 10 compares all the metrics leading to each state and picks the path bit which corresponds to the best one. This bit is multiplexed to the previous path and the metric is stored.

Block 11 makes sure there is enough path delay to guarantee a near optimum bit decision. It was shown in Task 2 that five (5) constraint lengths was sufficient.

Block 12 adds one to the path length counter and the algorithm is recycled.

Block 13 ejects the most delayed information bit estimate after the path delay reaches thirty-five. The algorithm is then recycled.

With the above in mind it is relatively easy to derive a number which represents the speed at which a computer must operate in order to perform the algorithm. The reasoning is as follows. Aside from the "housekeeping" operations that must be taken care of, there are a minimum number of additions and comparisons to be done. Block 3 dictates 4 additions; Block 4 dictates 128 additions; Block 10 dictates 64 comparisons. The

comparison is equivalent to an addition, so there are at least 196 additions to be performed. Rounding 196 to 200 gives an easier number to work with.

Now these additions must be done within a bit period hence Table 3.21 shows the speed required of the computer versus the input information bit rate (1/2 the coded rate).

| speed (μsec) | 9.8 | 4.9 | 2.4 | 1.2 | 0.6 | 0.3 |
|---|---|---|---|---|---|---|
| bit rate (KBPS) | 0.5 | 1.0 | 2.0 | 4.1 | 8.2 | 16.4 |

TABLE 3.21 COMPUTER SPEEDS REQUIRED PER ADDITION

The major computers available at the ground stations in the 1975 to 1977 time frame of interest will be the ones used for Stadac I and Stadac II.[34] These machines require over 2 μsecs per addition[35][36] (Digital Equipment Corporation PDP/11 and Univac 642B computers). As can be seen from the Table 3.21 only the IMEH mission at its lower rates could possibly make use of the station computers.

The above rationale eliminates the station computers, however, it could be possible for a more sophisticated machine at some remote location to perform the algorithm. A quick look at reference 35, however, readily shows that only very advanced machines such as the IBM 370 series or a Univac 1110 could handle the 16.4 kbps rate from the IMEMD.

It should also be noted that the other parts of the algorithm have not even been considered hence if the machine barely handles the number of additions required, it will fail to do the job when the extra load is placed on it by the rest of the algorithm.

It may be of interest to note why the computer cannot achieve the speed required. Computers are usually set up to read an instruction, say an add of A and B, go to the memory to fetch A and B, load them into registers, add them, and finally store the result. All of this consumes time, and if each addition must be done sequentially, i.e., one after another, then a large number of additions cannot be handled.

The conclusion is that a hard wired decoder is the most cost effective implementation of the Viterbi algorithm.

As a side comment to the hardware decision above, it can be noted that parallel operation is possible in hardware, whereas it is difficult to justify in a general purpose computer. The sequential machine must perform 200 additions one after another, but a hard wired machine can be built to perform, say 10 additions in parallel, thereby decreasing the speed necessary by a factor of 10. With the integrated circuit technology available today it is possible to package a large number of full adders in an extremely small space; also the advent of CMOS logic reduces the power requirement to a reasonable level even though this is not a prime consideration at a ground installation.

### 3.3.2 TELEMETRY/CODEC CONFIGURATION A

A straightforward mechanization of a system for receiving and decoding convolutionally coded data is shown. This method was used on the earlier Interplanetary Monitoring Platforms (IMP) and provided satisfactory results. A description of the method is as follows. The output of the receiver demodulator is recorded on a station tape recorder. Since the bit rates were so low (~400 bps) the data could be readily recorded on the FM

track of the tape recorder without encountering tape timing problems or exceeding the response of the FM track.

The tapes were then mailed to Goddard Space Flight Center Information Processing Division (IPD) where they were fed into a bit synchronizer with soft decision capability and decoded. In the case of the IMP series the decoding algorithm was the sequential version rather than the maximum likelihood one considered in this report.

In the present study the bit rates are higher thus necessitating a concern about the tape recorder. This subject will be taken up in Section 3.3.3 since the configuration A is not considered to be desirable due to the tape mailing required. Many procedural problems arise when tape mailing is involved. These problems are not reflected in a cost analysis, but are important when considered in the context of network operation, e.g., tape costs dictate that full tapes be mailed, however, full tapes inject confusion into the data processing when stripping out each experimenter's data. Other problems are tape costs, reuse of tapes, rework of tapes after "?" number of uses, mail delays, tape handling at the site, at GSFC, and in between. These and other drawbacks have led to the decision that direct transmission via NASCOM is highly desirable. Appendix H reproduces a Goddard study on tape costs which was done after the present study and is therefore included for "completeness."

It should be stated, however, that there are several positive features of configuration A among which are:

- simplicity in concept
- central processing facility
- relatively reliable
- moderate cost
- minimum station equipment loading.

Some unfavorable features other than those mentioned above are:

- human factor in handling and mailing
- indexing of projects requirement
- suseptability of tapes to damage.

The conclusion is that configuration A should not be used unless direct NASCOM transmission is not feasible.

### 3.3.3 TELEMETRY/CODEC CONFIGURATION B

The next simplest approach to the telemetry/codec problem is to place a decoder at each support site as shown in Figure 3.46b. This gets around the mail handling problem that was the chief reason for rejecting configuration A discussed in the previous section. The rest of the system is the same as that which would be employed in a real time transmission uncoded telemetry system.

The advantages of configuration B are:

- All decoding is done at the site
- Lower data rates for transmission over NASCOM due to the decoder output being just the information rate originally sent to the spacecraft encoder
- No tape recorder record/playback degradation prior to decoding (bit synchronizer timing jitter, etc.)
- The placing of the bit synchronizer directly behind the demodulator ensures that the matched filter internal to it will indeed be "matched"; that is, up to the demodulator output of a PCM/PM system the noise spectrum and statistics are very predictable, whereas, tape recorder effects and transmission anomalies over NASCOM can make the assumed white gaussian noise an invalid model.

The disadvantage* of configuration B is:

- Decoders needed at each support site.

---

* Other than the problems of NASCOM transmission treated later.

Let it be immediately stated, however, that once the decoders are at the site, and if they are designed with some degree of flexibility, then this disadvantage becomes an advantage. The reason is that future missions can make use of them to save transmit power and/or increase their data rates over and above an uncoded system. This can be done since the K=7 Viterbi encoder is an almost trivial addition to a spacecraft in terms of power and complexity.

It is the author's opinion that more and more coded systems will be used in the future because of two reasons:

- Proven performance on prior spacecraft
- More familiarity with coded systems in general.

3.3.3.1 BIT SYNCHRONIZER CONSIDERATIONS

It is appropriate here to discuss some of the practical aspects of implementing configuration B. Consider the bit synchronizer. Suppose that a bit error rate of $10^{-5}$ is desired. Theoretically an energy per bit to single sided noise density ratio ($E_b/N_o$) of 9.6 dB is needed, however, practical bit synchronizers of a state of the art design (so called third generation) will perform within 1 dB of theoretical for input SNR's of 0 dB[37] in the signaling bandwidth, i.e., the symbol rate seen by the bit sync. Thus 10.6 dB is required in an uncoded system.

In a coded system, however, the symbol rate into the bit sync is twice the information rate (1/2 rate code assumed). The bit sync must integrate over a period equal to each symbol to estimate it, thus the bandwidth must be larger in a coded system. This degrades the SNR into the bit sync making it work harder, so to speak. Also since the decoder

provides gain, say 5 dB for example purposes, the required $E_b/N_o$ into the bit sync must be 10.6 dB - 5 dB = 5.6 dB. Now the SNR is found by adding 10 log($R_b/W$), where $R_b$ is the information rate ($E_b R_b = S \neq E_b R_s$*) and W is the bit sync bandwidth.

Say that the data is NRZ-L then it is common to pass the first nulls of the power spectrum, thus $W = R_s$, where $R_s$ is the symbol rate; but $R_s = 2R_b$ resulting in an SNR at the bit sync of

$$\text{SNR} = 5.6 \text{ dB} - 3 \text{ dB} = 2.6 \text{ dB}. \tag{3.39}$$

The previous manipulation seems to cause great mystification among engineers. It is the author's opinion that the confusion lies in intermixing $E_b/N_0$ and SNR. Consider the following. Assume that all noise-free waveforms are rectangular of height "A" (Figure 3.48).

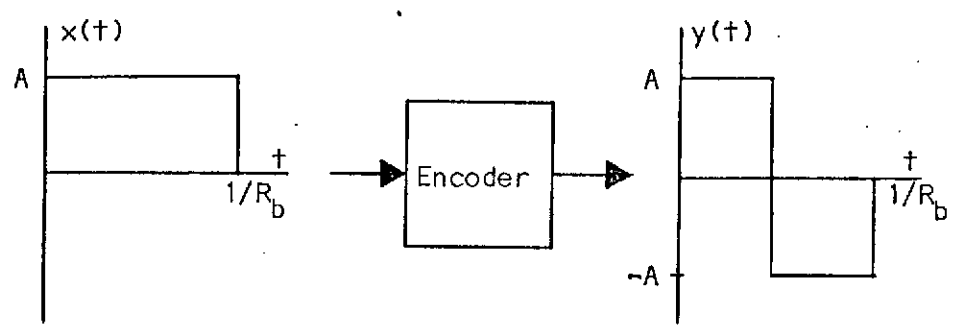


FIGURE 3.48 ENCODED WAVEFORMS

Since energy is given by

$$E = \int_{-\infty}^{\infty} S^2(t)\,dt, \tag{3.40}$$

* $R_s$ is the symbol rate

the energy per bit (x(t) over the time interval $1/R_b$) is

$$E_b = \int_0^{1/R_b} A^2 dt = A^2/R_b \ . \tag{3.41}$$

Out of the encoder the energy per bit is

$$E_b = \int_0^{1/2R_b} A^2 dt + \int_{1/2R_b}^{1/R_b} (-A)^2 dt = A^2/R_b \ . \tag{3.42}$$

The energy <u>per bit</u> has <u>not</u> changed! Consider, however, the energy per <u>symbol</u> out of the decoder

$$E_s = \int_0^{1/2R_b} A^2 dt = \int_{1/2R_b}^{1/R_b} (-A)^2 dt = A^2/2R_b = E_b/2. \tag{3.43}$$

Consider the power, i.e., the energy per unit time.

$$P_b = E_b R_b = A^2 \tag{3.44}$$

$$P_s = E_s R_s = \frac{E_b}{2} (2R_b) = A^2 \ . \tag{3.45}$$

The power hasn't changed! Since the noise density is constant the signal power to single sided noise density ratio is constant at

$$S/N_0 = P_b/N_0 = P_s/N_0 = A^2/N_0 \ . \tag{3.46}$$

The confusion occurs in the bandwidths throughout the system. Prior to the encoder $W=R_b$ (1st nulls again); after encoding $W=2R_b$, i.e., more bandwidth is required due to coding, thus the SNR is

$$SNR = S/N_0 W = (S/N_0)(1/W) \tag{3.47}$$

and the SNR has decreased. This is, unfortunately, the quantity that is significant to the bit sync.

To finally put the point to rest consider the block diagram of Figure 3.49.

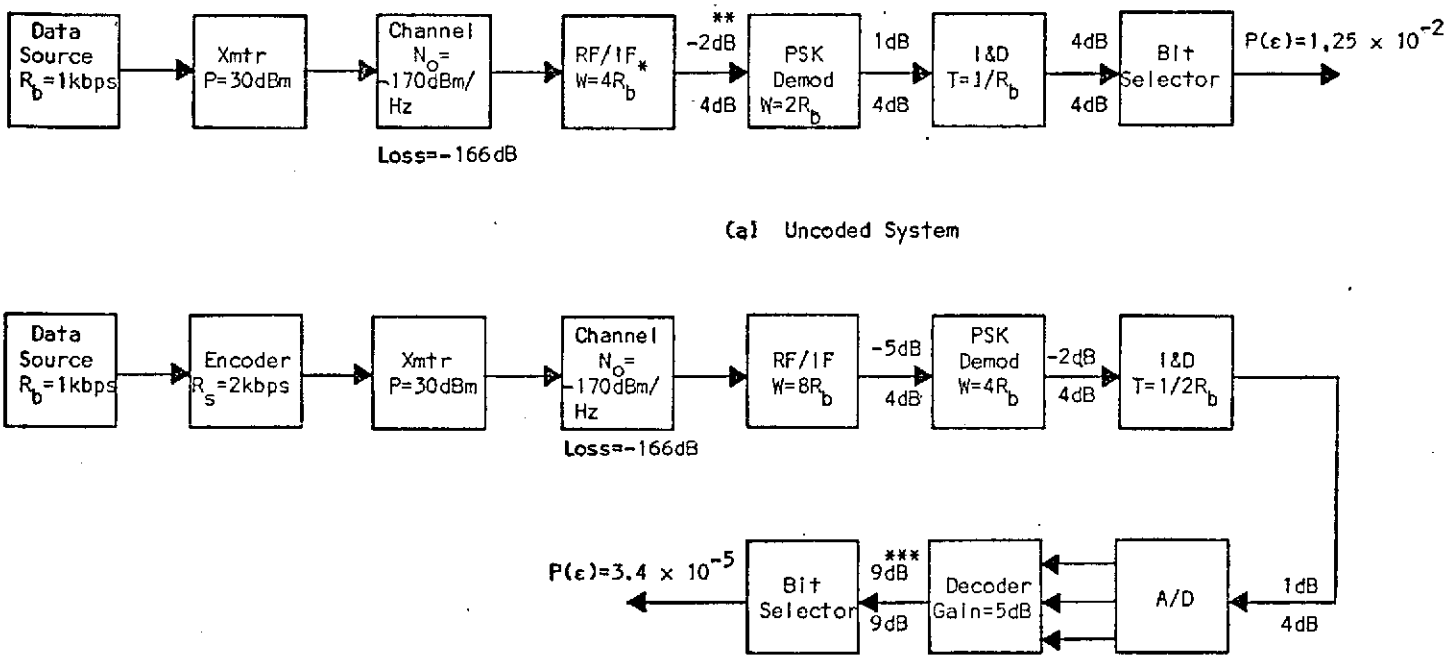


* W is the low pass equivalent of the RF/IF bandwidth (i.e., single sided)

** S/N values are above the line; $E_b/N_0$ values are below the line

*** 5 dB gain due to algorithm and 3 dB gain due to demultiplexing code bits, i.e., bit rate is now the information rate

FIGURE 3.49 SYSTEM POWER/NOISE BUDGETS FOR CODED AND UNCODED SYSTEMS

The conclusion to all of the above is that due to coding gain by the decoder and the decreased integration time available to the bit sync, the bit sync for a coded system must be better than an uncoded one in terms of efficient operation.

A further requirement of a bit sync to be used with the proposed soft decision system is that it have incorporated within it an analog to digital (A/D) converter which quantizes the analog voltage out of the matched filter into eight levels (3 bit word).

It has been learned by the author that a bit sync with the A/D, state of the art design (for the low SNR's expected), and appropriate clock outputs has been procured by NASA/GSFC from "Moniter Systems" and these units will be deployed throughout the STDN by the end of 1973. It is then concluded that no problems should be encountered due to the bit sync block in Figure 3.46.

3.3.3.2 TAPE RECORDER CONSIDERATIONS

The next topic to be discussed in connection with Figure 3.46b is the tape recorder. As can be seen from Figure 3.46 all of the configurations have the option of recording the data at the ground station as a backup to the direct data transmission via NASCOM. A tape recorder can also be used, if such is desired, to slow down the data rate prior to NASCOM transmission, thereby resulting in near real time data (the advantage here is that less bandwidth is required to send the data).

Consider for the moment the station backup recorder. The output of the bit sync was chosen as the point of recording rather than the MFR output because the matched filter operation has been performed at this stage of the system. The optimum estimate of the received signal

is therefore available at its output. As mentioned in the section on configuration A the closer that the system prior to the integrate and dump filter is to the AWGN model the better the system will perform. Again tape jitter, etc. would cause the channel to deviate from this AWGN model. Another advantage of the choice of backup recorder position made here is that digital recording can be made less sensitive to anomolies than analog recording. A treatise of digital recording will now be presented and is drawn mainly from references 38, 39, and 40.

There are two common methods used in recording digital data with a magnetic tape recorder, viz., direct and FM. Direct recording is merely an extension of the familiar audio (home entertainment) recorder. Without delving too deeply into the physics and mathematics the following basics together with the advantages and disadvantages of direct recording will be discussed.

It is well known that an audio recorder cannot record and play-back video, e.g., TV, signals. The reason is that the high end response is not wide enough, i.e., high frequency signals are attenuated and therefore lost. Since the electronics can be designed to handle the high frequencies the basic limitation must be in the magnetic recording (tape to head to tape) mechanism and indeed it is.

The voltage out of the playback head is a decreasing function of the recording wavelength, i.e.,

$$V = g(\lambda) \tag{3.48}$$

where

$$\lambda = \frac{v}{f} \tag{3.49}$$

v is the tape velocity past the head, and f is the frequency recorded. These equations reflect the fact that signal is averaged across the head gap and as such, when the frequency rises, it finally reaches the point that it is averaged over a full cycle and is thus zero (relation (3.50)).

$$g(\lambda) \rightarrow 0 \quad \text{as} \quad \lambda \rightarrow d \tag{3.50}$$

where d is the head gap (d/v is the time to traverse the head gap).

For a given frequency two things can be done to avoid the averaging problem (see Figure 3.50).

1) decrease d thereby raising the value of f in (3.50) needed to make the average zero.

2) increase v with the same result as in 1).

Obviously gap length can only be decreased so far due to head wear, etc.; also the increased tape speed requires a more stable tape drive mechanism and allows less total data to be recorded on a given length of tape. To quote an achievable high end response, the Ampex FR-2000 recorder can handle frequencies up to 2 MHz in the direct mode.

The basic limitation at the low end of the record spectrum is that the playback output is proportional to frequency, e.g., if Ø is the recorded flux on the tape, the output for a sinusoid is

$$V = \frac{K d\emptyset}{dt} = K \frac{d(\sin 2\pi ft)}{dt} = 2\pi fK \cos(2\pi ft) \tag{3.51}$$

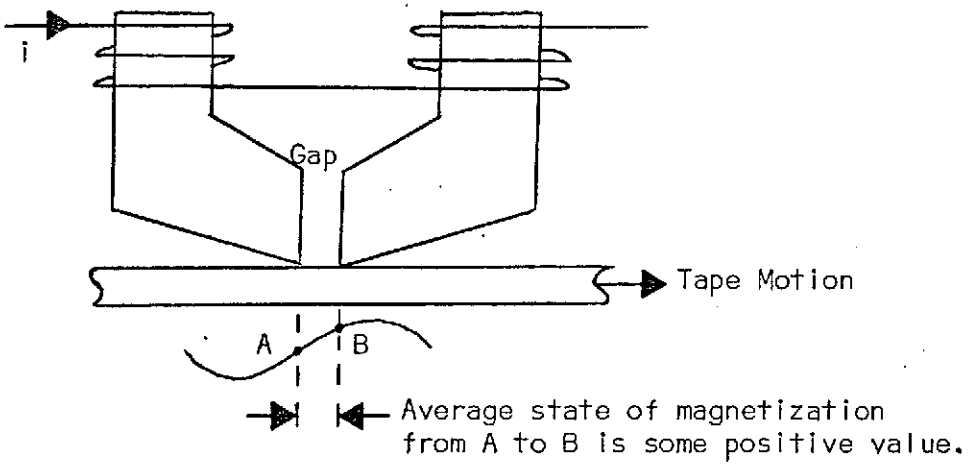


FIGURE 3.50a GAP EFFECT AT LOW FREQUENCY

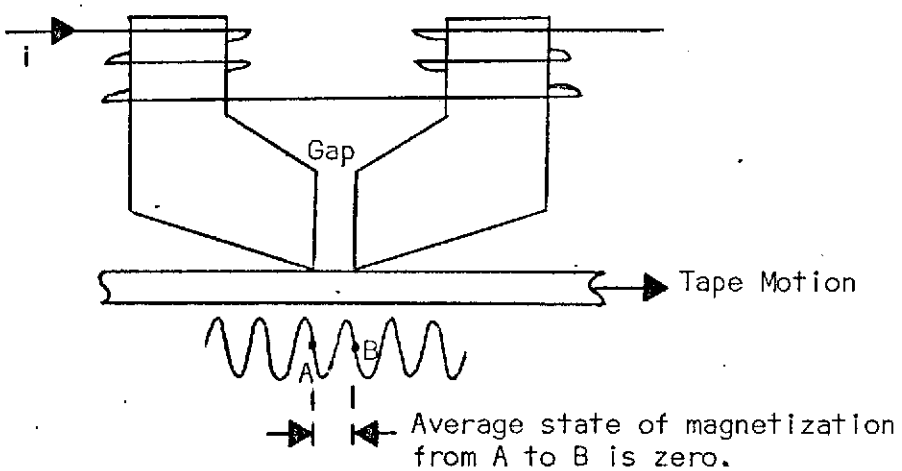


FIGURE 3.50b GAP EFFECT AT HIGH FREQUENCY

Figure 3.51 illustrates this relationship

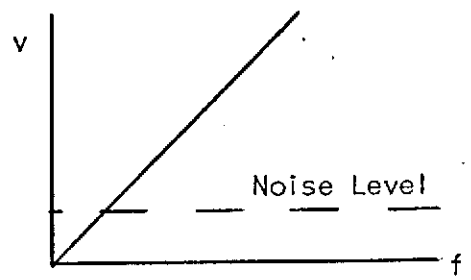


FIGURE 3.51 RECORDER PLAYBACK OUTPUT VERSUS FREQUENCY OF INPUT

As can be seen from the figure the output at low frequencies eventually drops down into the system noise and is thus unusable. The conclusion is that the low end response does not go to zero and thus signals with d-c averages cannot be faithfully reproduced. A typical low frequency cutoff is 400 Hz.

Two other limitations of direct recording will now be discussed. The first is data drop out. A simple explanation would be that the playback recorded amplitude drops due to the tape pulling away from the gap. This could be caused by "bumps" in the tape or vibration of the tape (Figure 3.52) (the farther away the tape gets from the head the less the recorded or played back signal).

The second limitation is due to timing errors. "A multichannel[40] instrumentation tape recorder exhibits some predictable time differences

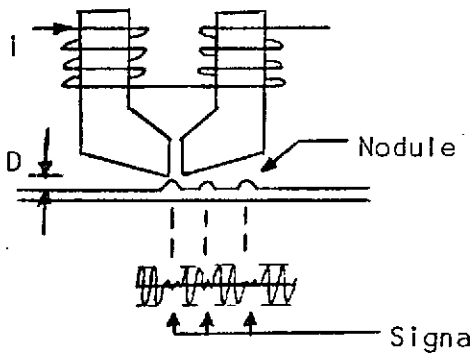


Drop in playback level (in dB) $= 54\frac{D}{\lambda}$

where: D = Separation of tape from head

$\lambda$ = Recorded wave length on tape

FIGURE 3.52 TAPE DROPOUT EXAMPLE

between its various data channels. These may or may not cause a problem in a given application depending upon how accurately you need to correlate time between events recorded on different channels. Interchannel timing errors can be attributed to three main factors: 1) Static delays (skew) caused by head manufacturing tolerances and any guiding misalignment of the tape path relative to the heads; 2) Dynamic delays (also commonly called skew) caused by the tape transport and the flexibility of the tape; 3) Static and dynamic delays caused by the electronics.

3.3.3.2.1 Static Time Errors

The major cause of static timing errors in a multichannel recorder is the manufacturing tolerances of the heads. To illustrate, take as an example the specifications of the Inter Range Instrumentation

Group (IRIG) for head design which furnish the standards adhered to by most tape recorder manufacturers (IRIG 106-66, Section 6).

| | |
|---|---|
| Gap Scatter . . . . . | 100 microinches |
| Stack Spacing . . . . . | 1.500 $\pm$ 0.001 inch |
| Head Tilt . . . . . | $\pm$1 minute of arc |

3.3.3.2.1.1 Gap Scatter

A multiple track instrumentation head stack has a number of individual heads (typically 7 for a 1-inch staggered head stack), incorporated in the stack. It is mechanically impossible to exactly align these gaps, so the term gap scatter refers to the actual tolerance of alignment of each of these tracks in relation to a line through the mean position of all gaps in the stack. The positional tolerance of these head gaps within a given stack is a band 100 microinches in width. The worst case condition of timing between two tracks would be when the gaps in question on the record head stack were at one limit of the tolerance while those at the reproduce stack were at the opposite end of the tolerance band. This gives a worst case error of 200 microinches between two tracks allowing 100 microinches in the record and 100 microinches in the opposite direction on the reproduce head. As a final note it should be stated that this error is somewhat random in occurence within a stack, and heads with the widest spacing or error may occur adjacent to each other or at the opposite ends of the stack.

3.3.3.2.1.2 Head Stack Spacing

In order to achieve the normal recording density of 14 tracks for 1-inch tape (or 7 tracks for 1/2-inch tape), it is necessary to place

half the heads, the odd numbered tracks, in one stack and the even numbered tracks in a second stack. This allows sufficient shielding to be provided between tracks in the head stack to minimize undersirable signal coupling and crosstalk. The normal spacing difference between the odd and even head stacks is 1.500 inches with a tolerance of $\pm$0.001 inch. This means that under worst case conditions (record stacks spaced at one limit of this tolerance and reproduce stacks at the other limit), adjacent odd and even tape tracks could be displaced from each other by a possible 0.002 inch (2000 microinches).

3.3.3.2.1.3 Head Tilt

This measurement and specification refers to the difference between the mean gap azimuth of a given head stack and a line perpendicular to the edge of the tape. In practice this may be caused either by lack of perpendicularity between the head stack and base plate, or the misalignment of the tape path of the transport relative to the head. These effects are difficult to separate and are usually tested as one measurement. No attempt will be made here to separate them. The value permissible under IRIG specifications is $\pm$1 minute of arc or a distance approximately 280 microinches across a 1-inch tape width. Again this is an additive specification. Thus in a worst case condition this figure could be doubled between record and reproduce head stacks.

3.3.3.2.1.4 Time Dimensional Changes

Additional effects are caused by the inherent characteristics of the magnetic tape which are not a function of head manufacturing tolerances. The backing of tape is an elastic material. As such, the distance between any two points on the tape depends on the tape tension

to some extent. This shows up primarily as a change in the 1.5-inch gap-to-gap dimension. Large temperature changes between the time of recording and reproducing and uncontrolled long term tape storage conditions can have the same effect. This tape tension effect is not as significant as other head spacing tolerances as its value is approximately 240 microinches change across the 1.5-inch head spacing with a 1-ounce tension change between the record and reproduce process on 1/2-inch tape (1 mil backing thickness). A more significant change is observed if the temperature is varied between the record and reproduce process. For a 50°F difference, the 1.5-inch spacing will change 750 microinches.

An even more interesting change is observed if the relative humidity of the air around the tape is varied over its full range between record and reproduce. In this case, a relative humidity change from zero to 100% would vary the 1.5-inch head spacing by 1650 microinches, more than all other effects put together. These phenomena, although seldom considered, result from the physical properties of polyester base materials of magnetic tape.

3.3.3.2.2 Dynamic Changes

Dynamic skew and dynamic registry changes between channels are caused by runout of the tape transport, which is always present to some degree, as well as tape guiding eccentricities, tape slitting errors, and tape damage. While static skew can be allowed for and ignored to some extent in the data, dynamic skew is a time variable phenomenon and thus is much more difficult to eliminate. The only known method for minimization of this is control of the record and reproduce transport guiding. Typical values of dynamic skew on a state of the art basis are 250 microinches from

record to reproduce across the full width of a 1-inch tape. Typical tape transports of the instrumentation variety have a normal value of 500 microinches.

3.3.3.2.3 Electronic Delays

The delay variation between channels caused by the signal record and reproduce electronics are normally inconsequential compared to the mechanical delays shown above.

3.3.3.2.4 Measurement Conversion

In the previous discussion, dimensional changes caused by heads and tape are expressed in two different units: linear measurement in microinches and time measurement in microseconds. The conversion between units can be easily made if you remember that a tape recorder running at 120 inches per second moves tape 120 microinches per microsecond. This would mean a linear error of 240 microinches would occupy 2 microseconds of time at 120 ips, 4 microseconds at 60 ips, etc.

3.3.3.2.5 Tape Head Considerations

The minimization of stack to stack errors by the use of an in-line head assembly is possible. However, manufacturing a single in-line head stack with the same number of tracks as two staggered head stacks creates two main problems. First, it requires that the amount of inter-track shielding be reduced. This increases the crosstalk between data channels. Second, the track width must be reduced which cuts the signal-to-noise ratio, since it is impossible to make a full width track because there is only a 20-mil space between them. Little or no room remains for shielding, mounting, or wirewinding. An alternative to special in-line heads is to put all data needing precise time correlation in the same head stack."

In summary, then, the advantages of the direct record mode are:

- Wide response
- Simple electronics.

The disadvantages are:

- No d-c response
- Sensitivity to tape dropout
- Sensitivity to time base error.

The second most common recording mechanism is the FM record mode. Basically, the signal frequency modulates a carrier which is then recorded. On playback it is demodulated to retrieve the original signal. Since the information is now carried in the frequency changes, amplitude level changes, e.g., tape dropouts, are not as catastrophic; also a d-c signal can now be recorded. Since the carrier is in the center of the direct record band the phase shift characteristics are very good (in direct record the band edges severely distort the signal phase).

The disadvantages of FM recording are the decreased bandwidth available (due to FM spectral spreading and double sidebands about the carrier), more complex electronics to implement the FM process, and the greater sensitivity to tape transport fluctuations. This last drawback is due to the fact that these fluctuations appear on playback as a noisy recorded signal.

With the above in mind the best mode of operation of the tape recorder and its effect on the system in configuration B will now be determined. First and foremost the highest bit rate in the system is for the

IMEMD mission at 32,768 bps; if the recorder can accommodate this rate then the lower rates will take care of themselves.

Coming out of the bit synchronizer is the quantized data and a clock at the code rate. These outputs could be time multiplexed and recorded on one track, however, the frequencies involved would be high, but more important than this the need to identify the start of each quantized block (block sync) and the susceptability to time base errors would be a problem. A much simpler approach would be to record the four signals on four tracks. This alleviates the high rate problem and the block sync problem, and if the proper tracks are chosen (all odd or all even) then the time errors are minimized to acceptable levels. Also multiplex/demultiplex equipment is not needed. The only disadvantage is the requirement of four tracks, thereby, using a good deal of the tape recording capacity.

It is felt that the four track method is the best approach. As a side comment the time errors due to the tape transport and the tape itself are minimized since the clock encounters these same errors.

The next decision is whether direct or FM recording should be used. The basic NRZ-L format coming out of the bit sync requires a d-c response from the recorder. This would seem to dictate the FM mode, however, there are techniques to circumvent this problem and still use the direct mode, thereby utilizing the wide bandwidth capability and the relative insensitivity of the direct over the FM mode of operation. One such technique is to convert the NRZ-L data to split phase data. This, however, doubles the bandwidth requirement, and in so spreading the spectrum

it increases the phase distortion of the data. Figure 3.53 illustrates the advantage of split phase coding whereby, the requirement of d-c response is eliminated.

Another method of coding the data is to use a Miller code. Figure 353 shows that the bandwidth required is decreased, and the d-c response is minimized to about the same extent as the split phase code.

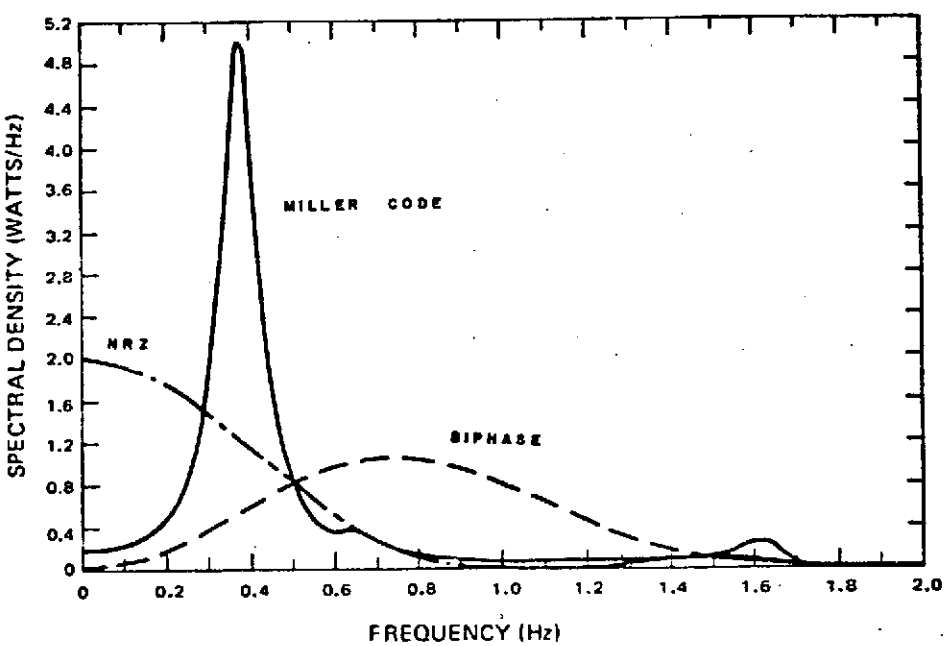


FIGURE 3.53 SPECTRAL DENSITY OF DATA CODES

Figure 3.54 shows the time waveforms for a sample of NRZ-L data. In coding with a Miller code it is possible to pack 20K bits per inch of

tape with less than a $10^{-6}$ error rate as compared to 12K bits per inch at $10^{-6}$ for split phase codes and 10K bits per inch at $10^{-6}$ for NRZ codes. Note that a $10^{-6}$ error rate prior to the convolutional decoding will not impact significantly on its performance since $10^{-6}$ is negligible relative to the pre-decoded error rate (e.g., $10^{-3}$). It should be noted that Miller coding also desensitizes the recorded data to dropouts due to the coupling of bits in the code.

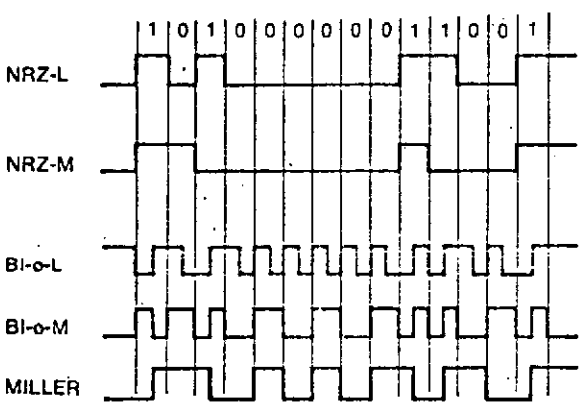


FIGURE 3.54 DATA FORMAT WAVEFORMS

The above discussion on direct recording with format coding was really for completeness only since the 32,768 bps rate is well within the capability of present day recorders (Table 3.22 lists the minimum FM record responses of four Ampex tape recorders which will accommodate 32,768 bps)*, and so cost and complexity factors dictate its choice.

* Higher tapes speeds increase the upper response limit.

| Model | Tape Speed (ips) | Response |
|---|---|---|
| AR-700 | 60 | dc to 40KHz |
| AR-1700 | 60 | dc to 40 KHz |
| FR-1900 | 15 | dc to 62.5 KHz |
| FR-2000 | 15 | dc to 62.5 KHz |

TABLE 3.22 EXAMPLE FM MODE TAPE RECORDER RESPONSES

Since the FM mode seems to be the best choice so far it is in order to investigate its distortion characteristics. The major culprit in degrading the signal is the flutter in the recorder. Flutter frequency modulates the already frequency modulated carrier, thus producing inter-modulation distortion. The net effect is to raise the noise level of the system. The amount that it raises the level is dependent upon the deviation of the carrier by the desired signal. If the signal deviation is high and the flutter deviation is low then the noise effect is small.

Appendix F presents the specifications of the four Ampex recorders mentioned above. As can be seen the total harmonic distortion, signal to noise ratio, and flutter are such that there would be negligible degradation to a recorded bit stream of 33 kbps or lower, especially in light of the fact that the clock will also be recorded along with the data.

The use of the tape recorder as a data rate reducer will be treated in the next section on the data transmission system.

### 3.3.3.3 DATA TRANSMISSION SYSTEM CONSIDERATIONS[41]

In configuration B the data entering the Data Transmission System (DTS) will have been decoded; thus the highest rate which will be seen by

the system will be the 16,384 bps rate from the IMEMD mission. The highest bit rate which can be transmitted over NASCOM narrow band lines (assuming that a good error rate is desired) is 7.2 kbps; hence the narrow band lines cannot be used unless some technique is employed to either lower the bit rate to be sent or increasing the DTS capacity. For example, if the 16,384 bps rate is only needed for short periods of time, then it can be recorded at say 120 ips and reproduced at 30 ips. The data rate is now 4,096 bps which is well within the capacity of the narrow band lines.

Another possibility is to multiplex the lines, e.g., feed every third bit to a narrow band line. This decreases the effective rate to 5,461 bps which again is well within the capacity of the 7.2 kbps lines. The problem with this approach, however, is that the bits must be reassembled at the receive end which is no small task; also delay differences among the lines present added problems. Another comment would be that it is an inefficient use of the lines themselves, i.e., it ties up three data channels.

The last alternative* for transmitting the high rate data is to use wide band lines. Relative to the rate handling capacity of these lines the 16,384 bps rate is very slow, thus no problem "capacity-wise" exists.

The above discussion was mainly for the 16,384 bps rate from the NEMD. The next lowest rate is 8,192 bps and the preceeding comments still apply. The lowest rate on IMEMD is 4,096. When this rate is sent then clearly a single narrowband line is in order.

On the IMEH mission the highest rate is only 2,048 bps, thus it is a simple matter to transmit it, or any of the lower rate options via a single narrowband line.

---

* Data compression was assumed undesirable due to the degradation of the experimental results.

With the above options set forth, the next order of business is to study the effect of NASCOM on the overall quality of data. The first thing to notice in connection with configuration B is that no burst error patterns due to NASCOM will affect the decoder since it is located prior to the DTS. This is an ideal configuration in this respect since the convolutional codes recommended for the missions are designed for a random error channel rather than a burst error channel. It will be recalled, though, that a reason for deciding in favor of the Viterbi decoder over the Sequential decoder was that it was less sensitive to burst errors and recovered more rapidly when overwhelmed by a long burst pattern. Although the preceeding is true, the fact still remains that burst errors are undesirable and so placing the decoder ahead of the DTS is optimum from that standpoint.

Any errors due to NASCOM can only degrade the quality of the data, hence considering channel errors and DTS errors as two sets, an upper bound to the overall (end to end) probability of error is:

$$P_0(\varepsilon) = P_c(\varepsilon) + P_d(\varepsilon), \tag{3.52}$$

where $P_0(\varepsilon)$ is the overall error rate, $P_c(\varepsilon)$ is that of the channel, and $P_d(\varepsilon)$ is the DTS error rate. The $P_d(\varepsilon)$ of NASCOM is specified to be (as a goal) as shown in Table 3.23.

| | |
|---|---|
| $P_d(\varepsilon) < 10^{-5}$ | on single communications circuits |
| $P_d(\varepsilon) < N \times 10^{-5}$ | on N tandem communications circuits |

TABLE 3.23 NASCOM DATA QUALITY GOALS

Using the values of Table 3.23 and the channel error rate of less than $10^{-5}$ with convolutional coding, the overall error rate can be expected to be

$$P_0(\varepsilon) < (N+1) \times 10^{-5} \tag{3.53}$$

### 3.3.4 TELEMETRY/CODEC CONFIGURATION C

The bulk of the difference between configuration C and B treated above is that the decoder is now remote from the ground station. The obvious advantage of this approach is that less decoders are needed. The disadvantages created, however, will be seen shortly to far outweigh the gain.

#### 3.3.4.1 BIT SYNCHRONIZER CONSIDERATIONS

Due to the placement of the bit sync (same as the configuration B) the pros and cons are the same as treated in Section 3.3.3.1.

#### 3.3.4.2 TAPE RECORDER CONSIDERATIONS

The only significant change in the tape recorder requirement is that the one used for data rate reduction must now handle the highest coded rate of 32,768 bps. The discussion in connection with the station backup recorder then applies. As a matter of fact the backup recorder and the rate reduction recorder will most likely be the same machine. The only reason for showing two machines in the Figure 3.46c is that the <u>function</u> played by each of the blocks is different; one machine, of course, can perform both functions.

#### 3.3.4.3 DATA TRANSMISSION SYSTEM CONSIDERATIONS

Here is where the major departure from configuration B becomes apparent. The outputs of the bit sync, whether rate reduced or not, are multiplexed onto a single line for transmission over NASCOM. (It should be

noted here that transmission of each output was rejected outright because of its inefficient, and therefore costly, use of NASCOM lines and because of the delay equalization problems involved.)

The only ramification of the parallel to serial (P/S) conversion is that the increase data rate eliminates the consideration of narrowband lines, e.g., the 2048 bps IMEH rate becomes 12,288 bps with the coding and P/S conversion. The higher IMEMD rates, of course, present an even worse problem, e.g., 16,384 bps implies 98,304 bps. Assuming that wideband lines are used these rates can be transmitted, but they greatly tax the transmission capacity. The techniques discussed in Section 3.3.3.3 can be applied to this problem.

Having transmitted the multiplexed data, the next task is to demultiplex it. The major problem here is to identify the 3 bit half-branches so that the decoder can properly process them. It will be recalled that the decoder searches for branch sync by slipping 3 bits at a time; it was assumed that these 3 bits were correctly grouped by the bit sync.

There are several ways of approaching the above problem. The easiest and most straightforward is to consider each (or an integral number) half-branch group as frames of data and to tag them appropriately. This framing is done in addition to the spacecraft frame sync. The obvious disadvantage of this method is that special equipment is needed, i.e., the P/S converter could be designed with the framing function built into it. The serial to parallel (S/P) converter would, of course, need a frame sync search function incorporated into it.

Another approach would be to identify the sub-bits by their distribution. Such a scheme was investigated in reference 42 and was found to be inadequate except at high SNR's which are absent in coded systems.

A third method is to obtain the spacecraft frame sync. This was also shown not to work at low SNR's[42].

A fourth method is to have a device similar to the decoder itself which moniters the metric of the decoder and slips by 1 bit instead of 3 bits. Of course the decoder could be designed to do this, but again cost is a factor.

The last method to be considered is to simply send the clock over a separate line and use it to obtain half-branch sync. This ties up a wide or narrowband line (depending upon the rate), however, it takes the least complexity and development cost to implement.

In summary, then, while the central location of the decoder away from the remote sites is desirable, it introduces many problems as a result of the higher rates and the need for half-branch sync. It should also be stressed that data rates are more likely to increase rather than decrease in the future; thus the problems discussed above will be further aggravated rather than relieved.

### 3.3.5 TELEMETRY/CODEC CONFIGURATION D

In this configuration the data is frequency multiplexed, sent over several wideband lines, demultiplexed, and fed to the Viterbi decoder. As noted in Section 3.3.4.3 this method taxes heavily the capacity of NASCOM, however, it could be that due to the larger available bandwidth that suitable

spectral packing (choice of subcarriers) could result in only one wideband channel being utilized at the lower rates of IMEMD or for the rates of the IMEH.

As can be seen from the figure no parallel to serial conversion takes place, thus no half-bit sync is required at the receive end. There is still the problem of delay differences among bit sync outputs, however, if one wideband line is used then the problem is partially solved.

For the high bit rate on IMEMD this configuration necessitates the employment of multiple wideband lines and thus is not considered to be cost effective. The alternative of slowing down the rate via a tape recorder at the station discussed in an earlier section could be used to get around the excessive rates.

### 3.3.6 TELEMETRY/CODEC CONFIGURATION E

This is the last configuration to be taken under consideration in this task report. It is unique in that while it has the advantages of placing the matched filter at the ground site and not requiring individual site decoders, it does not simultaneously incur the increased bit rate problems due to quantization which plagued configurations C and D. As can be seen from Figure 3.46e, the output of the matched filter is not quantized at the site, but rather it is sent via NASCOM in a pulse amplitude modulated (PAM) form.

The bandwidth requirements for the PAM out of the matched filter are the same as the noisefree PCM of the same rate (The power spectrum is derived in Appendix G). This means that the highest bandwidth which must be transmitted is 32,768 hertz. This would require a wideband line or group from the station to Goddard. Another drawback is that the

amplitude level variation over NASCOM is a function of many random parameters, thus when the PAM was received at Goddard the amplitude would bear little or no relationship to the output of the matched filter.

A way of avoiding the amplitude problem would be to FM or PM a carrier or subcarrier with the PAM baseband, but this would require more bandwidth and the additional cost of the modems.

## 4.0 CONCLUSIONS AND RECOMMENDATIONS

In this part of the report the tradeoffs and conclusions which were proposed in Section 3 will be reviewed. After a limited amount of discussion a set of recommendations will be stated. It is hoped that these recommendations will result in guidelines for the design of mission hardware and support.

Also included in this section will be special topics which are either specifically called for in the contract statement of work or are worthy of interest in themselves.

### 4.1 TASK 1 CONCLUSIONS

The first point to be made is that an Apollo type of transponder should not be used. As was shown in the main body of the report, the rising density severely limits the ability of the transponder to provide a noisefree turnaround ranging signal. At this point in the IME design a non rising density type of transponder is proposed. This is a wise choice and should not be compromised.

The next point of interest was that due to the large field of view of the command antennas on IME spacecraft, the effect of solar noise was negligible relative to the large system temperature of the IME receivers. This was seen to not be the case on the ground due to the narrow field of view of the dishes and the low system noise temperature on the ground.

Referring to Table 3.2 it will be recalled that the worst case Heliocentric mission required an 85' dish. This was due mainly to the null in the command antenna pattern. It was noted in connection with this item that this case is unlikely to occur because of the stabilized platform on which the antennas are mounted, that is, there will always be at least one channel onboard IME-Heliocentric which will operate at or

near the peak of the pattern of the command antenna. This chart, however, shows that the mission can be supported even in a tumble situation.

As a general comment it can be said that the uplink under nominal operating conditions is in good shape "marginwise."

Turning now to the downlink, it was seen that an 85' receiving antenna used with a maser front end was necessary on all the cases. This was because of the bit rates being considered sacred and thus only being lowered, as in the Heliocentric worst case, when all other parameters had been adjusted. More will be said about this later in connection with the recommendations portion of the report.

Another major tradeoff which was made for the downlink was to increase the minimum halo orbit radius from 40,000 km to 60,000 km. This resulted in a 1.4 dB improvement in the receiver system temperature due to the decrease in solar interference.

At this point it is appropriate to list the modulation indices and factors for the various cases discussed in the report. This is done in Table 4.1.

## 4.2 TASK 1 RECOMMENDATIONS

With the above tradeoffs and parameters in mind, this section will propose support requirements for the IME missions.

First and foremost, it is recommended that the minimum coding gain that be employed be 5 dB at $10^{-5}$ BEP. This is about the maximum that can be expected for a reasonable hardware/software implementation.

| Case | Range Index | Telemetry Index | Carrier Loss | Range Loss | Telemetry Loss |
|---|---|---|---|---|---|
| A | 0.5 (0.4)* | | -1.1 (-0.7) | -6.4 (-8.2) | |
| A | | 0.8 (1.4) | -3.1 (-15.4) | | -2.9 (-0.1) |
| B | 0.5 (0.4) | | -1.1 (-0.7) | -6.4 (-8.2) | |
| B | | 0.8 (1.4) | -3.1 (-15.4) | | -2.9 (-0.1) |
| C | 0.5 (0.4) | | -1.1 (-0.7) | -6.4 (-8.2) | |
| C | | 0.8 (1.4) | -3.1 (-15.4) | | -2.9 (-0.1) |
| D | 0.5 (0.4) | 1.2 (2.2) | -4.6 (-19.9) | -9.9 (-27.3) | -4.2 (-2.8) |
| E | 0.4 (0.4) | | -0.7 (-0.7) | -8.2 (-8.2) | |
| E | | 1.2 (1.4) | -8.8 (-15.4) | | -0.6 (-0.1) |
| F | 0.4 (0.4) | | -0.7 (-0.7) | -8.2 (-8.2) | |
| F | | 1.2 (1.4) | -8.8 (-15.4) | | -0.6 (-0.1) |

* The parenthetical values are for Mother-Daughter; others are for Heliocentric

TABLE 4.1 MODULATION INDEX/LOSS MATRIX

With this gain, the 85' receiving antennas, and maser front end, the Heliocentric mission is marginal for telemetry in Case C (0.6 dB), acceptable in Case D (2.3 dB), and unacceptable in Case F (-4.3).

The main reason for the above margins is the solar noise factor (-9.8 dB). If this were not present all the margins would be acceptable. Per direction from Goddard the largest halo radius minimum acceptable is 60,000 km. It is then recommended that it be used. Also if any beam shaping can be done to minimize the solar noise further, then it should be done.

When near the earth-sun line on Heliocentric the highest bit rate which can be supported is 256 bps; on all other cases the highest bit rates designed for can be used.

On the Heliocentric spacecraft the hemispheric antennas cannot be used on the downlink due to insufficient carrier power among other reasons.

4.2.1 Uplink Minimum Support Recommendations

- IME-Heliocentric: hemispheric spacecraft receive antenna, 20 kw command transmitter, 85' ground antenna, search for strongest channel then range on that channel
- IME-Mother-Daughter: hemispheric spacecraft receive antenna, 20 kw command transmitter, 30' ground antenna

4.2.2 Downlink Minimum Support Recommendations

| IMP | Range, Tlm Range/Tlm | Best/ Worst Situation | Downlink Case | Grd Ant. (feet) | Front End | Bit Rate (bps) | Range Index | Tlm Index |
|---|---|---|---|---|---|---|---|---|
| H. | R/T | W | D | 85 | Maser | 256 | 0.5 | 1.2 |
| H. | R/T | B | D | 85 | Maser | 2048 | 0.5 | 1.2 |
| H. | R | W | A | 85 | Maser | | 0.5 | |
| H. | R | B | A | 30 | Hot P. | | 0.5 | |
| H. | T | W | B | 85 | Maser | 256 | | 0.8 |
| H. | T | B | B | 85 | Maser | 2048 | | 0.8 |
| M.-D. | R/T | W | D | 85 | Maser | 16384 | 0.4 | 2.2 |
| M.-D. | R/T | B | D | 30 | Cold P. | 16384 | 0.4 | 2.2 |
| M.-D. | R | W | E | 30 | Hot P. | | 0.4 | |
| M.-D. | R | B | E | 30 | Hot P. | | 0.4 | |
| M.-D. | T | W | B | 85 | Maser | 16384 | | 1.4 |
| M.-D. | T | B | B | 30 | Hot P. | 16384 | | 1.4 |

## 4.3 TASK 2 CONCLUSIONS

The main conclusions to be reached as a result of this task are that either a Maximum Likelihood Decoder (MLD) or a Sequential Decoder (SD) will provide the coding gain required by the IMEMD/H missions when used with their corresponding convolutional encoder. It was found that the MLD had several "saving graces." Among these were no restart requirements and better burst error recovery than the SD.

Block diagrams for both of the decoders were presented and it was seen that "blockwise" they were about equal. The main differences were that the MLD required more storage than the SD. The SD was seen to require a

large input buffer to store the received coded bits. This was because the SD had to back up in time (code tree search) whenever it reached a point where the current data path violated a running threshold.

A minor conclusion was that Feedback Decoding (FD) of the convolutional code would not provide the coding gain necessary to do the job. This was because it had no power to back track, as in the SD, and as such had to rely on looking at many tree branches to get its error correction gain, however as the number of branches increased so did the complexity. Since the increase was exponential things soon got out of hand, hardwarewise.

Another conclusion which can be reached from the material in Section 3 is that the difference in complexity in a software implementation of the two decoders would be negligible. This can be reasoned as follows. It will be recalled that the definition of complexity bits was on a functional rather than hardware basis, thus any implementation would result in the same relative complexity between the two decoders.

The bit sync interface with the demodulator in use at the ground station is straightforward. The output of the decoder if used at the ground station on the other hand, can interface with either a tape recorder or a data transmission system. In either case the output data from

the decoder would be treated in the same way as any other telemetry data which was not coded. No special equipment is needed.

## 4.4 TASK 2 RECOMMENDATIONS

It is recommended that a K=7 encoder with a Maximum Likelihood Decoder be used for the IMEMD/H missions. This choice was primarily based on the marginal signal to noise ratios available on the Heliocentric mission when it is near the sun. The presence of the sun with the periods of possibility of frequent solar activity giving rise to short periods of higher levels of noise makes it imperative that the decoder be graceful when it degrades. Also the possibility of decoding at Goddard would introduce transmission line burst errors thus further supporting the recommendation. It is not to be construed from the above that the burst error mode is dominant, on the contrary, the AWGN applies most of the time, however, the high likelihood of the burst errors must be accounted for.

The complexity factor was not deemed to be sufficient to rule out the MLD since the state of the art in integrated circuit technology is such that storage requirements can be easily met and this was the main reason for the complexity of the MLD.

The other features of the MLD in Section 3.2.4 were also weighed and found to be desireable for the present application. It is felt that a close study of the material presented in Section 3 will support the conclusion reached in this section.

## 4.5 TASK 3 CONCLUSIONS

The five configurations of Figure 3.46 were discussed in detail on a block by block (or subsystem such as NASCOM) basis in Section 3. In this part of the report the salient features of each configuration will be reviewed. After this is done the appropriate conclusions will be drawn with the constraints of the IMEMD/H missions taken into account.

The first configuration was that of Figure 3.46a. It was seen to be the least complex, "hardware-wise," of the five. It did however require magnetic tape mailing. The following table lists its advantages and disadvantages.

| Advantages | Disadvantages |
|---|---|
| ° Central decoding location | ° Requires tape mailing |
| ° Least* number of decoders required | ° Matched filter removed from channel by record/playback characteristics of recorder |
| ° Simplicity of design | ° Delay in the data to the experimenter by mail delay time |
| Least* ground site impact | |

TABLE 4.2 CONFIGURATION A TRADEOFFS

Since the trend of future network support is for a minimum of tape handling and as near to real time data transmission as possible,

* of the five configurations of Figure 3.46

this configuration cannot be given the number one rating in terms of system optimality.

The next system is configuration B. This is the one that is best in the author's opinion. The chief reason for this selection is that it fulfills the real time data transmission criterion and also is cost effective (see Section 4.6). Table 4.3 presents its advantages and disadvantages.

| Advantages | Disadvantages |
|---|---|
| ° Simple to implement | ° Requires several decoders (one for each support station) |
| ° Moderate station impact | ° More station impact and complexity than configuration A |
| ° Matched filter located at the site | |
| ° Uncoded data rates for DTS transmission | |
| ° No post DTS resync problems | |
| ° Moderate cost impact | |
| ° Decoders can be used for other missions | |

TABLE 4.3 CONFIGURATION B TRADEOFFS

As mentioned in Section 3, if the decoders are at the site as part of the station inventory then they are an asset. This is because of the power savings on future spacecraft and/or the increased data rate and quality.

Configuration C was seen to be merely the result of locating the decoder of configuration B at a remote site. The major stumbling block was the requirement of obtaining half-branch synchronization due to

the loss of it in the parallel to serial conversion at the site. Great pains must be taken to reacquire this sync and therefore this configuration is not highly desirable. Table 4.4 lists its pros and cons.

| Advantages | Disadvantages |
|---|---|
| ° Central decoding location | ° Half-branch resync required |
| ° Less decoders required | ° Excessive complexity and station impact |
| ° Matched filter located at the site | ° High data rates to be transmitted via NASCOM (~100 kbps) |

TABLE 4.4 CONFIGURATION C TRADEOFFS

Configurations D and E will only have their tradeoff factors listed since as it will be shown in Section 4.6 the cost factors involved completely eliminate these options from consideration in a practical support system.

| Advantages | Disadvantages |
|---|---|
| ° No post DTS resync required | ° Requires many wide band lines or a super group channel |
| ° Match filter located at the site | ° Requires FDM Mux/Demux |
| ° Moderate station impact | ° High data rates involved |
| ° Moderate theoretical complexity | |

TABLE 4.5 CONFIGURATION D TRADEOFFS

| Advantages | Disadvantages |
|---|---|
| ° No post DTS resync required | ° Requires precise DTS analog level transmission |
| ° Matched filter located at the site | ° Requires PAM/FM transmitter/receiver |
| ° Moderate data rates involved | ° Requires additional bit sync |
| ° Moderate theoretical complexity | |

TABLE 4.6 CONFIGURATION E TRADEOFFS

## 4.6 TASK 3 RECOMMENDATIONS

The pros and cons of Section 4.5 together with cost factors will be used to arrive at an optimum support system for the IMEMD/H missions. Cost factors which were instrumental in eliminating various configurations will also be listed.

It should be mentioned here that the costs presented in this section of the report are estimates only since a prediction of future costs in this day and age is somewhat of a mystic art. However there will be a clear dividing line between systems with respect to the cost aspect of its implementation as will be seen shortly, and so the "order of magnitude" nature of the numbers presented will not compromise their effectiveness in grading the systems.

In order to look at cost factors and to be able to form some reasonable support conclusions, three stations were chosen as support sites. These are:

- Madrid (MAD)
- Orroral (ORR)
- Goldstone (GDS).

These three were chosen for their geographic location since worldwide coverage will be required for the missions and since mail rates, data transmission rates, etc. will be representative of those which would be encountered in that area of the world.

Per reference 44, it is believed that by the time of mission launch (late 1977) that there will be 28.5 kbps data lines to these sites

and possibly others as well. These data lines are being implemented for the Mariner/Mercury mission; they will be one part of a group channel leased via a satellite link.

The point of the above is that the highest bit rate of 16,384 bps can be transmitted over this link, however, this requires decoding at the sites.

To get a better feel for the numbers involved, the following Table 4.7 lists the present costs of Voice Band lines and a Group channel for each of the three stations under consideration. It also lists an estimate of a group channel cost if the Comsat "Spade" system under investigation by Goddard is employed by NASCOM. (An explanation of Spade is found in Appendix I.)

| | VOICE BAND | GROUP(50 kbps Capacity) |
|---|---|---|
| Madrid (1973) : | $13,000/mo | $117,000/mo |
| (1977 estimate) : | | $ 39,000/mo |
| Orroral (1973) : | $26,000/mo | $200,000/mo |
| (1977 estimate) : | | $ 78,000/mo |
| Goldstone (1973) : | $ 1,500/mo | $ 15,000/mo |
| (1977 estimate): | | $ 15,000/mo* |

TABLE 4.7 DTS COSTS

The cost for a supergroup can be estimated by multiplying by five (5) since five groups are in a supergroup.

It can be easily deduced that wideband lines are to be avoided if at all possible.

* The lower rates only apply to overseas locations.

Consider the following hypothesis and its associated costs. Assume that continuous coverage is required and that each station provides one third of it (this assumes a circular orbit and symmetrically placed sites, however it provides a case for study). This means that 8 hours per day is required for the transmission lines. For a three (3) year support schedule and assuming that the lines are time shared with other projects so that the costs are one third of the total Table 4.8 lists the costs of the configurations employing NASCOM. Also assumed is the lowest rate, i.e., the Spade system; thus the estimates can be considered to be conservative (e.g., there may not be time sharing among projects and the Spade system may not be employed).

As can be seen the decoder costs are small relative to the wide band alternatives; also they are a nonrecurring cost whereas the line costs grow with time.

In Table 4.8 only configuration C was compared against configuration B. This is because the others, viz., D and E, require even wider bandwidths and thus even higher costs. Since it is clear that configuration C is not cost effective relative to B, the others would not be either.

| Configuration | Mother or Daughter | Heliocentric |
|---|---|---|
| B | $ 13,500 ① Decoders<br>$234,000 ② (1/2 Group) MAD<br>$468,000 (1/2 Group) ORR<br>$ 90,000 (1/2 Group) GDS<br>$805,500 TOTAL ③ | $ 13,500 ① Decoders<br>$156,000 (Voice Band) MAD<br>$312,000 (Voice Band) ORR<br>$ 18,000 (Voice Band) GDS<br>$499,500 TOTAL ③ |
| C | $ 4,500 ① Decoder<br>$ 936,000 (2 Groups) MAD<br>$1,872,000 (2 Groups) ORR<br>$ 360,000 (2 Groups) GDS<br>$3,172,500 TOTAL ③ | $ 4,500 ① Decoder<br>$234,000 (1/2 Group) MAD<br>$468,000 (1/2 Group) ORR<br>$ 90,000 (1/2 Group) GDS<br>$796,500 TOTAL ③ |

① It is assumed that two spacecraft can be supported per site. The two can be the Mother and Daughter, Mother and Heliocentric, or Daughter and Heliocentric; hence two decoders per station are needed if local decoding is used or one decoder per spacecraft if remote decoding is used.

② Example calculation: $39,000/mo. for full group times 1/2 group needed for 16 kbps (it is assumed that the other half can be utilized by other NASA projects on a cost share basis) times 36 mo. project support times 1/3 support per site (it is assumed that other projects will use the site and NASCOM for the other 16 hours/day thus sharing costs).

③ Total 3 year support cost for that spacecraft.

TABLE 4.8 COMPARATIVE MISSION SUPPORT COSTS

## 4.7 THE OPTIMUM SYSTEM FOR IMEMD/H MISSIONS

Using all of the preceeding tasks and text as support material it is concluded and recommended that configuration B of Figure 3.46 be chosen as the telemetry system for both missions. It is optimum in the following sense:

- It is cost effective.
- It provides quality data to the user.
- It is practical to implement.
- It does not unduly load the network.

## 4.8 SPECIAL CONSIDERATIONS

In the statement of work of the contract the customer has requested "definitive answers" to the following questions.

1) What can be done with the present on-site equipment for the tasks I, II, and III of the contract?

2) What would be the nature of a cost limited modification to accomplish some of the coding advantages?

3) What would be an optimum system with state of art approaches including costs and advantages?

The purpose of this section is to fulfill the request.

Concerning question 1), the optimum system required no impact on the station inventory with the exception of the purchase of the decoder since the soft decision bit synchronizers will have been installed prior to the support time frame. Since the decoder was required to be hardwired (Section 3.3.1) there is nothing to be done with the present on-site equipment.

Question 2) addresses itself to a "cost limited modification." Since the decoders cost between $4,500 and $5,000 each (depending on order lots) the only less costly option in terms of initial cash outlay would be to use configuration A, that is, use the present system of mailing tapes. The pros and cons of this option were treated in detail in Sections 3 and 4.

Finally the optimum system, per question 3) was arrived at as an end result of this study, i.e., configuration B. The only improvement which could be made would be to purchase a decoder using state of the art circuitry, however, this would be costly and would not result in significantly better coding performance (the "state of the art" would be mainly to increase operating speed and lower power requirements, neither of which is needed).

## 5.0 REFERENCES


1. Cartier, D.E., Interplanetary Monitoring Platform - Heliocentric and Mother/Daughter Missions Study, Parameter Optimization, Task Report No. 1, Contract No. NAS5-20386, December 1972.

2. Brandt, J.C., The Solar Wind Blows Some Good for Astronomy, Smithsonian, January 1973.

3. The Magnavox Company, ASAO, Technical Proposal for the Interplanetary Monitoring Platform Mother/Daughter and Heliocentric Missions Study, ASAO-TP72-0035, Part 2, September 1972.

4. Support Instrumentation Requirements Document, Project NASA/ESRO/Mother/Daughter (NEMD) and NASA Heliocentric (NH) Spacecraft, June 1972.

5. Oglivie, K.W., and Trainor, J.H., A Solar Terrestrial Project - A Feasibility Study, GSFC Document, April 1971.

6. Advanced Network Support Study for the Interplanetary Monitoring Platforms (IMP) KK', L, MM', N, GSFC, X-831-72-42, February 1972.

7. Lin, Shu, An Introduction to Error-Correcting Codes, Prentice-Hall Electrical Engineering Series, 1970.

8. Cartier, D.E., An Introduction to Coding, ASAO Document, ASAO-TM72-0003, April 1972.

9. Peterson, W.W., Error Correcting Codes, MIT Press and John Wiley and Sons, Inc., 1961.

10. Huth, G.K., Performance Versus Complexity of Viterbi and Sequential Decoding, National Telemetry Conference, December 1972, pp. 13B-1 - 13B-7.

11. Cartier, D.E., Telemetry Coding Study for the NASA/ESRO Mother/Daughter and NASA Heliocentric Missions, Convolutional Coding Theory and Implementation, Task Report No. 2, Contract No. NAS5-20386, March 1973.

12. Northrop, G.M., Aids for the Gross Design of Satellite Communication Systems, IEEE Transactions on Communication Technology, Vol. Com-14, No. 1, February 1966.

13. SAS-D Antenna Pattern, Memo from T. Ryan to R. Cortez, F. Shelton, T. Standish, March 1972, (GSFC Internal Memo).

14. Kalil, F., and Uvaas, C., GSFC Document I-834-71-162, April 1971.

15. Gardner, F.M., Phaselock Techniques, John Wiley & Sons, Inc., April 1967.

16. Jones, S.C., IMP Circuit Margins and Signal Design Considerations, Memo to E.A. Beck, CSC-2-188, APL, July 1972.

17. AS205 Predicts, MSC Internal Note, EB-R-68-8, 05952-H482-R0-00.

18. Technical Manual, Mark IA Ranging Subsystem (JPL), NAS5-10750, September 1967, Revised January 1969.

19. Lindsey, W.C., Design of Block-Coded Communications Systems, IEEE Transactions on Communication Technology, Vol. Com-15, No. 4, August 1967.

20. Viterbi, A.J., Convolutional Codes and Their Performance in Communications Systems, IEEE Transactions on Communications Technology, Vol. Com-19, No. 5, October 1971.

21. Bucher, E.A., and Heller, J.A., Error Probability Bounds for Systematic Convolutional Codes, IEEE Transactions on Information Theory, Vol. IT-16, March 1970, pp. 219-224.

22. Cheng, D.K., Analysis of Linear Systems, Addision-Wesley Publishing Company, Inc., 1961.

23. Massey, J.L., Threshold Decoding, MIT Press, Cambridge, Massachusetts, 1963.

24. Viterbi, A.J., Error Bounds of Convolutional Codes and an Asymptotically Optimum Decoding Algorithm, IEEE Transactions on Information Theory, Vol. IT-13, April 1967, pp. 260-269.

25. Heller, J., Private Communication to Linkabit Corporation, San Diego, California, 9 February 1973.

26. Savage, J., The Computation Problem with Sequential Decoding, Ph.D. Dissertation, Dept. of Electrical Engineering, MIT, Cambridge, Mass., February 1965.

27. Jordan, K.L., The Performance of Sequential Decoding in Conjunction with Efficient Modulation, IEEE Transactions on Communication Technology, Vol. Com-14, No. 3, June 1966, pp. 283-297.

28. Barrows, J.T., and Leiter, M., Sequential Decoder Simulation Study, Mitre Corporation Report, MTP-106, January 1970.

29. Cahn, C.R., Huth, G.K., Moore, C.R., Simulation of Sequential Decoding with Phase Locked Demodulation, IEEE Transactions on Communications, Vol. Com-21, No. 2, February 1973, pp. 89-97.

30. Barnes, W.P., A Simulation of Convolutional Encoding with Sequential Decoding with Application to IMP-I and AIMP-H, J Data Processing, NASA/Goddard Space Flight Center, Document X-563-68-65.

31. Sos, J.Y., Data Handling Requirements for Convolutional PCM Telemetry, NASA/Goddard Space Flight Center Document, Information Processing Division.

32. Lumb, D.R., and Hofman, L.B., Efficient Coding System for Deep Space Probes with Specific Application to Pioneer Missions. NASA TN D4104.

33. Forney, Jr., G.D., and Bower, E.K., A High Speed Sequential Decoder Prototype Design and Test, IEEE Transactions on Communications Technology, Vol. Com-19, No. 5, October 1971, pp. 821-835.

34. Network Integration Study, Parts A and B, STDN No. 809, Networks Directorate, Goddard Space Flight Center, Greenbelt, Maryland, June 1972.

35. Computers and Automation, Computer Directory and Buyers Guide Issue, Vol. 20, No. 6B, June 30, 1971.

36. Univac, Programing Manual for 1230 Computer (15 Bit Mode), PX3892, February 1966.

37. Peavey, B., Performance Characteristics and Specification of PCM Bit Synchronizer/Signal Conditioners, ITC 1968, pp. 407-419.

38. Weber, Paul, J., The Tape Recorder as an Instrumentation Device, Ampex Corporation Document, 1967.

39. Multitrack Digital Recording of Wideband Analog Signals, Applications Engineering Department, Instrumentation Division, Ampex Corp.

40. Signal Time Coincidence in an Instrumentation Tape Recorder, Instrumentation Technical Information Number 4, Reprinted from Readout, Vol. 7, No. 4, 1968.

41. Data Development Plan, NASCOM Network, Revision B, FY 73-1, Goddard Space Flight Center, Greenbelt, Maryland.

42. Greene, Edward, P., Resynchronization of RAE-B Telemetry Data at MSOCC, Memorandum to Dr. Robert J. Coates, Advanced Data Systems Division, M&DOD, November 5, 1971 (Mr. Greene is with the Computer Applications Branch, ADSD, M&DOD).

43. Cartier, D.E., Baseband Power Spectrums, Magnavox Technical Memorandum, ASAO-TM72-0004.

44. Mansberg, J., Private Conversation, (from D.E. Cartier), March 27, 1973, (Mr. Mansberg is with NASCOM).

45. Private Correspondence between F. Kalil, Advanced Systems, Code 860, and G. Rall, Network Support Manager for NEMD/NH, International Magnetosphere Explorers, April 19, 1973.

46. Private Correspondence between F. Kalil, Advanced Systems, Code 860, and R. J. Augenstein, Code 850, Goddard Space Flight Center, April 16, 1973.

47. Private Correspondence between F. Kalil, Advanced Systems, Code 860, and G. Mansberg, Code 841.1, Goddard Space Flight Center, April 20, 1973.

48. Spaceflight Tracking and Data Network Mission Requirements Summary, Revision 5, GSFC, STDN No. 802, January 1973.

49. Werth, A. M., SPADE: A PCM FDMA Demand Assignment System for Satellite Communications, London Conference on Digital Satellite Communications, November, 1969.

## 6.0 GLOSSARY

- IMP - Interplanetary Monitoring Platform
- Dish - Parabolic Antenna
- PN - Pseudonoise
- MUX - Multiplexer
- S/C - Spacecraft
- PM - Phase modulation
- Xmtr - Transmitter
- Ant - Antenna
- Atm - Atmosphere
- Xpdr - Transponder
- Tlm - Telemetry
- Demod - Demodulator
- Grd - Ground
- Rec - Receiver
- Sys - System
- Convol - Convolutional
- PSK - Phase shift keyed
- Mod - Modulator
- BPF - Bandpass Filter
- MHz - Megahertz ($10^6$ Hertz)
- GHz - Gigahertz ($10^9$ Hertz)
- Temp - Temperature
- Car - Carrier
- ΔCoding - Phase Transistion Coding
- DTS - Data Transmission System

- Nascom - NASA Communications Network
- Rcdr - Recorder (Tape, Pen, etc.)
- S/P - Split Phase (Manchester)
- Polariz - Polarization (E-field orientation)
- VSWR - Voltage Standing Wave Ratio
- USB - Unified S-band
- STADAN - Space Tracking and Data Acquisition Network
- AGC - Automatic Gain Control
- S - Signal Power
- BPS - Bits Per Second
- $E_b$ - Energy Per Bit
- $N_o$ - Single Sided Noise Spectral Density (White Noise)
- BEP - Bit Error Probability
- ESRO - European Space Research Organization
- NEMD/NH - NASA/ESRO - Mother Daughter/NASA Heliocentric
- $E_b/N_0$ - Energy per bit/Single sided noise density
- GSFC - Goddard Space Flight Center
- AWGN - Additive White Gaussian Noise
- $P(\varepsilon)$ - Probability of error
- encoder - A device for applying a coding scheme to information bits
- decoder - A device for recovering information bits from coded bits
- $E_s/N_0$ - Energy per signal/Single sided noise density
- mod-2 addition - $0 + 0 = 1 + 1 = 0$, $0 + 1 = 1 + 0 = 1$
- $R_0$ - Channel exponential bound parameter
- MLD - Maximum Likelihood Decoder

- SD - Sequential Decoder
- d(x,y) - Absolute distance between x and y.
- $\Delta d(x,y)$ - Transition distance between x and y
- CPSK - Coherent Phase Shift Keying
- DCPSK - Differentially Coherent Phase Shift Keying
- $\Delta$-decoding - Coherent decoding of a differentially encoded bit stream
- Code Polynomial - Register tap configuration for a given code
- Biphase (two phase) - Phase modulation employing one constant phase shift for a binary 0 and another for a binary 1.
- TTL - Transistor Transistor Logic
- IC - Integrated Circuits
- CE/SD - Convolutional Encoder/Sequential Decoder combination
- $R_{comp}$ - Channel computational cutoff rate
- Modem - Modulator/Demodulation combination
- MECL III - Motorola high speed logic
- AGC - Automatic gain control
- sgn(x) - Signum function: $sgn(|x|) = 1 = -sgn(-|x|)$; $sgn(0) = 0$
- STDN - Space Tracking and Data Network
- SNR (S/N) - Signal Power to Noise Power Ratio
- FDM - Frequency Division Multiplex
- PAM/FM - Pulse Am plitude Modulation/Frequency Modulation (Baseband Modulation Format/Carrier Modulation Format)
- PCM - Pulse Code Modulation
- FM - Frequency Modulation
- Codec - Encoder/Decoder system
- P/S - Parallel to Serial
- S/P - Serial to Parallel (in connection with NASCOM discussion)

- ips - Inches per second
- NRZ-L - Non return to zero-level
- NRZ-M - Non return to zero-mark
- $B_1Ø$-L - Binary Phase-level
- $B_1Ø$-M - Binary Phase-mark
- Sync - Synchronization
- A/D - Analog to digital
- MFR - Multifunctional Receiver
- $R_b$ - Information bit rate
- $R_s$ - Signaling rate
- W - bandwidth
- I&D - Integrate and Dump detector
- CMOS - Complementary Metal Oxide Semiconductor
- Stadac - Station Data Acquisition and Control
- R - the practical channel capacity, R = b/n, where
  b is the number of information bits encoded and
  n is the number of resulting code bits.

APPENDIX A

SYSTEM PARAMETERS

A listing of the various parameters used throughout the test will be given here. Several of these parameters appear in the text, but it is felt that a concise listing is helpful for reference purposes.

- Ground Transmitter Power: 20 kw maximum at the USB sites
- 85 foot Antenna Gain: 52.5 dB at 2.1-2.3 GHz
- 30 foot Antenna Gain: 43 dB at 2.1-2.3 GHz
- IMP Antenna Gain: 9 dB maximum (medium gain); 2 dB maximum, -3 dB minimum (omnidirectional)
- IMP-Heliocentric Distance from Earth: $1.5 \times 10^6$ km maximum
- IMP-Mother-Daughter Distance from Earth: $1.5 \times 10^5$ km maximum
- IMP Transponder Noise Temperature: 1500°K (at threshold)
- Ground Receiver Noise Temperature: Maser 70°K, Cooled Parametric Amplifier 96°K, Uncooled Parametric Amplifier 170°K
- Uplink Modulation Indices: 0.8 radians (ranging), 0.9 radians (command)
- Transponder IF Ranging Bandwidth: 2 MHz
- IMP-Heliocentric Transmitter Power: 2.5 w
- IMP-Mother-Daughter Transmitter Power: 1.0 w
- Ground Receiver Carrier Threshold: 12 dB in 30 Hz bandwidth (loop)
- Ground Receiver Ranging Threshold: 23 dB-Hz
- Ground Receiver Telemetry Treshold: 11.6 dB ($E_b/N_o$ at $10^{-5}$ BEP)
- Ranging Chip Rate: 991.6 kcps (NRZ-L)
- Uplink Frequency Range: 2090-2120 MHz
- Downlink Frequency Range: 2200-2300 MHz
- IMP-Heliocentric Bit Rate: 2048 bps maximum, 256 bps minimum
- IMP-Mother-Daughter Bit Rate: 2048 bps minimum; 16,384 bps maximum
- Telemetry Subcarrier Frequency: 1.024 MHz

APPENDIX B

## SPECTRAL POWER DISTRIBUTION

In this appendix, the theory used in the text will be developed. The reader is referred to references 12 and 19 for details. Consider the following waveform

$$S_1(t) \triangleq \sqrt{2P}\sin[\omega_c t + \tau b(t)], \qquad (B.1)$$

where P is the total power, $\omega_c$ is the carrier frequency in radians per second, $\tau$ is the modulation index, and b(t) is a random bit stream taking on the values $\pm 1$. This waveform is a mathematical representation of a carrier phase modulated by a telemetry bit stream as would be the case if no ranging were present on the downlink of the IMP spacecrafts, i.e., the prime carrier option.

The power spectrum of $S_1(t)$ contains a discrete component, i.e., a concentration of power at a specific frequency (the carrier frequency here) with the rest of the spectrum spread out over a band of frequencies on both sides of the carrier. Any receiver using coherent demodulation will have to create a local version of the carrier for mixing purposes. This is done by placing a very narrowband bandpass filter about the discrete component in the above spectrum, thereby passing only it (the sidebands are rejected). Actually a tracking filter is used which keeps the center of the filter on the discrete component.

Having locked onto the carrier, so to speak, the detection of the information carrying sidebands can be accomplished by multiplying $S_1(t)$ by the created local reference and low pass filtering to remove double frequency components.

In the above two factors determine how well the processing can be done, the amount of discrete component power, $P_c$, and the sideband power, $P_{tlm}$. The higher $P_c$ is, the more stable the carrier lock is, and the better the reference carrier, whereas the higher $P_{tlm}$ is, the lower is the error in making information bit decisions in detection of the telemetry. Per reference 19 or by integrating the power spectrum appropriately the powers $P_c$ and $P_{tlm}$ are given by

$$P_c = P \cos^2 \tau \tag{B.2}$$

$$P_{tlm} = P \sin^2 \tau \tag{B.3}$$

In equations B.2 and B.3 the effects of local reference phase jitter have been neglected since at this stage in the IMP design these effects are secondary relative to the overall system.

In Appendix C, $(P_c/P)$ and $(P_{tlm}/P)$ are listed in dB. This allows $P_c$ and $P_{tlm}$ to be found as a function of $\tau$ by

$$P_c(\text{dBm}) = P(\text{dBm}) + 20 \log \cos \tau \tag{B.4}$$

$$P_{tlm}(\text{dBm}) = P(\text{dBm}) + 20 \log \sin \tau. \tag{B.5}$$

It is with these equations and the set of bounds discussed in the text that the optimum value of $\tau$ was chosen.

Consider now

$$S_2(t) = \sqrt{2P} \sin[\omega_c t + \sqrt{2P_{sc}} \cos[\omega_{sc} t + (\cos^{-1} m)X(t)] + \tau b(t)], \tag{B.6}$$

where P, $\omega_c$, $\tau$, and b(t) are as before, and $P_{sc}$ is the total subcarrier power, $\omega_{sc}$ is the subcarrier frequency, m is the subcarrier modulation index, and X(t) is a random bit stream with values ±1. The waveform $S_2(t)$ mathematically represents a prime carrier modulated by a subcarrier with telemetry and also by a pseudo-random ranging signal, i.e., $\tau b(t)$.

Arguments similar to those previously given hold here as well, i.e., there is power in the carrier (a discrete component of the spectrum); there is power in the subcarrier and its sidebands (taken together); there is power in the ranging sidebands. Due to the subcarrier presence extra terms are involved. Also Bessel functions appear due to the cosine modulation of a sine carrier. Again reference 19 gives

$$P_c = P \cos^2 \tau \, J_o^2 \, (\sqrt{2P_{sc}}) \tag{B.7}$$

$$P_{tlm} = P \, 2 \cos^2 \tau \, J_1^2 \, (\sqrt{2P_{sc}}) \tag{B.8}$$

$$P_{pn} = P \sin^2 \tau \, J_o^2 \, (\sqrt{2P_{sc}}). \tag{B.9}$$

Appendix C lists the factors $P_c/P$, $P_{tlm}/P$, and $P_{pn}/P$ as a function of the two indices $\tau$ and $(\sqrt{2P_{sc}})$. As a result these indices can be optimized to give the desired power margins for the carrier, ranging, and telemetry subsystems.

Coding Gain

In the text the term "coding gain" was used. A discussion will be given here to elaborate on the term and its meaning.

It is well known that coding (and convolutional coding in particular) can be used to improve the accuracy of bit decisions in transmitting information over a channel (see reference 3). This is done at the expense of bandwidth occupancy and hardware complexity. To oversimplify the analysis, it can be said that the standard curve of (ideal PSK) bit error probability (BEP) versus bit energy per noise density ratio ($E_b/N_o$) is replaced by another curve which gives lower $E_b/N_o$ for a fixed BEP than before. Referring to Figure B.1, then, the coding gain is nothing more than the difference (at a given BEP) between the standard curve and the coding curve.

In the Figure B.1, the coding gain for a Sequential decoder is singled out at $10^{-5}$ BEP and $10^{-4}$ BEP. Note how the Sequential decoder gives more gain at very low BEP than the Viterbi decoder. This is due to the steepness of the coding curve and is a major factor in a system study such as this one.

In the text the standard curve was used to calculate margins and then a coding gain was employed to improve the margin.

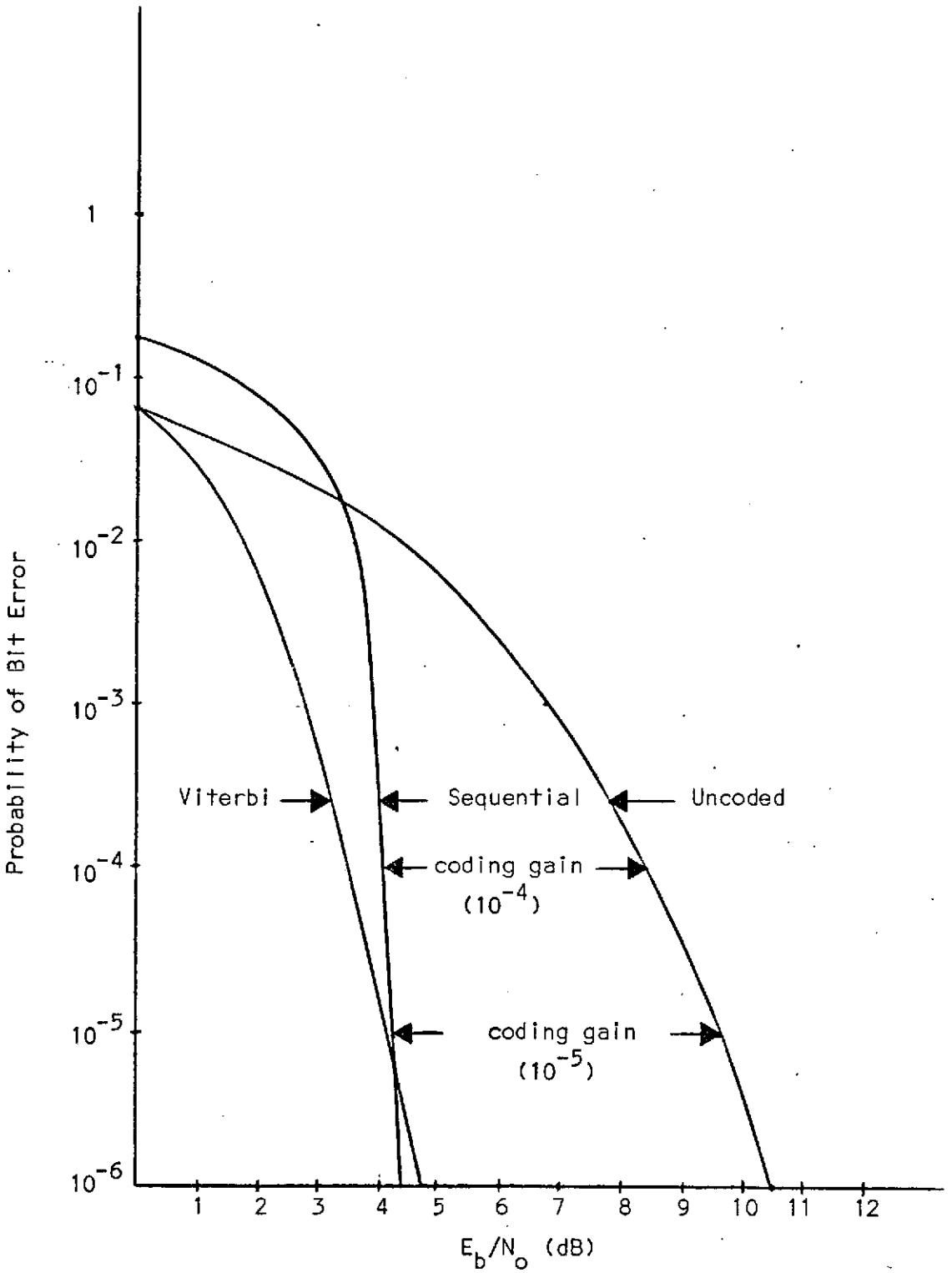


FIGURE B.1 CONVOLUTION CODING GAIN EXAMPLE

APPENDIX C

MODULATION INDEX TABLES

In this appendix are the results of solving the following equations by a digital computer.

$$\text{Loss}_1(\text{CAR.}) = 20 \log [J_o (\text{ITLM}) \cos (\text{IPN})] \quad (C.1)$$

$$\text{Loss}_1(\text{PN}) = 20 \log [J_o (\text{ITLM}) \sin (\text{IPN})] \quad (C.2)$$

$$\text{Loss}_1(\text{TLM}) = 20 \log [2J_1 (\text{ITLM}) \cos (\text{IPN})] \quad (C.3)$$

If $P_T$ is the total power (in dBm) in the prime carrier IF, then the carrier power (in dBm) accounting for modulation is (in dBm)

$$P_{CAR.} = P_T + \text{Loss(CAR.)}; \quad (C.4)$$

the ranging power is

$$P_{PN} = P_T + \text{Loss(PN)}; \quad (C.5)$$

the telemetry subcarrier power is

$$P_{TLM} = P_T + \text{Loss(PN)}. \quad (C.6)$$

The parameter IPN is the ranging modulation index, i.e., the prime carrier phase deviation in the absence of a subcarrier, and the parameter ITLM is the telemetry subcarrier index, i.e., the square root of two times the subcarrier power (Refer to Appendix B for details).

The results of equations C.1 through C.3 are used in the text the pick the optimum modulation indices in the downlink when ranging and telemetry are sent.

In the case of prime carrier modulation by the telemetry the following equations apply instead of C.1 and C.3.

$$\text{Loss}_2(\text{CAR.}) = 20 \log \cos (\text{ITLM}) \qquad \text{(C.1A)}$$

$$\text{Loss}_2(\text{TLM}) = 20 \log \sin (\text{ITLM}) \qquad \text{(C.3A)}$$

Equations C.4 and C.6 are then used as before. Equations C.1A and C.3A were also solved by computer with the results listed in the appendix.

As a side benefit of the program a listing of the solutions to the following equations is also presented in this appendix.

$$\text{Loss}_3(\text{CAR.}) = 20 \log J_o(\text{ITLM}) \qquad \text{(C.1B)}$$

$$\text{Loss}_3(\text{TLM}) - 3 = 20 \log J_1(\text{ITLM}) \qquad \text{(C.3B}$$

| IPN | ITLM | $LOSS_1$(CAR.) | $LOSS_1$(PN) | $LOSS_1$(TLM) |
|---|---|---|---|---|
| 0.1 | 0.1 | -0.07 | -20.04 | -23.07 |
| 0.1 | 0.2 | -0.13 | -20.10 | -17.09 |
| 0.1 | 0.3 | -0.24 | -20.21 | -13.62 |
| 0.1 | 0.4 | -0.39 | -20.37 | -11.20 |
| 0.1 | 0.5 | -0.60 | -20.57 | -9.36 |
| 0.1 | 0.6 | -0.84 | -20.81 | -7.89 |
| 0.1 | 0.7 | -1.14 | -21.11 | -6.70 |
| 0.1 | 0.8 | -1.49 | -21.46 | -5.71 |
| 0.1 | 0.9 | -1.90 | -21.87 | -4.87 |
| 0.1 | 1.0 | -2.37 | -22.34 | -4.17 |
| 0.1 | 1.1 | -2.90 | -22.87 | -3.58 |
| 0.1 | 1.2 | -3.51 | -23.48 | -3.09 |
| 0.1 | 1.3 | -4.19 | -24.17 | -2.69 |
| 0.1 | 1.4 | -4.97 | -24.95 | -2.36 |
| 0.1 | 1.5 | -5.86 | -25.83 | -2.11 |
| 0.1 | 1.6 | -6.88 | -26.85 | -1.93 |
| 0.1 | 1.7 | -8.05 | -28.02 | -1.81 |
| 0.1 | 1.8 | -9.41 | -29.39 | -1.75 |
| 0.1 | 1.9 | -11.04 | -31.02 | -1.76 |
| 0.1 | 2.0 | -13.04 | -33.01 | -1.82 |
| 0.1 | 2.1 | -15.61 | -35.58 | -1.95 |
| 0.1 | 2.2 | -19.19 | -39.16 | -2.14 |
| 0.1 | 2.3 | -25.15 | -45.12 | -2.40 |
| 0.1 | 2.4 | -52.06 | -72.03 | -2.72 |
| 0.2 | 0.1 | -0.20 | -14.06 | -23.21 |
| 0.2 | 0.2 | -0.26 | -14.12 | -17.22 |
| 0.2 | 0.3 | -0.37 | -14.23 | -13.75 |
| 0.2 | 0.4 | -0.53 | -14.39 | -11.33 |
| 0.2 | 0.5 | -0.73 | -14.59 | -9.49 |
| 0.2 | 0.6 | -0.97 | -14.84 | -8.03 |
| 0.2 | 0.7 | -1.27 | -15.14 | -6.83 |
| 0.2 | 0.8 | -1.62 | -15.49 | -5.84 |
| 0.2 | 0.9 | -2.03 | -15.89 | -5.01 |
| 0.2 | 1.0 | -2.50 | -16.36 | -4.30 |
| 0.2 | 1.1 | -3.03 | -16.90 | -3.72 |
| 0.2 | 1.2 | -3.64 | -17.50 | -3.23 |
| 0.2 | 1.3 | -4.33 | -18.19 | -2.82 |
| 0.2 | 1.4 | -5.11 | -18.97 | -2.50 |
| 0.2 | 1.5 | -5.99 | -19.85 | -2.24 |
| 0.2 | 1.6 | -7.01 | -20.87 | -2.06 |
| 0.2 | 1.7 | -8.18 | -22.04 | -1.94 |
| 0.2 | 1.8 | -9.55 | -23.41 | -1.88 |
| 0.2 | 1.9 | -11.18 | -25.04 | -1.89 |
| 0.2 | 2.0 | -13.17 | -27.04 | -1.96 |
| 0.2 | 2.1 | -15.74 | -29.60 | -2.08 |
| 0.2 | 2.2 | -19.32 | -33.18 | -2.27 |
| 0.2 | 2.3 | -25.28 | -39.15 | -2.53 |
| 0.2 | 2.4 | -52.19 | -66.05 | -2.85 |
| 0.3 | 0.1 | -0.42 | -10.61 | -23.43 |
| 0.3 | 0.2 | -0.48 | -10.68 | -17.44 |

| | | | | |
|---|---|---|---|---|
| 0.3 | 0.3 | -0.59 | -10.78 | -13.97 |
| 0.3 | 0.4 | -0.75 | -10.94 | -11.55 |
| 0.3 | 0.5 | -0.95 | -11.14 | -9.71 |
| 0.3 | 0.6 | -1.20 | -11.39 | -8.25 |
| 0.3 | 0.7 | -1.50 | -11.69 | -7.05 |
| 0.3 | 0.8 | -1.85 | -12.04 | -6.06 |
| 0.3 | 0.9 | -2.25 | -12.45 | -5.23 |
| 0.3 | 1.0 | -2.72 | -12.91 | -4.53 |
| 0.3 | 1.1 | -3.25 | -13.45 | -3.94 |
| 0.3 | 1.2 | -3.86 | -14.05 | -3.45 |
| 0.3 | 1.3 | -4.55 | -14.74 | -3.04 |
| 0.3 | 1.4 | -5.33 | -15.52 | -2.72 |
| 0.3 | 1.5 | -6.21 | -16.41 | -2.47 |
| 0.3 | 1.6 | -7.23 | -17.42 | -2.28 |
| 0.3 | 1.7 | -8.40 | -18.59 | -2.16 |
| 0.3 | 1.8 | -9.77 | -19.96 | -2.11 |
| 0.3 | 1.9 | -11.40 | -21.59 | -2.11 |
| 0.3 | 2.0 | -13.40 | -23.59 | -2.18 |
| 0.3 | 2.1 | -15.96 | -26.15 | -2.31 |
| 0.3 | 2.2 | -19.54 | -29.73 | -2.50 |
| 0.3 | 2.3 | -25.50 | -35.70 | -2.75 |
| 0.3 | 2.4 | -52.41 | -62.60 | -3.07 |
| 0.4 | 0.1 | -0.74 | -8.21 | -23.75 |
| 0.4 | 0.2 | -0.80 | -8.28 | -17.76 |
| 0.4 | 0.3 | -0.91 | -8.39 | -14.29 |
| 0.4 | 0.4 | -1.07 | -8.54 | -11.87 |
| 0.4 | 0.5 | -1.27 | -8.74 | -10.03 |
| 0.4 | 0.6 | -1.51 | -8.99 | -8.57 |
| 0.4 | 0.7 | -1.81 | -9.29 | -7.37 |
| 0.4 | 0.8 | -2.16 | -9.64 | -6.38 |
| 0.4 | 0.9 | -2.57 | -10.05 | -5.54 |
| 0.4 | 1.0 | -3.04 | -10.52 | -4.84 |
| 0.4 | 1.1 | -3.57 | -11.05 | -4.26 |
| 0.4 | 1.2 | -4.18 | -11.66 | -3.76 |
| 0.4 | 1.3 | -4.87 | -12.34 | -3.36 |
| 0.4 | 1.4 | -5.64 | -13.12 | -3.04 |
| 0.4 | 1.5 | -6.53 | -14.01 | -2.78 |
| 0.4 | 1.6 | -7.55 | -15.02 | -2.60 |
| 0.4 | 1.7 | -8.72 | -16.19 | -2.48 |
| 0.4 | 1.8 | -10.08 | -17.56 | -2.42 |
| 0.4 | 1.9 | -11.71 | -19.19 | -2.43 |
| 0.4 | 2.0 | -13.71 | -21.19 | -2.49 |
| 0.4 | 2.1 | -16.28 | -23.76 | -2.62 |
| 0.4 | 2.2 | -19.86 | -27.34 | -2.81 |
| 0.4 | 2.3 | -25.82 | -33.30 | -3.07 |
| 0.4 | 2.4 | -52.73 | -60.20 | -3.39 |
| 0.5 | 0.1 | -1.16 | -6.41 | -24.17 |
| 0.5 | 0.2 | -1.22 | -6.47 | -18.18 |
| 0.5 | 0.3 | -1.33 | -6.58 | -14.71 |
| 0.5 | 0.4 | -1.49 | -6.74 | -12.29 |
| 0.5 | 0.5 | -1.69 | -6.94 | -10.45 |
| 0.5 | 0.6 | -1.93 | -7.19 | -8.99 |
| 0.5 | 0.7 | -2.23 | -7.48 | -7.79 |
| 0.5 | 0.8 | -2.58 | -7.84 | -6.80 |

| | | | | |
|---|---|---|---|---|
| 0.5 | 0.9 | -2.99 | -8.24 | -5.96 |
| 0.5 | 1.0 | -3.46 | -8.71 | -5.26 |
| 0.5 | 1.1 | -3.99 | -9.24 | -4.68 |
| 0.5 | 1.2 | -4.60 | -9.85 | -4.18 |
| 0.5 | 1.3 | -5.29 | -10.54 | -3.78 |
| 0.5 | 1.4 | -6.06 | -11.32 | -3.46 |
| 0.5 | 1.5 | -6.95 | -12.20 | -3.20 |
| 0.5 | 1.6 | -7.97 | -13.22 | -3.02 |
| 0.5 | 1.7 | -9.14 | -14.39 | -2.90 |
| 0.5 | 1.8 | -10.51 | -15.76 | -2.84 |
| 0.5 | 1.9 | -12.13 | -17.39 | -2.85 |
| 0.5 | 2.0 | -14.13 | -19.38 | -2.91 |
| 0.5 | 2.1 | -16.70 | -21.95 | -3.04 |
| 0.5 | 2.2 | -20.28 | -25.53 | -3.23 |
| 0.5 | 2.3 | -26.24 | -31.49 | -3.49 |
| 0.5 | 2.4 | -53.15 | -58.40 | -3.81 |
| 0.6 | 0.1 | -1.69 | -4.99 | -24.70 |
| 0.6 | 0.2 | -1.75 | -5.05 | -18.71 |
| 0.6 | 0.3 | -1.86 | -5.16 | -15.24 |
| 0.6 | 0.4 | -2.02 | -5.32 | -12.82 |
| 0.6 | 0.5 | -2.22 | -5.52 | -10.98 |
| 0.6 | 0.6 | -2.47 | -5.76 | -9.52 |
| 0.6 | 0.7 | -2.77 | -6.06 | -8.32 |
| 0.6 | 0.8 | -3.12 | -6.41 | -7.33 |
| 0.6 | 0.9 | -3.52 | -6.82 | -6.50 |
| 0.6 | 1.0 | -3.99 | -7.29 | -5.80 |
| 0.6 | 1.1 | -4.53 | -7.82 | -5.21 |
| 0.6 | 1.2 | -5.13 | -8.43 | -4.72 |
| 0.6 | 1.3 | -5.82 | -9.12 | -4.31 |
| 0.6 | 1.4 | -6.60 | -9.90 | -3.99 |
| 0.6 | 1.5 | -7.48 | -10.78 | -3.74 |
| 0.6 | 1.6 | -8.50 | -11.80 | -3.55 |
| 0.6 | 1.7 | -9.67 | -12.97 | -3.43 |
| 0.6 | 1.8 | -11.04 | -14.34 | -3.38 |
| 0.6 | 1.9 | -12.67 | -15.97 | -3.38 |
| 0.6 | 2.0 | -14.67 | -17.96 | -3.45 |
| 0.6 | 2.1 | -17.23 | -20.53 | -3.58 |
| 0.6 | 2.2 | -20.81 | -24.11 | -3.77 |
| 0.6 | 2.3 | -26.78 | -30.07 | -4.02 |
| 0.6 | 2.4 | -53.68 | -56.98 | -4.34 |
| 0.7 | 0.1 | -2.35 | -3.84 | -25.36 |
| 0.7 | 0.2 | -2.42 | -3.91 | -19.37 |
| 0.7 | 0.3 | -2.53 | -4.02 | -15.90 |
| 0.7 | 0.4 | -2.68 | -4.17 | -13.48 |
| 0.7 | 0.5 | -2.88 | -4.37 | -11.64 |
| 0.7 | 0.6 | -3.13 | -4.62 | -10.18 |
| 0.7 | 0.7 | -3.43 | -4.92 | -8.98 |
| 0.7 | 0.8 | -3.78 | -5.27 | -7.99 |
| 0.7 | 0.9 | -4.19 | -5.68 | -7.16 |
| 0.7 | 1.0 | -4.65 | -6.14 | -6.46 |
| 0.7 | 1.1 | -5.19 | -6.68 | -5.87 |
| 0.7 | 1.2 | -5.79 | -7.28 | -5.38 |
| 0.7 | 1.3 | -6.48 | -7.97 | -4.97 |
| 0.7 | 1.4 | -7.26 | -8.75 | -4.65 |

| | | | | |
|---|---|---|---|---|
| 0.7 | 1.5 | -8.15 | -9.64 | -4.40 |
| 0.7 | 1.6 | -9.16 | -10.65 | -4.21 |
| 0.7 | 1.7 | -10.33 | -11.82 | -4.09 |
| 0.7 | 1.8 | -11.70 | -13.19 | -4.04 |
| 0.7 | 1.9 | -13.33 | -14.82 | -4.04 |
| 0.7 | 2.0 | -15.33 | -16.82 | -4.11 |
| 0.7 | 2.1 | -17.89 | -19.39 | -4.24 |
| 0.7 | 2.2 | -21.47 | -22.96 | -4.43 |
| 0.7 | 2.3 | -27.44 | -28.93 | -4.68 |
| 0.7 | 2.4 | -54.34 | -55.83 | -5.01 |
| 0.8 | 0.1 | -3.16 | -2.91 | -26.17 |
| 0.8 | 0.2 | -3.23 | -2.97 | -20.18 |
| 0.8 | 0.3 | -3.34 | -3.08 | -16.72 |
| 0.8 | 0.4 | -3.49 | -3.24 | -14.29 |
| 0.8 | 0.5 | -3.69 | -3.44 | -12.45 |
| 0.8 | 0.6 | -3.94 | -3.69 | -10.99 |
| 0.8 | 0.7 | -4.24 | -3.98 | -9.80 |
| 0.8 | 0.8 | -4.59 | -4.33 | -8.80 |
| 0.8 | 0.9 | -5.00 | -4.74 | -7.97 |
| 0.8 | 1.0 | -5.46 | -5.21 | -7.27 |
| 0.8 | 1.1 | -6.00 | -5.74 | -6.68 |
| 0.8 | 1.2 | -6.60 | -6.35 | -6.19 |
| 0.8 | 1.3 | -7.29 | -7.04 | -5.79 |
| 0.8 | 1.4 | -8.07 | -7.82 | -5.46 |
| 0.8 | 1.5 | -8.96 | -8.70 | -5.21 |
| 0.8 | 1.6 | -9.97 | -9.72 | -5.02 |
| 0.8 | 1.7 | -11.14 | -10.89 | -4.90 |
| 0.8 | 1.8 | -12.51 | -12.26 | -4.85 |
| 0.8 | 1.9 | -14.14 | -13.89 | -4.85 |
| 0.8 | 2.0 | -16.14 | -15.88 | -4.92 |
| 0.8 | 2.1 | -18.71 | -18.45 | -5.05 |
| 0.8 | 2.2 | -22.28 | -22.03 | -5.24 |
| 0.8 | 2.3 | -28.25 | -27.99 | -5.49 |
| 0.8 | 2.4 | -55.15 | -54.90 | -5.82 |
| 0.9 | 0.1 | -4.15 | -2.14 | -27.16 |
| 0.9 | 0.2 | -4.22 | -2.21 | -21.17 |
| 0.9 | 0.3 | -4.33 | -2.32 | -17.71 |
| 0.9 | 0.4 | -4.48 | -2.47 | -15.28 |
| 0.9 | 0.5 | -4.68 | -2.67 | -13.44 |
| 0.9 | 0.6 | -4.93 | -2.92 | -11.98 |
| 0.9 | 0.7 | -5.23 | -3.22 | -10.79 |
| 0.9 | 0.8 | -5.58 | -3.57 | -9.79 |
| 0.9 | 0.9 | -5.99 | -3.98 | -8.96 |
| 0.9 | 1.0 | -6.45 | -4.45 | -8.26 |
| 0.9 | 1.1 | -6.99 | -4.98 | -7.67 |
| 0.9 | 1.2 | -7.59 | -5.58 | -7.18 |
| 0.9 | 1.3 | -8.28 | -6.27 | -6.78 |
| 0.9 | 1.4 | -9.06 | -7.05 | -6.45 |
| 0.9 | 1.5 | -9.95 | -7.94 | -6.20 |
| 0.9 | 1.6 | -10.96 | -8.95 | -6.01 |
| 0.9 | 1.7 | -12.13 | -10.12 | -5.89 |
| 0.9 | 1.8 | -13.50 | -11.49 | -5.84 |
| 0.9 | 1.9 | -15.13 | -13.12 | -5.84 |
| 0.9 | 2.0 | -17.13 | -15.12 | -5.91 |

| | | | | |
|---|---|---|---|---|
| 0.9 | 2.1 | -19.70 | -17.69 | -6.04 |
| 0.9 | 2.2 | -23.27 | -21.26 | -6.23 |
| 0.9 | 2.3 | -29.24 | -27.23 | -6.48 |
| 0.9 | 2.4 | -56.14 | -54.13 | -6.81 |
| 1.0 | 0.1 | -5.37 | -1.52 | -28.38 |
| 1.0 | 0.2 | -5.43 | -1.59 | -22.39 |
| 1.0 | 0.3 | -5.54 | -1.70 | -18.92 |
| 1.0 | 0.4 | -5.70 | -1.85 | -16.50 |
| 1.0 | 0.5 | -5.90 | -2.05 | -14.66 |
| 1.0 | 0.6 | -6.15 | -2.30 | -13.20 |
| 1.0 | 0.7 | -6.45 | -2.60 | -12.00 |
| 1.0 | 0.8 | -6.80 | -2.95 | -11.01 |
| 1.0 | 0.9 | -7.20 | -3.36 | -10.18 |
| 1.0 | 1.0 | -7.67 | -3.82 | -9.48 |
| 1.0 | 1.1 | -8.21 | -4.36 | -8.89 |
| 1.0 | 1.2 | -8.81 | -4.96 | -8.40 |
| 1.0 | 1.3 | -9.50 | -5.65 | -7.99 |
| 1.0 | 1.4 | -10.28 | -6.43 | -7.67 |
| 1.0 | 1.5 | -11.16 | -7.32 | -7.42 |
| 1.0 | 1.6 | -12.18 | -8.33 | -7.23 |
| 1.0 | 1.7 | -13.35 | -9.50 | -7.11 |
| 1.0 | 1.8 | -14.72 | -10.87 | -7.06 |
| 1.0 | 1.9 | -16.35 | -12.50 | -7.06 |
| 1.0 | 2.0 | -18.35 | -14.50 | -7.13 |
| 1.0 | 2.1 | -20.91 | -17.07 | -7.26 |
| 1.0 | 2.2 | -24.49 | -20.64 | -7.45 |
| 1.0 | 2.3 | -30.46 | -26.61 | -7.70 |
| 1.0 | 2.4 | -57.36 | -53.51 | -8.02 |
| 1.1 | 0.1 | -6.89 | -1.02 | -29.90 |
| 1.1 | 0.2 | -6.95 | -1.09 | -23.91 |
| 1.1 | 0.3 | -7.06 | -1.20 | -20.44 |
| 1.1 | 0.4 | -7.22 | -1.35 | -18.02 |
| 1.1 | 0.5 | -7.42 | -1.55 | -16.18 |
| 1.1 | 0.6 | -7.67 | -1.80 | -14.72 |
| 1.1 | 0.7 | -7.97 | -2.10 | -13.52 |
| 1.1 | 0.8 | -8.32 | -2.45 | -12.53 |
| 1.1 | 0.9 | -8.72 | -2.86 | -11.70 |
| 1.1 | 1.0 | -9.19 | -3.32 | -11.00 |
| 1.1 | 1.1 | -9.72 | -3.86 | -10.41 |
| 1.1 | 1.2 | -10.33 | -4.46 | -9.92 |
| 1.1 | 1.3 | -11.02 | -5.15 | -9.51 |
| 1.1 | 1.4 | -11.80 | -5.93 | -9.19 |
| 1.1 | 1.5 | -12.68 | -6.82 | -8.93 |
| 1.1 | 1.6 | -13.70 | -7.83 | -8.75 |
| 1.1 | 1.7 | -14.87 | -9.00 | -8.63 |
| 1.1 | 1.8 | -16.24 | -10.37 | -8.58 |
| 1.1 | 1.9 | -17.87 | -12.00 | -8.58 |
| 1.1 | 2.0 | -19.87 | -14.00 | -8.65 |
| 1.1 | 2.1 | -22.43 | -16.57 | -8.78 |
| 1.1 | 2.2 | -26.01 | -20.14 | -8.97 |
| 1.1 | 2.3 | -31.97 | -26.11 | -9.22 |
| 1.1 | 2.4 | -58.88 | -53.01 | -9.54 |
| 1.2 | 0.1 | -8.84 | -0.63 | -31.85 |
| 1.2 | 0.2 | -8.90 | -0.70 | -25.86 |

| | | | | |
|---|---|---|---|---|
| 1.2 | 0.3 | -9.01 | -0.81 | -22.39 |
| 1.2 | 0.4 | -9.17 | -0.96 | -19.97 |
| 1.2 | 0.5 | -9.37 | -1.16 | -18.13 |
| 1.2 | 0.6 | -9.62 | -1.41 | -16.67 |
| 1.2 | 0.7 | -9.92 | -1.71 | -15.47 |
| 1.2 | 0.8 | -10.27 | -2.06 | -14.48 |
| 1.2 | 0.9 | -10.67 | -2.47 | -13.65 |
| 1.2 | 1.0 | -11.14 | -2.94 | -12.95 |
| 1.2 | 1.1 | -11.68 | -3.47 | -12.36 |
| 1.2 | 1.2 | -12.28 | -4.08 | -11.87 |
| 1.2 | 1.3 | -12.97 | -4.76 | -11.46 |
| 1.2 | 1.4 | -13.75 | -5.54 | -11.14 |
| 1.2 | 1.5 | -14.63 | -6.43 | -10.89 |
| 1.2 | 1.6 | -15.65 | -7.44 | -10.70 |
| 1.2 | 1.7 | -16.82 | -8.61 | -10.58 |
| 1.2 | 1.8 | -18.19 | -9.98 | -10.53 |
| 1.2 | 1.9 | -19.82 | -11.61 | -10.53 |
| 1.2 | 2.0 | -21.82 | -13.61 | -10.60 |
| 1.2 | 2.1 | -24.38 | -16.18 | -10.73 |
| 1.2 | 2.2 | -27.96 | -19.75 | -10.92 |
| 1.2 | 2.3 | -33.93 | -25.72 | -11.17 |
| 1.2 | 2.4 | -60.83 | -52.62 | -11.49 |
| 1.3 | 0.1 | -11.48 | -0.34 | -34.48 |
| 1.3 | 0.2 | -11.54 | -0.41 | -28.50 |
| 1.3 | 0.3 | -11.65 | -0.52 | -25.03 |
| 1.3 | 0.4 | -11.80 | -0.67 | -22.61 |
| 1.3 | 0.5 | -12.01 | -0.87 | -20.77 |
| 1.3 | 0.6 | -12.25 | -1.12 | -19.30 |
| 1.3 | 0.7 | -12.55 | -1.42 | -18.11 |
| 1.3 | 0.8 | -12.90 | -1.77 | -17.12 |
| 1.3 | 0.9 | -13.31 | -2.18 | -16.28 |
| 1.3 | 1.0 | -13.78 | -2.65 | -15.58 |
| 1.3 | 1.1 | -14.31 | -3.18 | -14.99 |
| 1.3 | 1.2 | -14.92 | -3.79 | -14.50 |
| 1.3 | 1.3 | -15.60 | -4.47 | -14.10 |
| 1.3 | 1.4 | -16.38 | -5.25 | -13.77 |
| 1.3 | 1.5 | -17.27 | -6.14 | -13.52 |
| 1.3 | 1.6 | -18.29 | -7.15 | -13.34 |
| 1.3 | 1.7 | -19.46 | -8.33 | -13.22 |
| 1.3 | 1.8 | -20.82 | -9.69 | -13.16 |
| 1.3 | 1.9 | -22.45 | -11.32 | -13.17 |
| 1.3 | 2.0 | -24.45 | -13.32 | -13.23 |
| 1.3 | 2.1 | -27.02 | -15.89 | -13.36 |
| 1.3 | 2.2 | -30.60 | -19.47 | -13.55 |
| 1.3 | 2.3 | -36.56 | -25.43 | -13.81 |
| 1.3 | 2.4 | -63.47 | -52.34 | -14.13 |
| 1.4 | 0.1 | -15.41 | -0.15 | -38.42 |
| 1.4 | 0.2 | -15.48 | -0.21 | -32.44 |
| 1.4 | 0.3 | -15.59 | -0.32 | -28.97 |
| 1.4 | 0.4 | -15.74 | -0.48 | -26.55 |
| 1.4 | 0.5 | -15.94 | -0.68 | -24.71 |
| 1.4 | 0.6 | -16.19 | -0.93 | -23.24 |
| 1.4 | 0.7 | -16.49 | -1.23 | -22.05 |
| 1.4 | 0.8 | -16.84 | -1.58 | -21.06 |

| | | | | |
|---|---|---|---|---|
| 1.4 | 0.9 | -17.25 | -1.98 | -20.22 |
| 1.4 | 1.0 | -17.72 | -2.45 | -19.52 |
| 1.4 | 1.1 | -18.25 | -2.99 | -18.93 |
| 1.4 | 1.2 | -18.86 | -3.59 | -18.44 |
| 1.4 | 1.3 | -19.54 | -4.28 | -18.04 |
| 1.4 | 1.4 | -20.32 | -5.06 | -17.71 |
| 1.4 | 1.5 | -21.21 | -5.94 | -17.46 |
| 1.4 | 1.6 | -22.22 | -6.96 | -17.28 |
| 1.4 | 1.7 | -23.40 | -8.13 | -17.16 |
| 1.4 | 1.8 | -24.76 | -9.50 | -17.10 |
| 1.4 | 1.9 | -26.39 | -11.13 | -17.11 |
| 1.4 | 2.0 | -28.39 | -13.13 | -17.17 |
| 1.4 | 2.1 | -30.96 | -15.69 | -17.30 |
| 1.4 | 2.2 | -34.54 | -19.27 | -17.49 |
| 1.4 | 2.3 | -40.50 | -25.24 | -17.75 |
| 1.4 | 2.4 | -67.41 | -52.14 | -18.07 |
| 1.5 | 0.1 | -23.03 | -0.04 | -46.04 |
| 1.5 | 0.2 | -23.09 | -0.11 | -40.05 |
| 1.5 | 0.3 | -23.20 | -0.22 | -36.58 |
| 1.5 | 0.4 | -23.36 | -0.37 | -34.16 |
| 1.5 | 0.5 | -23.56 | -0.57 | -32.32 |
| 1.5 | 0.6 | -23.81 | -0.82 | -30.86 |
| 1.5 | 0.7 | -24.11 | -1.12 | -29.66 |
| 1.5 | 0.8 | -24.46 | -1.47 | -28.67 |
| 1.5 | 0.9 | -24.86 | -1.88 | -27.84 |
| 1.5 | 1.0 | -25.33 | -2.35 | -27.14 |
| 1.5 | 1.1 | -25.86 | -2.88 | -26.55 |
| 1.5 | 1.2 | -26.47 | -3.49 | -26.06 |
| 1.5 | 1.3 | -27.16 | -4.17 | -25.65 |
| 1.5 | 1.4 | -27.94 | -4.95 | -25.33 |
| 1.5 | 1.5 | -28.82 | -5.84 | -25.08 |
| 1.5 | 1.6 | -29.84 | -6.85 | -24.89 |
| 1.5 | 1.7 | -31.01 | -8.02 | -24.77 |
| 1.5 | 1.8 | -32.38 | -9.39 | -24.72 |
| 1.5 | 1.9 | -34.01 | -11.02 | -24.72 |
| 1.5 | 2.0 | -36.01 | -13.02 | -24.79 |
| 1.5 | 2.1 | -38.57 | -15.59 | -24.92 |
| 1.5 | 2.2 | -42.15 | -19.17 | -25.11 |
| 1.5 | 2.3 | -48.11 | -25.13 | -25.36 |
| 1.5 | 2.4 | -75.02 | -52.03 | -25.68 |

| ITLM(RAD.) | $LOSS_2$(CAR.) | $LOSS_2$(TLM) |
|---|---|---|
| 0.1 | -0.04 | -20.01 |
| 0.2 | -0.17 | -14.04 |
| 0.3 | -0.40 | -10.59 |
| 0.4 | -0.71 | -8.19 |
| 0.5 | -1.13 | -6.39 |
| 0.6 | -1.67 | -4.96 |
| 0.7 | -2.33 | -3.82 |
| 0.8 | -3.14 | -2.89 |
| 0.9 | -4.13 | -2.12 |
| 1.0 | -5.35 | -1.50 |
| 1.1 | -6.87 | -1.00 |
| 1.2 | -8.82 | -0.61 |
| 1.3 | -11.45 | -0.32 |
| 1.4 | -15.39 | -0.13 |
| 1.5 | -23.01 | -0.02 |

| ITLM(RAD.) | $LOSS_3$(CAR.) | $LOSS_3$(TLM)-3 |
|---|---|---|
| 0.1 | -0.02 | -26.03 |
| 0.2 | -0.09 | -20.04 |
| 0.3 | -0.20 | -16.58 |
| 0.4 | -0.35 | -14.15 |
| 0.5 | -0.55 | -12.31 |
| 0.6 | -0.80 | -10.85 |
| 0.7 | -1.10 | -9.66 |
| 0.8 | -1.45 | -8.66 |
| 0.9 | -1.86 | -7.83 |
| 1.0 | -2.32 | -7.13 |
| 1.1 | -2.86 | -6.54 |
| 1.2 | -3.46 | -6.05 |
| 1.3 | -4.15 | -5.65 |
| 1.4 | -4.93 | -5.32 |
| 1.5 | -5.82 | -5.07 |
| 1.6 | -6.83 | -4.88 |
| 1.7 | -8.00 | -4.76 |
| 1.8 | -9.37 | -4.71 |
| 1.9 | -11.00 | -4.71 |
| 2.0 | -13.00 | -4.78 |
| 2.1 | -15.57 | -4.91 |
| 2.2 | -19.14 | -5.10 |
| 2.3 | -25.11 | -5.35 |
| 2.4 | -52.01 | -5.68 |

APPENDIX D

FORTRAN IME LINK CALCULATION COMPUTER PROGRAM

```
//mvxgdec1 job (0001,0051,1,1,0,,,,,0197313121,20046,masao,dec,n,
// ###),'038cartier20046',msglevel=1,msgclass=a,class=e
/*route  vts   042,save
//step1 exec fortgclg
//fort.sysin dd *
      dimension gtpwr(4),gtxl(4),codeg(12),srapwr(4),
     1gripwr(12),grden(12),gtant(4),upath(4),srant(4),srxl(4),
     2srden(4),sripwr(4),utosno(4),urfac(4),cofac(4),urth(4),
     3rban(4),bplim(4),prsn(12),grxl(4),grant(4),dpath(4),
     4spoint(4),stant(4),stxl(4),stpwr(4),dsol(4),grapwr(4),
     5dtosno(12),drfacs(12),dtfacs(12),rfban(12),
     6dcfacs(12),drsnos(12),dcsnos(12),dtsnos(12),
     7desnos(12),rmars(12),cmars(12),tmars(12),
     8comars(12),urmar(4),
     9usol(4),dcth(12),drth(12),dtth(12)
      read(5,5000)gtpwr,gtxl,gtant,upath,srant,srxl,usol,srden
5000  format(4f10.2)
      read(5,5001)iflag,jflag,kflag,lflag
5001  format(4i1)
      write(6,6000)
6000  format('1',t7,'IMP-H. BEST CASE',t34,'IMP-H. WORST CASE',t60,
     1'IMP-M.-D. BEST CASE',t87,'IMP-M.-D. WORST CASE'/)
6001  format(4(11x,f6.1,10x))
400   do 500 i=1,4
      srapwr(i)=gtpwr(i)+gtxl(i)+gtant(i)+upath(i)
      sripwr(i)=srapwr(i)+srant(i)+srxl(i)
      go to (401,403),jflag
401   srden(i)=rise(srden(i),sripwr(i))
403   utosno(i)=sripwr(i)-(srden(i)-usol(i))
500   continue
      write(6,6001)gtpwr,gtxl,gtant,upath,srapwr,srant,srxl,sripwr,
     1usol,srden,utosno
      if(iflag-1)600,4000,600
600   read(5,5000)urfac,cofac,urth,rban
      do 700 i=1,4
      rfban(i)=3.+rban(i)
      x=10.**((utosno(i)-rfban(i))/10.)
      bplim(i)=10.*alog10((1.+(2.*x))/(1.273239538+x))
      prsn(i)=(utosno(i)-rfban(i))+bplim(i)+urfac(i)+cofac(i)
      urmar(i)=prsn(i)-urth(i)
700   continue
      write(6,6001)bplim,urfac,cofac,(prsn(i),i=1,4),urth,
     1urmar,rban
      if(iflag-2)800,4000,800
800   read(5,5000)stpwr,stxl,stant,spoint,dpath,grant,grxl
      read(5,5002)dsol,(grden(i),i=1,3),(dcth(i),i=1,4),(drth(i),i=1,4),
     1(dtth(i),i=1,4)
5002  format(4f10.2/3f10.2/4f10.2/4f10.2/4f10.2)
      do 900 i=1,4
      grapwr(i)=stpwr(i)+stxl(i)+stant(i)+spoint(i)+dpath(i)
```

```
      gripwr(i)=grapwr(i)+grant(i)+grxl(i)
900   continue
      write(6,6001)stpwr,stxl,stant,spoint,dpath,grapwr,grant,grxl,
     1(gripwr(i),i=1,4),dsol
      do 1000 j=1,4
      i=5-j
      gripwr(3*i-2)=gripwr(i)+dsol(i)
      gripwr(3*i-1)=gripwr(i)+dsol(i)
      gripwr(3*i)=gripwr(i)+dsol(i)
      prsn(3*i-2)=prsn(i)
      prsn(3*i-1)=prsn(i)
      prsn(3*i)=prsn(i)
      rfban(3*i-2)=rfban(i)
      rfban(3*i-1)=rfban(i)
      rfban(3*i)=rfban(i)
      dcth(3*i-2)=dcth(i)
      dcth(3*i-1)=dcth(i)
      dcth(3*i)=dcth(i)
      drth(3*i-2)=drth(i)
      drth(3*i-1)=drth(i)
      drth(3*i)=drth(i)
      dtth(3*i-2)=dtth(i)
      dtth(3*i-1)=dtth(i)
      dtth(3*i)=dtth(i)
1000  continue
      do 1001 i=1,3
      grden(i)=grden(i)
      grden(i+3)=grden(i)
      grden(i+6)=grden(i)
      grden(i+9)=grden(i)
1001  continue
      do 1002 i=1,12
      go to (1111,1112),kflag
1111  grden(i)=rise(grden(i),gripwr(i))
1112  dtosno(i)=gripwr(i)-grden(i)
1002  continue
      write(6,6002)grden,dtosno
6002  format(t3,f6.1,11f9.1)
      if(iflag-3)302,301,302
301   write(6,6003)drth,dcth,dtth
6003  format(6(/),3(/t3,f6.1,11f9.1))
      go to 4000
302   read(5,5003)(drfacs(i),i=1,2),(dcfacs(i),i=1,2),
     1(dtfacs(i),i=1,2),
     2(codeg(i),i=1,2)
5003  format(2f10.1)
      do 303 k=1,2
      do 303 j=1,6
      i=3-k
      jsub=j+((i-1)*6)
```

```
      drfacs(jsub)=drfacs(i)
      dcfacs(jsub)=dcfacs(i)
      dtfacs(jsub)=dtfacs(i)
      codeg(jsub)=codeg(i)
303   continue
      do 304 i=1,12
      drsnos(i)=dtosno(i)+drfacs(i)
      dcsnos(i)=dtosno(i)+dcfacs(i)
      dtsnos(i)=dtosno(i)+dtfacs(i)
      y=10.**(prsn(i)/10.)
      z=10.**((drsnos(i)-rfban(i))/10.)
      desnos(i)=(10.*alog10((y*z)/(1.+y+z)))+rfban(i)
      rmars(i)=desnos(i)-drth(i)
      cmars(i)=dcsnos(i)-dcth(i)
      tmars(i)=dtsnos(i)-dtth(i)
      comars(i)=tmars(i)+codeg(i)
304   continue
      go to (305,306,307),iflag
305   write(6,6002)drfacs,dcfacs,dtfacs,drsnos,dcsnos,dtsnos,desnos,
     1drth,dcth,
     2dtth,rmars,cmars,tmars,codeg,comars
      go to 4000
306   write(6,6004)drfacs,dcfacs,drsnos,dcsnos,desnos,drth,
     1dcth,rmars,cmars
6004  format(2(t3,f6.1,11f9.1/)/2(t3,f6.1,11f9.1/)/
     13(t3,f6.1,11f9.1/)/2(t3,f6.1,11f9.1/))
      go to 4000
307   write(6,6005)dcfacs,dtfacs,dcsnos,dtsnos,dcth,dtth,
     1cmars,tmars,codeg,comars
6005  format(/2(t3,f6.1,11f9.1/)/2(t3,f6.1,11f9.1/)
     1//2(t3,f6.1,11f9.1/)/4(t3,f6.1,11f9.1/))
4000  continue
      stop
      end
      function rise(thres,pwrin)
      if(pwrin+120)4,4,1
1     if(pwrin+80)3,3,2
2     rise=pwrin-76.
      go to 5
3     rise=(thres+175.5)-(9.0246958e-6*pwrin**4
     1+3.5684297e-3*pwrin**3+.51151562*pwrin**2
     2+30.889069*pwrin+811.28955)
      go to 5
4     rise=thres
5     return
      end
/*
//go.sysin dd *
73.       73.       73.       73.
-.1       -.5       -.1       -.5
```

```
52.5        52.5        52.5        43.
-222.1      -222.1      -202.1      -202.1
2.          -3.         2.          -3.
-1.         -2.         -1.         -2.
0           0           0           0
-166.8      -166.8      -166.8      -166.8
4221
-4.7        -4.7        -4.7        -4.7
3.          3.          3.          3.
0           0           0           0
60.         60.         60.         60.
34.         34.         30.         30.
-1.5        -3.         -1.5        -3.
9.          9.          9.          9.
0.          -2.         0.          -2.
-223.1      -223.1      -204.9      -204.9
52.5        43.         52.5        43.
-.2         -.5         -.2         -.5
0.          -11.2       0.          0.
-180.1      -178.8      -176.3
30.         30.         30.         30.
23.         23.         23.         23.
35.7        44.7        44.7        53.8
-16.        -16.
-2.         -2.
-5.         -5.
6.          6.
/*
```

APPENDIX E

## CHOICE OF OPTIMAL METRIC FOR GAUSSIAN NOISE ENVIRONMENT

Let the noise on the channel be additive Gaussian noise with double-sided power spectrum $N_0/2$ watts/Hz. Given a state assumed to be the correct one and a transition incident out of this state, let $x_{j1}x_{j2}$ be the antipodal representation of the coded bit pair (i.e., $x_{j1}$ and $x_{j2} = \pm 1$) belonging to that transition at time j. Similarly, it is assumed that the modem assumes the bit 1(0) is received if the output signal is positive (negative). Again, here we are deriving results for the rate 1/2 code.

Let the received pair of signals from the modem be denoted by $(r_1, r_2)$.

We define

$$\hat{x}_{j1} = \text{sgn}(r_{j1}) \tag{E.1}$$

$$\hat{x}_{j2} = \text{sgn}(r_{j2}) \tag{E.2}$$

$$\alpha_{j1} = |r_{j1}| \tag{E.3}$$

$$\alpha_{j2} = |r_{j2}| \tag{E.4}$$

The maximum likelihood for sequences $\underline{x}_1$ and $\underline{x}_2$ of length n is obtained for

$$\underset{\underline{x}_1,\underline{x}_2}{\text{Max}} \prod_{j=1}^{n} \frac{1}{\pi N_0} \exp\left[-\frac{(r_{j1}-x_{j1})^2+(r_{j2}-x_{j2})^2}{N_0}\right] \tag{E.5}$$

Similarly, we obtain the result by minimizing a distance metric which is a monotonically decreasing function of the term above, i.e.,

$$\underset{\underline{x}_1,\underline{x}_2}{\text{Min}} \left\{ \sum_{j=1}^{n} [r_{j1}^2+x_{j1}^2-2r_{j1}x_{j1}+r_{j2}^2+x_{j2}^2-2r_{j2}x_{j2}] \right\} \qquad \text{E.6}$$

which is obtained by taking the negative logarithm of the product and deleting constant terms which do not affect the decision over $\underline{x}_1,\underline{x}_2$. Furthermore, terms within that expression which are independent of the choice of $x_{j1}$ or $x_{j2}$ may be neglected as only the relative values of the metric are of concern. Thus $r_{j1}^2, r_{j2}^2$ may be deleted and, since $x_{j1}$ and $x_{j2}$ are either plus or minus one, so can the terms $x_{k1}^2$ and $x_{j2}^2$.

Thus, the maximum likelihood decision is reduced to choose

$$\underset{\underline{X}_1\underline{X}_2}{\text{Min}} \sum_{i=1}^{n} \frac{1}{2}[-r_{j1}x_{j1}-r_{j2}x_{j2}] \qquad \text{E.7}$$

where a factor of 1/2 has been introduced. To each term we add a constant independent of $x_{j1}$ or $x_{j2}$ to yield

$$\underset{\underline{x}_1\underline{x}_2}{\text{Min}} \sum_{j=1}^{n} [\frac{1}{2}(-r_{j1}x_{j1}+r_{j1}\hat{x}_{j1}) + \frac{1}{2}(-r_{j2}x_{j2}+r_{j2}\hat{x}_{j2})] \qquad \text{E.8}$$

In view of the definitions, we have

$$r_{j1} = \hat{x}_{j1}\alpha_{j1} \qquad \text{E.9}$$

$$r_{j2} = \hat{x}_{j2}\alpha_{j2} \qquad \text{E.10}$$

Thus each term in the sum is

$$_jL_{c_1c_2} = \frac{1}{2}\hat{x}_{j1}\alpha_{j1}[\hat{x}_{j1}-x_{j1}] + \frac{1}{2}\hat{x}_{j2}\alpha_{j2}[\hat{x}_{j2}-x_{j2}] \qquad \text{E.11}^*$$

and reduces to

$$0 \text{ if } x_{j1} = \hat{x}_{j1} \text{ and } x_{j2} = \hat{x}_{j2} \qquad \text{E.12}$$

$$\alpha_{j1} \text{ if } x_{j1} \neq \hat{x}_{j1} \text{ and } x_{j2} = \hat{x}_{j2} \qquad \text{E.13}$$

---

* $C_i = (1 + x_{ji})/2$

$$\alpha_{j2} \text{ if } x_{j1} = \hat{x}_{j1} \text{ and } x_{j2} \neq \hat{x}_{j2} \qquad \text{E.14}$$

$$\alpha_{j1}+\alpha_{j2} \text{ if } x_{j1} \neq \hat{x}_{j1} \text{ and } x_{j2} \neq \hat{x}_{j2} \qquad \text{E.15}$$

The above table then specifies the construction of a simple metric which, for each state, is the accumulation of the absolute values of the quantized outputs of the modem for each of the transmitted bits. If hard decisions are used, all terms $\alpha_{j1}$, $j = 1,\ldots;n$ and $i = 1,2$ are unity and the count is the Hamming distance. If soft decisions are used, the count remains monotonic in the likelihood function and thus is optimal.

The transition equations 3.27 through 3.30 are derived as follows. Using the definition given before, i.e.,

$$C_i = \left(\hat{x}_{ji} + 1\right)/2, \; \overline{C}_i = 1 - C_i = \left(1 - \hat{x}_{ji}\right)/2, \qquad \text{E.16}$$

then the transition equations follow directly, e.g.,

$$\begin{aligned} {}^{j}L_{11} &= \frac{1}{2}\alpha_{ji}\left(\hat{x}_{ji}^2 - \hat{x}_{ji}\right) + \frac{1}{2}\alpha_{j2}\left(\hat{x}_{j2}^2 - \hat{x}_{j2}\right) \\ &= \alpha_{j1}\left(\frac{1}{2} - \frac{\hat{x}_{j1}}{2}\right) + \alpha_{j2}\left(\frac{1}{2} - \frac{\hat{x}_{j2}}{2}\right) \\ &= \alpha_{j1}\,\overline{C}_1 + \alpha_{j2}\,\overline{C}_2 \end{aligned} \qquad \text{E.17}$$

The transformation in E.16 is simply a logic level change.

AMPEX

TAPE RECORDER SPECIFICATIONS

# specifications

# AR-700
# instrumentation recorder

Effective December 1, 1971

## GENERAL DESCRIPTION

The AR-700 is a compact intermediate or wideband multichannel recorder designed for airborne and other stringent environments. It is ruggedly constructed, uses servo-controlled time base correction and may be electrically switched over a range of six speeds. Up to seven channels of record electronics are provided on machines using ¼" tape on 10½" or 12½" precision reels, or up to 14 channels on machines equipped for 1" tape.

The system design emphasizes small size, ease of operation and serviceability. Closed loop capstan design, concentric reels and a fast response capstan servo are featured. The AR-700 is designed for remote sequential operation for those needing uninterrupted recording. Additional optional features and custom modifications are available to satisfy every need.

## TAPE TRANSPORT

**Tape Speeds:** Six speeds—60, 30, 15, 7-1/2, 3-3/4 and 1-7/8 ips. Electrically selected with rotary switch.

**Reels:** 12-1/2 inch or 10-1/2 inch, precision reels.

**Flutter:** Percent measured per IRIG 106-71 (2 sigma).

| Tape Speed (ips) | Bandpass (Hz) | % Flutter[1] | % Flutter[2] |
|---|---|---|---|
| 60 | 0.2 to 10,000 | 0.30 | 0.40 |
| 30 | 0.2 to 5,000 | 0.32 | 0.60 |
| 15 | 0.2 to 2,500 | 0.35 | 0.80 |
| 7-1/2 | 0.2 to 1,250 | 0.40 | 1.50 |
| 3-3/4 | 0.2 to 625 | 0.6 | 1.80 |
| 1-7/8 | 0.2 to 312 | 0.7 | 2.0 |

**Dynamic Skew:** Measured between adjacent tracks on the same head stack.

| Tape Speed (ips) | Skew[1] (microseconds) | Skew[2] (microseconds) |
|---|---|---|
| 60 | ±0.5 | ±3.0 |
| 30 | ±1.0 | ±5.0 |
| 15 | ±2.0 | ±8.0 |
| 7-1/2 | ±4.0 | ±20.0 |
| 3-3/4 | ±6.0 | ±35.0 |
| 1-7/8 | ±12.0 | ±70.0 |

NOTES:
1) Under Laboratory conditions.
2) Reproduced under Laboratory conditions after recording subject to vibration specified by MIL-STD-810B, Notice 1, Figure 514.1-2 Curve D.

**Servo:** Fast response servo operates from internal crystal reference. All tape speeds are under servo control at all times.

**Time Base Error:** Measured as the difference between crystal reference and capstan tachometer. (No sync off tape provisions are included in the machine.)

| Tape Speed (ips) | TBE (microseconds) |
|---|---|
| 60 | ±1.0 |
| 30 | ±2.0 |
| 15 | ±4.0 |
| 7-1/2 | ±6.0 |
| 3-3/4 | ±8.0 |
| 1-7/8 | ±10.0 |

When reproduced in tape servo mode on an FR-2000 TBE will be less than ±0.6 microseconds at 60 ips.

**Tape Speed Accuracy:** ±0.2% maximum error in tachometer mode measured per IRIG 106-71.

**Servo Control Track:** Built-in 100 kHz reference standard at 60 ips; proportionately lower at lower tape speeds.

**Fast Wind Time:** For 12½-inch reel with 7200 feet of tape, less than thirteen minutes.

**Start Time:** Time required from start command to meet flutter specifications is 5 seconds or less at 60 ips. Lower at lower speeds.

**Stop Time:** Maximum of 2.5 seconds from 60 ips. Lower at lower speeds.

**Controls:** Momentary pushbutton to ground for Power ON/OFF, Stop, Drive, Fast Forward, Fast Reverse, Record, Airborne Record, Forward/Reverse Drive determined by toggle switch. Speed Selection by a seven position rotary switch. Indicator Lights are provided for Ready, Bias, and Sync.

**Tape Specifications:** Either ½ or 1 inch tape of 1 mil or 1½ mil polyester base. Ampex tape type 772 on precision reels is recommended.

**Heads:** Head geometry per IRIG 106-71.

## DIRECT SIGNAL ELECTRONICS

### INTERMEDIATE BAND, DIRECT

**Frequency Response and Signal-to-Noise:**

| Tape Speed (ips) | Bandwidth (±3 dB)** | SNR*[1] Monitor (dB) | SNR*[1] Ground Reproduce** (dB) |
|---|---|---|---|
| 60 | 300 Hz to 300 kHz | 33 | 36 |
| 30 | 150 Hz to 150 kHz | 33 | 36 |
| 15 | 100 Hz to 75 kHz | 33 | 36 |
| 7-1/2 | 100 Hz to 38 kHz | 32 | 36 |
| 3-3/4 | 100 Hz to 19 kHz | 31 | 36 |
| 1-7/8 | 100 Hz to 10 kHz | 30 | 34 |

**Input Level:** 0.25 to 4.0 volts rms.

**Input Impedance:** 10K ohms ±10% in parallel with no more than 100 pf to ground.

**Output:** When used with reproduce leads and preamps: 30 dB of gain available. Output is unequalized.

### WIDEBAND, DIRECT

**Frequency Response and Signal-to-Noise:**

| Tape Speed (ips) | Bandwidth (±3 dB)** | SNR*[2] Monitor (dB) | SNR*[2] Ground Reproduce** (dB) |
|---|---|---|---|
| 60 | 400 Hz to 1 MHz | 20 | 20 |
| 30 | 400 Hz to 500 kHz | 18 | 20 |
| 15 | 400 Hz to 250 kHz | 18 | 20 |
| 7-1/2 | 400 Hz to 125 kHz | 18 | 20 |
| 3-3/4 | 400 Hz to 63 kHz | 16 | 18 |
| 1-7/8 | 400 Hz to 31 kHz | 15 | 17 |

**Input Level:** 0.25 to 4.0 volts.

**Input Impedance:** Selectable 1K ohm ±10% or 75 ohms ±10%.

**Output:** When used with reproduce leads and preamps: 40 dB of gain available. Output is unequalized.

*[1] Measured at the output of an 18 dB per octave filter using a 1 kHz signal at 60 ips, normal record level and 1% third harmonic distortion.

*[2] Measured at the output of an 18 dB per octave filter using 100 kHz signal at 60 ips to set normal record level for 1% third harmonic distortion.

**Reproduced on an Ampex FR-2000 or equivalent. Monitor output response is ±4 dB.

## FM SIGNAL ELECTRONICS

### WIDEBAND GROUP II

| Tape Speed (ips) | Center Carrier Freq (kHz) | Bandwidth* | Signal-to-Noise** Monitor (dB) | Signal-to-Noise** Ground Reproduce (dB) |
|---|---|---|---|---|
| 60 | 450 | DC to 250 kHz | 29 | 32 |
| 30 | 225 | DC to 125 kHz | 28 | 31 |
| 15 | 112.5 | DC to 62.5 kHz | 27 | 30 |
| 7-1/2 | 56.25 | DC to 31.25 kHz | 26 | 29 |
| 3-3/4 | 28.125 | DC to 15.6 kHz | 23 | 26 |
| 1-7/8 | 14.06 | DC to 7.8 kHz | 22 | 25 |

**Input Level:** ±0.5 to ±5.0 volts for full deviation.

**Input Impedance:** 75 ohms ±5% shunted by 100 pf unbalanced to ground.

**D.C. Drift:** Less than ±0.5% of full deviation over any 10°C temperature change from −29°C to +55°C after 16 minute warmup. Less than 1.5% of full deviation over full temperature range.

**D.C. Linearity:** ±0.5% of total deviation measured per IRIG 106-71 at any temperature from −29°C to +55°C.

**Harmonic Distortion:** Less than 3% total for all frequencies up to 0.8 $F_{co}$.

*Frequency Response down no more than −1 dB at 0.32 $F_{co}$ −4 dB at 0.8 $F_{co}$ and −6 dB at $F_{co}$.

**Rms signal to rms noise ratio.

### WIDEBAND GROUP I

| Tape Speed (ips) | Center Carrier Freq (kHz) | Bandwidth (±1/2 dB) | Signal-to-Noise** Monitor (dB) | Signal-to-Noise** Ground Reproduce*** (dB) |
|---|---|---|---|---|
| 60 | 216 | DC to 40 kHz | 46 | 48 |
| 30 | 108 | DC to 20 kHz | 45 | 48 |
| 15 | 54 | DC to 10 kHz | 43 | 46 |
| 7-1/2 | 27 | DC to 5 kHz | 43 | 44 |
| 3-3/4 | 13.5 | DC to 2.5 kHz | 40 | 43 |
| 1-7/8 | 6.75 | DC to 1.25 kHz | 38 | 41 |

### INTERMEDIATE BAND

| Tape Speed (ips) | Center Carrier Freq (kHz) | Bandwidth (±1/2 dB) | Signal-to-Noise** Monitor (dB) | Signal-to-Noise** Ground Reproduce*** (dB) |
|---|---|---|---|---|
| 60 | 108 | DC to 20 kHz | 46 | 49 |
| 30 | 54 | DC to 10 kHz | 45 | 48 |
| 15 | 27 | DC to 5 kHz | 43 | 46 |
| 7-1/2 | 13.5 | DC to 2.5 kHz | 43 | 46 |
| 3-3/4 | 6.75 | DC to 1.25 kHz | 41 | 44 |
| 1-7/8 | 3.375 | DC to 625 Hz | 40 | 43 |

### LOW BAND

| Tape Speed (ips) | Center Carrier Freq (kHz) | Bandwidth (±1/2 dB) | Signal-to-Noise** Monitor (dB) | Signal-to-Noise** Ground Reproduce*** (dB) |
|---|---|---|---|---|
| 60 | 54 | DC to 10 kHz | 46 | 49 |
| 30 | 27 | DC to 5 kHz | 45 | 48 |
| 15 | 13.5 | DC to 2.5 kHz | 43 | 46 |
| 7-1/2 | 6.75 | DC to 1.25 kHz | 43 | 46 |
| 3-3/4 | 3.375 | DC to 625 Hz | 41 | 44 |
| 1-7/8 | 1.6875 | DC to 312 Hz | 40 | 43 |

### W1, I AND L BANDS

**Input Level:** ±0.5 to ±5.0 volts for full deviation.

**Input Impedance:** 100K ohms ±5% selectable with jumper resistor in parallel with no more than 100 pf unbalanced to ground.

**D.C. Drift:** Less than ±0.5% of full deviation over any 10°C temperature change from −29°C to +55°C after 15 minute warmup. Less than ±1.5% total drift over full temperature range.

**D.C. Linearity:** ±0.5% of total deviation measured per IRIG 106-71 at any temperature from −29°C to +55°C.

**Harmonic Distortion:** Less than 2% total for any frequency up to 0.8 $F_{co}$.

**Rms Signal to Rms Noise Ratio.

***Reproduced on an Ampex FR-2000 or equivalent

## POWER REQUIREMENTS (AIRBORNE)

**Voltage:** 24 to 28.v v dc per MIL-STD-704A, Category B.

**Power Consumption:** 175 watts steady state maximum at 60 ips in the record mode with 14 tracks of direct record electronics. Less than 140 watts at 1-7/8 ips under the same conditions. Starting surges may be as high as 15 amps depending on configuration, input voltage, and tape pack radius. Below 10°C heaters consume an additional 250 watts.

## ENVIRONMENT

**Temperature:** Operating per MIL-E-5400L Class 1, except the lower temperature limit of the transport with tape shall be −29°C. Heater power must be applied one hour before operation below 4°C. Temperature shall be altitude derated per MIL-E-5400L, Figure 3, Sheet 1, Curve A.

**Storage:** −54°C to +71°C without tape.

No degradation in system performance will be experienced due to temperature extremes.

**Altitude:** Operating to 50,000 feet. Non-Operating to 70,000 feet. Temperature derating as above.

**Humidity:** 30% to 95% non condensing.

**Vibration:** Tested to levels specified in MIL-STD-810B Notice 1, Figure 514.1-2 curve D. Degradation in performance as noted. Specifications are for vibration in any axis.

**Shock:** Recorder will meet full performance specifications after application of shock per MIL-STD-810B Figure 516.1-2 procedure I (15g half-sine−11 milliseconds) while operating. Recorder will meet crash safety requirements of procedure III of the above specification.

**Electromagnetic Interference:** Tested to levels specified in MIL-STD-461. Levels may be exceeded at discrete frequencies depending on specific system configuration.

## PHYSICAL CHARACTERISTICS

**Size:** 18.7 x 17.5 x 7.0", including shock mounts and mating cable connectors.

**Weight:** 48 pounds without tape for a 14 channel Direct System. 61 pounds without tape for a 14 channel FM System.

### METRIC CONVERSION TABLES

Applicable to all Ampex recorders–specific items may not apply to the unit described in this sheet.

**TAPE SPEEDS**

| | | | | | | |
|---|---|---|---|---|---|---|
| ips | 1-7/8 | 3-3/4 | 7-1/2 | 15 | 30 | 60 |
| cm/sec | 4.76 | 9.52 | 19.05 | 38.1 | 76.2 | 152.4 |

**TAPE DIMENSIONS**

| | | | | |
|---|---|---|---|---|
| Reels: inches | 12½ | 10½ | 8 | |
| cm | 31.75 | 26.67 | 20.48 | |

| | | | | | | | |
|---|---|---|---|---|---|---|---|
| Widths: inches | ¼ | ½ | 1 | 2 | | | |
| cm | 0.635 | 1.27 | 2.54 | 5.08 | | | |
| Base Thicknesses: inches | 1 mil | 1.5 mil | | | | | |
| mm | 0.0254 | 0.0381 | | | | | |
| Length: feet | 600 | 1200 | 1800 | 2500 | 3600 | 5000 | 7000 |
| meters | 185 | 366 | 549 | 762 | 1097 | 1524 | 2134 |

**HEAD DIMENSIONS**

| | | | | | | | |
|---|---|---|---|---|---|---|---|
| Gap Scatter | | Interstack Spacing* | | | Track Width & Spacing* | | |
| microinches | 100 | inches | 1.5 ±0.001 | | inches | 0.050 | 0.070 |
| mm | 0.00254 | cm | 3.81 ±0.00127 | | mm | 1.27 | 1.778 |
| | | | | | | | *(IRIG) |

AMPEX

# specifications

# AR-1700
# instrumentation recorder

Effective December 1, 1971

## GENERAL DESCRIPTION

The AR-1700 is a compact intermediate or wideband multichannel recorder designed for airborne and other stringent environments. It is ruggedly constructed, uses servo-controlled time base correction and may be electrically switched over a range of six speeds. Up to seven channels of record electronics are provided on machines using ½" tape on 10½", 12½" or 14" precision reels, or up to 14 channels on machines equipped for 1" tape.

The system design emphasizes small size, ease of operation and serviceability. Closed loop capstan design, concentric reels and a fast response capstan servo are featured. The AR-1700 is designed for remote sequential operation for those needing uninterrupted recording. Additional optional features and custom modifications are available to satisfy every need.

## TAPE TRANSPORT

**Tape Speeds:** Six speeds—120, 60, 30, 15, 7-1/2, and 3-3/4 ips. Electrically selected with rotary switch.

**Reels:** 14 inch, 12½ inch or 10½ inch, precision reels.

**Flutter:** Percent measured per IRIG 106-71 (2 sigma).

| Tape Speed (ips) | Bandpass (Hz) | % Flutter[1] | % Flutter[2] |
|---|---|---|---|
| 120 | 0.2 to 10,000 | 0.24 | 0.24 |
| 60 | 0.2 to 10,000 | 0.28 | 0.30 |
| 30 | 0.2 to 5,000 | 0.30 | 0.55 |
| 15 | 0.2 to 2,500 | 0.33 | 1.0 |
| 7-1/2 | 0.2 to 1,250 | 0.41 | 2.2 |
| 3-3/4 | 0.2 to 625 | 0.45 | 2.6 |

**Dynamic Skew:** Measured between adjacent tracks on the same lead stack.

| Tape Speed (ips) | Skew[1] (microseconds) | Skew[2] (microseconds) |
|---|---|---|
| 120 | 0.3 | 0.5 |
| 60 | 1.0 | 1.5 |
| 30 | 4.0 | 3.0 |
| 15 | 8.0 | 10 |
| 7-1/2 | 8.0 | 40 |
| 3-3/4 | 15.0 | 90 |

NOTES:
1) Under Laboratory Conditions.
2) Reproduced under Laboratory conditions after recording subject to vibration specified by MIL-STD-810B, Notice 1, Figure 514.1-2 Curve D.

**Servo:** Fast response servo operates either from internal crystal reference or external reference during record/reproduce modes. All tape speeds are under servo control at all times.

**Time Base Error:** Measured as the difference between crystal reference and capstan tachometer.

| Tape Speed (ips) | TBE (microseconds) |
|---|---|
| 120 | ±1 |
| 60 | ±1 |
| 30 | ±2 |
| 15 | ±4 |
| 7-1/2 | ±6 |
| 3-3/4 | ±8 |

When reproduced in tape mode on an FR-2000 TBE will be no more than ±0.4 microseconds at 120 ips.

**Tape Speed Accuracy:** ±0.2% maximum error in tachometer mode measured per IRIG 106-71.

**Servo Control Track:** Built-in 200 kHz reference standard at 120 ips; proportionately lower at lower tape speeds. May be jumpered to any record amplifier.

**Fast Wind Time:** For 14-inch reel with 7200 feet of tape, less than ten minutes.

**Start Time:** Time required from start command to meet flutter specifications is 9 seconds or less at 120 ips. Lower at lower speeds.

**Stop Time:** Maximum of 5 seconds from 120 ips. Lower at lower speeds.

**Controls:** Pushbuttons for: Power, Stop, Record, Reproduce, (Drive), Fast Forward or Reverse and Pilot Run. Forward/Reverse drive selected by toggle switch. Speed selection by rotary switch. Indicator lights for Ready, Bias and Sync.

**Tape Specifications:** Either ½ or 1 inch tape of 1 mil or 1½ mil polyester base. Ampex tape type 772 on precision reels is recommended.

**Heads:** Head geometry per IRIG 106-71.

## DIRECT SIGNAL ELECTRONICS

### INTERMEDIATE BAND, DIRECT

**Frequency Response and Signal-to-Noise:**

| Tape Speed (ips) | Bandwidth (±3 dB)** | Signal-to-Noise* Monitor (dB) | Signal-to-Noise* Ground Reproduce** (dB) |
|---|---|---|---|
| 120 | 300 Hz to 600 kHz | 33 | 36 |
| 60 | 300 Hz to 300 kHz | 33 | 36 |
| 30 | 150 Hz to 150 kHz | 33 | 36 |
| 15 | 100 Hz to 75 kHz | 33 | 36 |
| 7-1/2 | 100 Hz to 38 kHz | 32 | 36 |
| 3-3/4 | 100 Hz to 19 kHz | 31 | 36 |

*Measured at the output of an 18 dB per octave filter using a 1 kHz signal at 60 ips. Normal record level and 1% third harmonic distortion.
**Reproduced on an Ampex FR-2000 or equivalent. Monitor output response is ±4 dB.

**Input Level:** 0.25 to 4.0 volts rms.

**Input Impedance:** 10K ohms ±10% in parallel with no more than 100 pf unbalanced to ground.

**Output:** (When used with reproduce heads and preamps): 30 dB of gain is available. Output is unequalized.

### WIDEBAND, DIRECT

**Frequency Response and Signal-to-Noise:**

| Tape Speed (ips) | Bandwidth (±3 dB)** | Signal-to-Noise* Monitor (dB) | Signal-to-Noise* Ground Reproduce** (dB) |
|---|---|---|---|
| 120 | 400 Hz to 2 MHz | 20 | 20 |
| 60 | 400 Hz to 1 MHz | 20 | 20 |
| 30 | 400 Hz to 500 kHz | 18 | 20 |
| 15 | 400 Hz to 250 kHz | 18 | 20 |
| 7-1/2 | 400 Hz to 125 kHz | 18 | 20 |
| 3-3/4 | 400 Hz to 62.5 kHz | 16 | 18 |

*Measured at the output of an 18 dB per octave filter using a 200 kHz reference signal at 120 ips, set for 1% third harmonic distortion.
**Reproduced on an Ampex FR-2000 or equivalent.

**Input Level:** 0.25 to 4.0 volts rms.

**Input Impedance:** Selectable 75 ohms ±10% or 1K ohms ±10% in parallel with no more than 100 pf unbalanced to ground.

**Output:** (When used with reproduce heads and preamps): 40 dB of gain is available. Output is unequalized.

## FM SIGNAL ELECTRONICS

| Tape Speed (ips) | Center Carrier Freq (kHz) | Bandwidth* | Signal-to-Noise** Monitor (dB) | Signal-to-Noise** Ground Reproduce*** (dB) |
|---|---|---|---|---|
| 120 | 900 | DC to 500 kHz | 30 | 33 |
| 60 | 450 | DC to 250 kHz | 29 | 32 |
| 30 | 225 | DC to 125 kHz | 28 | 31 |
| 15 | 112.5 | DC to 62.5 kHz | 27 | 30 |
| 7-1/2 | 56.25 | DC to 31.25 kHz | 26 | 29 |
| 3-3/4 | 28.125 | DC to 15.6 kHz | 23 | 26 |

*Frequency response tolerance down no more than −1 dB at 0.32 $F_{co}$; down no more than −4 dB at 0.8 $F_{co}$; down no more than −6 dB at $F_{co}$.

**Rms Signal to Rms Noise Ratio.

**Input Level:** ±0.5 to ±5.0 volts for full deviation.

**Input Impedance:** 75 ohms ±5% shunted by 100 pf unbalanced to ground.

**D.C. Drift:** Less than ±0.5% of full deviation over any 10°C temperature change from −29°C to +55°C after 16 minute warmup. Less than 1.5% of full deviation over full temperature range.

**D.C. Linearity:** ±0.5% of total deviation measured per IRIG 106-71 at any temperature from −29°C to +55°C.

**Harmonic Distortion:** Less than 3% of total for all frequencies up to 0.8 $F_{co}$.

### WIDEBAND GROUP I

| Tape Speed (ips) | Center Carrier Freq (kHz) | Bandwidth (±1/2 dB) | Signal-to-Noise** Monitor (dB) | Signal-to-Noise** Ground Reproduce*** (dB) |
|---|---|---|---|---|
| 120 | 432 | DC to 80 kHz | 46 | 48 |
| 60 | 216 | DC to 40 kHz | 46 | 48 |
| 30 | 108 | DC to 20 kHz | 45 | 48 |
| 15 | 54 | DC to 10 kHz | 43 | 46 |
| 7-1/2 | 27 | DC to 5 kHz | 43 | 44 |
| 3-3/4 | 13.5 | DC to 2.5 kHz | 40 | 43 |

### INTERMEDIATE BAND

| Tape Speed (ips) | Center Carrier Freq (kHz) | Bandwidth (±1/2 dB) | Signal-to-Noise** Monitor (dB) | Signal-to-Noise** Ground Reproduce*** (dB) |
|---|---|---|---|---|
| 120 | 216 | DC to 40 kHz | 46 | 49 |
| 60 | 108 | DC to 20 kHz | 46 | 49 |
| 30 | 54 | DC to 10 kHz | 45 | 48 |
| 15 | 27 | DC to 5 kHz | 43 | 46 |
| 7-1/2 | 13.5 | DC to 2.5 kHz | 43 | 46 |
| 3-3/4 | 6.75 | DC to 1.25 kHz | 41 | 44 |

### LOW BAND

| Tape Speed (ips) | Center Carrier Freq (kHz) | Bandwidth (±1/2 dB) | Signal-to-Noise** Monitor (dB) | Signal-to-Noise** Ground Reproduce*** (dB) |
|---|---|---|---|---|
| 120 | 108 | DC to 20 kHz | 46 | 49 |
| 60 | 54 | DC to 10 kHz | 46 | 49 |
| 30 | 27 | DC to 5 kHz | 45 | 48 |
| 15 | 13.5 | DC to 2.5 kHz | 43 | 46 |
| 7-1/2 | 6.75 | DC to 1.25 kHz | 43 | 46 |
| 3-3/4 | 3.375 | DC to 625 Hz | 41 | 44 |

### W1, I AND L BANDS

**Input Level:** ±0.5 to ±5.0 volts for full deviation.

**Input Impedance:** 100K ohms ±5% selectable with jumper resistor in parallel with no more than 100 pf unbalanced to ground.

**D.C. Drift:** Less than 0.5% of full deviation over any 10°C temperature change from −29°C to +55°C after 15 minute warmup. Less than 1.5% total drift over full temperature range.

**D.C. Linearity:** ±0.5% of total deviation measured per IRIG 106-71 at any temperature from −29°C to +55°C

**Harmonic Distortion:** Less than 2% total for any frequency up to 0.8 $F_{co}$.

**Rms signal to rms noise.
***Reproduced on an Ampex FR-2000 or equivalent.

## POWER REQUIREMENTS (AIRBORNE)

**Voltage:** 24 to 28.5 v dc per MIL-STD-704A, Category B.

**Power Consumption:** 300 watts steady state maximum at 120 ips in the record mode with 14 tracks of direct record electronics. Maximum surge will not exceed 420 watts. Below 10% C heaters consume an additional 250 watts.

## ENVIRONMENT

**Temperature:** Operating per MIL-E-5400L, Class 1, except the lower temperature limit of the transport with tape shall be −29°C. Heater power must be applied one hour before operation below 4°C. Temperature shall be altitude derated per MIL-E-5400L, Figure 3, Sheet 1, Curve A.

**Storage:** −54°C to +71°C without tape.

No degradation in system performance will be experienced due to temperature extremes.

**Altitude:** Operating to 50,000 feet. Non-operating to 70,000 feet. Temperature derating as above.

**Humidity:** 30% to 95% non condensing.

**Vibration:** Tested to levels specified in MIL-STD-810B dated June 15, 1967 Figure 514-1 Curve A. Degradation in specifications as noted. Specifications are for vibration in any axis.

**Shock:** Recorder will meet full performance specifications after application of shock per MIL-STD-810B Figure 516.1-2 procedure I (15g half-sine – 11 milliseconds) while operating. Recorder will meet crash safety requirements of procedure III of the above specification.

**Electromagnetic Interference:** Tested to levels specified in MIL-STD-461. Levels may be exceeded at discrete frequencies depending on specific system configuration.

## PHYSICAL CHARACTERISTICS

**Size:** 20" x 16¾" x 10", excluding shockmounts but including mating cable connectors.

**Weight:** 72 pounds, excluding tape, for a complete 14 track Direct Record system. 92 pounds excluding tape for a complete 14 track FM Record system.

## METRIC CONVERSION TABLES

Applicable to all Ampex recorders—specific items may not apply to the unit described in this sheet.

**TAPE SPEEDS**

| | | | | | | |
|---|---|---|---|---|---|---|
| ips | 3¾ | 7½ | 15 | 30 | 60 | 120 |
| cm/sec | 9.52 | 19.05 | 38.1 | 76.2 | 152.4 | 304.8 |

**TAPE DIMENSIONS**

| | | | | | |
|---|---|---|---|---|---|
| Reels: inches | 14 | 12½ | 10½ | 8 | |
| cm | 35.56 | 31.75 | 26.67 | 20.48 | |

| | | | | | | | | | |
|---|---|---|---|---|---|---|---|---|---|
| Widths: inches | ½ | 1 | | | | | | | |
| cm | 1.27 | 2.54 | | | | | | | |
| Base Thicknesses: inches | 1 mil | 1.5 mil | | | | | | | |
| mm | 0.0254 | 0.0381 | | | | | | | |
| Length: feet | 600 | 1200 | 1800 | 2500 | 3600 | 5000 | 7000 | 7200 | 9200 |
| meters | 185 | 366 | 549 | 762 | 1097 | 1524 | 2134 | 2195 | 2804 |

**HEAD DIMENSIONS**

| | | | | | | |
|---|---|---|---|---|---|---|
| Gap Scatter | | Interstack Spacing* | | Track Width & Spacing* | | |
| microinches | 100 | inches | 1.5 ±0.001 | inches | 0.050 | 0.070 |
| mm | 0.00254 | cm | 3.81 ±0.00127 | cm | 1.27 | 1.778 |

*(IRIG)

AMPEX

# specifications

# FR-1900 multiband instrumentation recorder

Effective July 15, 1969

## GENERAL

The FR-1900 system consists of the following outstanding features:

- Proven High Performance Transport
- Low Non-Orthogonal Timing Errors
- 7-Speed Electrically Switchable Transport and Electronics
- Multiband Electronics
- FM Intra-Cal
- FM Recirculating Charge Dispenser
- Zero Loop Drive
- Variable Speed Operation
- Bi-directional Operation

## TAPE TRANSPORT

**Tape Speeds:**

Discrete by switch selection for continuously variable with variable oscillator in tach mode). Discrete Speed Selection with seven speeds: 120, 60, 30, 15, 7-1/2, 3-3/4 and 1-7/8 inches per second. Tape speeds and forward and reverse drive directions are electrically selectable.

**Tape Speed Accuracy:**

±0.2% maximum, long term, with input power variations from 105–125 volts AC, 47–63 Hz.

**Fast Wind Time:**

Fast forward and reverse for 14-inch reel with 7200 feet of tape is less than five minutes. Tape is continuously under capstan control. Tape speed never exceeds 360 inches per second.

**Time Base Error:**

| Tape Speed (ips) | Error in Microseconds |
|---|---|
| 120 | ±1.5 |
| 60 | ±3.0 |
| 30 | ±5.0 |
| 15 | ±10.0 |
| 7-1/2 | ±15.0 |
| 3-3/4 | ±25.0 |
| 1-7/8 | ±30.0 |

**Dynamic Skew:**

The relative time displacement of an event recorded simultaneously on any two adjacent tracks within the same head stack as observed on playback is less than:

| Tape Speed (ips) | ΔT Microseconds (Zero-to-Peak) |
|---|---|
| 120 | 0.15 |
| 60 | 0.30 |
| 30 | 0.60 |
| 15 | 1.20 |
| 7-1/2 | 2.40 |
| 3-3/4 | 4.80 |
| 1-7/8 | 9.60 |

**Non-Orthogonal Timing Error (NTE):**

Between outside tracks in same head stack (1 to 13 for one inch tape:

| Tape Speed (ips) | NTE (μsecs) Zero-to-Peak |
|---|---|
| 120 | 2.4 |
| 60 | 4.8 |
| 30 | 8.6 |
| 15 | 17.2 |
| 7-1/2 | 29.4 |
| 3-3/4 | 53.8 |
| 1-7/8 | 87.6 |

**Flutter:** Percent measured per IRIG 106-66 (2-Sigma)

| Tape Speed (ips) | Flutter Bandwidth | % Flutter |
|---|---|---|
| 120 | 0.2 Hz to 10 kHz | 0.15 |
| 60 | 0.2 Hz to 10 kHz | 0.15 |
| 30 | 0.2 Hz to 5 kHz | 0.15 |
| 15 | 0.2 Hz to 2.5 kHz | 0.25 |
| 7-1/2 | 0.2 Hz to 1.25 kHz | 0.30 |
| 3-3/4 | 0.2 Hz to 625 Hz | 0.45 |
| 1-7/8 | 0.2 Hz to 312 Hz | 0.60 |

**Start Time:**

The start time required to meet flutter specifications is eight seconds or less at 120 ips.

**Stop Time:**

Four seconds maximum at 120 ips.

**Servo Reference Frequency:**

The servo reference frequency recorded shall be 200 kHz ±0.01% at 120 ips and proportionately lower at the lower tape speeds (per IRIG 106-66).

**Heads:**

Comply with IRIG 106-66 for 7 tracks with 1/2 inch tape or 14 tracks with one-inch tape.

**Tape:**

All specifications and head life are based upon the use of Ampex recommended tape.

## SIGNAL ELECTRONICS

**DIRECT SYSTEM:**

All measurements per IRIG 106-66, reference paragraph 5.6.3.3.

**Input Level:**

0.25 to 10 volts RMS adjustable.

**Input Impedance-Selectable:**

75, 1000 or 20,000 ohms in parallel with 100 picofarads unbalanced to ground.

**Output Impedance:**

75 ohms ±10% for all frequencies.

**Output Level:**

1.0 volts RMS nominal across 75 ohms.

**Intermediate Band:**

| Tape Speed (ips) | Bandwidth (±3 dB) | S/N (RMS Signal to RMS Noise) (dB) |
|---|---|---|
| 120 | 300 Hz to 600 kHz | 36 |
| 60 | 300 Hz to 300 kHz | 36 |
| 30 | 150 Hz to 150 kHz | 36 |
| 15 | 100 Hz to 75 kHz | 36 |
| 7-1/2 | 100 Hz to 38 kHz | 36 |
| 3-3/4 | 100 Hz to 19 kHz | 36 |
| 1-7/8 | 100 Hz to 10 kHz | 34 |

**Wideband I**

| Tape Speed (ips) | Bandwidth (±3 dB) | S/N (RMS Signal to RMS Noise) (dB) |
|---|---|---|
| 120 | 400 Hz to 1.5 MHz | 30 |
| 60 | 400 Hz to 750 kHz | 29 |
| 30 | 400 Hz to 375 kHz | 29 |
| 15 | 400 Hz to 187 kHz | 28 |
| 7-1/2 | 400 Hz to 93 kHz | 27 |
| 3-3/4 | 400 Hz to 46 kHz | 26 |
| 1-7/8 | 400 Hz to 23 kHz | 24 |

**Wideband II**

| Tape Speed (ips) | Bandwidth (±3 dB)[1] | S/N (RMS Signal to RMS Noise)[2] (dB) |
|---|---|---|
| 120 | 400 Hz to 2 MHz | 20 |
| 60 | 400 Hz to 1 MHz | 20 |
| 30 | 400 Hz to 500 kHz | 20 |
| 15 | 400 Hz to 250 kHz | 20 |
| 7-1/2 | 400 Hz to 125 kHz | 20 |
| 3-3/4 | 400 Hz to 62 kHz | 18 |
| 1-7/8 | 400 Hz to 31 kHz | 17 |

1 Zero dB reference level, half way between the total excursions over the bandwidth.

2 Normal record level set-up 1% 3rd harmonic distortion of 150 kHz sinusoidal signal at 120 ips.

**Envelope Delay:**

The envelope delay at 120 ips shall be less than 500 nanoseconds peak-to-peak for a bandwidth of 100 kHz to 1.2 MHz.

**FM SYSTEM:**

All measurements per IRIG 106-66

**Input Impedance:**

Selectable 75, 1000 or 20,000 ohms in parallel with 100 picofarads unbalanced to ground.

**Input Sensitivity:**

0.5 volts peak to 25 volts peak adjustable.

**Output Impedance:**

75 ohms nominal.

# specifications
# FR-1900 multiband instrumentation recorder

## SIGNAL ELECTRONICS (continued)

**DC Drift:**

Less than ±0.5% of full deviation over a 20°F temperature change in eight hours, after 15 minute warm-up.

**DC Linearity:**

+0.5% of total deviation. Measured per IRIG 106-66.

**Low Band:**

| Tape Speed (ips) | Center Carrier Freq (kHz) | Bandwidth (±1/2 dB) | S/N (RMS Signal to RMS Noise) (dB) |
|---|---|---|---|
| 120 | 108 | DC to 20 kHz | 55 |
| 60 | 54 | DC to 10 kHz | 55 |
| 30 | 27 | DC to 5 kHz | 54 |
| 15 | 13.5 | DC to 2.5 kHz | 53 |
| 7-1/2 | 6.75 | DC to 1.25 kHz | 50 |
| 3-3/4 | 3.375 | DC to 625 Hz | 48 |
| 1-7/8 | 1.6875 | DC to 312 Hz | 47 |

Total Harmonic Distortion for 120 and 60 ips 1.5%

**Intermediate Band**

| Tape Speed (ips) | Center Carrier Freq (kHz) | Bandwidth (±1/2 dB) | Total Harmonic Distortion | S/N (RMS Signal to RMS Noise) (dB) |
|---|---|---|---|---|
| 120 | 216 | DC to 40 kHz | 1.2% | 51 |
| 60 | 108 | DC to 20 kHz | 1.2% | 51 |
| 30 | 54 | DC to 10 kHz | 1.2% | 50 |
| 15 | 27 | DC to 5 kHz | 1.2% | 48 |
| 7-1/2 | 13.5 | DC to 2.5 kHz | 1.2% | 48 |
| 3-3/4 | 6.75 | DC to 1.25 kHz | 1.5% | 46 |
| 1-7/8 | 3.375 | DC to 625 Hz | 1.5% | 45 |

**Wideband Group I**

| Tape Speed (ips) | Center Carrier Freq (kHz) | Bandwidth (±1/2 dB) | Total Harmonic Distortion | S/N (RMS Signal to RMS Noise) (dB) |
|---|---|---|---|---|
| 120 | 432 | DC to 80 kHz | 1.2% | 50 |
| 60 | 216 | DC to 40 kHz | 1.2% | 50 |
| 30 | 108 | DC to 20 kHz | 1.2% | 50 |
| 15 | 54 | DC to 10 kHz | 1.2% | 48 |
| 7-1/2 | 27 | DC to 5 kHz | 1.2% | 46 |
| 3-3/4 | 13.5 | DC to 2.5 kHz | 1.5% | 45 |
| 1-7/8 | 6.75 | DC to 1.25 kHz | 1.5% | 43 |

**Wideband Group II**

| Tape Speed (ips) | Center Carrier Freq (kHz) | Bandwidth* | S/N (RMS Signal to RMS Noise) (dB) |
|---|---|---|---|
| 120 | 900 | DC to 500 kHz | 33 |
| 60 | 450 | DC to 250 kHz | 32 |
| 30 | 225 | DC to 125 kHz | 31 |
| 15 | 112.5 | DC to 62.5 kHz | 30 |
| 7-1/2 | 56.25 | DC to 31.25 kHz | 29 |
| 3-3/4 | 28.125 | DC to 15.6 kHz | 26 |
| 1-7/8 | 14.06 | DC to 7.8 kHz | 25 |

*Frequency response tolerance down no more than -1 dB at 0.32 $F_{co}$; down no more than -4 dB at 0.8 $F_{co}$; down no more than -6 dB at $F_{co}$.

**Output Level:**

Adjustable up to 4 volts peak-to-peak into a 75 ohm load (±40% deviation). Adjustable up to 3 volts peak-to-peak into a 75 ohm load (±30% deviation).

**Harmonic Distortion:**

Less than 2% total harmonic distortion for modulation indices greater than 3; less than 3% for modulation indices less than 3. For all harmonic frequencies up to 0.8 $F_{co}$.

## POWER REQUIREMENTS

**Voltage:**

105 to 125 volts standard (210 to 250 volts also available).

**Frequency:**

47 to 63 Hz, single phase

**Power Consumption:**

Approximately 2000 watts for a 14-track system.

## ENVIRONMENT

**Temperature:**

Operating: 5°C to 43°C
Non-Operating: -20°C to 55°C

**Altitude:**

Operating: to 10,000 feet (3048 meters)
Non-Operating: to 50,000 feet (15,000 meters)

**Relative Humidity:**

25 to 90% without condensation (tape limited)

## PHYSICAL CHARACTERISTICS

**Size:**

Single Cabinet: 77-5/16 inches (196.4 cm) high by 23 inches (58.4 cm) wide by 24 inches (60.9 cm) deep.

**Weight:**

Approximately 800 pounds (363 kg) for a 14-track system in a single rack cabinet.

## METRIC CONVERSION TABLES

Applicable to all Ampex recorders—specific items may not apply to the unit described in this sheet.

**TAPE SPEEDS**

| ips | 1-7/8 | 3-3/4 | 7-1/2 | 15 | 30 | 60 | 120 |
|---|---|---|---|---|---|---|---|
| cm/sec | 4.76 | 9.52 | 19.05 | 38.1 | 76.2 | 152.4 | 304.8 |

**TAPE DIMENSIONS**

| Reels: inches | 14 | 10-1/2 | 7 | 5-3/4 | 5 |
|---|---|---|---|---|---|
| cm | 35.56 | 26.67 | 17.78 | 14.62 | 12.70 |

| Widths: inches | 1/4 | 1/2 | 3/4 | 1 | 2 |
|---|---|---|---|---|---|
| cm | 0.635 | 1.27 | 1.905 | 2.54 | 5.08 |

| Base Thicknesses: inches | 1 mil | 1.5 mil |
|---|---|---|
| mm | 0.0254 | 0.0381 |

| Length: feet | 600 | 1200 | 1800 | 2500 | 3600 | 5000 | 7200 | 9200 |
|---|---|---|---|---|---|---|---|---|
| meters | 185 | 366 | 549 | 762 | 1097 | 1524 | 2195 | 2800 |

**HEAD DIMENSIONS**

| Gap Scatter | | Interstack Spacing* | | Track Width & Spacing* | | |
|---|---|---|---|---|---|---|
| microinches | 100 | inches | 1.5 ±0.001 | inches | 0.050 | 0.070 |
| mm | 0.00254 | cm | 3.81 ±0.00127 | mm | 1.27 | 1.778 |
| | | | | | | *(IRIG) |

**STANDARD PANELS FOR 19-INCH (48.25 cm) RACK**

| in | 1-3/4 | 3-1/2 | 5-1/4 | 7 | 8-3/4 | 12-1/4 | 14 | 15-3/4 | 17-1/2 | 19-1/4 | 21 | 35 |
|---|---|---|---|---|---|---|---|---|---|---|---|---|
| cm | 4.45 | 8.89 | 13.34 | 17.78 | 22.23 | 31.12 | 35.56 | 40.01 | 44.45 | 48.9 | 53.34 | 88.9 |

AMPEX

# specifications

# FR-2000 multiband instrumentation recorder

Effective January 1, 1972

## GENERAL

*Outstanding features of the FR-2000 are:*

- *High performance transport with exceptionally low flutter, TBE and dynamic skew (NTE), due to Ampex's exclusive zero loop drive, vacuum chambers and an advanced design servo that provides 40,000 information samples per revolution.*
- *System is designed for maintainability with complete front accessibility as the criterion.*
- *Multiband ES-200 electronics . . . one set does the same job as three or more single purpose sets.*
- *Accommodates 16" reels for long playing time (33% more total playing time than 14" reels).*
- *Modular packaging allows easy integration into data handling system, simplifies maintenance.*
- *Control panel mounted in transport module to save front panel space; functional grouping of buttons simplifies operation.*
- *Power panel assembly in standard FR-2000 rack is integrated into the base of the rack assembly to save front panel space for other signal and monitoring equipment.*

## TAPE TRANSPORT

**Tape Speeds:** Discrete by switch selection (or variable within each speed range with external variable frequency oscillator in tach mode). Direct activation between any of seven discrete speeds. 120, 60, 30, 15, 7½, 3¾, and 1⅞ inches per second. Tape speeds and forward and reverse drive directions are electrically selectable.

**Tape Speed Accuracy:** ±0.15% maximum error, long term, with input power variations from 105–125 volts AC, 47–63 Hz.

**Fast Wind Time:** Fast forward and reverse for 14-inch reel with 7200 feet of tape is less than 4½ minutes. Tape is continuously under capstan control. Tape speed never exceeds 360 inches per second.

**Time Base Error:**

| Tape Speed (ips) | Error in Microseconds |
|---|---|
| 120 | ±0.30 |
| 60 | ±0.40 |
| 30 | ±0.50 |
| 15 | ±1.00 |
| 7½ | ±1.50 |
| 3¾ | ±3.00 |
| 1⅞ | ±6.00 |

**Dynamic Skew:**

The relative time displacement of an event recorded simultaneously on any two adjacent tracks within the same head stack as observed on playback is less than:

| Tape Speed (ips) | ΔT Microseconds (Zero-to-Peak) |
|---|---|
| 120 | 0.10 |
| 60 | 0.20 |
| 30 | 0.50 |
| 15 | 1.00 |
| 7½ | 2.00 |
| 3¾ | 4.00 |
| 1⅞ | 8.00 |

**Non-Orthogonal Timing Error (NTE):** Between outside tracks in same head stack 1 to 13 for one inch tape:

| Tape Speed (ips) | NTE (μsecs) Zero-to-Peak |
|---|---|
| 120 | 1.0 |
| 60 | 2.0 |
| 30 | 3.5 |
| 15 | 5 |
| 7½ | 8 |
| 3¾ | 15 |
| 1⅞ | 30 |

**Flutter:** Percent measured per IRIG 106-69 (2-Sigma)

| Tape Speed (ips) | Flutter Bandwidth | % Flutter |
|---|---|---|
| 120 | 0.2 Hz to 10 kHz | 0.13 |
| 60 | 0.2 Hz to 10 kHz | 0.15 |
| 30 | 0.2 Hz to 5 kHz | 0.15 |
| 15 | 0.2 Hz to 2.5 kHz | 0.18 |
| 7½ | 0.2 Hz to 1.25 kHz | 0.25 |
| 3¾ | 0.2 Hz to 625 Hz | 0.32 |
| 1⅞ | 0.2 Hz to 312 Hz | 0.38 |

**Start Time:** The start time required to meet flutter specifications at 120 ips with reels 14-inch diameter is five seconds or less (seven seconds is allowable for a 16-inch reel).

**Stop Time:** Four seconds maximum at 120 ips.

**Servo Reference Frequency:** The servo reference frequency recorded is 200 kHz ± 0.01% at 120 ips and proportionately lower at the lower tape speeds.

**Heads:** Comply with IRIG 106-69 for 7 tracks with ½ inch tape or 14 tracks with one-inch tape.

**Tape:** All specifications are based upon the use of Ampex recommended tape.

## SIGNAL ELECTRONICS

**DIRECT SYSTEM:**

All measurements per IRIG 106-69, reference paragraph 5.6.3.3.

**Input Level:** 0.25 to 10 volts RMS adjustable for 20 K ohm and 1 K ohm input impedances and 0.25 to 3.0 volts RMS for 75 ohm input impedance.

**Input Impedance-Selectable:** 75, 1,000 or 20,000 ohms in parallel with 100 picofarads unbalanced to ground.

**Output Impedance:** 75 ohms ±10% for all frequencies.

**Output Level:** 1.0 volt RMS nominal across 75 ohms.

**Intermediate Band:**

| Tape Speed (ips) | Bandwidth (±3 dB) | S/N (RMS Signal to RMS Noise) (dB) |
|---|---|---|
| 120 | 300 Hz to 600 kHz | 37 |
| 60 | 300 Hz to 300 kHz | 37 |
| 30 | 150 Hz to 150 kHz | 37 |
| 15 | 100 Hz to 75 kHz | 36 |
| 7½ | 100 Hz to 38 kHz | 36 |
| 3¾ | 100 Hz to 19 kHz | 36 |
| 1⅞ | 100 Hz to 10 kHz | 34 |

**Wideband I**

| Tape Speed (ips) | Bandwidth (±3 dB) | S/N (RMS Signal to RMS Noise) (dB) |
|---|---|---|
| 120 | 400 Hz to 1.5 MHz | 30 |
| 60 | 400 Hz to 750 kHz | 29 |
| 30 | 400 Hz to 375 kHz | 29 |
| 15 | 400 Hz to 187 kHz | 28 |
| 7½ | 400 Hz to 93 kHz | 27 |
| 3¾ | 400 Hz to 46 kHz | 26 |
| 1⅞ | 400 Hz to 23 kHz | 24 |

**Wideband II**

| Tape Speed (ips) | Bandwidth (±3 dB)[1] | S/N (RMS Signal to RMS Noise)[2] (dB) |
|---|---|---|
| 120 | 400 Hz to 2 MHz | 22 |
| 60 | 400 Hz to 1 MHz | 22 |
| 30 | 400 Hz to 500 kHz | 22 |
| 15 | 400 Hz to 250 kHz | 22 |
| 7½ | 400 Hz to 125 kHz | 21 |
| 3¾ | 400 Hz to 62 kHz | 20 |
| 1⅞ | 400 Hz to 31 kHz | 19 |

[1] Zero dB reference level, half way between the total excursions over the bandwidth.
[2] Normal record level set-up 1% 3rd harmonic distortion of 150 kHz sinusoidal signal at 120 ips.

**Envelope Delay:** The envelope delay at 120 ips shall be less than 500 nanoseconds peak-to-peak for a bandwidth of 100 kHz to 1.2 MHz.

# specifications
## FR-2000 multiband instrumentation recorder

**SIGNAL ELECTRONICS (continued)**

**FM SYSTEM:**

All measurements per IRIG 106-69.

**Input Impedance:** Selectable 75, 1,000 or 20,000 ohms in parallel with 100 picofarads unbalanced to ground.

**Input Sensitivity:** 0.5 volt peak to 25 volts peak adjustable for 20 K ohm and 1 K ohm input impedances and 0.5 to 10 volts peak for 75 ohm input impedance.

**Output Impedance:** 75 ohms nominal.

**DC Drift:** Less than ±0.5% of full deviation over a 20°F temperature change in eight hours, after 15 minute warm-up.

**DC Linearity:** ±0.5% of total deviation.

**Low Band:**

| Tape Speed (ips) | Center Carrier Freq (kHz) | Bandwidth (±½ dB) | S/N (RMS Signal to RMS Noise) (dB) |
|---|---|---|---|
| 120 | 108 | DC to 20 kHz | 55 |
| 60 | 54 | DC to 10 kHz | 55 |
| 30 | 27 | DC to 5 kHz | 54 |
| 15 | 13.5 | DC to 2.5 kHz | 53 |
| 7½ | 6.75 | DC to 1.25 kHz | 50 |
| 3¾ | 3.375 | DC to 625 Hz | 48 |
| 1⅞ | 1.6875 | DC to 312 Hz | 47 |

Total Harmonic Distortion for 120 and 60 ips 1.5%

**Intermediate Band**

| Tape Speed (ips) | Center Carrier Freq (kHz) | Bandwidth (±½ dB) | Total Harmonic Distortion | S/N (RMS Signal to RMS Noise) (dB) |
|---|---|---|---|---|
| 120 | 216 | DC to 40 kHz | 1.2% | 54 |
| 60 | 108 | DC to 20 kHz | 1.2% | 52 |
| 30 | 54 | DC to 10 kHz | 1.2% | 51 |
| 15 | 27 | DC to 5 kHz | 1.2% | 51 |
| 7½ | 13.5 | DC to 2.5 kHz | 1.2% | 50 |
| 3¾ | 6.75 | DC to 1.25 kHz | 1.5% | 47 |
| 1⅞ | 3.375 | DC to 625 Hz | 1.5% | 45 |

**Wideband Group I**

| Tape Speed (ips) | Center Carrier Freq (kHz) | Bandwidth (±½ dB) | Total Harmonic Distortion | S/N (RMS Signal to RMS Noise) (dB) |
|---|---|---|---|---|
| 120 | 432 | DC to 80 kHz | 1.2% | 52 |
| 60 | 216 | DC to 40 kHz | 1.2% | 51 |
| 30 | 108 | DC to 20 kHz | 1.2% | 50 |
| 15 | 54 | DC to 10 kHz | 1.2% | 50 |
| 7½ | 27 | DC to 5 kHz | 1.2% | 47 |
| 3¾ | 13.5 | DC to 2.5 kHz | 1.5% | 46 |
| 1⅞ | 6.75 | DC to 1.25 kHz | 1.5% | 43 |

**Wideband Group II**

| Tape Speed (ips) | Center Carrier Freq (kHz) | Bandiwdth* | S/N (RMS Signal to RMS Noise) (dB) |
|---|---|---|---|
| 120 | 900 | DC to 500 kHz | 35 |
| 60 | 450 | DC to 250 kHz | 35 |
| 30 | 225 | DC to 125 kHz | 34 |
| 15 | 112.5 | DC to 62.5 kHz | 33 |
| 7½ | 56.25 | DC to 31.25 kHz | 32 |
| 3¾ | 28.125 | DC to 15.6 kHz | 32 |
| 1⅞ | 14.06 | DC to 7.8 kHz | 29 |

* Frequency response tolerance down no more than −1 dB at 0.32 $F_{co}$; down no more than −4 dB at 0.8 $F_{co}$; down no more than −6 dB at $F_{co}$.

**Output Level:** Adjustable up to 4 volts peak-to-peak into a 75 ohm load (±40% deviation). Adjustable up to 3 volts peak-to-peak into a 75 ohm load (±30% deviation).

**Harmonic Distortion:** Less than 2% total harmonic distortion for modulation indices greater than 3; less than 3% for modulation indices less than 3. For all harmonic frequencies up to 0.8 $F_{co}$.

### POWER REQUIREMENTS

**Voltage:** 105 volts to 125 volts standard (210 to 250 volts also available).

**Frequency:** 47 to 63 Hz, single phase.

**Power Consumption:** A complete 14 track record/reproduce system, excluding monitor accessories and non-standard options will operate at a nominal 1,000 watts and consume less than 1,500 watts at initial turn-on.

### ENVIRONMENT

**Temperature:**
Operating: +5°C to +50°C
Non-Operating: −20°C to +60°C

**Altitude:**
Operating: to 12,000 feet
Non-Operating: to 40,000 feet

**Relative Humidity:** The system, excluding tape limitations, will operate from 5% to 90% without condensation. For tape limitations see appropriate tape manufacturer's specification limits.

### PHYSICAL CHARACTERISTICS

**Size:** Single Cabinet: 77¼ inches high by 23 inches wide by 25 inches deep. Including standard rack dolly: 79⅝ x 23 x 39¼.

**Weight:** Approximately 750 pounds for a 14-track system in a single rack cabinet including a rack dolly. Multitap International transformer increases the weight by 75 pounds.

### METRIC CONVERSION TABLES

Applicable to all Ampex recorders—specific items may not apply to the unit described in this sheet.

**TAPE SPEEDS**

| | | | | | | | |
|---|---|---|---|---|---|---|---|
| **Ips** | 1⅞ | 3¾ | 7½ | 15 | 30 | 60 | 120 |
| **cm/sec** | 4.76 | 9.52 | 19.05 | 38.1 | 76.2 | 152.4 | 304.8 |

**TAPE DIMENSIONS**

| | | | | | |
|---|---|---|---|---|---|
| **Reels: inches** | 16 | 14 | 12½ | 10½ | 8 |
| **cm** | 40.64 | 35.56 | 31.75 | 26.67 | 20.32 |

| | | |
|---|---|---|
| **Widths: inches** | ½ | 1 |
| **cm** | 1.27 | 2.54 |

**Base Thicknesses:** inches 1 mil 1.5 mil; mm 0.0254 0.0381

| | | | | | | | | | | |
|---|---|---|---|---|---|---|---|---|---|---|
| **Length: feet** | 600 | 1200 | 1800 | 2500 | 3600 | 5000 | 7000 | 7200 | 9200 | 12500 |
| **meters** | 185 | 366 | 549 | 762 | 1097 | 1524 | 2134 | 2195 | 2800 | 3810 |

**HEAD DIMENSIONS**

**Gap Scatter** microinches 100; mm 0.00254
**Interstack Spacing*** inches 1.5 ±0.001; cm 3.81 ±0.00127
**Track Width & Spacing*** inches 0.050 0.070; mm 1.27 1.778 *(IRIG)

**STANDARD PANELS FOR 19-INCH (48.25 cm) RACK**

| | | | | | | | | | | | | |
|---|---|---|---|---|---|---|---|---|---|---|---|---|
| **In** | 1¾ | 3½ | 5¼ | 7 | 8¾ | 12¼ | 14 | 15¾ | 17½ | 19¼ | 21 | 35 |
| **cm** | 4.45 | 8.89 | 13.34 | 17.78 | 22.23 | 31.12 | 35.56 | 40.01 | 44.45 | 48.9 | 53.34 | 88.9 |

## APPENDIX G

## BANDWIDTH REQUIREMENTS FOR THE OUTPUT OF AN INTEGRATE AND DUMP FILTER ON THE AWGN CHANNEL

This appendix will derive the power spectrum of the PAM output of an I&D detector operating on an NRZ-L signal with additive white Gaussian noise. In the text this was needed to determine the bandwidth required to transmit the PAM before quantizing it and converting it into PCM.

Consider Figures G.1 and G.2. As can be seen from Figure G.2 the I&D output on any given bit period is just the addition of signal with a Gaussian random variable. Thus the waveform of Figure G.1 can be written as the sum of two random variables, one equally likely and the other zero mean Gaussian. Since they are also independent their power spectrums simply add giving

$$S_r(f) = S_s(f) + S_n(f), \tag{G.1a}$$

where r = s+n is the output of the I&D, s is the signal part and n is the noise part.

Most bit syncs convert the input PCM format into NRZ-L in the integration process thus

$$S_s(f) = E_b Sa^2(\pi f T), \tag{G.1b}$$

(43)

where $E_b$ is the bit energy, $Sa(x) = \frac{\sin x}{x}$, and T is the integrate period (usually T $\doteq$ 1/bit rate).

The spectrum $S_n(f)$ is found as follows[43]

$$S_n(f) = \lim_{N\to\infty} \frac{1}{NT} \sum_{m=0}^{N} \sum_{n=0}^{N} E\left\{F_m(f) F_n^*(f)\right\}, \tag{G.2}$$

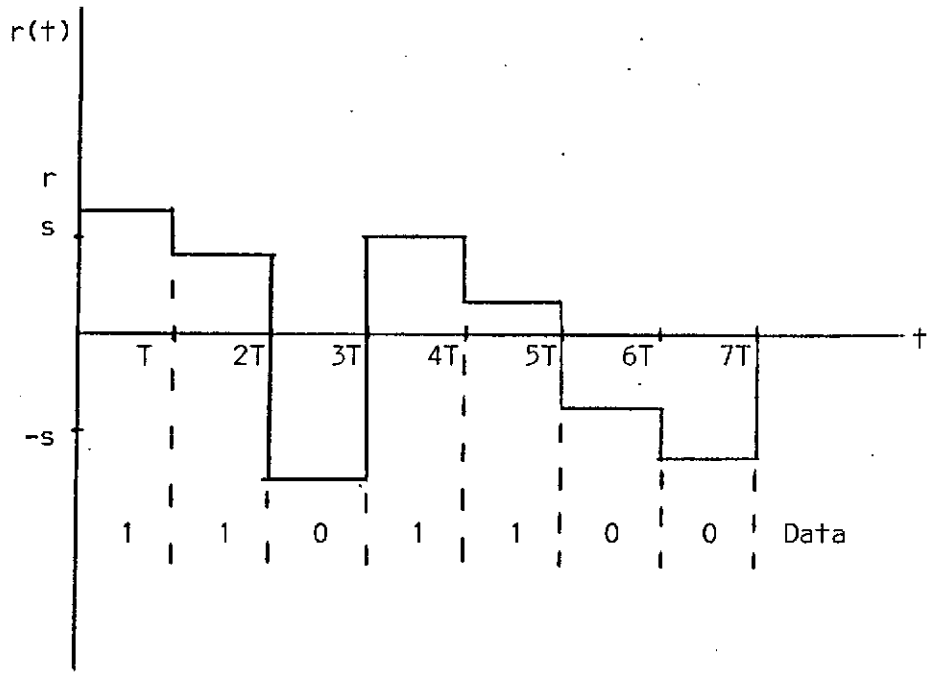


FIGURE G.1 I&D OUTPUT WAVEFORM

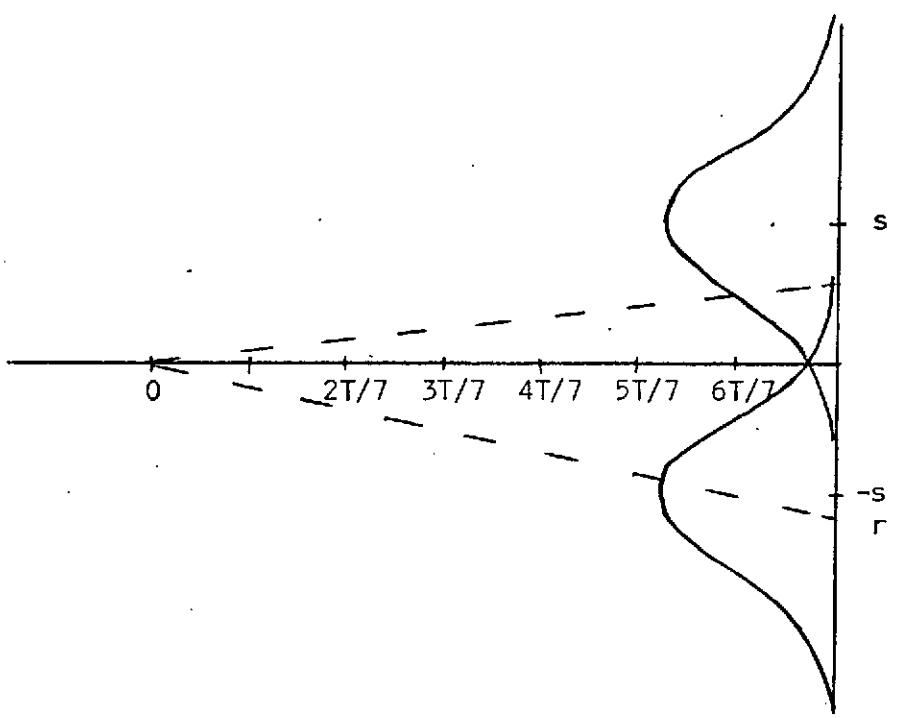


FIGURE G.2 I&D PROCESS AND DISTRIBUTIONS

where

$$F_n(f) = \int_{nT}^{(n+1)T} a_n e^{-jwt}\, dt, \qquad (G.3)^*$$

where $a_n$ is a zero mean Gaussian random variable with variance $N_0W$, $\frac{N_0}{2}$ is the channel noise spectrum and W is the bandwidth of the channel (usually the prefilter preceeding the I&D).

$$E\left\{F_m(f)\, F_n^*(f)\right\} = \overline{a_m a_n} e^{-jw(m-n)T}\, T^2\, Sa^2(\pi fT)$$

$$= N_0WT^2\, Sa^2(\pi fT), \qquad (G.4)$$

where independence of $a_n$ with $a_m$ for $m \neq n$, $\overline{a_n} = 0$, and $\overline{a_n^2} = N_0W$ was employed. Using (G.2)

$$S_n(f) = N_0WT\, S_a^2(\pi fT). \qquad (G.5)$$

Thus defining $S = E_b/T$ and $N = N_0W$

$$S_r(f) = \left(1 + \frac{N}{S}\right) E_b Sa^2(\pi fT) \qquad G.6)$$

Conclusion: The bandwidth requirement for the output of an I&D is the same as that of the noisefree signal! The only modification to the power spectrum is an increase in its amplitude as the S/N decreases.

---

* $F_n(f)$ is the Fourier transform of one rectangular pulse of height $a_n$ and duration T.

APPENDIX H

## TAPE RECORDING WITH REMOTE DECODING VS. SITE DECODING COST CONSIDERATIONS

This appendix is an edited version of a study done by Dr. F. Kalil of the Advanced Systems Code 860 of GSFC/NASA. Due to the lateness of its completion it was not integrated into the main body of this final report.

### H1. TAPE RECORDING AND SHIPPING COSTS

#### H1.1 MOTHER/DAUGHTER DATA

To obtain a 5 dB coding gain, the PCM Decom must provide soft decisions. This means that for each input bit, the Decom must provide at least 3 output bits in parallel. The best approach is to record these three parallel bit streams plus a timing signal on four tracks of the same head stack with a multiple track tape recorder, which is available at the remote sites.

Thence, the bit rate being recorded on the three data tracks is 32,768 bps including the 1/2 convolutional code.

Assume the FR-1900 or FR-2000 recorders are used. These are the predominant recorders at the USBS stations, which will be prime for these missions. Then, the tape speed must be 15 inches/sec (ips) to give the required response. These tape recorders use 1 inch by 9600 feet wideband analog tape, which cost \$52.45/reel per present contract[45] and weigh 14 lbs.

The time required to fill this tape at 15 ips is:

$t_1$ = 9600 ft. x 12 inches/ft. x 1 sec/15 inches x 1 hr/3600 sec

= 2.13 hrs/tape .

The coverage time ($t_2$) in three years for mother and daughter craft is:

$t_2$ = 2 craft x 3 years/craft x 365 days/yr x 24 hrs/day

= $5.25 \times 10^4$ hrs.

Number of tapes N is

$N = t_2/t_1 = 5.25 \times 10^4$ hrs/2.13 hrs/tape = $2.46 \times 10^4$ tapes

= 24,600 tapes (1" x 9600 ft. reels) for Mother Daughter Missions over a three year lifetime.

Purchase cost of tapes, $C_{tapes}$

$C_{tapes}$ = $2.46 \times 10^4$ tapes x \$52.45/tape

= $1.2930 \times 10^6$ dollars

= \$1,293,000 for Mother/Daughter mission

Shipping costs of tapes, $C_{shipping}$ is

$C_{shipping}$ = $2.46 \times 10^4$ tapes x 14 lbs/tape

x \$2.00/1 lb (ave. cost round trip)*

= \$690,000 for Mother/Daughter missions

Cost of tapes plus shipping for Mother/Daughter missions, $C_{M/D}$ is

$C_{M/D}$ = \$1,983,000 (assuming all new tapes)

## H1.2 HELIOCENTRIC MISSIONS

Heliocentric mission tapes costs, $C_H$ is computed as follows. Full coverage is required for the three year lifetime. Hence, the mission time is 1/2 that for both mother and daughter. Also, since the data rate permits a lower tape speed of 1 7/8 ips, which is 1/8 the speed needed for the

---

*Round trip cost is used because tape must first be shipped to the site, used and shipped back to GSFC.

mother/daughter missions, the total tape costs

$$C_H = 1/2 \times 1/8 \times C_{M/D}$$

= $125,000 (costs of tapes and shipping for Heliocentric Mission, assuming all new tapes).

H1.3 OTHER FACTORS

A tape may be erased and reused up to 6 times maximum, then rehabilitated and reused up to 6 more times maximum. A tape can be rehabilitated up to 6 times depending on wear-out factors such as tape speed. However, in addition to the cost of erasing, packaging, receiving, unpacking, inspecting, and storing for ready use, the two-way shipping must be taken into account again. That is, after the data has been extracted from the tapes at GSFC, and the tapes erased or rehabilitated, they must be shipped to the remote site(s) for reuse and shipped back to GSFC for data extraction. These two-way shipping costs are more than 1/2 the original cost of the tape.

Regarding tape logistics, each site must be equipped with spare tapes, facilities for tape handling and storage, as well as personnel. For instance, Rosman has 4 men (1 man/shift) for logging shipping of tapes,[46] even though Rosman transmits via NASCOM a large portion of their acquired data. Also, Code 860 has 2 civil service and 3 or 4 contractor personnel for intermediate handling of tapes prior to shipping them to Code 500 for information processing. However, these manpower costs, prorated by project, are difficult to assess. Furthermore, if one wishes to compare total tape costs with total NASCOM costs, prorated by project, then one must also consider the NASCOM, prorated manpower costs, which could be very difficult and highly subjective. Therefore, it appears that a less subjective yet acceptable approach for comparison purposes

would be to compare only the tape and shipping costs versus the NASCOM line costs on a prorated basis. Hence, manpower costs will not be discussed further.

Assuming an average tape can be reused a total of 6 times then the tape costs computed earlier are reduced by one-sixth, i.e.

$C_{tapes}$ = 1/6 x \$1,293,000

= \$215,500 for M/D missions, assuming reuse of tapes six times.

The two-way shipping costs remain the same whether a tape is new, erased, or rehabilitated, i.e.

$C_{shipping}$ = \$690,000 for M/D missions.

Then, cost of tapes plus shipping for Mother/Daughter missions is

$C_{M/D}$ = \$905,500, assuming reuse of tapes.

Since the Heliocentric Mission will use one-sixteenth as many tapes, its tape costs are:

$C_H$ = 1/16 x \$905,000 = \$56,500, assuming reuse of tapes six times.

Total tape costs for M/D and H missions including shipping, for the mission life of 3 years is

$C_{M/D,\ H}$ = \$962,000, assuming reuse of tapes six times

This does not include any handling costs.

Assume inflation is 5%, compounded yearly for 6 years up to midway in the mission life. (Launch is planned for August 1977, and the mission life is 3 years). Then, inflation could increase these costs by over 33%.

## H2. DECODING AND WIRE TRANSMISSION (NASCOM) COSTS

The following considers the decoder and prorated NASCOM costs.

### H2.1 DECODER COSTS

Assuming the Linkabit, model LV7015 Viterbi Decoder costs given earlier are used, i.e. $5,000/unit for quantities less than 4 and $3,950/unit for quantities greater than 10. To be conservative, the $5,000/unit cost will be used. Again to be conservative, assume each of the sites in the 15 station network will be equipped with two of these decoders, one of which may be considered a back-up or a spare. Then any one of the sites can support any two of the M/D and H missions simultaneously, if necessary, when they are in the same beamwidth, or the site has adequate antennas and receivers.

Then the decoder costs are

$C_{Decoders}$ = 2 decoders/site x 15 sites x $5,000/decoder

$C_{Decoders}$ = $150,000, including spares.

Although these decoders can be used to support other missions and these costs prorated, this will not be considered here to be conservative.

### H2.2 PRORATED NASCOM COSTS

Consider the following, 1973, voice band costs as provided by NASCOM,

| | | |
|---|---|---|
| Madrid | $13,000/mo = | $156,000/yr |
| Orroral | $26,000/mo = | $312,000/yr |
| Goldstone | $ 1,500/mo = | $ 18,000/yr |
| | Total | $486,000/yr |

Each of these sites would spend an average of 8 hrs per day or 1/3 of their time supporting the NH mission. Since the decoded data is 2 Kbps only one

voice line/site would be needed to transmit the decoded data to GSFC. Hence, the prorated NASCOM costs for NH would be about

$$C_{NASCOM,\ NH} = 1/3 \times \$486,000 = \$162,000/yr$$

Assume that in the IME time frame (first launch August 1977) the 9.6 Kbps modems are operational, then only two voice lines in parallel would be needed to transmit the Mother or Daughter decoded data of 16 Kbps. Hence to provide continuous coverage to both mother and daughter, the prorated NASCOM costs are

$$C_{NASCOM,\ M/D} = 2 \text{ craft} \times 2 \text{ lines/craft} \times \$162,000 = \$648,000/yr$$

Hence, the total prorated NASCOM cost for NEMD/NH, i.e. the 3 IME craft is

$$C_{NASCOM,\ M/D,\ H} = \$810,000/yr$$

$$C_{NASCOM,\ M/D,\ H} = \$2,430,000/3 \text{ yrs the mission lifetime}$$

Including cost of decoders and spares this is

$$C_{M/D,\ H} = \$2,580,000; \text{ prorated NASCOM, decoders and spares for 3 years mission life.}$$

As a gross check on this latter cost, consider the following rationale. FY-73 NASCOM leased channel costs are \$26,000,000 + \$4,000,000 for operations.[41][47] In FY-73 the number of unmanned spacecraft missions supported was about 39.[48] A large part of these NASCOM costs are for the Lyndon B. Johnson Space Center, manned flight support requirements and the Deep Space Network requirements. Hence, only about half (very approximate) of these NASCOM costs can be prorated over the above 39 unmanned missions. Thence, the average prorated NASCOM cost per mission per FY-73 is \$334,000, neglecting NASCOM operations. Therefore, for the three IME spacecraft (M/D, H) over three years, this computes to \$3,000,000 NASCOM channel costs, which satisfactorily checks the earlier computation, i.e. it is within 17% of the earlier computation.

H3. COST SUMMARY FOR IME, NEMD/NH OVER 3 YR. MISSION LIFE

| Option 1 (Record On-Site & Ship Tapes to GSFC) | Total Cost |
|---|---|
| 1. All new tapes + shipping, excluding handling (probably pessimistic cost) | $2,108,000 |
| 2. Tapes reused 6 times + shipping, excluding handling (probably optimistic cost) | $ 962,000 |
| 3. More realistic cost of tapes + shipping, excluding handling costs, i.e. average of the above plus inflation | $2,000,000 |
| **Option 2 (Decode On-Site and NASCOM to GSFC)** | |
| 1. Prorated NASCOM + decoders and spares<br>° May be pessimistic since SPADE System could reduce these costs, if SPADE is time shared with other missions. | $2,580,000 |

H4. CONCLUSIONS

The costs are so comparable that Option 2 may be considered as being the more cost-effective, with emphasis on the word effective, for the following reasons: (1) it can provide the experimental data to the GSFC/POCC in essentially real time; (2) it could satisfy the project's expectations for considerable real-time control of some experiments where spacecraft and experiment status need to be monitored in real-time for/during such control.

However, if it develops that the project will have no real-time requirement for quick-looks and related experiment control, and if the analog downlink data could be recorded on another channel of the same tape which is recording the convolutionally coded data, then recording and shipping of tapes becomes more attractive. On the other hand, if NASCOM voice channels will be available anyway, whether the spacecraft data is recorded or not, the more

realistic costs for option 2 might not need to include NASCOM costs in the trade-off analyses. In that case, option 2 again could be more attractive, especially since the decoders could be used for support of other missions. Also, if decoders with capability of handling 2 Mbps, information data rate, are desired, then the decoder costs are approximately doubled from $150,000 to less than $300,000 for 30 decoders, excluding installation and other costs.

The above conclusions bring to mind a third and very interesting option not discussed earlier

Option 3 (Decode at the Remote Sites, then Record and Ship Tapes)

Cost of decoders, as before = $150,000 for 30 decoders.

The bit rate to be recorded will be reduced from three channels at 32 Kbps per channel (soft decision coded data) to 16 Kbps if only one channel. The tape speed can then be reduced from 15 to 7.5 ips. (See Appendix F which includes the recorder specifications for several of the network recorders.) Thus, the costs for tapes and shipping will be reduced by one-half; i.e. from about $2,000,000 to about $1,000,000 for the three year life of the three spacecraft (M/D and H), so that:

Total cost for this option is

~ $1,150,000 (decoders, spares, some new tapes, some reused tapes, plus shipping, excluding handling).

This is a saving of $850,000 over option 1, where the data is recorded and shipped prior to decoding. Also, the STDN ground stations could use the same decoders for support of other missions which may use this convolutional coding scheme to get the advantage of 5 dB coding gain. This could result in further, similar cost savings to the STDN.

Thus, it now appears timely for Network Engineering, NASCOM, and the Project (or Projects) to further evaluate the merits of decoding at the remote sites. This preliminary study shows that it could be very attractive in terms of both economics and efficiency.

APPENDIX I

## THE COMSAT "SPADE" SYSTEM [49]

The term "SPADE" is derived from Single Channel per carrier, PCM, multiple Access Demand assignment Equipment and is used to describe a Comsat accessing system for the Intelsat satellite system. In the SPADE system a frequency bin consisting of some 800 frequencies is formed. As each user requires a link up to and down from the satellite it is assigned by SPADE by randomly selecting frequencies from the bin (the randomness enhances the channel separation characteristics). The system is completely flexible in that neither end of a channel is permanently associated with any terminal, rather the channels are paired to form a link as required within the demand assignment bin.

Figure I1 is a block diagram of a SPADE terminal. Telephone

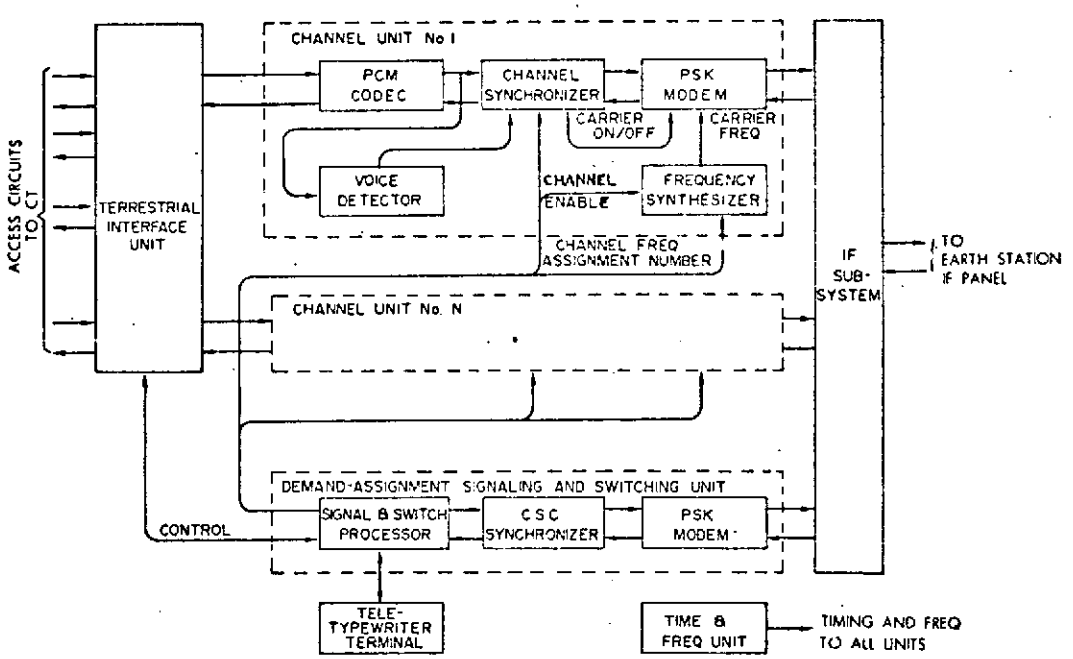


FIGURE I1 BLOCK DIAGRAM OF A SPADE TERMINAL

circuits are interconnected between the local transit center and the SPADE terminal by way of the terrestrial interface unit. When a call request is received the demand assignment signaling and switching unit selects a frequency pair from the bin, notifies the destination station of the incoming call, and also notifies it of the frequency to be used for responding. The two frequencies selected are removed from the list of those available to other users.

The frequency synthesizer is commanded to generate the assigned frequency for the carrier. Once the connection has been established an analog signal is converted to a PCM bit stream by the PCM codec. The codec also reverses the process for received PCM. The channel synchronizer sets the timing, buffers, and frames the data. The PSK modem modulates the carrier which is then frequency multiplexed with other modem outputs so that the total PCM/FDM spectrum can be transmitted to the satellite. For received modulated signals the reverse of the above process takes place. The carrier on/off function makes use of the lulls in conversations to save power by disabling the carrier during the dead time.

It should be noted that for digital data the PCM codec is simply bypassed; thus the system can readily provide PCM channels for the data received by the STDN.

The potential for the SPADE system is to provide low cost high data rate communications since the PCM bit rate which can be accommdated is 56 kbps. As stated in the text of the report the cost for a 56 kbps channel using SPADE is estimated to be on the order of three times the cost of a voice band channel at present. This opens up the possibility of real time

data transmission to and from STDN sites at a relatively low cost (compared with wide band line costs today).